INVESTIGATING THE EFFECTS OF ARIDITY AND ITS IMPACTS ON WATER RESOURCES AVAILABILITY IN THE LUVUVHU RIVER CATCHMENT

by

Nkuna, Tinyiko Rivers
Student no. 11532038

A thesis submitted to the Department of Earth Sciences in Fulfilment of the requirement for the Degree of Doctor of Philosophy in Environmental Sciences (Hydrology)

Promoter: Prof R. Makungo

April, 2025

DECLARATION

I, Tinyiko Rivers Nkuna, declare that this dissertation is my research for PhD Environmental Sciences (Hydrology) at the University of Venda has not previously been submitted for this degree at this or any other university. It is my original work in design and execution and all the references contained therein have been duly acknowledged.

Student's signature… …………   Date…22 April 2025.

DEDICATION

I dedicate this thesis to my late father Gezani Samuel Nkuna.

ACKNOWLEDGEMENTS

First and foremost, I would like to thank the Almighty for giving me the strength to complete this thesis. This work would not have been completed if Prof R. Makungo, the promoter, had not stepped in to guide the work to completion. I want to acknowledge the late Prof J.O. Odiyo for nurturing me into what I am today and for his patience, help, positive criticism and guidance on my research. I would also like to thank Prof Diana Liverman for hosting me on an exchange programme at the University of Arizona. You gave proper guidance during my lifetime's difficult times at the beginning of the COVID-19 pandemic.

I am deeply grateful to Prof JR Gumbo for his unwavering encouragement and support throughout the research. I also want to express my thanks to Mr Ndaedzo Nthulane for his assistance with data collection to analysis. Mr Nthulane's contributions have been instrumental in the success of this research. I also acknowledge the support from the staff members in the Department of Earth Sciences at the University of Venda. Their expertise and resources have significantly enhanced the quality of this study.

I would like to gratefully acknowledge Prof N.S. Nethengwe, who led the University of Venda's University Staff Doctorate Programme (USDP) from the former School of Environmental Sciences. I am also thankful to Prof S Shackleton and Prof M New from the University of Cape Town for providing necessary workshops during the PhD progress. Ms Nondumiso Mginywa is thanked for regularly checking the progress and organizing workshops for the USDP programme. I am also deeply grateful to the University of Venda for providing me with the opportunity to advance my academic pursuits through their offerings.

I would also like to thank Mr Hlulani Clayton Sithole for introducing me to multivariate statistical analysis. The South African Weather Service (SAWS) and Department of Water and Sanitation (DWS) are also acknowledged for providing the temperature and rainfall data, and streamflow data, respectively. The Council for Scientific and

Industrial Research (CSIR) is acknowledged for Conformal Cubic Atmospheric Model (CCAM) data.

I would like to express gratitude towards my grandmother, Mphephu Munwanati, who unfortunately passed away before the completion of my research despite being present and involved from the very beginning. She gave birth to my mother and her support will always be cherished.

I would like to convey my heartfelt appreciation to my beloved parents, Mr. G.S. Nkuna, who, regrettably, passed away before witnessing the completion of this important journey, and Mrs. M.M. Nkuna, for their steadfast love and support. Their financial aid and emotional encouragement have been the bedrock of my determination. Friends and family who supported me during the challenging work time are also acknowledged.

ABSTRACT

The study investigated aridity and its impacts on water resource availability in the Luvuvhu River Catchment (LRC). Hydrological information indicates gradual changes towards more arid conditions in the LRC. The shift towards aridity has impacted negatively on water resources availability. Aridity indices for the LRC were determined using both meteorological and hydrological data. The 5-year or 10-year rainfall or streamflow averages were used to detect drought thresholds, except during flood events. A significant study was done on drought conditions using Standardised Precipitation Index (SPI), Standardised Precipitation-Evapotranspiration (SPEI) and Standardised Streamflow Index (SDI). The study hypothesised increased inter-station variations (spatial and temporal) observable from 5-year or 10-year rainfall or streamflow averages over a historical hydrological period. The study used rainfall and temperature data from the Agricultural Research Council (ARC) and South African Weather Service (SAWS) spanning 58 years (1961 - 2018). National Centers for Environmental Prediction (NCEP) data with a resolution of 10 km was used to determine historical and future aridity in the LRC. The spatiotemporal variations and trends of aridity are reflected in the availability and distribution of water resources. The study developed the aridity indices using United Nations Environment Programme (UNEP) Aridity Index (AI) to determine the spatiotemporal variability of water resources in the LRC. The variations and trends of aridity indices were determined using the coefficient of variation and Mann Kendall test, respectively. Due to a limited number of weather stations in the study area, the Kriging method was used to interpolate aridity indices for areas with no stations. The temporal changes of the 5-year or 10-year cycles of hydrological data analyses show progressive, gradual increases linked to global environmental changes such as global warming. The Hierarchical clustering (HC) analysis revealed the presence of two factors that account for 59.7% and 39.3% of the variability in rainfall within the LRC. The results show that upstream of the catchment experiences more rainfall and lower temperatures than downstream. The increase in temperature and decrease in rainfall might negatively impact the availability of water resources for downstream users. Thus, more arid conditions are experienced downstream of the catchment than upstream. Flood events have become rare and more intense, a characteristic associated with areas prone to droughts. The results of the study reveal significant year-to-year variability in floods and drought events. The increase in aridity should be considered when allocating water resources and implementing sustainable water resources management in the LRC. Thus, the study provides a baseline for monitoring and modelling hydrological processes in arid environments.

Keywords: Aridity; drought; land-use change; Luvuvhu River Catchment; streamflow; and water resources availability

CONTRIBUTIONS OF THE STUDY

This section indicates the publications and presentations emanating from the study and contributions to knowledge.

List of publications

- **Nkuna, T.R.** and Makungo, R. Orographic influence on the distribution of rainfall in the Luvuvhu River Catchment (Manuscript in preparation)
- **Nkuna, T.R.** and Makungo, R. Spatiotemporal variation and trends of aridity indices in the Luvuvhu River Catchment, South Africa (Manuscript in preparation)

Conference presentations

- **Nkuna, T.R.** and Makungo, R. (2022) Orographic influence on distribution of rainfall in the Luvuvhu River Catchment. 1st South African Hydrological Society SAHS) Symposium - Building a Community of Practice, 10 - 12 October 2022, 26 Degrees South Hotel, Muldersdrift, South Africa.
- **Nkuna, T.R.** and Odiyo, J.O. (2019) Spatiotemporal variation and trends of aridity indices in the Luvuvhu River Catchment, South Africa. 20th WaterNet/WARFSA/GWP-SA Symposium on Integrated Water Resources Management (IWRM), 29 October – 01 November 2012, Indaba Hotel, Fourways, Johannesburg, South Africa.

The study’s contributions to knowledge include:

- Determination of arid indices and conditions at a catchment scale will aid in decision-making by water resources managers.

- The study established the rainfall distribution in the LRC based on orographic influence. This information is useful in understanding the distribution of water resources availability in the LRC.

- The current study also provided a forecast for the availability of water in the LRC using a standardized measure for computing standardized arid index.

- This present study provided the importance of integrating drought and floods analysis on water resource availability.

- This study could bring valuable understandings into water resource management economic and sustainable development.

TABLE OF CONTENTS

LIST OF FIGURES

LIST OF TABLES

LIST OF PLATES

LIST OF ACRONYMS

AET	Actual Evapotranspiration
AI	Aridity Index
AWC	Availability Water Content
CMIP5	Coupled Model Inter-comparison Project 5
CV	Coefficient of variation
DWAF	Department of Water Affairs and Forestry
DWS	Department of Water and Sanitation
ENSO	El Nino Southern Oscillation
FAO	Food and Agricultural Organisation
FFA	Flood Frequency Analysis
GEV	Gumbel's Extreme Value
IHP	International Hydrological Programme
IPCC	International Panel on Climate Change
ITCZ	Inter-Tropical Convergence Zone
KNP	Kruger National Park
LRC	Luvuvhu River Catchment
ML	Maximum likelihood
PWM	Probability-weighted moments
RCP	Representative Concentration Pathways
SA	South Africa
SDI	Streamflow Drought Index
SPI	Standardised Precipitation Index
SPEI	Standardised Potential Evapotranspiration
SSP	Shared Socioeconomic Pathways
UAI	UNEP Aridity Index
UNEP	United Nations Environment Programme
UNESCO	United Nations Education and Scientific committee
VDM	Vhembe District Municipality
WMO	World Meteorological Organisation
WRC	Water Research Commission

CHAPTER ONE: INTRODUCTION

1.1 Background

Climate variability and change that are a result of both natural processes and human activity are highly important environmental concerns. These issues have the potential to significantly impact the world throughout the 21st century (Abram et al., 2021; Hulme, 2001; Kenny et al., 2001). Distinguishing between the latter two is a challenging task. Furthermore, it presents a significant difficulty in distinguishing the effects of climate change from long-term fluctuations in climate over several decades (Berdowski et al., 2001).

Variations in rainfall are controlled by the distribution and amount in both time and space. In some instances, these variations are reported to be influenced by El Nino Southern Oscillation (ENSO). For example, a study by Manatsa and Matarira (2009) among others has shown that ENSO events influence rainfall variability in southern Africa. However, it is essential to note that variations cannot be linked to the latter in some instances. As a result, a gap for further investigation exists with the purpose of identifying and quantifying the other causes.

Aridity is a climatic characteristic characterised by low annual precipitation, inadequate water, and significant spatial and temporal fluctuations (Ahmed et al., 2019). This leads to reduced moisture levels and ecosystem support for living organisms (Pereira *et al.*, 2009). According to Adamo and Crews-Meyer (2006), aridity may be a result of high frequency of droughts occurrence. This has been reported in studies such as Maliva and Missimer (2012) which indicated the negative impact on water resources availability. Areas with arid climates are defined by their limited and unpredictable rainfall patterns, typically accumulating between 100 to 600 mm of precipitation each year (Muli, 2014). The primary characteristic of aridity is the presence of dry conditions, which arises due to an imbalance between the amount of annual precipitation and the process of evaporation (Martano et al., 2015). This poses a threat to areas which rely on these water resources. According to Sun (2009), aridity may occur due to frequent occurrence of droughts. The availability of water resources is adversely affected by this situation (Kabanda, 2004). Thus, in recent times, the issues of aridity and drought have gained significant importance at a global level due to their wide-ranging implications on the environment and socio-economic factors (Salvati et al., 2012). According to the International Hydrological Programme (IHP, 1999) approximately 33 percent of the land surface on Earth can be considered as either arid or semi-arid. This is further worsened when one considers the fact that more than two thirds of South African land surface is considered as both arid and semi-arid (Dennis and Nell, 2002).

1.2 Problem statement

Rainfall in Luvuvhu River Catchment (LRC) is characterised by seasonal and annual variations. Rainfall is mainly received in the summer season which is associated with high temperatures. Thus, high rates of evapotranspiration are experienced in this area. Both rainfall and evapotranspiration amounts vary in both time and space with droughts becoming more frequent with a few floods in transition as reported by (Kabanda, 2004). Additionally, Singo et al. (2012) has shown that there are temporal variabilities in both the rainfall and streamflow in the study area. Odiyo et al. (2015) also confirm the above findings in a study on long-term trends and variability in streamflow and rainfall in the same area.

Arid and semi-arid zones are characterised by low annual rainfall and very high evaporation rate, resulting in to severely limited water resources availability (Hadji et al., 2010). Climatic variation and climate change have a significant impact on the hydrology in arid and semi-arid regions, highlighting its sensitivity (Misra, 2014). In these areas, even slight alteration in temperature and precipitation can lead to significant variations in runoff, which in turn raises the chances of experiencing severe droughts and floods (Field et al., 2012).

Several studies such as Odiyo et al. (2015), Singo et al. (2012) and Odiyo et al. (2020) have shown that the LRC has been prone to variations of both rainfall and streamflow over the years. This variability in hydrological variables is responsible for major shifts in the hydrological cycle as reported by Elhag (2006). This can manifest itself in the form of aridity in areas which used to be semi-arid. Thus, semi-arid conditions can be converted into arid conditions if there is a decrease in rainfall. This in most cases is coupled by high temperatures. Aridity may be one of the permanent conditions replacing the normal conditions in most parts of the world including the LRC (Hulme, 2001, Quesada-Hernandez et al., 2019). With evidence of climate change having effects on the hydrology of the LRC, it is likely to impact on the semi-arid environment (Mukwada et al., 2021). The regions of the world currently and expected to experience the greatest water stress are the arid and semi-arid areas (Masoud et al., 2022).

Recently, there has been a noticeable shift towards a drier and more unpredictable climate in certain areas (Wasti et al., 2022). This has contributed to an increase in the occurrence of intense precipitation events on a global scale, while more moderate precipitation events have decreased. This phenomenon has had a particularly strong impact on semi-arid or arid regions. As a result, damage from extreme flood events has steadily increased despite the ongoing challenges of water scarcity in certain areas (Kundzewicz and Kaczmarek, 2000).

Most studies dealing with aridity have been done at the regional scale. These include studies such as that of Araghi et al. (2018), Yin et al. (2015) and Brutsaert and Stricker (1979) amongst others, all of which overlooked the fact that water resources are mostly managed on a catchment scale. Studies at a provincial level have indicated that the Limpopo Province where the LRC is located has water deficit (Monashane, 2011, Muller et al., 2009). In other words, evapotranspiration is higher than the precipitation received. The latter excludes the requirement by water users. Thus, there is a need to undertake research on aridity at a catchment scale where decisions on water resources and supply can be made. This study will aid in decision making by water resources managers. It will also help reservoir operators in knowing when to release water. It is therefore essential that appropriate research methods are developed and applied for the former and that strategies for the development of water resources in arid and semi-arid regions consider the main features of in situ hydrological processes.

1.3 Justification of the study

Water scarcity is a critically significant issue, but when compared to other climatic regions, semi-arid hydrology has not been given as much focus (Govender et al., 2022). Additionally, historical hydrological data have been largely inadequate and basins with this type of data may be regarded as ungauged basins due to the potential irrelevance of the information (Wheater, 2008). The restricted nature of the data arises from the scarce number of hydrological monitoring networks in those areas, where construction and upkeep are challenging and costly. It is therefore important to understand aridity and its influence on water resources availability in semi-arid areas.

Rainfall and streamflow in LRC are characterised by seasonal and annual variations. Rainfall is mainly received in the summer season which is associated with high temperatures. Thus, a high rate of evaporation is experienced in this area. The rainfall amounts vary in both time and space with droughts becoming more frequent and a few floods as reported by (Kabanda, 2004). A study by Nkuna (2012) has shown that there are temporal variations in both rainfall and streamflow in the study area. Through allowing hydrologists, hydrological and hydraulic engineers to construct adequate flood mitigation measures, accurate flood recurrence estimation can save human lives and property damage (Haghighatafshar et al., 2020).

Aridity research at a catchment scale will aid in decision-making by water resources managers. It will also help reservoir operators in knowing when to release water i.e., manage water resources in the catchment effectively to sustain economic and social development of the livelihoods that depend on them. Thus, the study establishes the nature and distribution of rainfall in the LRC. The study also developed a forecast for the availability of water in the LRC using a standardized measure for computing standardized aridity index. It also provides the most useful information on the distribution of available water over an area. This study is justified by the need to better understand the consequences of drought and floods on water resource availability. This study could bring valuable understandings into water resource management economic and sustainable development.

1.4 Research objectives

1.4.1 Main objective

The main objective of this study was to investigate the effect of aridity and its impacts on water resources availability in the LRC.

1.4.2 Specific Objectives

- To determine the inter-station variability (spatial and temporal) observable from 5-year or 10-year rainfall time series data of at least 30 years in the study area.
- To assess variations and trends in rainfall, temperature and streamflow of 5-year or 10-year cycles over at least 30 years of time series data in the study area.
- To determine flood and drought thresholds, duration, magnitude/intensity and frequency in the study area.
- To determine aridity indices in the study area.
- To assess the historical and future impact of spatial-temporal variation of aridity on water resources in the LRC.

1.5 Research questions

- Is inter-station variability (spatial and temporal) detectable in the study area from 5-year or 10-year rainfall time series data spanning at least 30 years?
- To what extent are variations and trends in rainfall, temperature, and streamflow explained by 5-year or 10-year cycles in the study area, using at least 30 years of time series data?
- What are the flood and drought thresholds, duration, magnitude/intensity and frequency in the study area?
- What are the aridity indices in the study area?
- How does historical and future spatial-temporal variation of aridity impact on water resources availability in the LRC?

1.6 Research assumption

The present study assumed that the LRC is changing towards arid conditions which pose serious impacts on the availability of water resources.

1.7 The study area

1.7.1 Location

The Luvuvhu River Catchment (LRC) is a large and diverse area in the Limpopo Province's Northern Region. It is located within one of the five districts within the latter province called Vhembe District Municipality (VDM). It spans a significant distance between the longitudes 29°49'46.16"E and 31°23'32.02"E and the latitudes 22°17'33.57"S and 23°17'57.31"S. It covers an area of approximately 5941 km^2 (Figure 1.1).

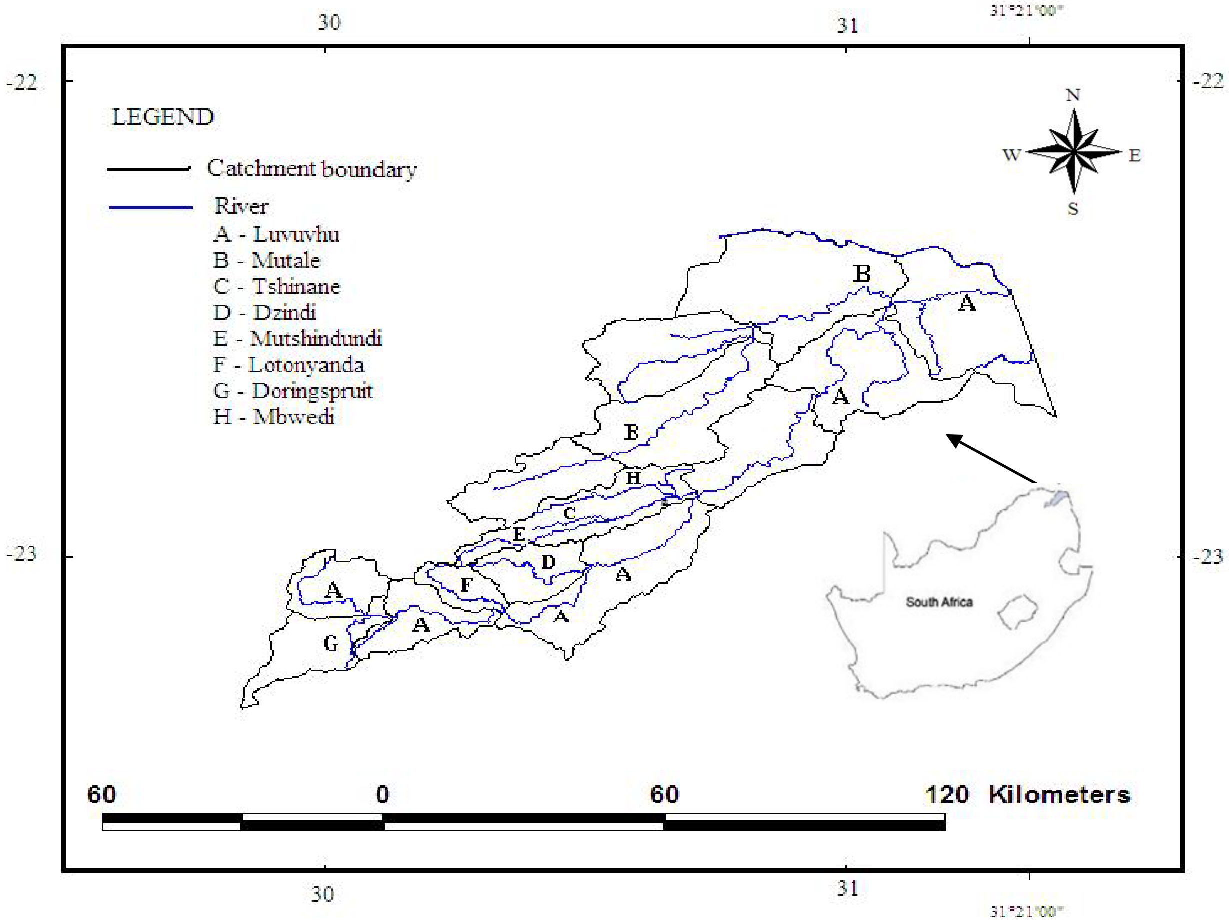

Figure 1.1: A map of the Luvuvhu River Catchment

1.7.2 Climate

The LRC experiences distinct seasons that bring about varying weather patterns. During the summer season, the area is characterised by hot and wet conditions, with an average daily temperature of 28°C and an average rainfall of 450 mm per annum. In contrast, the winter season brings about cold and dry weather conditions. The contrast between the seasons in this region is clear, with temperatures and rainfall patterns shifting dramatically between the two seasons. Thus, some areas of the catchment with very low rainfall and high temperature can be described as semi-arid to arid.

1.7.3 Topography

The predominant topographical feature in the LRC is the Soutpansberg Mountain range. The upper section of the LRC holds the most elevated points and steepest slopes (Figure 1.2). The altitude ranges from 200 m in the northeast to 1600 m in the southwest. The study area encompasses a blend of gently rolling plains, where slopes of less than 5% predominate across over 80% of the region, as well as lowlands, hills, and mountains characterized by varying degrees of elevation (Kundu et al., 2015). The topographic influence has a substantial impact on the hydrology of the remaining catchment, resulting in a notable increase in rainfall.

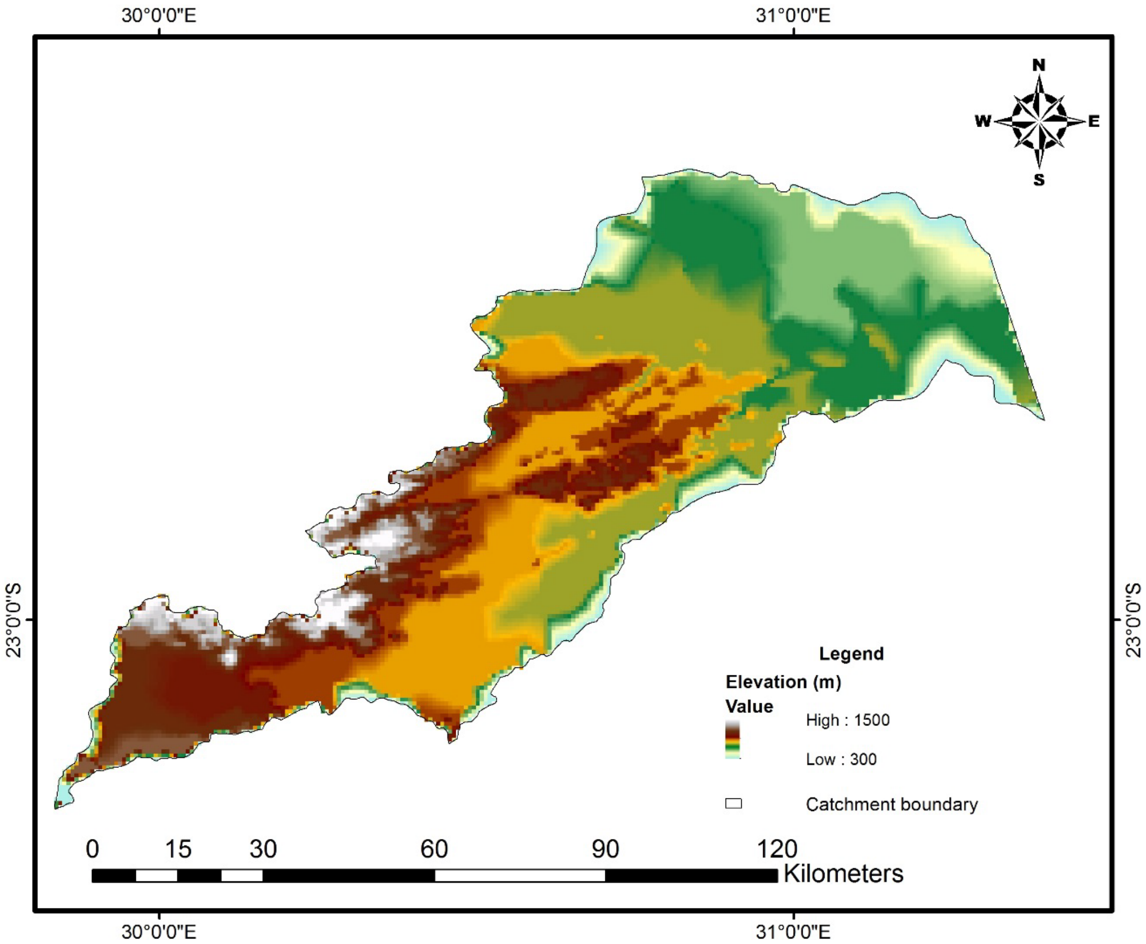

Figure 1.2: Topography of the Luvuvhu River Catchment

1.7.3 Hydrology

The study area is drained by the Luvuvhu River and its seven tributaries, namely Doringspruit, Latonyanda, Dzindi, Mutshundudi, Mutale, Mbwedi, and Tshinane. This can be seen in Figure 1.1. As it flows towards Kruger National Park, the Luvuvhu River merges with the Limpopo River, which extends into Mozambique and eventually meets the Indian Ocean. Originating from the perennial streams in the Soutpansberg, both the Luvuvhu River and its tributaries maintain a constant flow. The annual average precipitation in the area stands at 608 mm, resulting in an annual runoff of 519 million cubic meters, with a range between 85 and 1900 million cubic meters according to the State of the Rivers Report in 2001 (WRC, 2001).

1.7.4 Geology

The geology of the area is varied and complex, with sedimentary rocks dominating in the northern regions while metamorphic and igneous rocks reign supreme in the southern territories. The contrast between the two types of rock formations is evidence of the dynamic and ever-changing nature of the earth's crust. In addition to the diverse rock formations, high-quality coal deposits can be found near Tshikondeni and in the northern part of the KNP, adding yet another layer of complexity to the landscape. With the exception of sandy aquifers found in the Limpopo River Valley, the composition of the formation exhibits a comparatively limited capacity to hold water (Busari, 2008). The presence of the Sibasa basalt has played a significant role in shaping the fundamental geological formation of the mountains within the Sibasa region, as well as certain adjacent areas (Magakane, 2019). Dolerite dykes and unclassified surface deposits are found sporadically in various locations within the vicinity of Thulamela. These dikes are the most heavily aquifer bearing structures and are considered locally important. It is of great importance to acknowledge the intricate network of faults present within the region, predominantly aligned with the Fundudzi and Sibasa basalt formations.

1.7.5 Vegetation and land use

Land use activities in the LRC include forestry, agriculture and settlement. Forest plantations cover the upper reaches of the Luvuvhu and Latonyanda rivers and decrease towards the Albasini Dam. Land cover in the southern highlands of the LRC is dominated by exotic tree plantations of pine and eucalyptus, with some remaining and fragmented patches of indigenous forest (Griscom et al., 2010). Subsistence farming is about a third of the total agricultural component. Riparian vegetation is a sight to behold, characterised by dense stands of large trees, shrubs, and reeds that grow along the banks of rivers, streams, and other bodies of water. The trees that make up this vegetation are often tall and imposing, creating a canopy that shades the water below. The shrubs and reeds, on the other hand, are often smaller and more delicate, but they play a critical role in stabilizing the soil and preventing erosion. Together, these plants create a thriving ecosystem (WRC, 2001). The dry acacia forest species make up the riparian vegetation. To accommodate increasing demand for agriculture, space for orchards are created by clearing extensive portions of the riparian area in the LRC (Riddell et al., 2022). Additionally, alien vegetation such as eucalyptus, poplar and Mauritius thorn have encroached on the riparian zone (Butt et al., 1994).

Community farms are located on the steep slopes near the upper parts of the Dzindi River, while activities such as grazing and tree felling take place in the riparian zone. Subsistence farming dominates in the upper parts of the Mutshindudi and Mbwedi rivers, with a significant area of the sub-catchment covered by plantations. The Mutale catchment is occupied by subsistence farming. In the proximity Albasini foothills, huge citrus, mango, banana, and vegetable farms are plentiful.

CHAPTER TWO: LITERATURE REVIEW

2.1 Preamble

This chapter reviewed the historical trends in aridity encroachment and determination using applicable methodologies and the contemporary research in this field. It begins by reviewing the global issue of aridity with specific emphasis on the causes of aridity and its effects on water resources in Southern Africa. This is because it is a crucial issue that influences water resources management and planning. The physical characteristics and processes associated with aridity are discussed in this chapter. According to Andersen (2008), semi-arid regions have received little attention mainly due to their complexity in the hydrological settings and the lack of hydrological data. This chapter also reviews key hydrological processes occurring in semi-arid regions and how they can be measured or estimated. Hydrological extremes (droughts and floods) are reviewed with specific emphasis to arid and semi-arid areas. The issue of water scarcity and stress are discussed on a global and local scale.

The sustainability of water resources is being hindered by several factors. These include the natural location of the country within the arid zone, where water is already scarce, as well as groundwater deterioration due to excessive pumping and pollution. Additionally, the population growth has increased the demand for water, while agriculture consumes a significant amount of water resources for irrigation (Murad et al., 2010).

The concept of spatial-temporal aridity indices, their importance in assessing aridity, and how they are calculated was explored. different types of aridity indices discussed including their use and limitations. By the end of this literature, a better understanding of the significance of spatial-temporal aridity indices in monitoring and predicting aridity in arid regions is revealed.

2.2 Arid environment

It is important to differentiate between drought and aridity when looking at arid environments. An arid environment is defined as a region that is very dry and has little vegetation (Basso et al., 2000). Thus, the arid environment is regarded as a climatic phenomenon characterised by a temporary and periodic anomaly caused by a prolonged lack of precipitation (Wilhite and Glantz, 1985). Several authors have linked drought to a shortage of water resources availability (Rossi, 2000, Tsakiris and Vangelis, 2005). Aridity, on the other hand, is an enduring feature of climate associated with dry regions that are subject to frequent or continuous occurrences of drought (Incoom et al., 2020). Due to the complexity in the requirements such as temperature, rainfall, and evaporation, aridity is difficult to quantify (Zomer et al., 2022). Arid and semi-arid zones are known for their scanty annual rainfall and very high rates of evaporation, resulting in water resources being extremely insufficient (Hadji et al., 2010). However, it is essential to note that an arid area can also be defined as an area that receives less than 250 mm of rainfall each year (Botkin and Keller, 2010). Very arid regions are deserts in nature. Desert is a landscape form or region that receives very little precipitation. According to Laity (2009), deserts are areas with an average annual rainfall of less than 200 mm. An arid area is also defined as an area falling within the rainfall zones of 0 -300 mm. This implies that the arid environments are very diverse in landforms, soil, fauna, flora, water balances and human activities.

Aridity is typically expressed as a function of rainfall and temperature (Rojas et al., 2014). A region is arid when it is characterised by a severe lack of water availability that prevents the development of plants and animals. Areas exposed to arid climates tend to deficiency vegetation and are referred to as Xeri or Dexeric. The majority of dry climates are located around the equator including Africa and parts of South America, Central America and Australia (Mason and de Blij, 2016).

In the United States of America areas that receive 500 mm and above of rainfall do not irrigate their crops while areas that receive less than 500 mm irrigate their crops (Lillesand et al., 2015). The above statement should be compared with the South African (SA) scenario with more than 50 percent considered arid and that SA receives rainfall less than the global average per annum as indicated by Joubert et al. (1996).

Arid regions are also facing problems such as soil erosion, over cultivation, deforestation, biological invasion, overgrazing, population growth and overexploitation of resources that result in desertification in certain areas (Becerril-Piña and Mastachi-Loza, 2021). Thus, the characteristics below are amongst the ones that make arid regions unable to support some human activities:

- *Rainfall pattern.*

  The rainfall is not reliable. People are unable to predict whether they will receive rain or not in the next season. Because of unreliable rainfall, it is impossible to practice agricultural activities and supply communities with sufficient surface water (Konapala et al., 2020). Despite repeated attempts at forecasting, the weather patterns have become highly unpredictable, making it nearly impossible for farmers to plan their harvests. This has led to much uncertainty and anxiety among the farming community, as their livelihoods depend entirely on the rainfall, they receive each year.

- *High rate of potential evapotranspiration.*

  Evapotranspiration, the combination of water evaporation and plant transpiration, is known to be a crucial component of the water cycle. However, when evapotranspiration rates are high, they can result in structural land degradation. This occurs because excessive water absorption can cause soil erosion, leading to an increased risk of landslides, reduced soil fertility, and decreased plant growth. As such, it is important to monitor evapotranspiration levels and take steps to mitigate the effects of high rates, such as preventing over-irrigation and promoting sustainable land management practices.

- *Low organic matter level.*

  When an area has low organic matter naturally, it can be difficult for plants to grow and thrive. To increase the amount of organic matter in these areas, people often turn to artificial means. This can include adding fertilizers, compost, and other materials to the soil to help create a nutrient-rich environment for plants. While these methods can be effective in the short-term, they may not be sustainable in the long-term. Artificial means of increasing organic matter can also negatively impact the environment, contributing to soil erosion and water pollution. Therefore, it is important to consider more natural and sustainable ways of increasing organic matter, such as crop rotation, cover crops and organic fertilisers.

- *The arid soil tends to support more weeds than cultivated crops.*
  Weeds outcompete selected crops for resources, which is a significant challenge for farmers and agricultural practitioners. The soil supports more weeds than selected crops, making optimum crop yield difficult to achieve. Weeds grow faster and more aggressively than selected crops, and as a result, they outcompete them for food, sunlight, and other essential resources. This can result in stunted growth and low yields for the crops in question. Agricultural practitioners must devise weed-management strategies to ensure that selected crops thrive and produce high yields. A study by Zhang et al. (2020b) showed how maize production can be improved areas with limited water.

- *Prone to flash floods.*
  Arid regions, characterised by their low precipitation and high evaporation rates, often receive heavy showers of rain within a short period of time. However, due to the sandy or compacted soil, much of the water is lost through runoff and less infiltration into the ground. As a result, the area remains dry even after rainfall, and the water that does seep into the soil is quickly absorbed by plants or evaporates (Sharma, 2021). Additionally, the lack of vegetation in arid regions means there is little to no water retained in the ground, exacerbating the issue of water scarcity. This highlights the importance of sustainable water management in arid regions, including methods such as rainwater harvesting and soil conservation to help prevent water loss and promote long-term water availability.

- *Arid regions are typically windy.*
  Arid regions are characterised by their high levels of wind due to the lack of vegetation that can impede air movement. The scarcity of plant life in these

regions means that the wind can move freely across the landscape, unencumbered by obstacles. This can have a significant impact on the water cycle in these areas, as wind removes moist air around the plants and soil due to the absence of any barrier to slow it down. As a result, arid regions are often subject to drought conditions as the moisture is quickly carried away by the wind, leaving the soil dry and barren. The high levels of wind in these regions also contribute to the formation of sand dunes and other geological features, which can have a dramatic impact on the local environment.

- *Vegetation in arid regions is scarce.*
  They have vegetation, a mixture of grasses, herbs, small plants, shrubs, and trees, but they are scarce. The plant species in arid areas are scattered, and most of the plant species in those areas survive short life cycle. In that short life cycle, they can germinate, grow and produce during a short period of available moisture. Plant species with dead and extensive root systems can adapt to such an environment. They can gather water over a wide area. Those areas also have species which store water in their tissues and release that water very slowly. It makes them adapt to such conditions.

2.2.1 Types of arid environments

The types of arid environment include hyper-arid covers (4.2 percent), the arid zone (14.6 percent), and the semi-arid zone (12.2 percent) (Goyal et al. 2013). Almost a third of the total surface of the earth is therefore arid land (Figure 2.1).

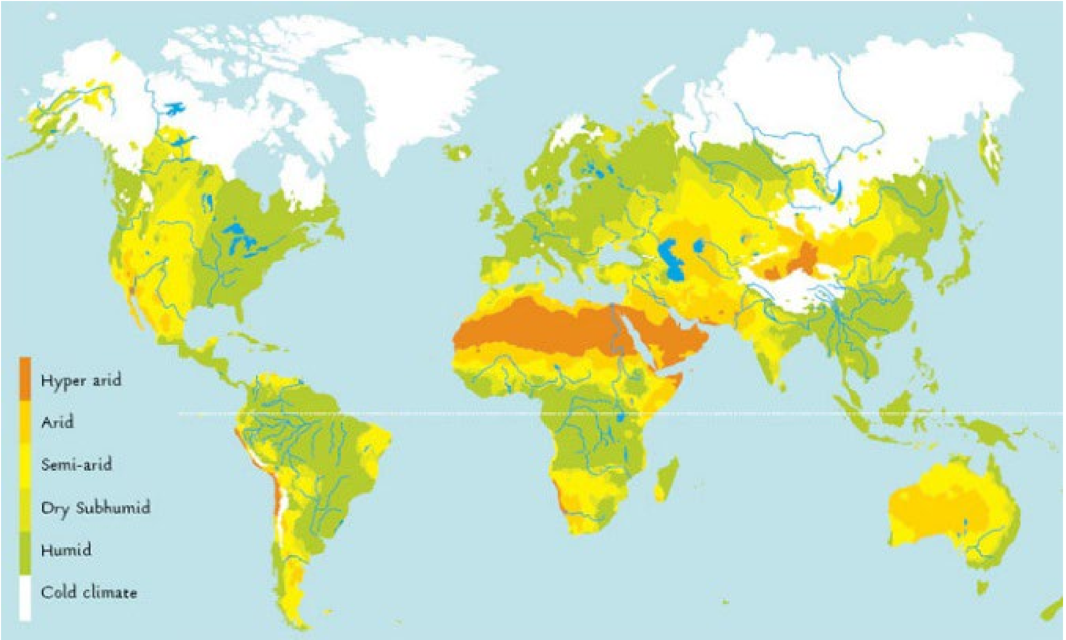

Figure 2.1: World aridity zones (IPCC, 2001)

Arid environments are characterised by dry and hot conditions and are home to diverse flora and fauna that have adapted to survive in these extreme conditions. These environments can be classified into three main types based on their level of aridity. The first type is hyper-arid covers, which comprise only 4.2 percent of arid environments. These areas are extremely dry and have little to no vegetation. The second type is the arid zone, which covers 14.6 percent of these environments. These areas are also dry but can support some vegetation and wildlife. The third and final type is the semi-arid zone, which covers 12.2 percent of these environments. These areas have a slightly higher moisture level and can support more vegetation and wildlife than hyper-arid and arid zones. Understanding the different types of arid environments is crucial for conservation efforts and developing sustainable practices in these regions.

Drought refers to less availability of water compared to the usual or average condition for certain periods. The aridity indicates permanent state of the climate over the given location. The aridity index (AI) is a measure of climatic condition over a given place. However, the drought is a temporary phenomenon. Deterioration of rainfall regime or degradation of the environment by human activities may cause aridity (Verheye, 2009).

Aridity occurs when moist air is cooled either by rising, mixing, radiant cooling, or contact cooling. The processes that contribute to the development of aridity generally hinder the occurrence of cooling by promoting air stability, creating temperature inversions, or raising atmospheric temperatures. When air descends, it tends to warm up, resulting in decreased relative humidity and increased aridity. The majority of arid regions are located in the tropics, where they receive substantial amounts of solar radiant energy that can be harnessed for environmental heating, wind power generation, or evaporation purposes (Thompson, 1975, Walton, 1969). Regional aridity can be attributed to four primary factors: elevated atmospheric pressure, continental air currents, the rain shadow effect, and frigid oceanic currents (Agnew, 1991, Thompson, 1975).

High pressure

Air heated at the equator has a significant role in shaping the Earth's climate. This air rises due to its lower density and moves towards the poles where it cools, becoming denser and heavier. The cooled air then sinks in the subtropics, roughly around 20^{o} to 30^{o} north and south latitude. This sinking motion creates high-pressure areas that are responsible for producing dry and sunny weather conditions. This process is known as the Hadley cell circulation and it affects the climate and weather conditions globally. Understanding the Hadley cell circulation is vital for predicting and managing weather patterns, which can have significant impacts on human activities, such as agriculture, transportation, and energy production.

Continental winds

Continental interior winds possess a distinct characteristic that distinguishes them from their oceanic counterparts (Bradley and Diaz, 2021). Due to the absence of water bodies, these winds have less chance of absorbing moisture, resulting in low humidity levels. This phenomenon is evident in several regions of the world, including South-west Asia and the Middle East. The dry, stable winds that blow across these areas have significant impacts on the climate and weather patterns. For instance, they contribute to the formation of arid and semi-arid landscapes, which are characterised by low rainfall and high temperatures. The stability of these winds also makes them ideal for certain economic activities, such as wind energy production and aviation. Overall, the unique properties of continental interior winds make them an important factor to consider when studying climate and weather phenomena. In the context of moist airstreams, the distance along their flow paths from the ocean holds greater significance than the actual distance itself (Villiger et al., 2022).

Rain shadow effect

When air masses interact with mountain ranges, the cooling of the air causes precipitation and moisture loss. As air is forced to rise over the mountains, it cools and reaches its dew point, forming clouds and eventually, precipitation. This process, called orographic lifting, is responsible for the creation of many weather patterns, such as snowfall and rainfall. However, as the air cools and loses moisture, it becomes drier and less humid. This can result in arid conditions on the leeward side of the mountains, where the air mass descends, with little precipitation and a lack of moisture. The cooling of air by mountain ranges is an important factor in the regional climate, affecting both the precipitation and moisture levels in an area.

Cold ocean currents

The temperature of the lower atmosphere can be significantly affected by cool ocean currents near the shore. As these currents move along the coast, they can cool the surrounding air and create a stark contrast between the air temperature on land and the ocean. However, this phenomenon can also lead to a temperature inversion, where warmer air aloft does not allow cooler air near the surface to rise. This can create a stable layer of air that can cause a variety of weather conditions, such as fog and low-level clouds. In addition, temperature inversions can also trap pollutants near the surface, leading to poor air quality in the affected areas. Understanding the impact of cold ocean currents on the atmosphere is essential for predicting weather patterns and mitigating the potential effects of temperature inversions. This decreases humidity in areas such as coastal Peru, Oman, and Namibia (Warner, 2009).

The increasing occurrence of radioactive trace gases in the atmosphere is expected to lead to changes in climatic conditions. These changes could have significant impacts on the spatial and temporal distribution of land and water resources, water quality, the hydrological cycle of water bodies, water supply systems, and water resource needs in different regions. To effectively address potential water resource issues related to industrial use, domestic consumption, power generation, transportation, agriculture, future planning and management of water resource systems, and protection of the natural environment, it is crucial to have reliable quantitative estimates of the hydrological impacts of climate change.

The phenomenon of climate change is anticipated to bring about alterations in both soil moisture and water resources. The accurate prediction of regional precipitation, which stands as the most crucial climate variable subject to change, poses considerable challenges. In semi-arid regions, even slight alterations in precipitation can have a significant impact on water supply and utilisation, given their high sensitivity to such variations. Regarding the impact of increased temperature on precipitation, it is worth mentioning that the majority of precipitation is retained through natural processes such as infiltration and evapotranspiration initiated by vegetation (Hanel et al., 2018). While higher temperatures may promote more evapotranspiration, it is expected that this effect will be partly mitigated by reduced plant water usage under a CO_2-enriched atmosphere. Furthermore, in areas with transitional winter snow zones, an increase in temperature could potentially lead to more winter precipitation in the form of rain, thereby increasing runoff during the winter season and reducing snowmelt flows in the spring and summer. Unfortunately, when the surplus winter runoff cannot be retained due to flood control regulations or inadequate storage capacity, it may lead to an undesirable reduction in the available water resources. According to Tsakiris and Vangelis (2005), the following types of arid conditions were proposed by Food and Agricultural Organisation and can be distinguished based on aridity:

The hyper-arid zone (arid index 0.3)

The hyper-arid zone includes dryland areas with no vegetation, except for a few dispersed shrubs. Nomadic pastoralism is commonly practiced where rainfall on an annual basis low, seldom exceeding 100 mm (Swift, 2019). The rains are infrequent and irregular, sometimes without rain for long periods of several years according to Sharma (2021) and Dlamini et al. (2022).

Arid zone (arid index 0.03-0.20)

Arid zone is characterised by pastoralism. Agriculture can only be possible with irrigation. Native vegetation is mostly sparse and consist of annual and perennial grasses and other herbaceous plants, as well as shrubs and small trees (Sharma, 2021). High rainfall variability with annual amounts between is predominant in this area.

The semi-arid zone (arid index 0.20-0.50)

Semi-arid zone can support rain-fed agriculture with sustained levels of production (Zhang et al., 2020b). There is also a presence of sedentary production in the area. The native flora consists of a diverse range of species, including grasses, grass-like plants, subshrubs, and trees. The amount of annual rainfall fluctuates from 200 to 250 mm to 450 to 500 mm, with a predominance of winter precipitation.

The sub-humid zone (with an arid index of 0.50-0.75) also experiences arid conditions. In this context, the term "arid zone" encompasses the hyper-arid, arid, semi-arid, and sub-humid zones collectively. Therefore, the term "aridification" is generally used to describe an arid index that falls below 0.75.

2.2.2 Aridity Index (AI)

An aridity index (AI) is a numerical indicator of the aridity of the climate at a given location (Thornthwaite, 1948). It provides a simple way of understanding or expressing the ratio of precipitation to evapotranspiration. High AI represents a humid climate whereas low AI represents an arid area. The use of AI has the potential to measure the amount of precipitation that is accessible for use against the atmospheric water requirements (UNEP, 1997). AI can also be employed to represent aridity and is used to determine the suitability of rainfall in satisfying the water requirements crops (Tsiros *et al*., 2008). In addition, low AI signifies insufficient levels of moisture for prospective plant development, as well as a lack of capacity for soil to retain moisture. This may be associated with high drought vulnerability.

The aridity index has been used to predict inter-annual variability of the evapotranspiration and runoff fluxes (Koster and Suarez, 1999). This has been used to estimate the change in annual runoff due to changes in climate. This required data on precipitation and potential evaporation. More complex indices consider evapotranspiration and even wind and solar radiation. For time series analysis, it is necessary to have a complete set of variables for a long period to retrieve statistically significant results (Scordo et al., 2009). In a separate study, De Martonne (1926) used characteristics of soil hydrologic regime to classify climate by determining the aridity index. In this study, low values indicated dry conditions. Harouna and Carlson (1994) used the normalized deviation from the mean of monthly precipitation and subtracted it from the normalized deviation from the mean of monthly maximum temperatures, applied in the same way to calculate an aridity index.

2.2.3 Determination of aridity

Determination of aridity can be dated back to as early as early 20th century (De Martonne, 1926). This looked at the ratio between precipitation and temperature plus 10^{o}C. It was followed by several methods afterwards. This included among others more complex methods such as the use of reference evapotranspiration (ET_o). The latter was developed by (Thornthwaite, 1948). Despite the two methods above, there was still no standard method for determining aridity. This led to further development of these methods. Penmann and Monteith were the first to get international recognition since they included crop evapotranspiration and irrigation water requirements (Allen et al., 1998).

Aridity can also be used to determine soil moisture holding capacity in certain areas such as in Romania (Paltineanu et al., 2007). Despite the differences in the requirements of the equations used to determine aridity, the resulting aridity index has been used to check the relationship between soil type and soil moisture regime in some areas. Some of the key internationally recognised aridity indices are discussed and further summarised in Table 2.1. The ranking criteria for the aridity index was based on the requirement of data and the applicability of the method in different parts of the world.

Table 2.1: The climatic indices, along with their corresponding equations, classifications, and rankings (Modified from Chowdhury, 2018)

Index	Equation	classification	Rank number
UNEP Arid Index, UAI	$UAI = \frac{P}{PET}$ P = Precipitation, PET= Potential evapotranspiration	UAI< 0.05: Hyper-arid 0.05≤UAI<0.2: Arid 0.2≤ UAI< 0.5: Semi-arid 0.5≤ UAI< 0.65: Dry sub-humid 0.65 ≤ UAI<1: Sub-humid > 1: Humid	1
De Martonne's aridity index, I_{DM}	$I_{DM} = \frac{P}{T+10}$ P= average rainfall, T= average temperature.	I_{DM} < 10: Arid 10 ≤ I_{DM} < 20: Semiarid 20 ≤ I_{DM} < 24: Mediterranean 24 ≤ I_{DM} < 28:Semi-humid 28 ≤ I_{DM} < 35: Humid 35 ≤ I_{DM} < 55: Very humid > 55: Extremely humid	2
Thornthwaite index	$PE = \sum_{n=1}^{12} 115 \left(\frac{P}{T+10}\right)^{10/9}$	$PE < 16: Arid$ 16 ≤ PE ≤ 31: Semi-arid 32 ≤ PE ≤ 63: Semi-humid PE > 63: Humid	3
Minar's moisture certainty, I_M	$I_M = \frac{P - 30(T-30)}{T}$	I_M<0: Highly-Arid 1≤ I_M < 7: Arid 8≤ I_M < 14: Semi-Arid 15≤ I_M < 21: Stable 22≤ I_M < 28: Semi-Humid 29 I_M < 35: Humid > 35: Per- Humid.	4
Pinna Combinative, I_P	$I_p = \frac{1}{2}\left(\frac{P_y}{T_y+10} + \frac{12P_d}{T_d+10}\right)$ I_p= Pinna Combinative Index, P= Yearly precipitation, T= Temperature means, P_d and Td= Precipitation and Temperature means in the	Ip<10 arid climate; 10≤Ip<20 Semi-dry; Ip >20 Humid	5
Lang's Rainfall Factor, I_L	$I_L = \frac{P}{T}$ I_L= Lang's rainfall factor, P = Average rainfall, T= Average temperature	I_L< 40: Arid 40≤ I_L <60: Semi-arid 60≤ I_L <100: Humid >100: Per-Humid	6
The Emberger Index	$I_E = \frac{2000T_{max}P}{T_{max} - T}$ Average rainfall, T= Average temperature, T_{max}= maximum temperature	I_E <10 Per-arid 10≤ I_E<30 Arid 30≤ I_E<65 Semi-arid 65≤ I_E<120 Sub-humid 120≤ I_E<170 Humid >170 Per-humid	7
Lobova Index	$V_a = \frac{P}{6.12\sum T_{A-O} - 30.6}$ V_a= Lobova index, P = Average rainfall, T= Average temperature, A=April, O=October		8

UNEP Arid Index

UNEP arid index (UAI) is the ratio of the precipitation (P) and potential evapotranspiration (PET) (UNEP, 1997). UIA can give a reliable calculation of water balance (Greve et al., 2019). This index is better for assessing the availability of water resources because it is not solely based on precipitation (Zarch et al., 2015). Using this method can better understand precipitation patterns over time and how they may change due to climate change or other factors. It is a reliable tool for mitigating and adapting to climate change impacts. This is because it helps to identify areas that are susceptible to drought and water scarcity. This information can be critical for predicting weather patterns and planning for future water resources. This index has been widely used by researchers and policymakers to assess the water resources of a region and make informed decisions about water management. By understanding the UAI arid index, we can gain valuable insights into the water availability, drought risk, and climate variability of a region, which is key for effective water resource planning and management. Thus, the UAI is ranked number one in most studies of aridity.

De Martonne's aridity index (IDM)

The De Martonnes index is employed to assess the aridity of a specific location by comparing the mean annual precipitation and average annual air temperature. The de Martonne aridity index is expressed as precipitation divided by temperature proposed by de Martonne in 1926. It is the oldest method used to measure aridity. The de Martonne is sometimes referred to as de Martonne drought index wherein its computation is based on the ration between precipitation and temperature plus 10 (Greve et al., 2019). It can be computed monthly. Although it is considered as one of the most ancient indices, De Martonne's aridity index remains a reliable tool implemented to recognise aridity levels in diverse regions (Araghi et al., 2018).

Thornthwaite index

The Thornthwaite index, sometimes referred to as the Precipitation Effectiveness index, is a measure used to assess the effectiveness of precipitation in sustaining vegetation growth (Thornthwaite, 1948). This index considers both the amount and distribution of precipitation throughout the year, as well as the temperature and evapotranspiration rates in the area. By using this index, researchers and environmentalists can better understand the relationship between precipitation and vegetation growth in a given region (Wang et al., 2012). The Thornthwaite index serves as a valuable tool for assessing the overall health and sustainability of ecosystems in various regions of the world. The precipitation effectiveness index (PE), a comprehensive measure of the impact of weather conditions on precipitation, combines monthly measurements of both precipitation and temperature (Marani-Barzani et al., 2017).

Minar's Moisture certainty

Minar's Moisture certainty, a reliable method for determining moisture levels in specific locations, is directly influenced by the amount of rainfall and temperature (Chowdhury, 2018). The ratio of average rainfall in each period to average air temperature in the same period yields the amount of rainfall that falls on every degree of average temperature in a specific time interval. Minar's Moisture certainty is a valuable tool that allows users to determine the presence of moisture in specific locations. However, it is important to note that this measure is closely related to both rainfall and temperature. As such, it's crucial to take these factors into account when interpreting data gathered by Minar's Moisture certainty. By analysing moisture levels in conjunction with climate patterns, users can gain valuable insights into the overall health and condition of their environment. This information can be used to make informed decisions about land use, farming practices, and other important environmental factors. Ultimately, Minar's Moisture certainty is a powerful tool that provides critical information for anyone looking to better understand and manage moisture in their environment.

Pinna Combinative Index

Pinna combinative index is a tool that was developed by Pinna and has been used extensively in the field of environmental science. This index considers the mean value of precipitation and temperature, and it has been shown to be particularly useful in predicting weather patterns and identifying potential changes in the climate. The development of this index has been well-documented in various scientific journals, including works by Deniz et al. (2011) and Ullah et al. (2022) among others. As such, the Pinna combinative index is a valuable resource for researchers and professionals in the field of environmental science and continues to be widely used and studied today. However, there are certain disadvantages associated with this technique that need to be considered. One of the main disadvantages is the complexity of the combinative index itself.

This index can be difficult to understand and interpret, particularly for those who are not well-versed in climate analysis. Additionally, the accuracy of the analysis can be compromised if the data used to calculate the index is not reliable or consistent. It is also important to note that the results obtained from this technique may not always be applicable to other regions or areas with different geographical and climatic conditions. Therefore, while Pinna climate analysis using combinative index can provide valuable insights into climatic changes, it is important to approach it with caution and to consider its limitations when interpreting the results (Moral et al., 2016). Additionally, the index may not consider important local factors that can impact climate, such as topography, vegetation, and urbanization. Finally, the combinative index may not be suitable for all regions or climates, as it was developed based on specific environmental conditions and may not be applicable to other areas. Therefore, while the Pinna climate analysis using combinative index may provide some insights into climate patterns, it should be used with caution and in conjunction with other methods for a more comprehensive analysis.

Lang’s Rainfall factor

Lang's rainfall factor is an important tool used in assessing the natural irrigation conditions of a landscape. This factor considers the relationship between rainfall and air temperature, which are two key factors that influence the ability of a landscape to retain moisture. By analysing this relationship, Lang's rainfall factor can provide valuable information on the water needs of a landscape and help identify areas where irrigation may be necessary. This information is particularly important for farmers and other individuals involved in land management, as it can help them make informed decisions about crop selection and irrigation practices. Overall, Lang's rainfall factor is a valuable tool for anyone looking to optimize the natural irrigation conditions of their landscape. The Lang rainfall factor value is determined by assessing the correlation between the average annual rainfall and the average temperature.

Emberger index

The Emberger index is a useful tool for studying climate and weather patterns. This index is calculated by comparing the annual precipitation to the difference in temperature between the hottest and coldest months of the year (Benaradj et al., 2022). The result is a ratio that provides insight into the conditions of an area. The Emberger index can be used to compare different regions and determine which areas are more arid or humid. By analysing data obtained from this index, scientists can make predictions about future weather patterns and assess the impact of climate change on various regions. Overall, the Emberger index is an important tool for understanding the dynamics of weather and climate in different parts of the world (Shaban et al., 2019). This index helps in understanding the climatic conditions and planning water management strategies accordingly.

The Emberger Index is a commonly used method to quantify the aridity of a given climate zone. While it has its benefits, there are some notable disadvantages to using this index in climatology. This means that its accuracy can be compromised in areas where these variables have a significant impact on the climate. Additionally, the Emberger Index assumes a constant relationship between precipitation and evapotranspiration, which may not hold true in regions with complex hydrological cycles (Arkian et al., 2018, Moral et al., 2016). Finally, the index does not account for any changes in land use or land cover, which can have a significant impact on the water balance of an area. Therefore, while the Emberger Index can provide some insights into the aridity of a given region, it should be used with caution and in conjunction with other climatic indices for a more complete analysis.

Lobova Index

Lobova index is another way of assessing aridity. It uses average annual precipitation minus the monthly temperature of the wet period by subtracting the monthly temperature from the average annual precipitation, the Lobova index can accurately identify regions with low moisture availability, such as deserts or semi-arid regions. Burić et al. (2018) used it Montenegro that experiences low rainfall amount between April and October. This measurement is particularly useful in areas where water availability is critical for agriculture, human habitation, or natural ecosystems. The Lobova index is a valuable tool for researchers and policymakers who need to understand the aridity of a region to make informed decisions about land use, water management, and environmental conservation.

2.3 Challenges of water resources in an arid environment

Water availability in an area is associated with the water scarcity index developed by Asheesh (2007). The Water Scarcity Index (WSI) takes into consideration various factors such as population growth rate, water availability, and the utilisation of water for domestic, industrial, and ecological purposes. The increasing population and recent periods of drought are placing significant strain on water resources. As a result, there is a pressing need for innovative strategies in water planning and management to prevent escalating conflicts and reverse environmental degradation. However, it is concerning that countries are utilising their water resources with greater intensity.

Insufficient precipitation is progressively causing significant water shortages at a national level, resulting in the decline of water tables and the depletion of reservoirs, wetlands, and rivers (Forootan et al., 2019). Global warming is expected to lead to additional alterations, fluctuations, and a heightened level of unpredictability. Numerous factors pose challenges to the long-term viability of water resources. These factors encompass the inherent geographical positioning of the country in an arid zone, degradation of groundwater quality, rapid population expansion, agricultural and industrial operations, as well as the impact of tourism.

Climatic variation and climate change have a significant impact on the hydrology of arid and semi-arid regions (Raulino et al., 2021). It is noteworthy that even slight fluctuations in temperature and precipitation within these regions may lead to significant variations in runoff percentages, ultimately enhancing the possibility and intensity of both droughts and floods (Parry et al., 2007). Throughout the twentieth century, there was a notable shift towards arid and unpredictable weather patterns, leading to a substantial rise in the occurrence of intense precipitation events worldwide (IPCC, 2001). This increase came at the expense of more moderate weather events. The influence of this climate alteration is significantly prominent in regions of the world characterised as semi-arid and arid. Despite the challenge of water scarcity being widespread, this modification has resulted in a constant surge of harm associated with catastrophic flood occurrences (Kundzewicz and Kaczmarek, 2000).

The Limpopo Province is facing the issue of deforestation, which is coupled with a change in species composition (Musakwa et al., 2020). Communal areas are also affected by this problem, with a significant portion of the province being overrun by non-native or alien plants (Maema et al., 2016). According Hoffman and Ashwell (2001), Limpopo Province has been identified as one of the most environmentally damaged provinces in South Africa, especially in communal areas. According to Orimoloye (2023) drought is the most significant contributor to degradation.

Drought conditions which are persistent have been reported to enhance arid conditions in the Volta River Basin in West Africa (Totin et al., 2014). These conditions are also associated with changes in hydrological regimes. To be specific, surface runoff reduced by 13% over a period of 40 years. This poses a threat on water resources availability.

It is anticipated that global climate variations will give way to dwindling levels of precipitation in many areas of the world. However, due to the impending rise in temperatures, evaporation rates will likely surge, leading to arid climate. In addition, downpours are anticipated to decrease in frequency while intensifying in nature. These elements combined will most likely result in more frequent occurrences of both droughts and floods. Anticipated reductions in precipitation, as per climate models, are expected to exacerbate the already arid conditions in regions like northern Africa (Schilling et al., 2020). According Döll (2002) has projected a rise in crop water requirements by more than 5% by 2070. However, it is important to note that this increase may vary in different regions and could even reach up to a 15% surge (Cline, 2007, Kundzewicz et al., 2007). The latter will have serious repercussions not only on water resources availability, but also on food security (Garrity et al., 2010).

2.4 Hydrological Extremes

Hydrological extremes entail both floods and droughts. These are among the topmost challenges that hydrologists have been faced with for a very long period. Fighting the consequences of these has been a challenge for both developing and developed countries. Thus, this section will provide an overview of hydrological extremes. It will also explore how the most talked about hydrological extremes, i.e., floods and droughts, are linked to arid conditions. These are expected, in some areas they come in handy while in some they are considered disastrous. Droughts in the tropics produce more disastrous situations than floods. The repercussions of flooding events tend to receive significant coverage in media and scientific publications. Their swift and conspicuous effects make them a prominent subject of interest. The most significant difference probably lies in the duration of the extremes. Several studies including Ponce (1995), Greve et al. (2014) and Molini (2016) have indicated that hydrological extremes are common in arid climates. These studies found that the following reasons are responsible:

- Precipitation levels remain relatively low throughout the year, but when it does rain, it comes down in intense storms that cover only a small area,
- The potential evaporation rates are quite high, and
- Low volume of runoff throughout the year with occasional short-term flash floods do occur

Despite the intricate projected spatial variations of hydroclimate change, it is highly probable that many regions with existing heavy rainfall may experience even heavier precipitation, and conversely, drier regions will suffer from even more severe droughts. In addition, certain intermediate regions lying on the fringes of current subtropical dry zones are predicted to face progressively increasing aridity (Seager et al., 2013). Anticipated modifications can intensify issues throughout the water cycle, placing more pressure on the already constrained water resources in arid and semi-arid regions, whilst also heightening the possibility of floods and erosion in wet regions. Adjustments in precipitation strength have the potential to intensify the complexity of managing water in the future (Sun et al., 2021). Furthermore, the instrumental, historical, and prehistorical records of hydrological variations suggest that drastic changes between wet and dry conditions can happen swiftly. These transitions can impact the availability of water resources and have significant consequences for ecosystems, agriculture, and society. Therefore, understanding the mechanisms and triggers of hydrological extremes is crucial for developing effective water management strategies and adapting to potential future changes.

Studying past hydroclimatic events can provide valuable insights into the range and frequency of natural variability, as well as the potential impacts of human activities on the hydrological cycle. By taking a proactive approach to water management, we can mitigate the risks associated with extreme hydrological events and ensure sustainable water use for future generations (Seager et al., 2013). For example, within decades, transitions between wet conditions and dry can occur within a year and last for several years (Clark et al., 1999).

Some of the recent studies in the study area on drought include Mathivha et al. (2020), Mazibuko et al. (2021) and Mukwada et al. (2021). The study by Mathivha et al. (2020) used several indices to assess the drought characteristics in the study area. These methods were mainly rainfall and streamflow based. The latter study found that drought is a common phenomenon in the study area as earlier indicated in studies by Kabanda (2004) and Nkuna and Odiyo (2016). Mukwada et al. (2021) used the NDVI to show the prevalence of drought events in the LRC. It showed that the number of years with low NDVI has increased over the years by a significant percentage. The study further showed that this does not show the effects of floods. Thus, a study by Mazibuko et al. (2021) asserted the impacts of both floods and droughts in the same study area. The above study looked at both the phenomenon using the La Nina and El Nino years coupled with the SPI. This leads to the conclusion that both floods and droughts are a challenge in the study area. The study, however, did not indicate the magnitude of the flood as well as their return periods. This is crucial for planning and water allocation purposes. This suggests that integration of flood and drought studies is crucial for areas such as the one in the study.

Floods and drought are accountable for more than 60% of natural disasters occurring worldwide (EM-DAT, 2019). This is responsible for most of the budgets set aside for dealing with disasters by most governments. According to Zhao et al.

(2020), this needs to be looked at holistically because they alternate and in certain case they occur abruptly.

2.4.1 Floods

Flood is defined as an extreme amount of rainfall received in a particular location with measurements that are above normal measurements (Heim Jr, 2015). However, it is important to note that the definition of flood differs with respect to amount of precipitation and its perceived purpose. Flat or low-lying areas (flood plains) are common causes of flooding. At high tide, the ground is saturated and the rate of runoff is always reduced. Floods can also occur when water falls onto an impervious surface such as concrete, pavement or frozen ground, and cannot rapidly be drained quickly into the ground (Barnes et al., 2001).

Floods are associated with disastrous effects in some areas while in some areas they are associated with good recharge of water sources. Their negative effects are associated with washing away of crops; erosion of fertile topsoil; destruction of hydraulic structures such as weirs and bridges. According to Akpalu and Hassan (2009) flooding impacts differently on maize depending on the stages of growth. The topography of the LRC is characterised by many gentle slopes in the lower reaches where vulnerable communities are concentrated, for example, Bende Mutale neighbouring the KNP. Plate 2.1 indicates some of the impacts associated with floods in the study area.

Plate 2.1: Impacts of flood on road infrastructure

The over-saturation of water during floods on seasonal crops such as tomato plant, maize and other crops becomes a fatal disaster on the root's hairs and the underground part of the crop because the xylem is over filled with water and this lead to roots rotting (Akpalu and Hassan, 2009). This usually occurs on maize that are in their early growth as the stem becomes more water filled leading to rapid growth followed by premature pollination (Jain et al., 2019). A flood occurs as a result of an excess amount of surface water runoff that surpasses the capacity limit of either natural or man-made channels. Consequently, the water spills over stream banks and onto lower-level regions. Nevertheless, a flood only becomes a hazardous situation when it poses a threat to human life and property. The occurrence of flooding in a riverline is a direct result of its varying dynamics, greatly influenced by the surrounding terrain. The flat regions are more susceptible to this kind of flood, whereby the land may remain submerged in shallow and sluggish floodwater for an extended duration ranging from several days to several weeks. In contrast, mountainous areas experience floods a few minutes after heavy rain.

The short duration, great depths and high speeds of flash floods make this type of flooding, which is common in arid and semi-arid areas, particularly dangerous. Riverline floodplains vary in width and topography, ranging from narrow, constrained channels to expansive, level zones. In steeper, narrower valleys, flooding can transpire rapidly and briefly, but it is liable to be swift and profound. In contrast, in floodplains that are relatively flat, inundated areas can persist for several days, or even weeks, but the flooding is generally gradual and superficial.

For a hydrologist, the most suitable method of conveying flood magnitude is through the measurement of instantaneous peak discharge. On the other hand, when assessing the risk of flooding, it is more pertinent to consider the noteworthy level that water can attain. Flash floods can happen in a variety of situations. For instance, they may occur due to heavy rainfall occurring within a short period of time, or as a result of sudden releases of large quantities of water from dams or river blockages. Their impact is rapid and intense, causing immediate flooding in low-lying geomorphological areas including, but not limited to, dry lakes, rivers, and mudflats. The occurrence can be attributed to intense precipitation resulting from a severe thunderstorm, hurricane, tropical storm, as well as meltwater from ice or snow traveling over ice sheets or snowfields (Ryu et al., 2017). Flash floods may happen as a result of the failure of a natural obstruction like a debris or ice dam, or as an outcome of infrastructure failures including those of man-made dams. A good example may be the Johnstown flood of 1889 which occurred after a dam wall collapsed in Pennsylvania in the USA (McCullough, 1968).

Distinguishing flash floods from regular floods is determined by the duration of the event, which is typically less than six hours (Seo et al., 2013). Flash floods have the potential to happen in different scenarios. This natural phenomenon takes place when there is a sudden downpour on soil that is already soaked or on soil that has low absorption capacity. The water from the excessive rainfall mixes with rivers and gullies, creating a strong surge of water accompanied by debris. These floods are frequent in arid regions that receive sudden rainfall, and can even be seen far away from the actual source, several kilometres downstream (Schmittner and Giresse, 1996). Flash floods are most common in dry areas due to soil type and permeability, and the lack of vegetation conducive to infiltration. Flash floods can be amplified by the increase in impervious areas (Plate 2.2).

Plate 2.2: Flash floods in Thohoyandou (February 2016)

Flood frequency analysis

Flood magnitude and frequency are performed simultaneously (Archer, 1998). This is because flood magnitude alone may not divulge some of the important information about floods behaviour in an area. Thus, it is necessary to consider the frequency of these events. In this case, historical records are used to mimic the expected behaviour of future events. Mann et al. (2004) discuss methods of estimating flood frequency and return periods. The intensity of floods caused by rainstorm occurrences varies based on the amount and duration of rainfall. The magnitude of the event can be assessed statistically to indicate the likelihood of a recurrence of the same magnitude.

The study of Flood Frequency Analysis (FFA) is important since it helps find the most appropriate model that can determine extreme events of a natural phenomenon like flood (Alam et al., 2018). In most flood frequency analyses, the probability of occurrence of events is determined. This results in establishing the relationship between the magnitude of extreme events and their frequency. To achieve the latter, probability distribution functions are used. Flood frequency was estimated by studies such as Abida and Ellouze (2008), Ahilan et al. (2012) and Alam et al. (2018) amongst others. Flood frequency and magnitude provide essential information for communities affected by tropical cyclones and other extreme weather events.

Several studies were conducted on the frequency of floods were conducted in the study area (LRC). However, it is important to note that such studies were focusing on streamflow as an input into the flood model. For example, Odiyo and Maluleke (2005) used Log Pearson Type III (LP3) method to determine the flood frequency and magnitude in the LRC using data from one streamflow gauging station at Makhovha Village. In another study, Singo et al. (2012) used a combination of methods including the Gumbel Extreme Value (EV1) and Log Pearson Type III (LP3) to determine the frequency of floods in the LRC. The above studies showed that the Log LP3 and EV1 methods perform better in estimating the return period and the corresponding magnitude well. This is in agreement with a study by Alexander (2002) that showed the LP3 is suitable for analysing flood frequency analysis in South Africa.

Smithers and Schulze (2004) created a database to estimate design rainfall for various time periods for South Africa. An analysis was conducted on return durations that spanned from 5 minutes to 7 days, and even as far as 200 years. This analysis was conducted simultaneously with the application of goodness of fit testing. The purpose of these tests is to aid in the selection of suitable distribution based on the data provided. Thus, it is important to note that these tests are not meant to determine the ideal distribution, but rather to eliminate potential distributions. The test statistics generated through these tests can then be utilized to evaluate the degree of conformity between the data and specified distribution. These tests identify discrepancies involving observed and predicted data values from the distribution under investigation.

2.4.2 Droughts

Defining drought can be challenging as it varies according to people's professions and their reliance on precipitation (Backeberg and Viljoen, 2003). However, most of the definitions have one thing in common i.e., lack of moisture (water). According to Shaw et al. (2011) drought is characterised as a prolonged duration of inadequate rainfall, commonly encountered in arid and semi-arid climates. Its numerous dimensions can impact soil moisture, streams, groundwater, ecosystems, and human beings, which vary across each specific region. However, the initial cause of a drought is always the absence of precipitation. The occurrence of drought is a frequent global phenomenon, with distinct spatial and temporal features that differ markedly across regions (Tallaksen and Van Lanen, 2004). Due to its recurrence in nature, it is often confused with aridity which has already been discussed in the earlier section. The duration and severity of droughts have increased, often persisting throughout the rainy season, and their underlying factors remain insufficiently comprehended (Nicholson, 2017).

This section reviews how droughts may affect the availability of water resources in arid areas. Different types of droughts are meteorological, agricultural, hydrological and socio-economic in nature. Each type of drought reflects different sectors' perspectives on water scarcity and is discussed later in this section. Various types of drought can occur, each representing distinct stages of an ongoing and natural phenomenon (Smakhtin and Hughes, 2004). Figure 2.4 below shows different types of droughts and their impacts according to Tallaksen and Van Lanen (2004).

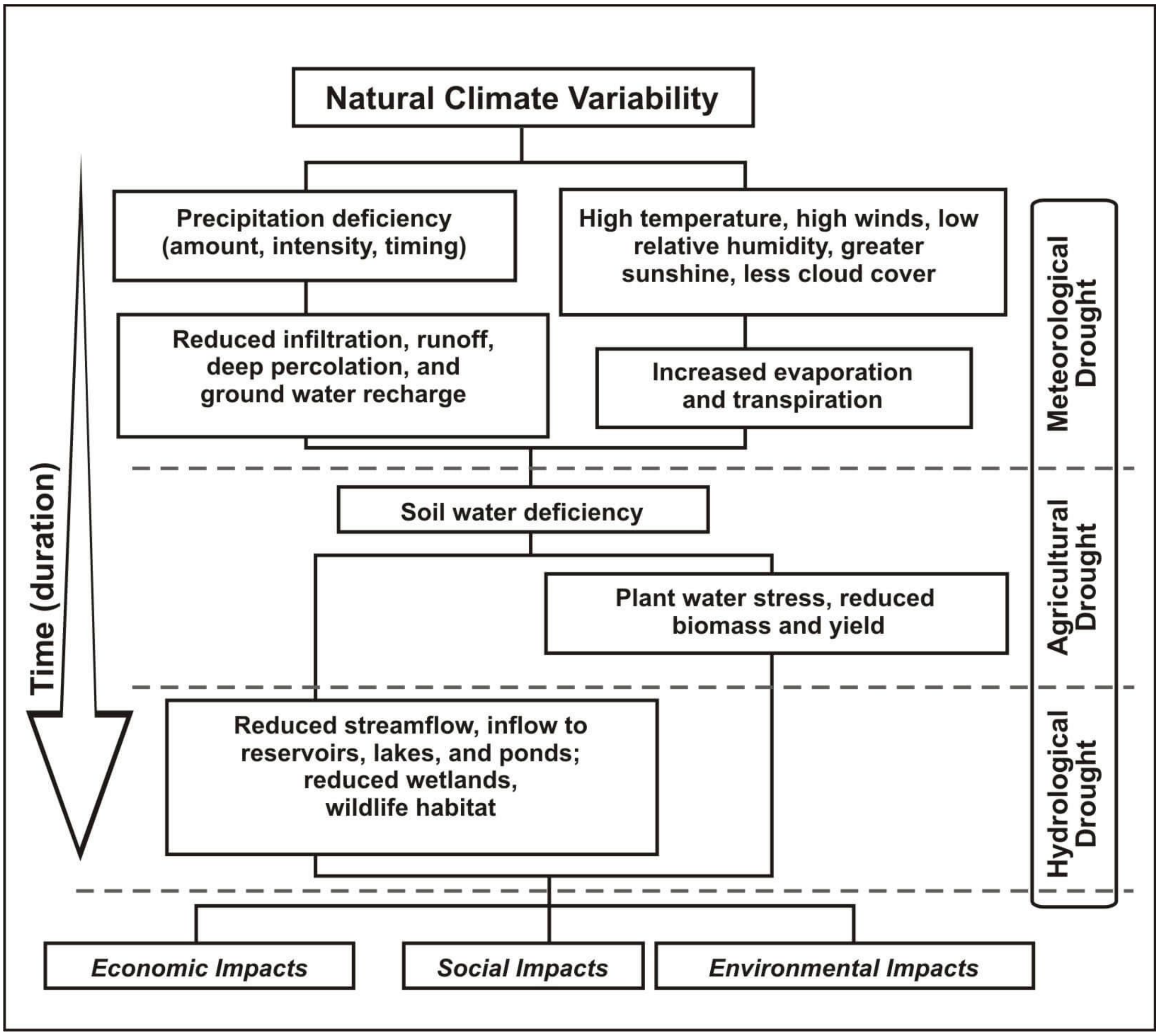

Figure 2.2: Types of droughts

The agricultural sector is particularly susceptible to the effects of drought as compared to other sectors, primarily because the impacts on crops tend to arise during harvesting periods. Additionally, droughts are often accompanied by increased atmospheric temperatures, leading to a rise in surface temperatures. This poses a greater threat to crops such as maize, as the warmer soil conditions result in reduced oxygen absorption capabilities by plant roots (Rouanet, 1987). The primary reason for the drying up of maize roots is the lack of oxygen absorbability, leading to oxygen deficiency.

Meteorological drought

The definition of meteorological drought commonly pertains to the intensity of aridity as well as the length of the period without precipitation (Maliva et al., 2012). This is usually compared to something normal or average. The onset of a drought generally begins with a meteorological drought. It is imperative to consider that meteorological drought definitions should be tailored to a specific region, as the atmospheric factors that result in precipitation shortage differ significantly depending on the area (Wilhite and Buchanan-Smith, 2005). For example, in the realm of meteorology, drought is defined as a period characterised by a scarcity of precipitation, as determined by the frequency of days wherein the amount of rainfall falls below a certain threshold. This condition is specifically applicable to geographical areas that consistently experience precipitation throughout all seasons. These areas include tropical rainforests, where the climate is characterised by high rainfall and constant humidity, as well as humid subtropical regions and humid mid-latitude climates, which also have a significant amount of precipitation throughout the year. Meteorological droughts are a cyclical form of disaster, triggered by insufficient precipitation levels that can result in substantial financial repercussions (Smakhtin and Hughes, 2004). Meteorological droughts are inevitable occurrences that cannot be prevented (Smakhtin and Schipper, 2008). However, with the aid of accurate forecasting and diligent monitoring, their detrimental impacts can be anticipated and minimized. Furthermore, despite their association with meteorological droughts, they only show a rainfall deficit compared to an expected amount over a given period. This type of drought occurs when dry weather patterns dominate an area. Meteorological droughts can begin and end quickly, before the other types of drought manifest themselves (Keyantash and Dracup, 2002, Rossi, 2000, Wilhite and Buchanan-Smith, 2005).

Agricultural drought

Agricultural drought is a phenomenon that encompasses different aspects of meteorological or hydrological drought, specifically examining the effects it has on agriculture (Moorhead et al., 2015). This includes inadequate levels of precipitation, insufficient soil moisture, diminished reserves of groundwater or reservoirs required for irrigation, and similar factors. In agriculture, the amount of water needed by plants is influenced by various factors such as weather conditions, biological traits of the plant, growth stage, as well as physical and biological qualities of the soil. A definition of agricultural drought that is comprehensive should factor in the varying susceptibility of crops during different developmental phases from emergence to maturity. Specifically, droughts in agriculture are linked to rain availability which can be measured by plant requirements during the growing season. Plate 2.3 shows the impact of rainfall shortage on maize. According to Sharma et al. (2020), short-term impacts dominate the nature of these droughts, which involve variations in both the amount and spatial distribution of rainfall. The quality of rainfall, as opposed to just its quantity, may also play a crucial role. The occurrence of this drought stems from the impact it has on crops (Walz et al., 2020).

Plate 2.3: Impacts of drought on agricultural production (February, 2015)

Hydrological drought

Hydrological drought typically manifests itself as a consequence of prolonged deficits in precipitation, which in turn affects the availability of water resources like streamflow, reservoir and lake levels, as well as groundwater. This can have far-reaching implications for society, potentially leading to significant impacts. Hydrological drought, in terms of frequency and severity, is typically characterised on a watershed or river basin scale. While all droughts stem from a lack of precipitation, hydrologists primarily focus on understanding how this deficiency impacts the hydrologic system. Hydrological droughts specifically affect various components of the hydrological system, such as soil moisture, streamflow, and levels of groundwater and reservoirs. Unlike other types of droughts, hydrological droughts are specifically associated with reduced discharge in rivers and streams, indicating long-term water deficits. This type of drought becomes apparent when there is a noticeable decrease in water supply, particularly in streams, reservoirs, and groundwater levels. Typically, these conditions develop after several months of meteorological and agricultural droughts have already occurred (Figure 2.2). The process of development and recovery requires a significantly greater amount of time (Keyantash and Dracup, 2002). It is worthwhile to note that it is hard to detect the changes of this type of drought and possibly attribute it to climate change. This occurs due to the possibility that the perceived impact of climate change in certain instances might actually be attributable to the influence of long-term climate fluctuations, as reported by Van Lanen et al. (2013).

Hydrological drought is a type of drought that can have significant societal impacts due to extended periods of precipitation shortfalls affecting water supply (Wilhite and Buchanan-Smith, 2005). Hydrologists have a specific focus on the implications of this insufficiency within the hydrological system, as it has the potential to affect critical aspects such as soil moisture, streamflow, as well as groundwater and reservoir levels. Unlike other types of drought, hydrological droughts are related to reduced discharge in rivers and streams, typically after many months of meteorological and agricultural droughts (Van Lanen et al., 2013). Plate 2.4 shows the impact of hydrological drought on streamflow. Detecting changes in this type of drought can be difficult and attributed to climate change because multi-decadal climate variability plays a role in some cases (Berdowski et al., 2001, Van Lanen et al., 2013).

Plate 2.4: Impacts of drought on hydrology (river discharge)

2.5 Drought assessment and monitoring

Drought indices integrate multiple factors such as precipitation, snow accumulation, streamflow, and other key water supply indicators to provide a comprehensive assessment. The value of a drought index is significant in facilitating decision-making processes, as it consolidates extensive data sets into a singular numerical value.. Various drought indices measure the level of precipitation deviation from historical standards over a particular period. It is worth noting that none of these indices can be deemed superior in all scenarios. Some indices are more appropriate for specific purposes compared to others. In international publications, different indices have been thoroughly discussed and applied, including the ones below:

Percent of Normal

The computation of this index involves dividing the current precipitation by the average precipitation, commonly referred to as the "normal" precipitation, which is typically based on a 30-year mean. The result is then multiplied by 100. This index has the flexibility to be calculated over different time periods, typically ranging from a single month to a collection of multiple months. Discloses the proportion of precipitation during a specified time in relation to the standard precipitation during the baseline period. The use of this method is limited in South African catchments. However, this method is mainly used on a seasonal scale.

$$P_N = \frac{p_i}{\bar{p}} \times 100 \qquad (2.1)$$

Where:

- p_i is annual rainfall and
- $\bar{p}$ is long time rainfall mean.

Deciles

The time series of accumulated precipitation for a specific duration is split into segments, referred to as deciles, which represent 10% of the overall distribution. These deciles serve as a means to examine and comprehend the patterns of precipitation over time. This approach facilitates the identification of the most prevalent and least frequent precipitation values. It proves to be an invaluable technique for studying and predicting weather patterns, empowering us to make well-informed choices and preparations by leveraging past data. However, it is worth noting that the applicability of this method is constrained within South African catchments.

$$P_i = \frac{i}{n+1} \times 100 \qquad (2.2)$$

Where:

- P_i is probability of rain in number ith,
- n is number of rainfall data

Palmer Drought Severity Index (PDSI)

Palmer (1965) devised an index that utilizes the water balance equation's supply-and-demand concept. The purpose of this index is to assess the moisture supply's deviation from regular conditions in a place. It considers variables such as precipitation and temperature data, as well as meteorological parameters and the soil's Available Water Content (AWC) at a local level. As per the PDSI classification, strong droughts are more frequent over eastern Europe's continental region. Conversely, areas along the northwest European seaboard, the Mediterranean seaboard, and the Alps rarely experience droughts. This index has been widely used in North America and Europe. Its implementation is gradually picking up speed in South Africa, and it has played a crucial role in studies such as Mbhamali and Jury (2021) and Theron et al. (2021) in assessing the impacts of drought on agriculture. The primary equation for the Palmer Drought Severity Index (PDSI) is relatively complex, encompassing several elements that must be derived from temperature, precipitation, and regional moisture information. The PDSI is based on the water balance equations below.

$$d = P - \dot{P} \qquad (2.3)$$

Where:

d, is the difference between the actual precipitation (P) and climatically appropriate for existing conditions precipitation $\dot{P}$ is an indicator of water deficiency or surplus.

$$\dot{P} = ET + R + RO - L \qquad (2.4)$$

Where:

- ET is the evapotranspiration (mm)
- R is the recharge of soil moisture (mm)
- RO is the runoff (mm); and
- L is the loss of soil moisture (mm)

Surface Water Supply Index (SWSI)

The SWSI (Snow Water Supply Index) was created by Shafer and Dezman (1982) as a supplementary tool to the Palmer Index. Its purpose is to address the challenges posed by significant variations in topography within a given region, while also taking into consideration the accumulation of snow and resulting runoff. To calculate the SWSI for a specific basin, one must gather monthly data from all precipitation stations, reservoirs, and snowpack/streamflow measuring stations located within that basin.

$$SWSI = \frac{[(a \times PN_{SP})(b \times PN_{PCP})(c \times PN_{RS}) - 50]}{12} \quad \text{(2.5)}$$

Where:

- PN is the probability of non-exceedance
- SP is snowpack
- RS reservoir components, during summer SP is replaced by SR for streamflow

Standardized Precipitation Index (SPI)

The Standardised Precipitation Index (SPI) was developed by McKee et al. (1993) with the purpose of measuring the shortage of precipitation for various time periods. Through its evaluation of different water resource availability, SPI reflects the impact of drought on soil moisture conditions on a shorter scale and on groundwater, streamflow, and reservoir storage on a longer scale. Thus, the index was originally determined for time periods of 3, 6, 12, 24, and 48 months (Moreira et al., 2015). The computation of SPI is based solely on precipitation records and involves calculating the difference between precipitation anomalies and their mean values for a given period, divided by the standard deviation of the data. This index is used worldwide because of its flexibility in data requirements.

$$Z = \frac{x_i - \bar{x}}{\sigma} \quad \text{(2.6)}$$

Where:

- Z = normalized standardised departure
- $\bar{x}$= sample mean
- x_i = raw value
- σ = sample standard deviation

The Standardized Precipitation Index (SPI) exhibits homogeneity in terms of the spatial occurrence of severe drought events. according to Hayes et al. (1999), one potential drawback of the SPI is its inability to identify regions that are more susceptible to drought. However, a standard classification system should prioritize standardization in both space and time, ensuring that the frequency of a specific event is not influenced by its location. Therefore, the SPI can be considered superior to the PDSI when it comes to categorizing droughts on a consistent scale. Additionally, aside from the spatial distribution of drought occurrence, the SPI12 index produces identical results to those obtained with the PDSI. The latter agreed with Oladipo (1985), demonstrated through the analysis of data specific to Nebraska, that precipitation-based indices can exhibit strong performance in comparison to intricate hydrological indices like the PDSI. Moreover, the SPI possesses the added benefit of a flexible time scale, which proves advantageous in examining the chronological progression of events. A good example of the use of this is reported by (Hayes et al., 1999) for US drought of 1996. Their research highlights the various implications of such environmental challenges and illustrates how drought not only impacted agricultural productivity but also had far-reaching effects on water supply, ecosystem health, and the economic stability of communities. Nkuna and Odiyo (2016) used the SPI to show the variability of rainfall in the upper reaches of the LRC.

Standardized Precipitation Evapotranspiration Index

The Standardized Precipitation-Evapotranspiration Index (SPEI) is an advanced tool that climatologists and environmental scientists employ to evaluate the intensity and consequences of drought conditions in different areas (Habeeb et al., 2023). This index builds upon the conventional Standardized Precipitation Index (SPI) by integrating precipitation data with evapotranspiration factors, including water loss through soil evaporation and plant transpiration. SPEI uses a climatic water balance obtained at various time scales. The SPEI is particularly useful for assessing the balance between precipitation and evapotranspiration, which is critical in understanding agricultural droughts and water availability. In addition, SPEI effectively captures the primary impact of rising temperatures on water demand, showcasing its high sensitivity and resilience to climate change (Elbeltagi et al., 2022). This is because one of the most important variables is temperature. Consequently, the SPEI offers a more thorough insight into hydrological conditions, enabling researchers and policymakers to analyse and address droughts more effectively.

The are a series of steps that can be followed to compute SPEI. Firstly, the difference between precipitation (P) and potential evapotranspiration (PET) over a given time period (typically on a monthly, seasonal, or annual basis) need to be calculated:

$$Water\ balance = P - PET \text{...(2.7)}$$

Where:

- P = Precipitation (mm),
- PET = Potential Evapotranspiration (mm)

Secondly, the difference between these two gives an indication of moisture deficit or surplus. Thus, the water balance values over a historical period are used to estimate a probability distribution (often a log-logistic distribution) to model the frequency and intensity of wet and dry periods. Thirdly, the water balance for each defined period, whether monthly or seasonal, is standardized. This involves transforming the water balance values into standard scores (z-scores) by comparing the observed water balance to the historical distribution.

$$SPEI = \frac{x_i - \bar{x}}{\delta} \text{..(2.8)}$$

Where:

- x_i = the observed water balance value
- $\bar{x}$= the mean of the historical water balance distribution
- σ= the standard deviation of the historical water balance distribution

Streamflow drought index

Streamflow drought index (SDI) is a highly sophisticated and comprehensive measurement tool utilized by hydrologists and environmental scientists who are dedicated to understanding the dynamics of water systems. This index serves a critical purpose in assessing both the severity and duration of drought conditions in a specific geographic area by analysing water flow in rivers and streams. To produce its evaluations, the index considers a multitude of factors, including but not limited to precipitation levels, temperature variations, and historical streamflow data. By synthesizing this diverse array of information, the SDI provides a clear, detailed understanding of water availability, which is crucial for managing water resources effectively (Malik et al., 2019). This thorough analysis enables policymakers, farmers, and conservationists to make well-informed decisions regarding agricultural practices, irrigation needs, and the conservation of vital ecosystems, ultimately supporting sustainability efforts in changing climate conditions. The SDI for each reference period k of the i-th hydrological year is determined based on the cumulative streamflow volume V(i, k) using equation 2.9 below.

$$SDI(i,k) = \frac{(V(i,k) - V_k)}{S_k} \quad \text{..........}(2.9)$$

Where:

- Vk represents the long-term average (mean) of the cumulative streamflow volume for the reference period k.
- Sk represents the standard deviation of the cumulative streamflow volume for the reference period k, calculated over a long historical period.

2.6 Water scarcity and stress

Scarcity of water resources is a growing concern worldwide. The condition of water scarcity arises from a disparity in the availability and utilisation of water resources within a specific region. It occurs when the amount of water available in an area does not meet the community's needs. Water scarcity is therefore defined as a situation where the demand for water is more than natural water availability in a river catchment (Liu et al., 2017). The precision of the indicators utilised to describe and chart water scarcity on a global scale is of significant significance. These indicators have brought to the forefront the discrepancy between the availability of and the demand for water, as well as recorded the progression of water scarcity over time. Water scarcity evaluations continue to underline worldwide assessments of food availability, poverty rates and human advancement, as well as economic and commercial opportunities and environmental well-being (Falkenmark, 2013). Given the widespread application of water scarcity indicators, their precision is of utmost importance. Figure 2.3 shows the number of months with water scarcity based on the period of 1996-2005 for the entire world in areas that have data (Hoekstra et al., 2012).

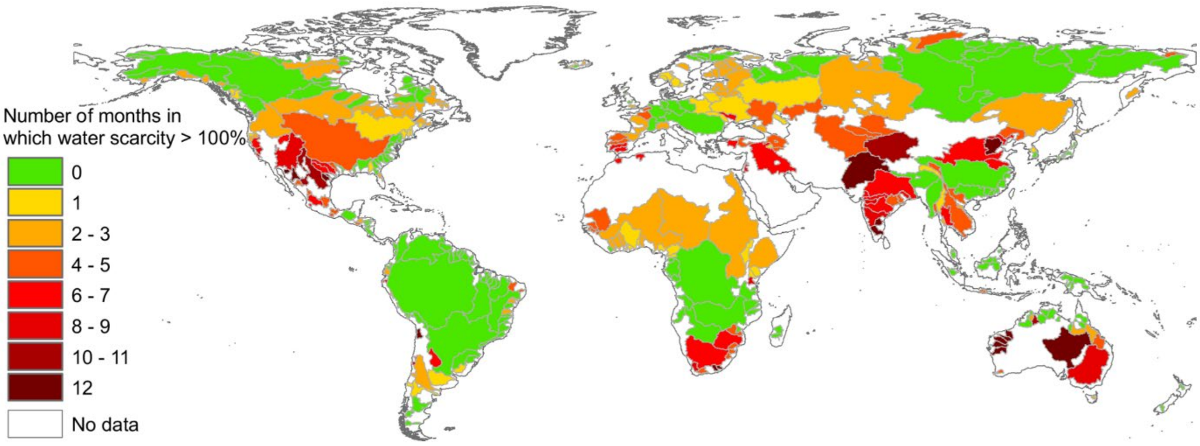

Figure 2.3: Number of months with water scarcity based on the period of 1996-2005

The impacts of population growth, urbanization, and human induced as well as natural climate change are anticipated to be experienced in developing countries, as the demand for resources continues to rise. Physical water scarcity is characterised by severe environmental deterioration, depleting groundwater reserves, and water distribution that prioritizes certain sectors over others (Molden, 2013). According to Falkenmark,s classification, the scarcity of water in southern Africa and some parts of the eastern Africa will experience a significant decline in the amount of water resources available for use (Howlett and Cuenca, 2017). This classification divides countries and areas into distinct categories based on their available freshwater resources in relation to their population sizes, providing critical insights into the challenges of water management (Figure 2.4). By taking into account factors such as annual renewable water availability, demographic pressures, and consumption patterns, Falkenmark's classification helps policymakers and researchers understand the complexities of water scarcity and develop effective strategies for sustainable water use. This framework serves as a vital tool for addressing issues like drought, over-extraction of water resources, and the impacts of climate change on global freshwater supplies. It is noteworthy that there is no consensus on which social and economic factors should be included and that these factors may be different for different countries and regions (Liu et al., 2017). Thus, determining the physical availability of water is key. Below is the world map of water scarcity according to the Falkenmark indicator.

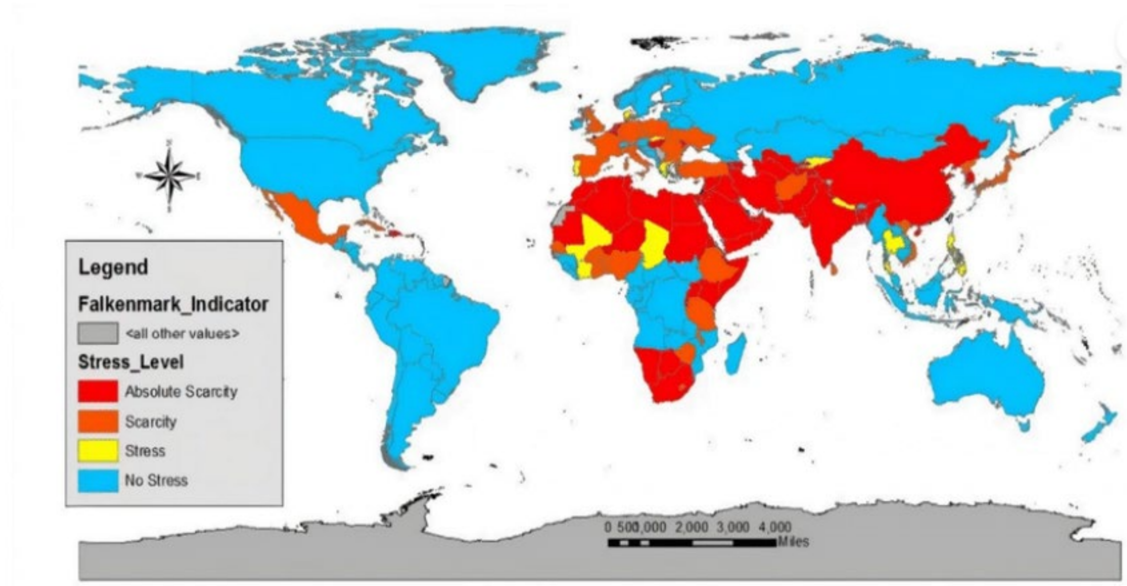

Figure 2.4: World map of water scarcity as per Falkenmark indicator

The development of economic water scarce infrastructure, which is designed to make limited water resources available for use, is widely acknowledged as critical in addressing the challenges of water scarcity. These infrastructure projects involve the construction of water storage facilities, such as reservoirs and dams, as well as the implementation of water distribution systems to ensure efficient and equitable access to water. Additionally, the use of innovative technologies, such as desalination plants and water recycling systems, plays a crucial role in maximizing the availability of water in regions facing water scarcity.

2.7 Rainfall variability

Rainfall variability pertains to the extent in which amounts of rainfall differ over time and space. According to Kizza et al. (2009), Liebmann et al. (2014), and Nicholson (2015), amongst others variability comes in different forms and shapes. Several studies have shown that rainfall is characterised by significant trends that can easily be discerned from different time and spatial scales (Giorgi, 2002). In some cases, variability is due to physiographic attributes. These may include topography, vegetation cover, distance from the ocean, prevailing winds, and latitude amongst others (Agnew and Palutikof, 2000, Makarieva et al., 2013). The above influence the spatial variability of rainfall. Studies such as Cammarano et al. (2019), Kalisa et al. (2019) and Srivastava et al. (2020) amongst others have reported the variability of rainfall with respect to physiography of an area. Rainfall variability varies form one geographical location to the other. According to Nicholls et al. (1997) some areas may be more variable than others despite having similar climates. This is because the are other factors involved apart from the physiography of an area. This may include amongst others the impact of ENSO (Wooldridge et al., 2001). Having a comprehensive comprehension of climate variability and trends proves to be highly advantageous when it comes to strategic planning and the sustainable development of water resources (Mengistu et al., 2014). This includes the vital aspect of equitable distribution and collaboration among riparian nations.

Understanding of rainfall variability helps managers of water resources to deal with the effects of too much or less water in a catchment. Additionally, it helps to allocate water resources in an area. The other side of rainfall variability is the temporal aspect. This helps managers to allocate water resources with respect to when to abstract what volume and when not to. In recent times, studies focusing on variability of rainfall have increased in numbers to climate change and urbanisation leading to rapid land use change. According to Nicholson (2017), efforts to regionalize the precipitation patterns of eastern Africa have been undertaken in order to better understand its complex regime and facilitate prediction, agricultural planning, and analysis of interannual fluctuations. Most of the researches have employed principal component analysis (PCA), sometimes coupled with clustering techniques or linear correlation. These diverse studies exhibit considerable variations in relation to the geographical areas and seasons examined, the number of stations engaged in the examination, and the time assessed. The meridional displacements of the Inter-Tropical Convergence Zone (ITCZ) are the primary driving force behind the seasonal patterns of rainfall in tropical Africa (Dedekind et al., 2016). According to (Konapala et al., 2020) the presence of consistent and sufficient precipitation, evenly spread across each month of the year, is an indicator of a reliable and ample source of atmospheric water. Similarly, significant levels of precipitation that are unevenly distributed over the course of a month signify an excess of water resources during a certain time within a year, while also indicating a shortage of water resources during another time within that same year. Consequently, it is necessary to account for seasonal fluctuation in precipitation magnitude to avoid misrepresentation of water availability in an area.

However, it is important to note that several studies have shown the disadvantages of correlation coefficients in determining the relationship between individual stations (Habib et al., 2001). Haile (2010) indicated that there are limitations in terms of the number of stations involved in interstation correlation. Variability and trend analysis categories. According to (Asfaw et al., 2018) variability analysis comprises the application of various statistical measures, including the Coefficient of Variation (CV), percentage deviation from the mean (Anomalies), Precipitation Concentration Index (PCI), and moving average amongst others.

The categorization of rainfall variability can be established based on three levels: low, moderate, and high in accordance with a study by (Thangamani and Raviraj, 2016). However, prior to the above study, Hare (1983) classified variability using CV (%) values as follows: < 20% as less variable, 20- 30% as moderately variable, and > 30% as highly variable. The study used CV to characterise the annual spatial variability of rainfall. Table 2.2 shows the degree of variation and the corresponding percentage. Higher CV indicates higher variability of the rainfall (Teyso and Anjulo, 2016). It can be discerned from it that high variability of greater than 30 percent indicate high degree of discrete rainfall distribution and very vulnerable to drought (Carroll et al., 2009). The low values of CV indicate regular temporal rainfall distribution.

Table 2.2: The degree of variation and the corresponding percentage

Percentage of CV	Degree of variability
<20%	Low
20%<35%	Moderate
>35	High

Rainfall variability can also be assessed using the rainfall variability index developed by the Australian Meteorological Bureau (AMB). In this case, the rainfall variability index is defined as the difference between ninetieth percentile and the tenth percentile divided by the fiftieth percentile (AMB, 2010). Table 2.3 show the rainfall variability index classes. Temporal variability is a good indicator for characterising climate and showing evidence of climate change.

Table 2.3: The rainfall variability index classes

Class	Index
>1.5	Very high
1.25-1.5	High
1-1.25	Moderate to high
0.75-1	Moderate
0.5-0.75	Low to moderate
<0.5	Low

2.8 Integrating flood and drought studies

In most studies, floods and droughts are seldom investigated combined. Even though their effects are tied to the availability of water resources. Examining the effects of the two gives a comprehensive approach to water resource management they are two sides of the same coin and are intrinsically linked. Figure 2.8 depicts the magnitude-frequency relationship for rain events. Most hydrological risk research focuses on either flood risk or drought risk, even though floods and droughts are two extremes of the same hydrological cycle . When formulating metrics and approaches for the purpose of mitigating disaster risks, it is imperative to thoroughly evaluate the interdependencies that exist among these interconnected occurrences. Thus, a comprehensive analysis is necessary as this may provide an understanding of the effects of water resource availability. In most studies conducted within the field of environmental science, floods and droughts are seldom investigated in tandem, despite the significant and intricate relationship that exists between these two extreme weather phenomena. Researchers often focus on each disaster in isolation, overlooking the critical insights that could be gained from examining their combined effects. This oversight is particularly concerning given that the impacts of both floods and droughts are intricately tied to the availability of water resources, which play a crucial role in agriculture, ecosystem health, and overall human well-being. By neglecting to study these events together, we may miss vital opportunities to understand their interdependencies and to develop more effective strategies for managing water resources in an increasingly unpredictable climate.

In the majority of research, floods and droughts are infrequently analyzed in conjunction, even though their impacts are closely related to water resource availability. Investigating the effects of both phenomena provides a holistic perspective on water resource management, as they represent two facets of the same issue and are fundamentally interconnected. The magnitude-frequency relationship for rainfall events is illustrated in Figure 2.8. Most hydrological risk studies tend to concentrate on either flood risk or drought risk, despite the fact that floods and droughts are extreme manifestations of the same hydrological cycle (Ward et al., 2020). When developing metrics and strategies aimed at mitigating disaster risks, it is essential to conduct a thorough examination of the interdependencies inherent in these related occurrences. Therefore, a comprehensive analysis is warranted, as it may yield insights into the implications of water resource availability.

In environmental science research, it is rare for floods and droughts to be studied simultaneously, despite the complex and significant relationship between these two extreme weather events. Researchers typically investigate each disaster independently, thereby overlooking critical insights that could emerge from analyzing their combined impacts (Tierney, 2007). This gap in research is particularly troubling given that the consequences of both floods and droughts are intricately linked to water resource availability. Failing to consider these events together risks missing important opportunities to comprehend their interdependencies and to devise more effective strategies for managing water resources in an increasingly erratic climate.

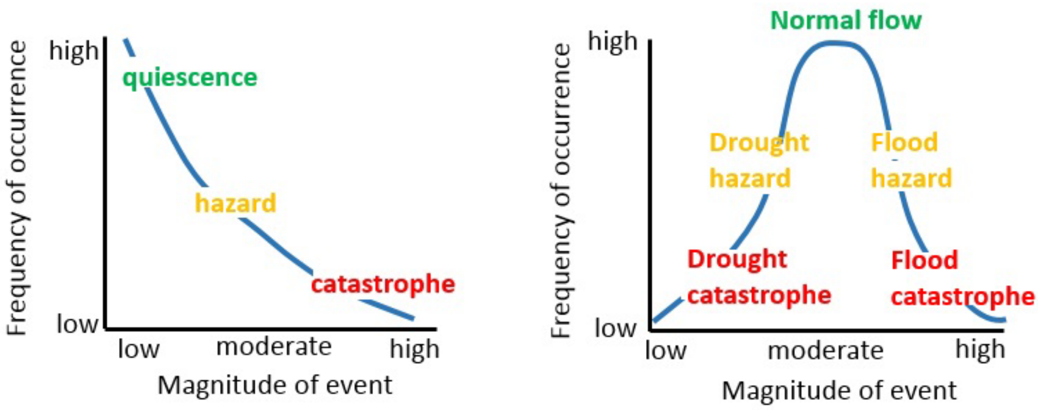

Figure 2.5: Relationship between the magnitude and frequency of rainfall-associated events

2.9 Impacts of climate change on water resources

The impact of climate change on water resources is a pressing concern that affects water resources. As global temperatures rise, the hydrological cycle is altered, leading to significant changes in precipitation patterns, evaporation rates, and water availability (Riedel and Weber, 2020). These shifts pose challenges to the availability of water resources. Thus, addressing these issues requires a concerted effort from governments, organisations, and communities to implement sustainable practices and develop adaptive strategies that ensure equitable access to water resources in an increasingly uncertain climate.

Climate change significantly influences precipitation patterns, increasing rainfall in some regions and prolonged droughts in others (Clarke et al., 2022). Climate change alters precipitation timing, intensity, and distribution (Trenberth, 2011). Some regions are experiencing more intense rainfall events, while others are facing droughts and reduced rainfall (Frame et al., 2020). Areas that have traditionally relied on consistent rainfall may experience erratic weather conditions, causing water shortages during critical growing seasons. Conversely, flood-prone regions may experience increased rainfall, overloading existing water management systems and causing damage to infrastructure. This contrast complicates the allocation of water resources, as regions can go from surplus to deficit in a short period of time. Additionally, rising temperatures contribute to increased evaporation rates, further reducing available freshwater supplies (Konapala et al., 2020). Lakes, rivers and reservoirs are particularly at risk, as higher temperatures can lead to falling water levels and changed drainage conditions. This not only impacts agricultural practices but also threatens aquatic ecosystems that rely on stable water conditions. In southern Africa, the effects of climate change on water resources have been reported in various studies such as Rouault and Richard (2005), Archer et al. (2018) and Konapala et al. (2020), amongst others.

There are several ways in which climate change impacts on water resources can be assessed. Shared Socioeconomic Pathways (SSP) and Representative Concentration Pathways (RCP) are both used in climate science to model and project future climate scenarios (Tang et al., 2023). However, they represent different aspects of future conditions and are used in different context. These pathways are critical for understanding the potential future impacts of climate change on water resources. Table 2.4 provides a summary of comparison between SSP and RCP.

Table 2.4: Summary of comparison between SSP and RCP

Aspect	SSP	RCP
Focus	Socioeconomic drivers (e.g., economic, technological, social)	Greenhouse gas concentration and radiative forcing
Number of Scenarios	5 (SSP1, SSP2, SSP3, SSP4, SSP5)	4 (RCP2.6, RCP4.5, RCP6.0, RCP8.5)
Use	Describes societal conditions that influence emissions	Represents potential future emissions and radiative forcing
Timeframe	Generally, through the 21st century and beyond	Primarily through 2100
Relation	Used with RCPs to create complete climate scenarios	Used to model climate impacts based on different emissions pathways

There are four primary RCPs, each representing different levels of global warming and carbon dioxide concentrations (Table 2.5). These pathways provide crucial scenarios that help scientists and policymakers understand the potential climate impacts associated with different greenhouse gas emission trajectories. Each RCP is characterised by its unique set of assumptions about socio-economic development, technological advancements, and land-use changes, illustrating the complex interplay between human activities and the environment as the planet responds to increasing levels of carbon emissions.

The RCP8.5 scenario, often regarded as the most extreme in its projections of fossil fuel consumption, has been carefully crafted to illustrate a range of possible futures (Schwalm et al., 2020). It suggests a persistent reliance on fossil fuels, leading to a scenario where greenhouse gas emissions soar unchecked, causing significant climate shifts and dire environmental impacts (Upreti, 2023). This scenario is essential for both researchers and policymakers, offering valuable perspectives on the possible consequences from existing energy habits and underscoring the critical necessity for sustainable solutions to address the imminent dangers of climate change (Khorram-Manesh et al., 2024).

Table 2.5: Climate change impacts on water resources based on RCPs

Impact	RCP 2.6	RCP 4.5	RCP 6.0	RCP 8.5
Water Availability	Minor to moderate change, some regions may face scarcity	Moderate reductions in availability	Significant reductions in availability, some regions face chronic shortages	Severe reductions in availability, widespread water stress
Flooding	Slight increase in frequency	Increased frequency in some areas	Increased frequency in many regions	Severe flooding in many regions
Droughts	Slight increase, mainly in dry regions	More frequent droughts, affecting agriculture	Increased droughts in many areas, especially arid regions	Widespread, severe droughts, particularly in semi-arid regions
Saltwater Intrusion	Limited to coastal areas	Increased risk in coastal zones	Major threat to coastal aquifers	Severe impact on coastal aquifers, rendering many sources unusable
Water Quality	Moderate changes	Water quality risks increase	Significant degradation in water quality	Severe water quality degradation, including high pollution and algal blooms

2.10 Summary

The chapter discusses historical trends in aridity, focusing on its causes and effects on water resources in Southern Africa. It highlights the complexity of semi-arid regions and the lack of hydrological data, reviewing key hydrological processes, droughts, and floods in these areas. The chapter explored spatial-temporal aridity indices, their significance in assessing aridity, and differentiates between drought (temporary) and aridity (permanent climatic feature) in arid environments.

The determination of aridity began in the early 20th century with methods like the precipitation-to-temperature ratio proposed by De Martonne (1926) and evolved to include more complex methods such as reference evapotranspiration (ETo) developed by Thornthwaite (1948). Despite various approaches, a standardised method was lacking, leading to more refined indices, including those developed by Penman and Monteith that factor in crop evapotranspiration. Aridity indices, like the UNEP Arid Index (UAI), assess water availability by comparing precipitation and potential evapotranspiration, providing insights into water resources, drought risk, and climate variability essential for effective water management. The UAI is highly regarded in research and policymaking for its reliability in water resource assessments.

Water resources in arid environments face significant challenges due to an increasing population, droughts, and climate change. Global warming contributes to unpredictable weather patterns, leading to both droughts and floods, particularly affecting arid and semi-arid regions. The Limpopo Province is specifically dealing with issues like deforestation and changes in species composition, adding to the environmental pressures. Innovative strategies in water management are urgently needed to address these challenges and prevent conflicts over dwindling resources.

Drought is a complex phenomenon characterised by a prolonged lack of moisture, affecting various regions differently. It is primarily caused by insufficient rainfall and can impact water resources, ecosystems, and human activities, particularly in arid and semi-arid areas. Droughts can be classified into four main types: meteorological, agricultural, hydrological, and socio-economic, each highlighting different aspects of water scarcity. The water sector is especially vulnerable to drought, as it affects water availability, exacerbated by higher atmospheric temperatures. The duration and severity of droughts have been increasing, but their underlying causes are not fully understood.

Water scarcity is an increasing global concern defined as a situation where water demand exceeds natural availability. It highlights the gap between water supply and community needs, impacting food security, poverty, and economic opportunities. Key factors contributing to water scarcity include population growth, urbanisation, and climate change, particularly in developing countries. Addressing these challenges involves building infrastructure like reservoirs and implementing technologies like desalination and water recycling to enhance water availability.

It further explores various spatial-temporal aridity indices, emphasising their vital significance in accurately assessing levels of aridity (Maliva et al., 2012). The text draws a clear distinction between the concepts of drought and aridity, considered a permanent climatic feature of arid environments, enhancing the reader's understanding of these critical distinctions. The impacts of climate change on water resources were also highlighted including the different ways in which they are assessed.

Despite introducing various approaches to measure aridity, the chapter notes that a standardised method has been elusive, leading to the development of increasingly refined indices aimed at providing clearer insights into the dynamics of aridity and its implications for environmental sustainability and resource management in the region. A good example is that of SPI being refined to SPEI to address temperature in the main that affects water demand in the environment (Hernandez and Uddameri, 2014). In addition, the impacts of climate change are reflected easily in the SPEI. In addition, the SDI was also considered since it included. The comprehensive flood analysis, which focused on both the magnitude and frequency of various flood events, was also considered in the broader context of environmental factors. Finally, the study reviewed how floods, often perceived as sudden disasters, can be linked to previous prolonged drought, creating a complex interplay between drought and subsequent floods. It examined how, by analysing historical data and meteorological patterns, researchers sought to uncover the underlying relationships that contribute to the occurrence of floods and develop a nuanced understanding of how climatic extremes can lead to such devastating water events.

CHAPTER THREE: METHODS AND MATERIALS

3.1 Preamble

Statistical techniques and computer software tools were used to analyze various data sets collected from various agencies in the study area. Initially, exploratory data analysis (EDA) was introduced to identify changes in time series - whether meteorological or hydrological. In addition, drought and flood evaluations were performed to determine hydrological extremes. Finally, spatial maps of the study area's aridity on different time scales were constructed to assess its impact on hydrology.

3.2 Data required and selection

The study used a combination of primary and secondary data, specifically focusing on instrumental records of hydrometeorological variables such as rainfall, temperature and streamflow. Selection of data was based on factors such as quality, length of record, percentage of missing data (gaps), and frequency of data. Majority of the stations considered in the study are not normally distributed except for Levubu and Matiwa. The study made use of the conceptual model shown in Figure 3.1.

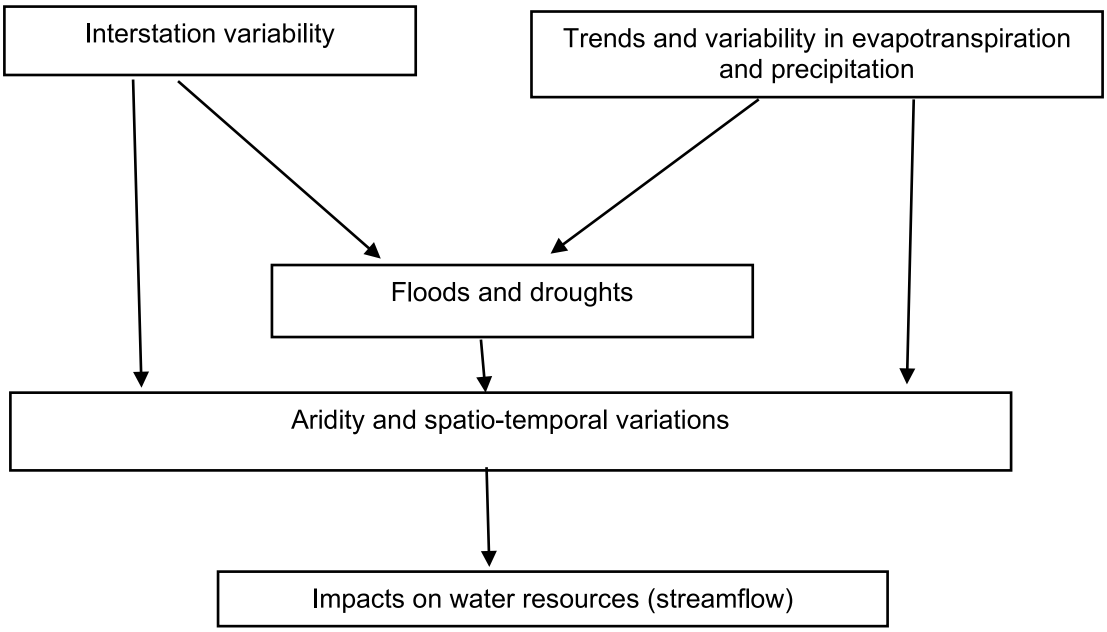

Figure 3.1: Conceptual framework

Hydrometeorological data

Climate data including temperature and rainfall data at different temporal scales were obtained from the South African Weather Service (SAWS) (Appendices 1A and 1B). These are stations that have long data sets within the catchment and represent almost all the topography of the catchment (i.e., high and low elevations). Of all the stations, Tshivhase and Thohoyandou had rainfall data which was used in the study with least records. Table 3.1 shows a list of stations used in the study including their location, length of records as well as the percentage of missing data in the records. Figure 3.2 shows the location of the stations used in the study. In cases where data were missing or there are gaps due to instruments malfunctioning and other reasons were spatially interpolated using Thiessen Polygon Method. Additionally, data from the (Lynch and Schulze, 2006) database was used, particularly for years prior to 2000. The data spans a period between 1960 and 2018 for most of the stations. However, some stations did not have the entire period but were included in the study since they satisfy the WMO (1976) requirement of at least 30 years long record. Hydrological data including streamflow at different timescales were obtained from the Department of Water and Sanitation (DWS) (Appendix 1C).

Table 3.1: Meteorological stations used in the study

Station name	Station number	Latitude	Longitude	Altitude (m)	Start year	End year	Percentage of missing data (<10%)
0812567	PAFURI	-22.42	31.22	210	1960	2018	Yes
0768011	PUNDA MARIA	-22.68	31.02	509	1960	2018	Yes
0766509	MATIWA	-22.98	30.28	1311	1960	2018	Yes
0723334	NOOITGEDACHT	-23.07	30.20	762	1960	2018	Yes
0723363	KLEIN AUSTRALIE	-23.05	30.22	702	1960	2018	Yes
0723513	TSHAKHUMA	-23.05	30.30	1158	1960	2018	Yes
0723363	LEVUBU	-23.09	30.29	610	1966	2016	Yes
0723155	GOEDEHOOP	-23.07	30.13	811	1960	2018	Yes
0722721	HANGLIP	-23.02	29.92	1036	1960	2018	Yes
0723603	TSIANDA	-23.05	30.35	671	1960	2018	Yes
0722614	ZWARTRANDJES	-23.23	29.86	1036	1960	2018	Yes
0723070	ELIM - HOSP	-23.15	30.06	808	1960	2018	Yes
0763603	THOHOYANDOU	-22.97	30.50	605	1983	2018	Yes
0766563	THATHE	-22.88	30.32	1250	1964	2014	Yes
0766480	ENTABENI BOS	-23.00	30.27	1376	1960	2018	Yes
0766779	PALMARYVILLE	-22.98	30.43	570	1960	2018	Yes
0766596	VONDO	-22.93	30.33	1130	1963	2016	Yes
0723182	SHAFEERA	-23.03	30.12	1214	1960	2018	Yes
0766827	RAMBUDA	-22.79	30.43	762	1960	2016	Yes
0723073	ROSSBACH	-23.21	30.05	1190	1974	2016	Yes
0766717	PHIPHIDI	-22.96	30.38	900	1986	2016	Yes
0766030	ROODEWAL	-23.01	30.03	440	1966	2016	Yes
0723664	THOHOYANDOU	-23.08	30.38	614	1985	2018	Yes

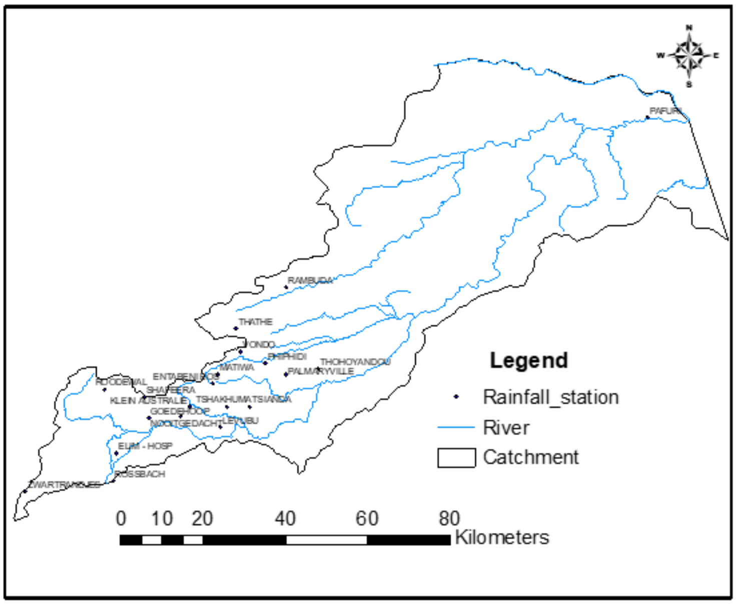

Figure 3.2: Location of hydrometeorological stations in LRC used for the study

3.3 Exploratory data analysis

In an effort to explore, comprehend and present data, Exploratory Data Analysis (EDA) graphs were employed. This served as the initial basis for presumptions made whilst reviewing the data. It is capable of transforming the questions raised and revealing crucial details which would have otherwise remained elusive. Visual examination facilitates the identification of statistical characteristics such as independence, distribution, assumptions, and contributes to the comprehension, elucidation, and presentation of analysis outcomes. As an example, it determined whether the dataset being considered is composed of discrete or continuous data. Additionally, EDA proved instrumental in exposing voids within the record and provided information regarding the duration and frequency of these gaps. Statistical analysis was used to check whether the pattern identified through the EDA approach is significant or not (Kundzewicz and Kaczmarek, 2000; Kundzewicz and Robson, 2004).

Data quality was performed using a range of methods including the reliability, normality and distribution test. This is in line with the best practice before one can perform any meaningful analysis. The extent to which data quality analysis was performed was limited to the quality and quality of data (Hunziker et al., 2017).

Quality control

Quality control for rainfall, streamflow, and temperature was performed. In cases where there were missing records, simple methods of infilling were used. This included an average between two observations. Appendix 2 shows the summarised normality plots for all the rainfall stations used in the study.

3.4 Data analysis

3.4.1 Trends detection and variations

The datasets' variations were derived from various statistical parameters, such as the mean, standard deviation, variance, and coefficient of variation for temperature, rainfall, evaporation, and streamflow. These were applied to all stations that fulfilled the requirements specified in subsection 3.2. Hydrological years were used to establish both seasonal and annual variations. The study tested numerous variables, including annual total rainfall and streamflow, monthly averages, annual total evaporation, and daily maximum and minimum temperatures. These were used to identify quinquennial and decadal variations within long-term datasets. Periods of five and ten years were employed to split the data for the latter. The outcomes were employed in assessing both spatial and temporal variations. The use of the quinquennial and decadal scale enabled the determination of the timing of the annual cycles.

Using equation 3.1, the arithmetic average of dataset was computed, taking into account each individual value's contribution to the final result.

$$\bar{x} = \frac{1}{n}\sum_{i=1}^{n} x_i \quad \text{...} \quad (3.1)$$

To calculate the variance of a data set, equation 3.2 was used. This involves finding the arithmetic average of the squared differences between each value in the set and the mean. This formula is a key tool in statistics, enabling researchers and analysts to assess the degree of variability within a given set of data. By understanding the variance of a data set, the distribution and patterns of the data can be identified.

$$S^2 = \frac{\sum_{i=1}^{n}(x-\bar{x})^2}{n-1} S^2 = \sum_{i=1}^{n}(x-\bar{x})^2 \quad \text{..} \quad (3.2)$$

Where:

- S = standard deviation
- N = number of individuals
- $(\sum \bar{x})^2$ = is the sum of squared mean

The standard deviation was computed using Equation 3.3. This measure considered the differences between each data point and the mean, giving us an idea of how spread out the data is. The larger the standard deviation, the larger the spread of data, indicating greater variability between individual data points.

$$s = \sqrt{\frac{n\sum \bar{x}^2 - (\sum x_i)^2}{n(n-1)}} \quad \text{.. (3.3)}$$

Where:

- S = standard deviation
- N = number of individuals
- $(\sum \bar{x})^2$ = is the sum of squared mean

$$\text{CV} = \frac{s}{\bar{x}} \quad \text{..(3.4)}$$

Where:

- $\bar{x}$ = sample mean
- Z = normalized standardised departure
- x_i = raw value
- σ = sample standard deviation

The Mann-Kendall (MK) test is widely recognized as the most commonly used method in natural time series data analysis, especially in hydrological time series data to detect trends (Odiyo et al., 2015). This statistical test is a non-parametric method that measures the correlation between data points over time, allowing for the identification of any significant upward or downward trends. With its robustness and ease of use, the Mann-Kendall test has become an essential tool for researchers and analysts in various fields, including environmental science, climate change studies, and finance. In this study, MK test was used for trend detection for rainfall, temperature and streamflow data used in the study.

$$S = \sum_{k=1}^{n-1} \sum_{j=k+1}^{n} \operatorname{sgn}(x_j - x_k) \quad \text{...................................... (3.5)}$$

$$\operatorname{sgn}(x_j - x_k) = \begin{cases} +1 if (x_j - x_k) > 0 \\ 0 if (x_j - x_k) = 0 \\ -1 if (x_j - x_k) < 0 \end{cases} \quad \text{.......................................(3.6)}$$

The value of zero mean and variance of S can be calculated by

$$\text{Var}\,(S) = \frac{[n(n-1)(2n+5) - \sum_t t(t-1)(2t+5)]}{18}$$ ……………………..…(3.7)

When dealing with cases where the value of n is greater than 10, it is necessary to compute the standard normal variate z by using equation 3.8 (Ashraf et al., 2021). This equation considered a range of factors, including the sample size, mean, and standard deviation, and uses mathematical principles to arrive at an accurate result. By utilizing this equation, researchers can gain a deeper understanding of complex statistical concepts and make informed decisions based on their findings.

$$Z=\begin{Bmatrix} \frac{s-1}{\sqrt{var(s)}} if s > 0 \\ 0 if s = 0 \\ \frac{s-1}{\sqrt{var(s)}} if s < 0 \end{Bmatrix}$$ …………………………..………(3.8)

3.4.2 Interstation correlation

The full matrix of interstation correlation of annual precipitation was entered in a cluster analysis that identifies a tree of linkages between stations. Linkages between stations and/or groups is defined by the average linkage method (Wolter, 1987), which maximises correlation between individuals or derived groups, by using the average correlation of each group. Statistically significant correlations (0.05 level) are recorded and mapped as correlation fields. To establish the characteristic within a geographical region, the individual fields of constituent stations are combined by placing each at the origin of the correlation field and superimposing its significance values of correlation at the appropriate locations relative to this origin (Berndtsson, 1988). The resulting field is indicative of the regional strength and structure of associations between annual precipitation, through the number and orientation of significant pairings.

Bivariate normal distribution

The bivariate normal distribution was employed to examine the relationship between two variables. The main objective was to identify patterns and trends that could inform predictions of hydrometeorological events. In this study, Pearson's correlation was used to measure the strength and direction of these relationships. This analysis was crucial for understanding how factors such as altitude influence rainfall distribution.

Canonical correlation analysis

Canonical correlation analysis (CCA) is one of the methods that can be used in comparing several variables. Within the fields of climatology and hydrology, the technique is employed to investigate the correlations that exist between two distinct sets of variables (Zhang et al., 2020a, Ahani et al., 2019, Forootan et al., 2019). It is important to note that the maximum number of years for which climate variables have been measured should statistically fall within canonical multivariate analysis (Ahani et al., 2019). Thus, certain assumptions were made on the data. The variables within each set, when combined with the first canonical coefficient, exhibit the strongest correlations with the variables in the other set. To identify the canonical variates with the highest correlations, correlation coefficients were computed and utilized for projecting x and y onto u and v. In this study, x represents the rainfall data vectors derived for LRC in equation 3.9, and y represents topographical data. XLSTAT's statistical analysis software was used for CCA.

$$\begin{aligned} R &= \frac{E[XY]}{sqrt(E[X^2]E[Y^2])} \\ &= \frac{E[u^T xy^T v]}{sqrt(E[u^T xx^T u]E[v^T yy^T v])} \\ &= \frac{u^T C_{xy} v}{sqrt(u^T C_{xx} uv^T C_{yy} v])}, \end{aligned} \quad \text{………………………………..(3.9)}$$

Where:

C_{xx} and C_{yy} are covariance matrices of *x* and *y*, respectively and the objective in above function is to maximize the correlation *R*

Hierarchical clustering

Hierarchical clustering (HC) is a statistical technique that is essential in canonical analysis. It systematically organises and classifies data points or variables based on their interrelationships within a dataset. This method produces a dendrogram, which is a tree-like diagram that effectively shows the degrees of similarity or dissimilarity among the data points. In this study, HC was particularly used for visualising and understanding the complex relationships revealed through canonical correlation analysis. This enables discovery of patterns and connections that might otherwise go unnoticed.

3.4.3 Analysis of Variance (ANOVA)

The ANOVA was performed to evaluate the source of variability in the dataset and to conduct significance tests. This procedure was first developed by Fisher (1918). Since the method was developed it has been widely used in many fields of science.

The analysis of variance result demonstrates that there is a significant difference between the mean rainfalls throughout the LRC, as the observed p-value is less than 0.05. This suggests that at least one of the rainfall stations evaluated differs significantly from the rest. Again, there is a substantial difference in mean rainfall across years, suggesting that at least one year's mean rainfall is significantly different from others.

3.4.4 Spatial interpolations

Geostatistical methods were applied to determine optimal weights for measurements at sampled locations for the estimation of values in locations not sampled such as Inverse Distance Weighting (IDW), Thiessen Polygon and Kriging, amongst others. Variogram modelling was used to characterise the spatial correlation in the station skew data as explained under interstation section (sub-section 3.5.2). The variogram model defines the linear weighting function used to krige the grid or lattice of skew estimates. Bossong (1999) have discussed in detail the variogram modelling and kriging procedure which were adopted in this study. Kriging is the most widely used method due to its computational ease and data availability in most applications (Gentile et al., 2013).

3.4.5 Drought analysis

Standardized Precipitation Index

The study area's drought magnitude and duration were assessed using the SPI to determine its spatial and temporal extent. The SPI has been widely used in drought analysis since it is not affected by geographical differences (Lana et al., 2001). The Standardized Precipitation Index (SPI) is based on precipitation probability at any time scale. In this study, the SPI was used to identify drought events since it is a reference index. The calculation of the SPI for a specific area depends on the historical data of precipitation over an extended period of time as shown in equation 2.6. The SPI classification values from McKee et al. (1993) were used to discern between wet and dry spells/events. In this study rainfall data for all the stations considered in this study was used. SPI has been widely adopted globally.

Standardized Evapotranspiration Index (SPEI)

The SPEI calculation process was carried out, as it integrates the original SPI calculation method. Instead of relying on monthly or weekly precipitation exclusively, the SPEI considers the variance between precipitation and PET on a monthly or weekly basis. The aforementioned statement pertains to the calculation of the Standardized Precipitation-Evapotranspiration Index (SPEI) through the utilization of Thornthwaite's climatic water balance methodology (Thornthwaite, 1948). This approach involved assessing the water balance at various temporal scales as shown in equation 2.7 and 2.8. The SPEI then considered the number of rainy days throughout the wet season, in order to estimate both the probability and frequency of dry spells. The SPEI was used in this study to show the effects of increasing temperature on droughts.

Streamflow Drought Index

The Standardized Drought Index (SDI) method was used to thoroughly assess the severity and impact of drought conditions in different regions, considering numerous environmental factors. This comprehensive method was specifically designed to assess and analyse the hydrological drought conditions prevailing in the study area and provides valuable insights not only into the severity and duration of these droughts but also their impacts on water resources, agriculture and ecosystems. Equation 2.9 was used to compute SDI for the study area.

3.4.6 Flood frequency analysis

Two methods were used to determine flood magnitudes and return periods. This was done for both rainfall and streamflow stations used in the study. For streamflow, three stations were used representing upstream, midstream and downstream of the LRC. Selection of the methods used in the study was given to those that are widely applicable in South Africa. Two methods were used to determine flood frequency and magnitude. This was done to minimize over and underestimation of flood magnitudes. The forms mentioned above are comprised of Gumbel's Extreme Value (EV1) and the Log Pearson Type three (LP3). The analysis of flood frequency and magnitude followed the guidelines developed by the USGS (England Jr et al., 2019). A threshold analysis was conducted for both floods.

Log Pearson Type three

The frequency of flood was determined by utilizing LP3 distribution along with parameter estimates that were derived through the moments obtained from the logarithms of the data. This method is reported to be most successful in the study and in South Africa (Alexandra et al, 2001). Thus, LP3 is recommended generally for flood frequency estimation (Singo et al., 2012). The descending order of the rainfall/streamflow data was employed in various statistical approaches and plotting positions to estimate the return period. Through the use of the rainfall/streamflow-return period equation derived from the graphs produced for various plot position methods, an assessment was conducted to compute the rainfall/streamflow magnitudes corresponding to distinct return periods.

$$G = \left[\frac{n^2\left(\sum x^3\right) - 3n\left(\sum x^2\right)\left(\sum x\right) + 2\left(\sum x\right)^3}{n(n-1)(n-2)\sigma_x^{\ 3}} \right] \quad \text{.................................... (3.10)}$$

Where:

G = skewness coefficient, σ_x, X_{av}, $\sum x$ and n are as defined above

The estimated discharge values for a given period can be evaluated using the logarithm of the design flood given by the following formula:

$$X_T = \log Q_T = X_{av} + K\sigma_x \quad \text{..} (3.11)$$

$$X_T = \log Q_T = X_{av} + K\sigma_x \quad \text{..} (3.12)$$

Where: Q_T = the outflow for the estimated T-year return period, K = the probability factor based on an n-year return interval, which can be determined using a frequency factor table (Appendix 3) for gamma and LP3 distributions (Haan, 1977), X_{av} = the mean of the logarithms of annual peak flows at the streamflow gauging station and X_T, $\sigma_x =$ the standard deviation from the mean of the logarithms of annual peak flows.

The calculation of the design flood involves the use of a equation 3.13, as provided below, that takes into account various factors and variables to determine the magnitude and characteristics of the flood event.

$$X_T = \text{antilog}Q_T = 10Q_T \quad \text{..} (3.13)$$

Gumbel Extreme Value

The utilization of GEV distribution parameter estimation was found to be possible. Although the method of parameter estimation via probability-weighted moments (PWM) may not be as efficient as maximum likelihood (ML), it is almost impartial, user-friendly, and usually not affected by outliers.

$$P(X \geq x_0) = 1 - e^{-e^{-y}} \quad \text{..} (3.14)$$

Where: P = the probability of occurrence, X = the event of the hydrologic series, x_0 = the desired value of the event and y = the reduced variate: $y = \sigma(x - a)$

Where: x = the variate value, $a = \bar{x} - 6_x$ and σ =standard deviation of variate X and $\bar{x}$ =mean of the variate X

The reduced variate is calculated as:

$$y = \frac{1.2825\left(x - \bar{x}\right)}{\sigma_x} + 0.577 \quad \text{.......................................} \quad (3.15)$$

The constants for reduced mean and variate, namely 1.2825 and 0.577, respectively, are utilized in calculating the estimated peak discharges for each return period in Gumbel's distribution according to the subsequent equation. The calculation of the Gumbel distribution's frequency factor (k) is accomplished by using equation 3.16:

$$K = \frac{Y_T - \bar{Y}n}{\sigma_n} \quad \text{..} \quad (3.16)$$

Where: K = the frequency factor, Y_T = the value of peak discharge for a given recurrence interval, Y_n = Gumbel's reduced mean and σ_n = Gumbel's reduced standard deviation.

$$Y_T = -\ln\left[\ln\left(\frac{T_r}{T_r - 1}\right)\right] \quad \text{..} (3.17)$$

3.5.7 Determination of aridity index and impacts on water resources

Aridity Index calculations were performed by using UNEP (1992) method based on the equation 3.18:

$$UAI = \frac{P}{PET} \quad \text{..} \quad (3.18)$$

Where:

- UAI is the UNEP aridity index;
- P is precipitation and
- PET is potential evapotranspiration

Combined graph of aridity indices was drawn for each station. Decadal averages and trend lines were built on each station's graph to show the trend in aridity with time over the study area (Sawa et al., 2015). The UAI's aridity indices used were annual relationship precipitation and potential evapotranspiration to classify aridity.

Spatial analysis to give descriptions of spatial distributions of rainfall conditions, land water balance and aridity index in the research area was performed using ArcGIS 10.8 software. Each of the parameters above was used to generate thematic maps from annual totals. The generated thematic maps were overlaid upon each other to identify aridity levels for the study area, areas that are severely affected by aridity.

The study used gridded rainfall and the minimum and maximum temperature time series data for arid index calculations. Gridded data was used due to limitations in the number of rainfall and temperature stations in the LRC. Future aridity indices were computed for the purpose of determining their potential impacts on water resources. A gridded climate dataset with a spatial resolution of 10 km × 10 km was used. National Centre for Environmental Prediction (NCEP) reanalysis downscaling was used in dealing with the computations of historical and future aridity indices. The projections were generated using RCP8.5 from the Max Planck Institute (MPI). For this purpose, projected data between 2021 and 2070 was used. Rainfall and temperature data (maximum and minimum) were obtained from the Council for Scientific and Industrial Research (CSIR). The model used for this reanalysis was the conformal-cubic atmospheric model (CCAM) which is a variable-resolution global atmospheric model. The details of the methodology followed can be obtained in Archer et al. (2018). Figure 3.3 shows the location of virtual stations used in the study. The data was collected through a comprehensive study that analysed range of factors, such as average temperature, rainfall, and evapotranspiration rates, to determine the aridity indices. UNEP AI was used to calculate aridity value trends, annual rainfall total and then test these using the Mann-Kendall rank correlation coefficient test. The critical significance level of the test was at least 0.05. The impact of aridity on water resources was inferred based on the correlation between the sensitivity of streamflow and aridity using the streamflow drought index (SDI).

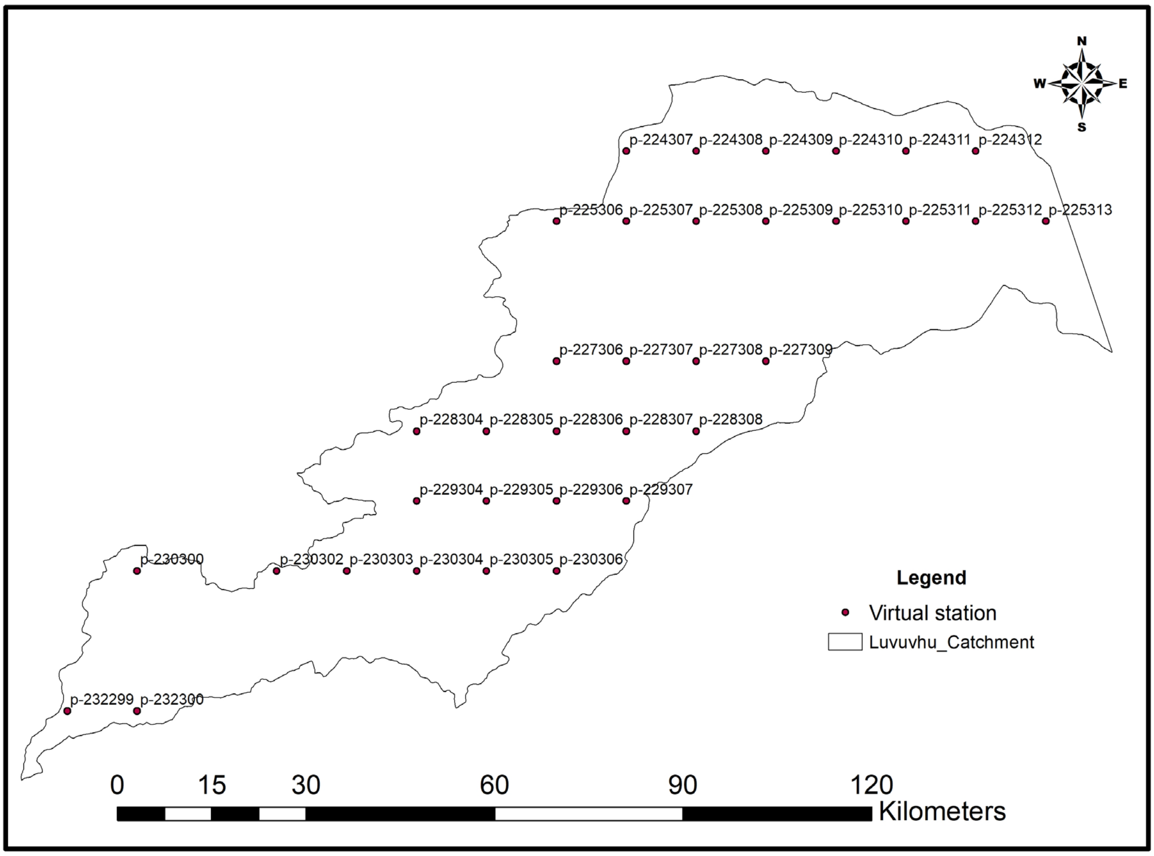

Figure 3.3: Location of virtual meteorological stations in LRC used for the study of aridity

CHAPTER FOUR: HYDROMETEOROLOGICAL VARIABILITY AND TRENDS

4.1 Preamble

In this chapter, findings pertaining to variations and trends in rainfall, temperature, and streamflow in the LRC are presented and deliberated with respect to changes over time and space. For temporal variation, different window periods are considered ranging from seasonal, annual, quinquennial and decadal. While for spatial variation, the distance between stations and the location of the stations with respect to the topography is investigated.

4.2 Temporal variability and trends

Several temporal scales are analysed and discussed. This ranged from annual, seasonal, quinquennial and decadal. The above was done for all the stations used in the study. The analysis of trends enables the identification of areas that are encountering notable rises or declines in rainfall patterns. This knowledge proves to be of great assistance in estimating the potential hazards posed by climate change and variability, thereby enabling prioritization of resources towards the most vulnerable regions. According to the study by Muthoni et al. (2019a), the comprehension of climate trends from the past can assist in predicting future developments and in turn, aid in the decision-making process towards deploying adaptive measures to specific areas.

Annual variability

Table 4.1 presents the yearly average rainfall statistics for the research region. The average precipitation measured ranged from 439 to 1832 mm with a mean of 800 mm. Moreover, the table indicates that there is considerable diversity in rainfall patterns by displaying significant standard deviation values. The range of standard deviation values observed across stations is between 162 and 550 mm. Thirteen out of twenty-one stations used in the study had a CV of greater than 0.35. The other stations had CV values ranging between 0.25 and 0.34. This suggests that LRC has high rainfall variability. This was portrayed by both temporal and spatial scales used in the study. The stations which portrayed a high degree of variability are those with low rainfall amounts in the study area. This study is consistent with studies such as that by Illius and O'Connor (1999) and Cheung et al. (2008) who found higher variability of rainfall in areas with low rainfall amounts. Individual stations that showed a high degree of variability are those in the downstream part of the catchment. The upstream was associated with a low CV. The variation contrast can be logically explained by the geographical position of the stations, primarily induced by the Soutpansberg Mountain range that plays a significant role in influencing the distribution of rainfall within the area. The overall CV for rainfall for the stations used in the study area. Only Matiwa and Entabeni stations received more rainfall than other stations. The difference is probably related to the extremely low variability of rainfall as shown in this present study.

Table 4.1: Basic long-term rainfall statistics and trends

STATION_NA	Minimum	Maximum	Average	Standard deviation	CV
Pafuri	103	880	439	179.99	0.41
Rambuda	67	2200	840	336	0.40
Thathe	263	2916	1200	324	0.27
Vondo	402	3020	1278	549.54	0.43
Phiphidi	431	3144	1282	538.44	0.42
Thohoyandou	193	1490	769	253.77	0.33
Matiwa	520	4295	1832	512.96	0.28
Palmaryville	228	2276	867	294.78	0.34
Entabeni Bos	523	4009	1747	436.75	0.25
Roodewal	292	2242	831	357.33	0.43
Shafeera	166	3153	1378	496.08	0.36
Klein australie	403	3304	1101	484.44	0.44
Tshakhuma	226	1385	1117	346.27	0.31
Tsianda	173	2095	877	359.57	0.41
Nooitgedacht	438	2685	962	375.18	0.39
Goedehoop	146	2758	843	404.64	0.48
Levubu	256	2239	950	361.00	0.38
Elim - hosp	172	1925	675	263.25	0.39
Rossbach	421	1973	927	342.99	0.37
Zwartrandjes	223	1385	507	162.24	0.32

The changes observed in precipitation trends are closely linked to climate change. As per the reports of IPCC 2007, the global surface temperature has displayed a consistent increase of 0.74 ± 0.18°C between the years 1906-2005. These changing climatic conditions may lead to a decline in the availability of fresh water in the future. Studies have also shown that by mid-21st century, the available water and average annual runoff may decrease by 10-30% (Parry et al., 2007). The temporal shift in precipitation patterns, observed through time-series analysis, represents the change in trend of precipitation over time. This change in trend, which can lead to either an increase or decrease in precipitation, is a significant factor contributing to climate variability. The MK Test and Cumulative Summation test were used in Zambia to investigate the long-term rainfall trend by Kampata et al. (2008). The investigation conducted by Xu et al. (2010) focused on the analysis of precipitation and runoff patterns in significant rivers across China. The researchers employed the Mann-Kendall statistical method as a means of detecting any existing trends in the data.

All the observations are consistent with the regional climate of the study area including Gbetibouo (2009), Dube et al. (2016) and Wright et al. (2021). High variation of spatial distribution of rainfall in the LRC is indicative of topographical and meteorological factors playing their roles. The two factors make the western part of the catchment receive high rainfall more resilient to high variation. In contrast, the eastern part is characterised by relatively low rainfall amount with high variability. Makungo and Mashinye (2022) explained trends in rainfall in the LRC is mostly not statistically significance, but substantive. They identified altitude and vegetation as some of the factors influencing rainfall behaviour in the LRC.

Most of the stations had negative Sen slope i.e., twelve out of twenty-one (Table 4.2). This indicates that there is a decline in annual rainfall which is not significant at a 95% confidence interval. This may have implications for floods and droughts. This suggestion is congruent with that made by Joshi et al. (2014) on the implications for extreme events. The study specifically focused on extreme precipitation in mountainous areas. The results show differences between minimum and maximum rainfall in the study area. The minimum ranged from 103 and 523 mm while the maximum ranged between 880 and 4295 mm (Table 4.1). This difference among the stations suggests that there is a high variability of rainfall in the study area.

The magnitude of the rainfall trends for the study period was calculated from Sen's slope estimator and presented in Table 4.2. The Sen's slope values ranged from -0.44 to 0.01 indicating that there is a shift in the behaviour of rainfall. Recent LRC climate change research anticipated that rainfall patterns in most locations have become extremely unreliable, uneven, and unpredictable (Odiyo et al., 2020). This finding is supported by Dourte et al. (2020), who indicated the effect of rainfall distribution on soil, hydrology, and plant health in general. This kind of climatic change makes it difficult for humans to survive in this environment. Thus, people must devise adequate solutions and plans for their personal safety, agricultural products, and livestock. Mann-Kendall test was used by Faiz et al. (2018) to determine rainfall trend analysis in China. The study revealed noteworthy variations in the monthly mean rainfall data, indicating a decline in some months and an uptick in others. Through analysis, the statistics displayed an upward slope trend in annual rainfall. Nonetheless, the results also showed a significant variation in rainfall patterns from year to year and season to season, suggesting the erratic nature of the country's overall rainfall patterns. The study by Muthoni et al. (2019b) analysed the spatial trends in rainfall in seven countries of the Eastern and Southern Africa (ESA). In the latter study, the occurrence of drought and flooding due to above-normal rainfall was detected through analysis of annual precipitation anomalies and their corresponding spatiotemporal distributions.

Table 4.2: Monthly rainfall trends and statistics

Station	No. of observations	Minimum	Maximum	Mean	Std. deviation	Kendall's tau	p-value	Sen's slope
Zwartrandjes	696	0.00	702.40	42.19	61.18	-0.01	0.72	0.00
Goodehoop	691	0.00	1388.00	70.12	104.85	-0.01	0.70	0.00
Hanglip	696	0.00	836.40	58.03	77.56	-0.02	0.63	0.00
Klein Australie	696	0.00	1483.50	91.80	128.90	0.01	0.73	0.01
Levubu	645	0.00	1153.00	72.33	102.66	-0.17	<0.00	-0.24
Entabeni	696	0.00	253.50	37.46	47.58	-0.07	0.193	0.00
Matiwa	696	0.00	1803.00	152.61	183.01	-0.10	0.01	-0.41
Mukumbani	306	0.00	1466.30	87.86	141.49	-0.17	0.01	-0.55
Pafuri	386	0.00	440.80	36.51	53.72	-0.018	0.68	0.00
Thate-bos	437	0.00	1159.20	96.14	138.75	-0.05	0.27	-0.08
Thohoyandou AWS	429	0.00	1016.20	62.92	93.64	-0.031	0.50	-0.04
Tshakhuma	579	0.00	1304.00	86.19	124.59	-0.09	**0.03**	-0.12
Elim	673	0.00	1173.50	55.54	82.89	-0.08	**0.03**	-0.05
Tsianda	696	0.00	799.50	71.66	100.00	-0.09	**0.02**	-0.08
Punda	696	0.00	515.10	43.23	66.68	-0.04	0.33	-0.01
Nooitgedacht	696	0.00	1364.10	80.13	110.77	-0.03	0.41	-0.04

Seasonal variability and trends of rainfall

Figure 4.1 presents a detailed analysis of the monthly rainfall patterns, indicating that the months of October, November, December, January, and February experience the highest average rainfall during the summer season, a period often characterized by fluctuating weather conditions. The standard deviation values for these months, show that they were comparatively lower than their corresponding mean values, suggesting a more consistent pattern of rainfall during this time. In contrast, the subsequent months exhibit larger standard deviation values relative to their mean rainfall, highlighting a greater variation in rainfall distribution over time and indicating that those months can be unpredictable. Additionally, the coefficient of variation and skewness are notably high in the month of August, reaching values of 1.02 and 2.5, respectively, which signifies a significant deviation from the average and a pronounced unevenness in the rainfall data. As a result of these findings, it is generally observed that the concentration of rainfall is significantly high during the summer months, particularly in the earlier part of the season, and this trend also notably decreases from west to east, revealing regional differences in rainfall distribution that are critical for understanding the availability of water resources in the LRC.

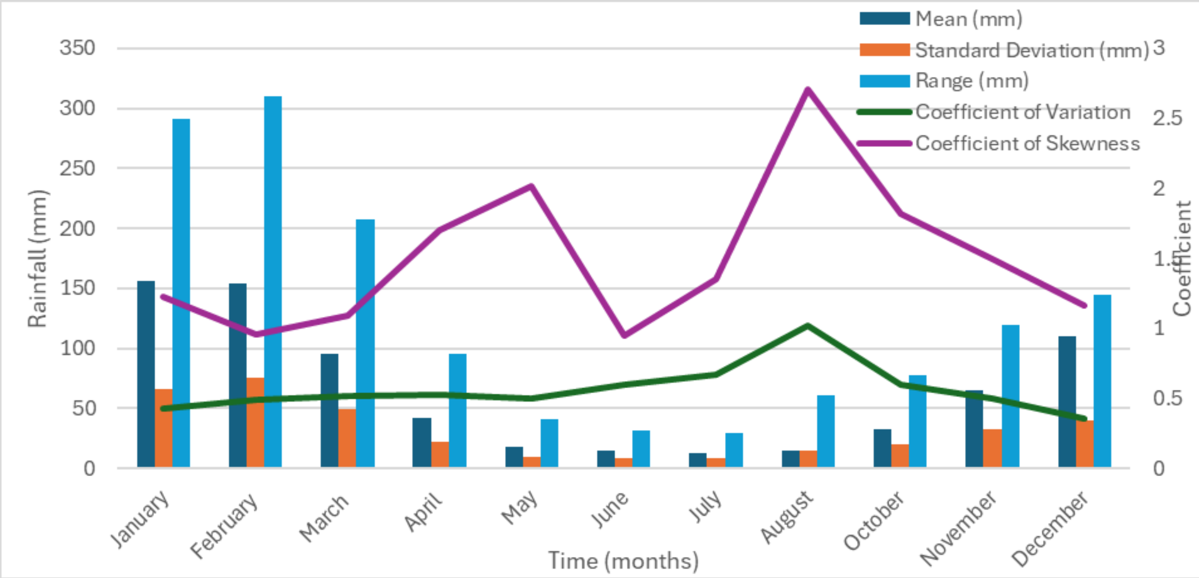

Figure 4.1: Statistical parameters for monthly rainfall analysis

Quinquennial (pentad) variability

The LRC experiences significant intraseasonal variability in rainfall. Only results from three stations representing upstream, mid-stream and downstream were presented. The other stations are presented Appendix 4. The rainfall standard deviation from pentad to pentad suggesting substantial variability. High average rainfall was recorded in pentads 4 and 9, which correspond to the years 1975-1979 and 2000-2004, respectively (Figures 4.2 to 4.4). This may be attributed to the high rainfall amounts received in the years 1977 and 2000. In the eastern region of southern Africa, tropical cyclones have been found to be associated with elevated levels of rainfall amounts (Chikoore et al., 2015). The El Nino-Southern Oscillation (ENSO) plays a significant role in causing fluctuations in climate patterns on an annual basis. Nicholson (2014), suggests that identified several drivers are responsible for spatial-temporal variability. However, Nicholson (2017) indicted that despite the strong relationship between ENSO and rainfall, overtime the relationship may weaken from region to region. These will affect water resources as well as managing water supplies. This may necessitate an awareness of climate variability in the LRC.

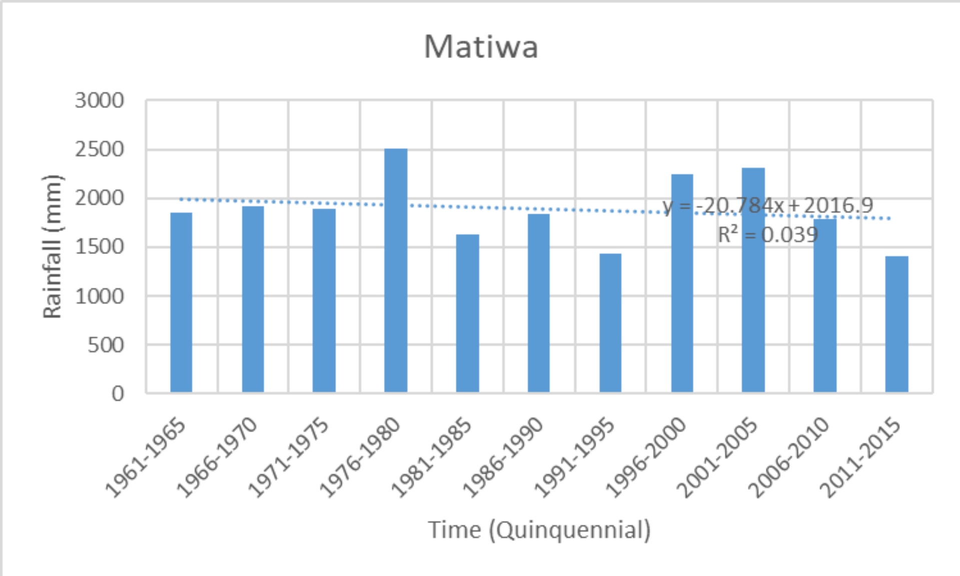

Figure 4.2: Quinquennial variability of rainfall for Matiwa

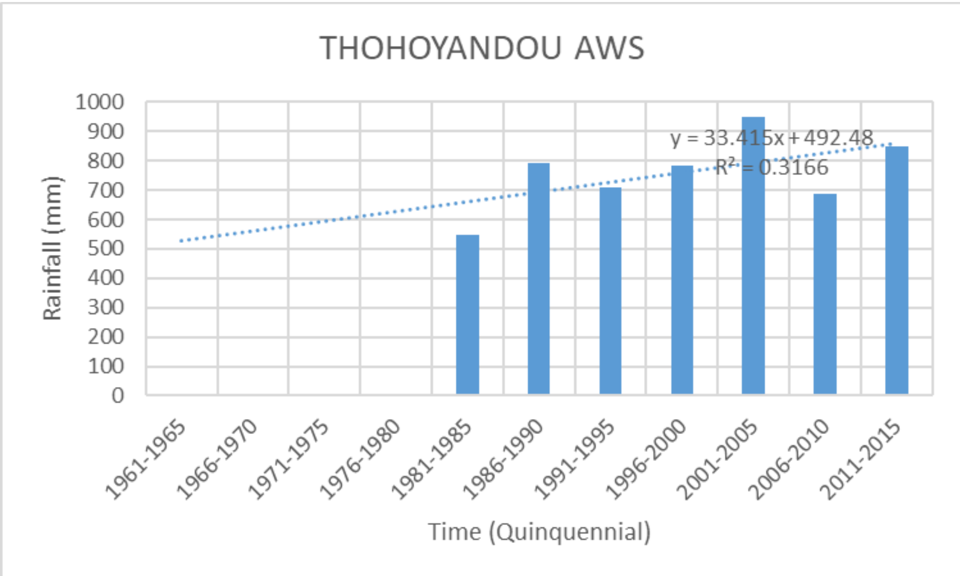

Figure 4.3: Quinquennial variability of rainfall for Thohoyandou

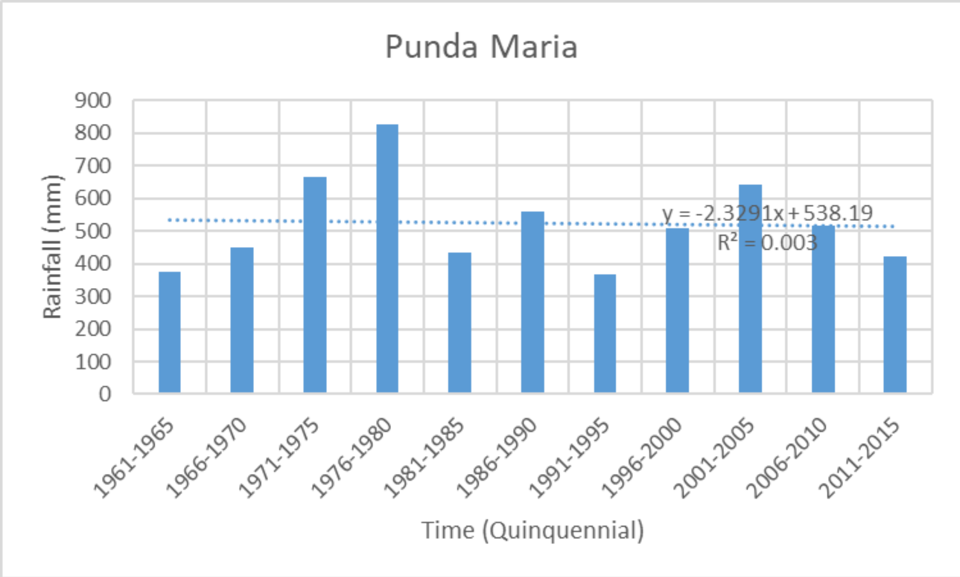

Figure 4.4: Quinquennial variability of rainfall for Punda Maria

Decadal variability

Figures 4.5 to 4.7 show the decadal variability of rainfall in the LRC. The other stations are presented Appendix 5. The results show that rainfall is highly variable on a decadal scale. It shows that there are some decades with high rainfall averages while some with low. All the stations used in the study show that their last decade considered in the study had the lowest average. The decadal variability of rainfall is considered less well defined (Malherbe et al., 2016). Thus, linking it to weather systems is necessary. The subject of rainfall variability in southern Africa has been researched without convincing conclusions. This may be because of the mechanisms and the forcing involved (Nicholson, 2017). This increased decadal variability may influence water resource availability. This finding is supported by Christensen and Christensen (2007) who found that increased variability may put pressure on the hydrology of southern Africa region in which the LRC is found.

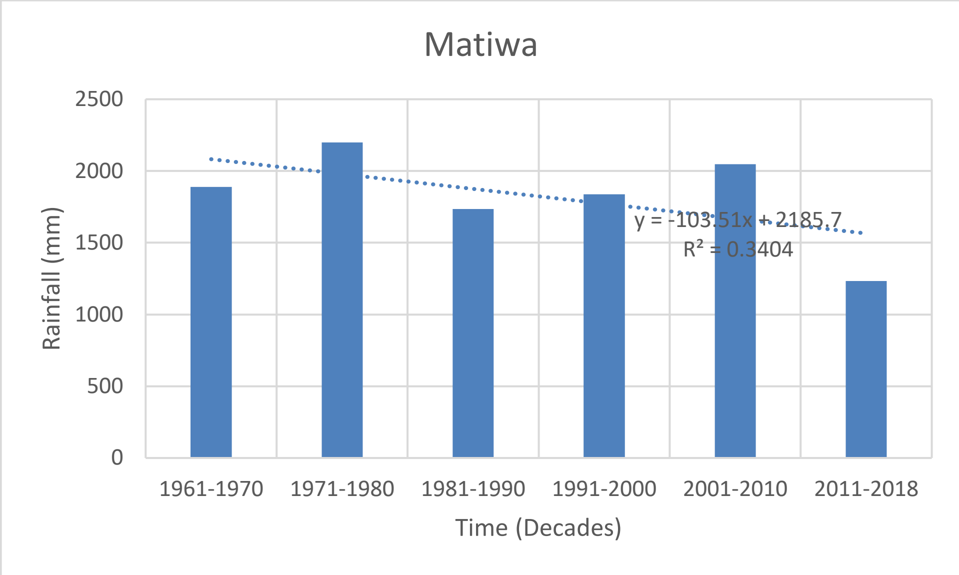

Figure 4.5: Decadal variability of rainfall for Matiwa

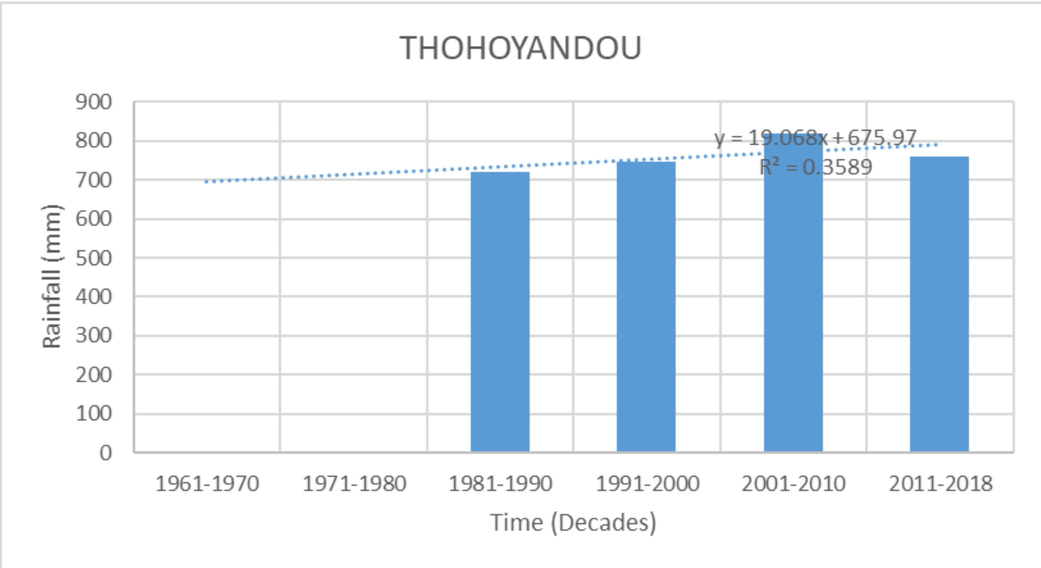

Figure 4.6: Decadal variability of rainfall for Thohoyandou

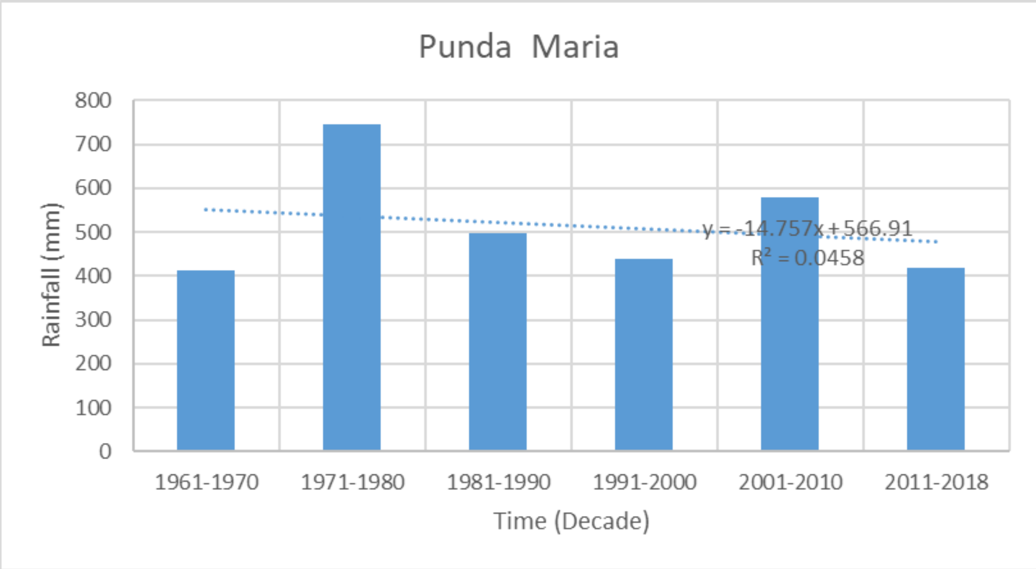

Figure 4.7: Decadal variability of rainfall for Punda Maria

4.3 Temperature trends and variability

Table 4.4 shows the minimum temperatures for three stations used in the study area. The minimum temperature in the period 1965-2018 was between 14.26 and 23.21 °C. The minimum temperature for Levubu and Thohoyandou increased by 1.5°C and 1.9°C, respectively. The increase is also observed in Tshivhase at 1.4°C for the period between 1990 and 2018. Higher maximum temperatures were recorded at Thohoyandou compared to the other stations used in the study. This could be related to the increase in residential areas for the growing town in contrast to Levubu and Tshivhase which are in predominantly densely vegetated areas. Densely vegetated areas can have relatively low temperatures. In addition, the altitude may also be a reason for the lower maximum temperatures in Levubu and Tshivhase. The results indicate that the temperature has shifted, which may result in higher evaporation rates. This could have a negative impact on the availability of water resources in the LRC.

Table 4.3: Temperature trends and variability

Variable	No. of observations	Minimum	Maximum	Mean	Std. deviation	Kendall's tau	p-value	Sen's slope
Min Tshivhase	29	14.23	16.83	15.11	0.52	0.207	<0.0001	0.016
Max Tshivhase	29	23.15	26.59	24.47	0.81	0.234	0.000	0.031
Min Thohoyandou	25	13.56	17.50	15.29	0.74	0.027	0.832	0.003
Max Thohoyandou	25	26.00	29.27	27.60	0.80	0.160	0.028	0.034
Min Levubu	54	14.175	16.34	15.09	0.41	0.205	0.018	0.007
Max Levubu	54	25.318	29.13	26.80	0.89	0.403	<0.0001	0.032

MK and linear regression both revealed an increase in temperature. These results are supported by findings from other studies, such as Banda et al. (2021), Ncongwane et al. (2021) and Kalumba et al. (2013) amongst others. The above studies revealed that temperature in most areas of South Africa is continually increasing warmer than in the past for both minimum and maximum values. The MK analysis showed statistical significance at an alpha level of 0.05, confirming that the temperature variations are significant. Studies by Tshiala et al. (2011) and Shikwambana et al. (2021) found that the Limpopo Province where the study area is located is experiencing increase in temperature since the early 1990’s. Figures 4.8 to 4.10 show a positive trend in temperature, but the linear regression trend for the period studied. It was also discovered that the temperature anomalies experienced between 1971 and 2003 were primarily negative in both minimum and maximum temperatures. It was also discovered that the minimum and maximum anomalies were much lower than the mean temperature between 1971 and 1986. However, the overall increase in temperature in the study area may suggest that rainfall may increase with time. This has been corroborated by a study carried out by Nkuna and Odiyo (2016) that showed there is a strong positive correlation between rainfall and temperature within the study area. The rainfall trends, however, displayed a declining as explained in sub-section 4.2.

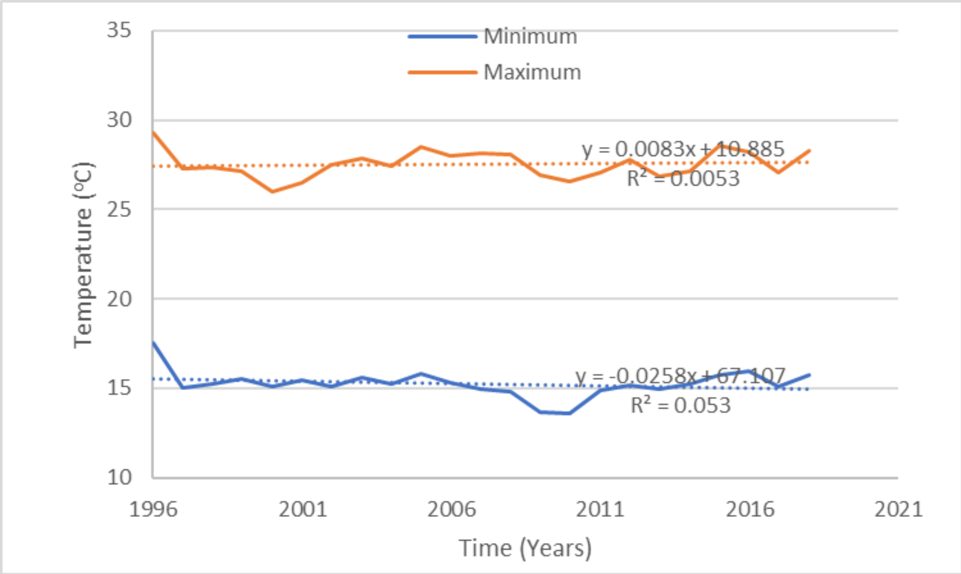

Figure 4.8: Temperature trends for Thohoyandou

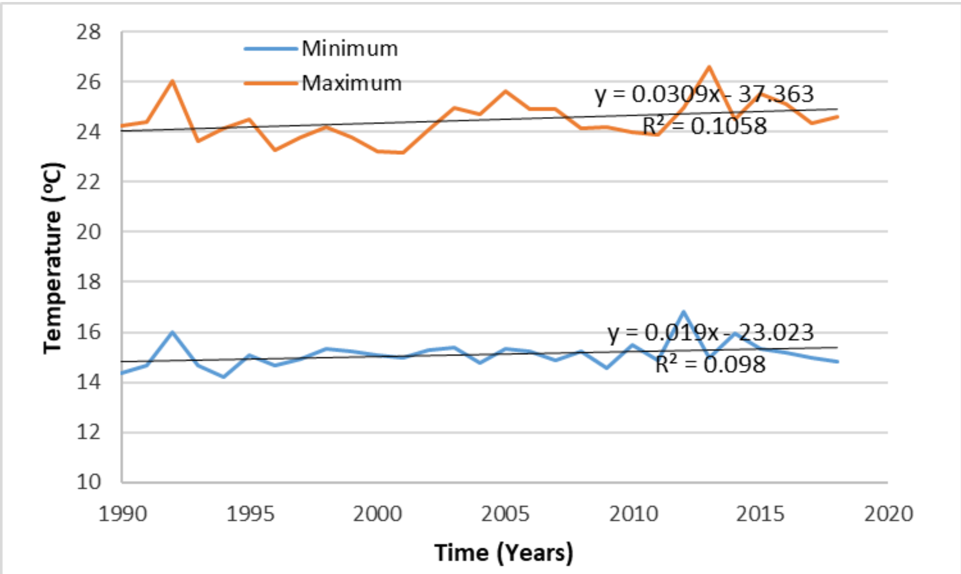

Figure 4.9: Temperature trends for Tshivhase

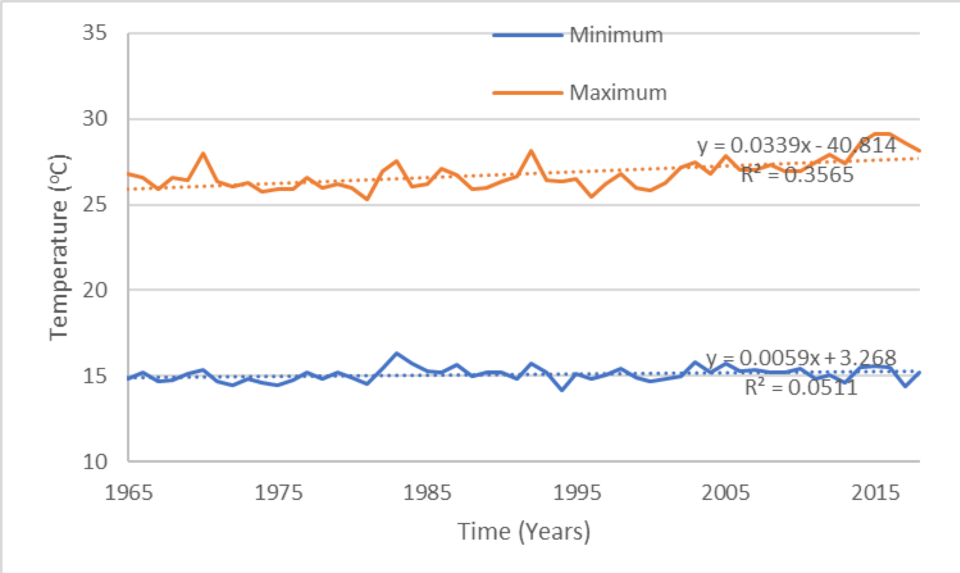

Figure 4.10: Temperature trends for Levubu

4.4 Streamflow trends and variability

Streamflow characteristics vary greatly, and this is noticeable even within the LRC, as shown in Table 4.4 and Figures 4.11 to 4.13. All stations had their highest annual flows in 2000/2001, which can be attributed to the renowned flood of the year 2000. Variations in streamflow were observed at the stations in the lower reaches of the catchment. The monthly streamflow measurements obtained from Mhinga station (A9H012) were utilized to calculate the mean value, providing an overview of the temporal pattern of streamflow within the designated study region. Table 4.5 shows that the months of February and March received 65% of the total streamflow. The annual streamflow data showed uneven variations between the stations (Figures 4.11 to 4.13). These disparities could be attributed to distinct meteorological and physiographic factors in the LRC. This results in uneven rainfall distribution and, thus, streamflow. The observed variations in the LRC align with what was suggested by Ashraf et al. (2021). The latter study found that different climatic regions were responsible for variations in streamflow in the Indus River basin.

Table 4.4: Streamflow trends

Variable	Observations	No. of observations	Min	Max	Mean	Std. deviation	Kendall's tau	p-value	Sen's slope
A9H012	32	32	1.25	18.79	6.29	4.86	0.00	0.97	0.00
A9H003	58	58	0.13	6.33	0.78	0.88	0.06	0.12	0.00
A9H006	58	58	0.00	2.40	0.29	0.41	-0.01	0.86	0.00

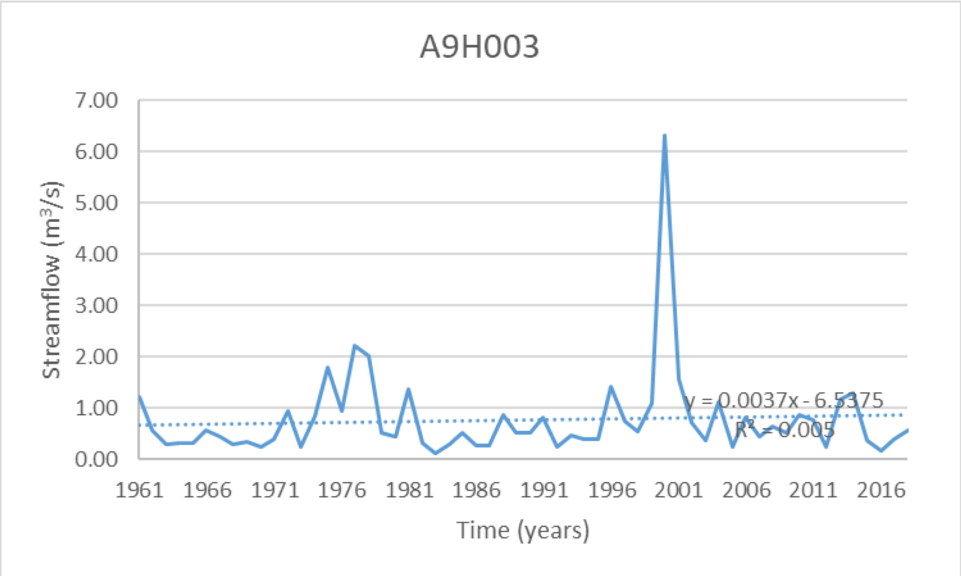

Figure 4.11: Average daily streamflow for station A9H003

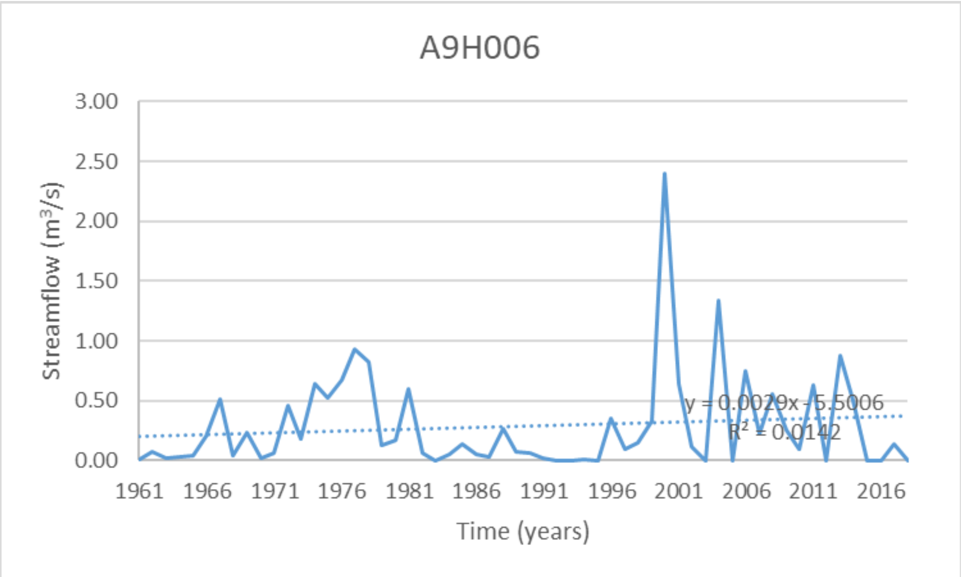

Figure 4.12: Average daily streamflow for station A9H006

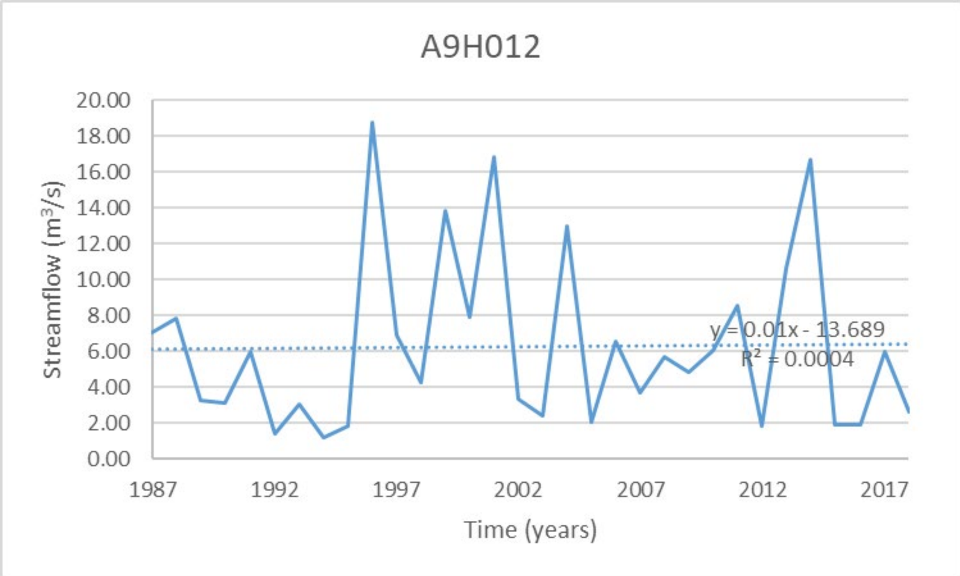

Figure 4.13: Average daily streamflow for station A9H012

The results presented above are in agreement with studies such as Pellicciotti et al. (2007) where over a period of 30 years, data was analyzed with the aim of identifying any patterns in precipitation and streamflow occurring annually, seasonally, or monthly within the Aconcagua River watershed - an arid Andes basin situated in Central Chile. Their findings have revealed a decrease in the average streamflow between years for the upper portion of the river and has also highlighted significant impacts resulting from El Niño Southern Oscillation (ENSO) occurrences. The study by Ávila et al. (2019) conducted an assessment of climate indicators for rainfall data in the upper basin area of the Cauca River with the objective of determining patterns in precipitation that occur spatially and temporally. Additionally, the study aimed to establish a correlation between historical floods and ENSO. The results of the study show a significant association between sea surface temperature (SST) and indicators of intense rainfall, backed by statistical evidence. In addition, the findings indicate a notable temporal delay of 2-3 months relating to ENSO and SST impacts. The findings of this study hold great importance in the realm of flood prediction and understanding of precipitation occurrences and climate fluctuations within the watersheds situated in the Colombian Andes. Puertas Orozco et al. (2011) conducted a study that examined the fluctuations in water availability caused by climatic variability in the gauging stations of the Upper and Middle Cauca River Basin. This analysis focused on the analysis of seasonal and monthly rainfall data.

Figure 4.14 shows that the average daily streamflow varied significantly during the study period. This variability can be seen through the fluctuations in the plotted data points, indicating that the streamflow values fluctuate significantly from day to day. Stations A9H003 and A9H006 showed high CV of 59 and 71 %, respectively. However, station A9H012 showed a very low CV of 11%. This finding has important implications for water resource management.

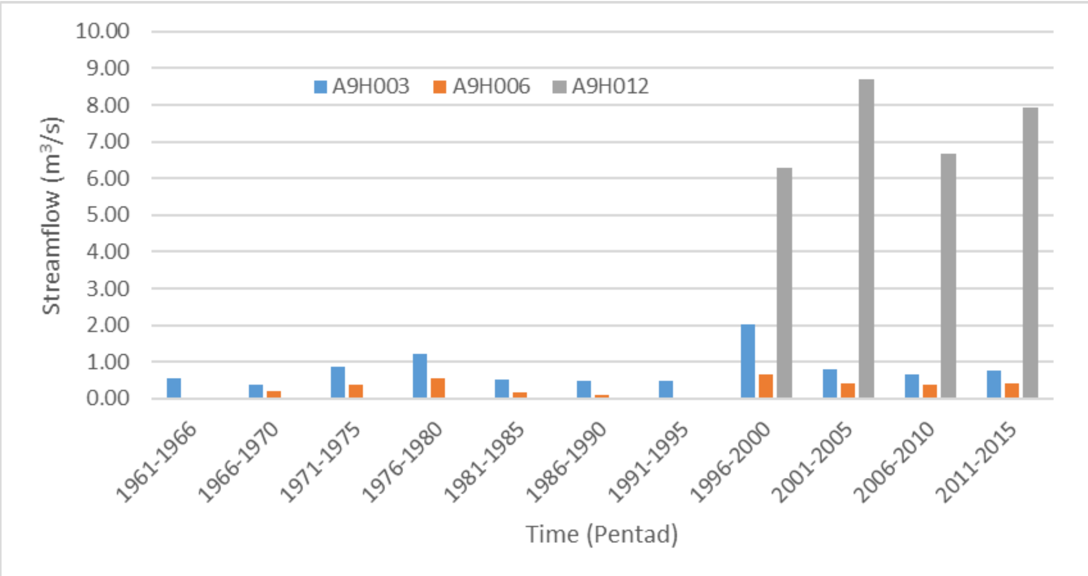

Figure 4.14: Average pentad streamflow stations used in the study

Based on the data shown in Figure 4.15, there has been a significant and notable decrease in the average daily streamflow over the last thirty years of this study. This was observed from all stations used in the study focusing on decadal daily average. Stations A9H003 and A9H006 showed high CV of 40 and 48 %, respectively. These results could indicate the presence of various factors, such as changing weather patterns, topography, and hydrological conditions in the catchment area. This could have significant environmental implications particularly on water resources. A significant decrease in CV was noted for station A9H012 with just 2%.

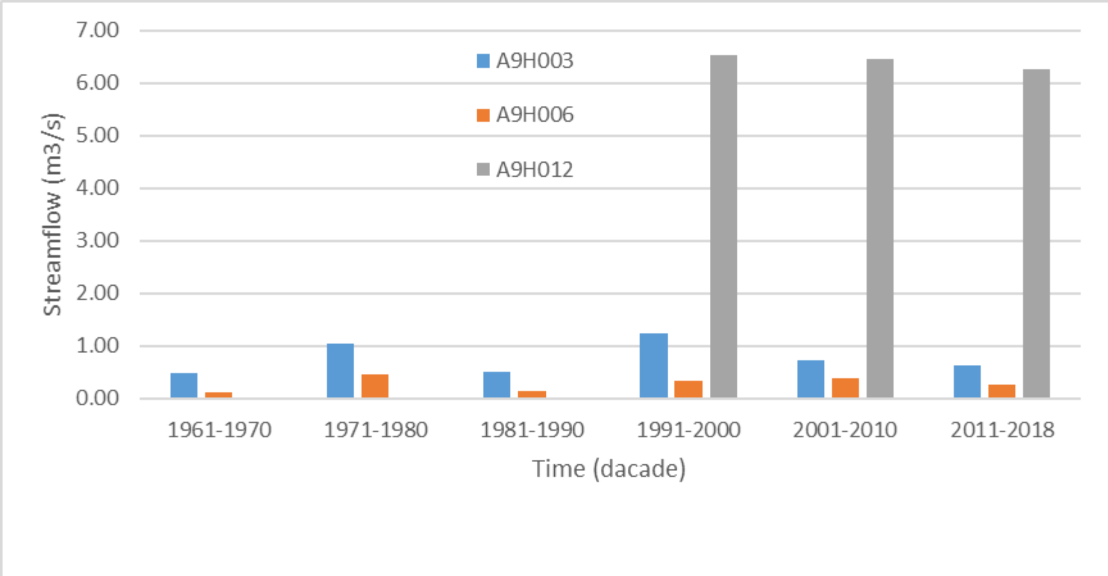

Figure 4.15: Average pentad streamflow stations used in the study

4.5 Rainfall interstation correlation

The analysis of spatial variability of rainfall was performed at different time scales in the study area. Table 4.5 shows the distance matrix of the stations used in the study. The longest distance apart from individual stations is 148.5 km, lying between Zwartrandjes and Pafuri upstream and downstream, respectively. The shortest distance is between Matiwa and Entabeni at 2.4 km. It is important to note that the rest have average distances of about 30 km between them.

Table 4.5: Distance matrices between rainfall stations in the LRC

	VONDO	PALMARYVILLE	ENTABENI BOS	PAFURI	PUNDA MARIA	THATHE	MATIWA	NOOITGEDACHT	KLEIN AUSTRALIE	TSHAKHUMA	LEVUBU	GOEDEHOOP	HANGLIP	TSIANDA	MAMPAKUIL	ZWARTRANDJES	ELIM - HOSP	THOHOYANDOU	MUKUMBANI	SHAFEERA	RAMBUDA
VONDO	0	12	10	107	75	6	8	20	17	13	19	26	43	13.5	51	59	37	18	7	24	19
PALMARYVILLE		0	17	102	69	16	15	26	23	16.3	19	32.3	52.4	11.3	58.2	65	42	7	7	32	21
ENTABENI BOS			0	117	85	14	2.5	11	8	6.4	10.2	17	36	10	42.3	49	27	24	16	15	29
PAFURI				0	36	106	115	127	124	117	121	133	149	113	159	166	144	96	100	132	90
PUNDA MARIA					0	36	82	95	92	8.4	88	101	119	80	127	134	111	62	68	99	61
THATHE						0	12	24	21.5	19	24	29	44	19	54	61	40	21	9	26	15
MATIWA							0	13	10	8	12	18	37	11	44	51	29	23	14	17	27
NOOITGEDACHT								0	3	10.5	9.5	7	29	16	33	39	17	33	26	9	39
KLEIN AUSTRALIE									0	8	8.4	9.5	31	13	35	42	20	30	24	10	36
TSHAKHUMA										0	5	18	39	5	43	49	27	22	18	18	32
LEVUBU											0	16	39	8	41	47	24	25	23	18	38
GOEDEHOOP												0	22	23	26	33	11	39	32	5	44
HANGLIP													0	44	16.5	24	20.3	60	50	20	60
TSIANDA														0	48	54	48	18	15	24	30
MAMPAKUIL															0	8	16.5	65	58	27	70
ZWARTRANDJES																0	22	72	65	35	77
ELIM - HOSP																	0	50	43	15	55
THOHOYANDOU																		0	11	39	21
MUKUMBANI																			0	31	15
SHAFEERA																				0	41.44
RAMBUDA																					0

Table 4.6 shows the interstation correlation between stations in the study area. The highest value for interstation correlation is 0.94 between Matiwa and Entabeni. This can be attributed to the shortest distance between stations as indicated in the previous paragraph. This is also further supported by the higher altitude at which the two stations are located as shown in Table 4.7. The lowest interstation correlation is between Shafeera and Pafuri with r=0.39. Though the two stations are not the ones with greatest distance in between, it is highly probably that altitude may be the explanation of this weak positive correlation. This may be due to variability topography. Additionally, factors such as land use, which can include agriculture, urban development, and natural reserves, may further contribute to the variability in measurements and outcomes between the two stations (Figure 5.16).

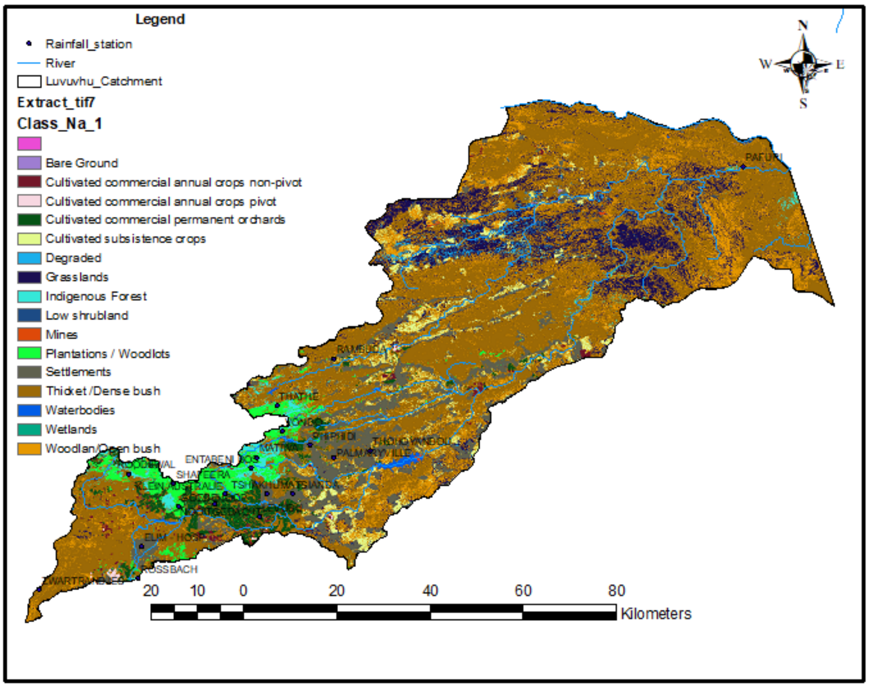

Figure 5.16: Land use map of the study area

Table 4.6: Correlation matrices between rainfall stations in the LRC

	THOHOYANDOU	RAMBUDA	SHAFEERA	ROODEWAL	PALMARYVILLE	ENTABENI BOS	GOEDEHOOP	HANGLIP	KLEIN AUSTRALIE	LEVUBU	MATIWA	PAFURI	THATHE BOS	ELIM	TSHAKHUMA	ZWAARTRANDJES	TSIANDA	PUNDA MARIA	NOOITEGEDACHT	PHIPHIDI	ROSSBACH
THOHOYANDOU	1.00																				
RAMBUDA	0.71	1.00																			
SHAFEERA	0.82	0.52	1.00																		
ROODEWAL	0.64	0.83	0.54	1.00																	
PALMARYVILLE	0.85	0.77	0.63	0.77	1.00																
ENTABENI BOS	0.81	0.82	0.61	0.85	0.84	1.00															
GOEDEHOOP	0.83	0.67	0.64	0.58	0.73	0.75	1.00														
HANGLIP	0.81	0.73	0.60	0.80	0.75	0.82	0.74	1.00													
KLEIN AUSTRALIE	0.85	0.75	0.59	0.76	0.86	0.86	0.85	0.83	1.00												
LEVUBU	0.82	0.84	0.54	0.86	0.85	0.86	0.63	0.75	0.77	1.00											
MATIWA	0.79	0.79	0.66	0.81	0.86	0.95	0.73	0.77	0.81	0.83	1.00										
PAFURI	0.62	0.63	0.39	0.66	0.67	0.67	0.50	0.60	0.61	0.72	0.61	1.00									
THATHE BOS	0.59	0.51	0.42	0.59	0.68	0.73	0.51	0.61	0.67	0.76	0.71	0.62	1.00								
ELIM	0.75	0.76	0.70	0.81	0.85	0.87	0.72	0.75	0.78	0.82	0.79	0.67	0.64	1.00							
TSHAKHUMA	0.73	0.63	0.53	0.70	0.77	0.77	0.59	0.70	0.68	0.79	0.78	0.52	0.74	0.75	1.00						
ZWAARTRANDJES	0.76	0.63	0.62	0.75	0.72	0.75	0.70	0.80	0.80	0.76	0.73	0.54	0.61	0.79	0.61	1.00					
TSIANDA	0.67	0.79	0.61	0.79	0.81	0.76	0.58	0.68	0.71	0.83	0.79	0.66	0.66	0.71	0.71	0.58	1.00				
PUNDA MARIA	0.85	0.77	0.52	0.80	0.79	0.77	0.57	0.75	0.72	0.83	0.71	0.73	0.62	0.72	0.73	0.68	0.70	1.00			
NOOITEGEDACHT	0.85	0.79	0.68	0.85	0.90	0.87	0.79	0.85	0.90	0.88	0.87	0.65	0.68	0.86	0.73	0.82	0.82	0.79	1.00		
PHIPHIDI	-0.11	-0.08	-0.05	0.04	0.12	-0.01	-0.06	-0.08	-0.03	-0.03	0.03	0.28	-0.19	-0.19	-0.05	-0.13	0.11	-0.18	0.03	1.00	
ROSSBACH	0.79	0.70	0.67	0.70	0.75	0.78	0.65	0.66	0.81	0.83	0.74	0.66	0.72	0.86	0.59	0.79	0.66	0.76	0.84	-0.26	1.00

The interstation variability per pentad and decade were investigated to show the trends of rainfall in the study area. Station by station variability showed that it has increased by 10% of the whole study period considered (Table 4.7). The overall variability of rainfall on a pentad and decadal scale shows varying coefficients of variation. The highest variability is observed on the pentad scale while low variability is observed from decadal scale. This can be attributed to the fact that within a decade some events tend to repeat themselves unlike the pentad case. This can be justified by the events such as ENSO which tend to repeat themselves from three to five years (Dieppois et al., 2015).

In a study conducted by Wazneh et al. (2017), the focus was on the examination of rainfall variability across different stations in Canada. To assess the extent of interstation variability and determine the representativeness of trend values, the researchers calculated the range of interstation variability among the station indices by dividing the absolute standard deviation by the mean absolute mean of the trends.

4.6 Rainfall versus altitude

The relationship between average rainfall and altitude in the LRC for the stations used produced a correlation coefficient of 0.76 (Figure 4.17). This shows that there is a strong effect of orography on the distribution of rainfall in the LRC association is moderately strong. Table 4.8 shows the relationship between rainfall and altitude in the LRC for the stations used in the study. This supports the theory that mountainous areas receive more rainfall and may have an influence on rainfall occurrence (Daly et al., 1994; Smith and Barstad, 2004; Tuladhar et al., 2020).

Table 4.7: Topography and rainfall variables used in the study

STATION_ NAME	LATITUDE	LONGITUDE	ALTITUDE	AVERAGE_ RAINFALL	CV	ASPECT	SLOPE
PAFURI	-22.42	31.22	210	439	0.41	68.88	0.64
RAMBUDA	-22.79	30.43	762	840	0.40	156.40	2.23
THATHE	-22.88	30.32	1250	1200	0.27	171.16	3.57
VONDO	-22.93	30.33	1130	1278	0.43	251.89	3.12
PHIPHIDI	-22.96	30.39	900	1282	0.42	143.67	5.66
THOHOYANDO U	-22.967	30.5	605	769	0.33	287.24	0.79
MATIWA	-22.98	30.28	1311	1832	0.28	333.57	4.321
PALMARYVILLE	-22.98	30.43	570	867	0.34	70.78	0.64
ENTABENI BOS	-23	30.27	1376	1747	0.25	181.18	4.72
ROODEWAL	-23.01	30.03	440	831	0.43	207.78	8.14
SHAFEERA	-23.03	30.12	1214	1378	0.36	197.00	12.92
KLEIN AUSTRALIE	-23.05	30.22	702	1101	0.44	137.56	1.38
TSHAKHUMA	-23.05	30.30	1158	1117	0.31	282.82	2.11
TSIANDA	-23.05	30.35	671	877	0.41	130.09	2.13
NOOITGEDACH T	-23.07	30.20	762	962	0.39	200.91	2.39
GOEDEHOOP	-23.07	30.13	811	843	0.48	67.25	1.35
LEVUBU	-23.09	30.30	610	950	0.38	68.92	1.04
ELIM - HOSP	-23.15	30.06	808	675	0.39	96.88	3.13
ROSSBACH	-23.21	30.05	1190	927	0.37	134.20	9.53
ZWARTRANDJE S	-23.23	29.86	1036	507	0.32	149.64	1.09

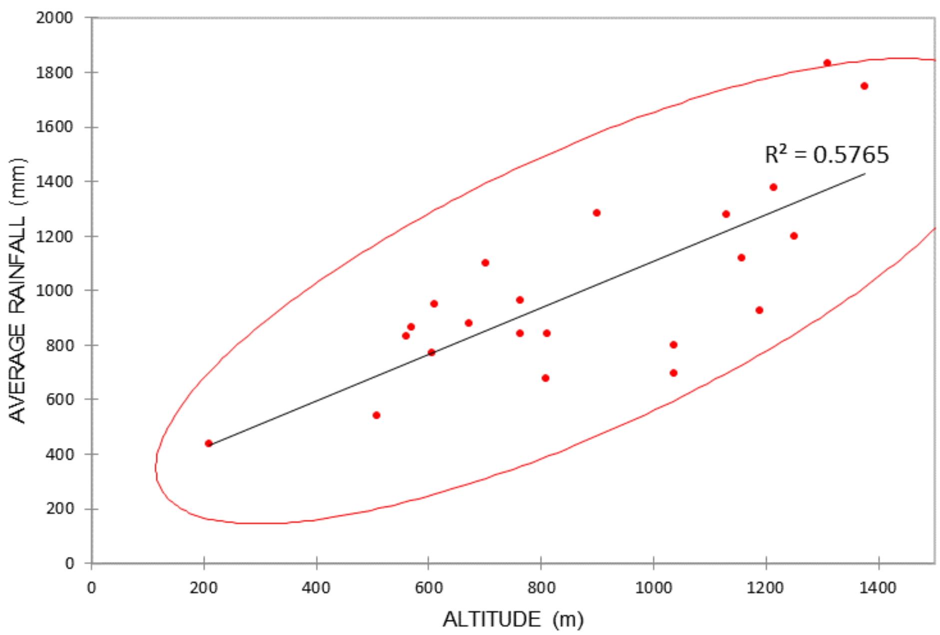

Figure 4.17: The correlation between altitude and rainfall in the study area

Figure 4.18 shows the location of rainfall stations in LRC with respect to altitude. The findings show that altitude has a statistically significant correlation with annual rainfall with a coefficient of determination of about 60% at a significant level of 0.05. Thus, altitude plays a vital role in the spatial distribution of rainfall while using annual series. Figure 4.19 shows the relationship between altitude and CV in the LRC for the stations used. It shows that there is a negative correlation of 0.56 with a co-efficient of determination of about 32% at a significant level of 0.05. This suggests that with increasing altitude, the variability of annual precipitation decreases significantly, highlighting the complex interplay between altitude and precipitation patterns in the study area. This shows that more consistent weather patterns may occur at higher elevations, potentially reducing the precipitation fluctuations seen at lower elevations. It also emphasizes the importance of understanding the geographical and climatic factors that influence water distribution, which is critical to its availability in the region

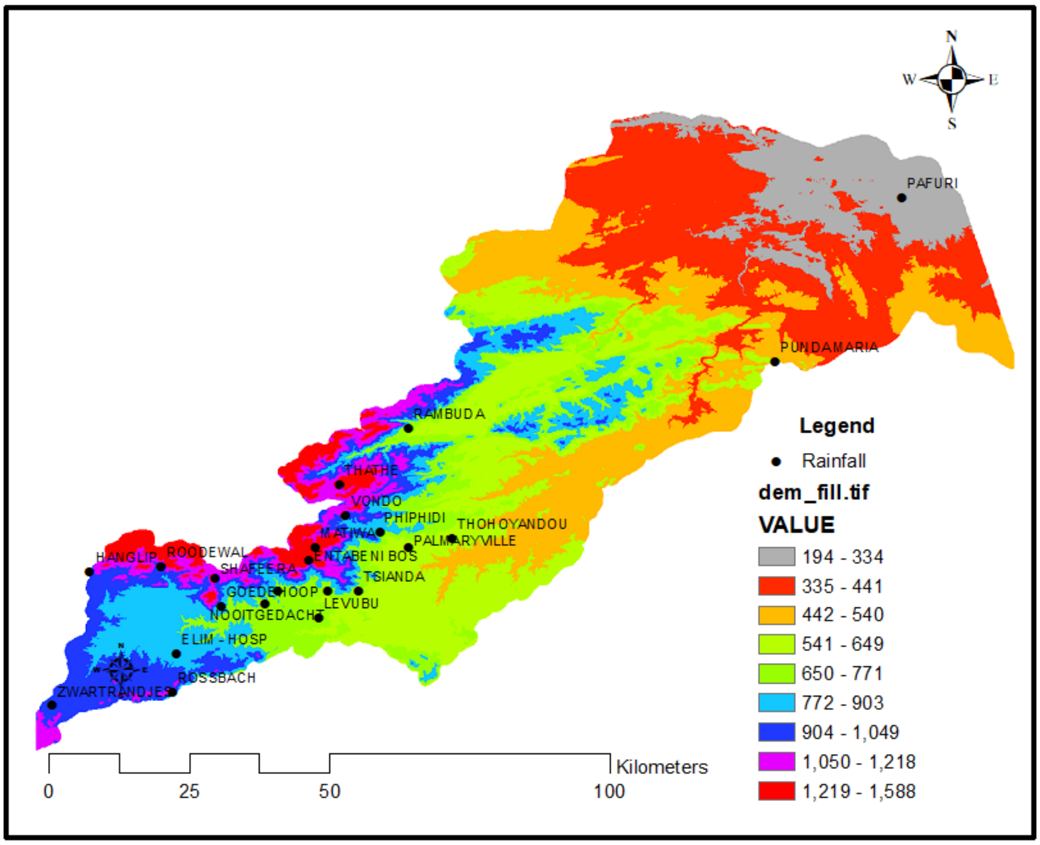

Figure 4.18: Location of rainfall stations in the LRC with their respective altitude

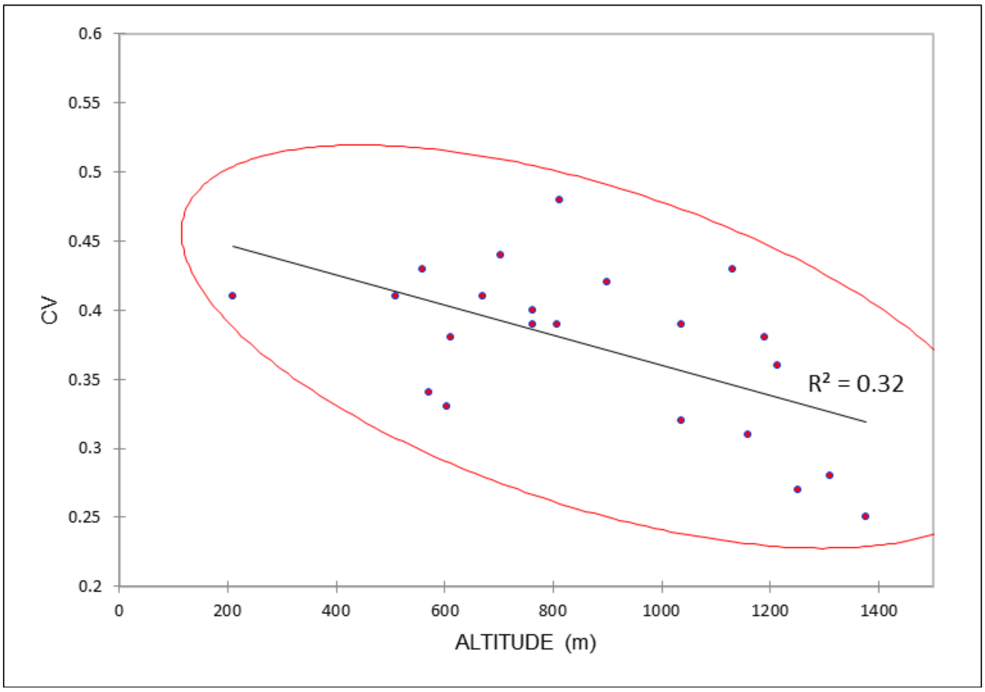

Figure 4.19: The relationship between the CV and the altitude of the stations calculated

The altitude and rainfall relationship indicate a positive correlation of 0.68. This clearly shows that the distribution of rainfall in the LRC is somehow influenced by the presence of the Soutpansberg Mountain. A further confirmation can also be explained by the distance among the stations located in the higher altitudes and those in the lower elevations. The highest amount of rainfall occurs along the Soutpansberg mountain in terms of spatial distribution. The patterns of change of annual rainfall shows varying percentages with some showing increase while others showing a decrease. These patterns of change vary from one season to the other. This synonymous to the findings by Christensen and Christensen (2007). The east-west gradient of rainfall distribution that was observed.

The spatial distribution of the rainfall received in the LRC for the study period was manifest that the northeast part of the catchment received the least amount of rainfall. The rainfall distribution was supported by the distribution of natural vegetation of the LRC (Mukwada et al., 2021). Despite the spatial variability of rainfall, the higher altitudes remain important sources of water since they receive high rainfall amount.

Detection of changes in the rainfall was performed using annual rainfall amount at a significance level of 0.05. In this study, rainfall was regressed against time. The interstation variability was performed using the coefficient of correlation for individual stations. This study found that most of the stations along the Soutpansberg Mountain range within 20 km on the south facing slopes were relatively homogeneous than those located at a further distance (Table 4.6). However, this homogeneity was applicable to stations that are in the upstream part of the catchment. Table 4.7 show the correlation coefficients for rainfall and altitude for individual stations in the LRC.

The implications of rainfall variability in the study area may have detrimental effects on different sectors of the economy and society. These may include domestic water supply, tourism, commercial and subsistence agriculture. Consequently, the results of this study may help the concerned groups in understanding the patterns of rainfall to encourage them to implement better water saving strategies.

The HC was performed on rainfall variables, including average rainfall and CV. The HC revealed two clusters in the LRC, with Cluster 1 explaining 46% of the total variation and Cluster 2 explaining 54% (Figure 4.20). These clusters were mainly influenced by topography. This is validated by various studies that attempted to show the effect of the Soutpansberg Mountain on the distribution of rainfall in the northern region of Limpopo Province (Kephe et al., 2016). The latter studies used composite rainfall and standardised anomaly index to make inferences on their findings. However, this overlooked other variables of topography and rainfall as indicated in a study by Mmbando and Kleyer (2018). However other studies demonstrate that topography (altitude) influences the distribution of rainfall in the LRC. This type of influence has been noticed in Kenya, where Camberlin et al. (2014) researched rainfall behaviour in Mount Kenya and nearby areas. The latter found that altitude and exposure played a vital role in the distribution of rainfall. However, in terms of variability, their study found high variability in high altitude as opposed to low altitude.

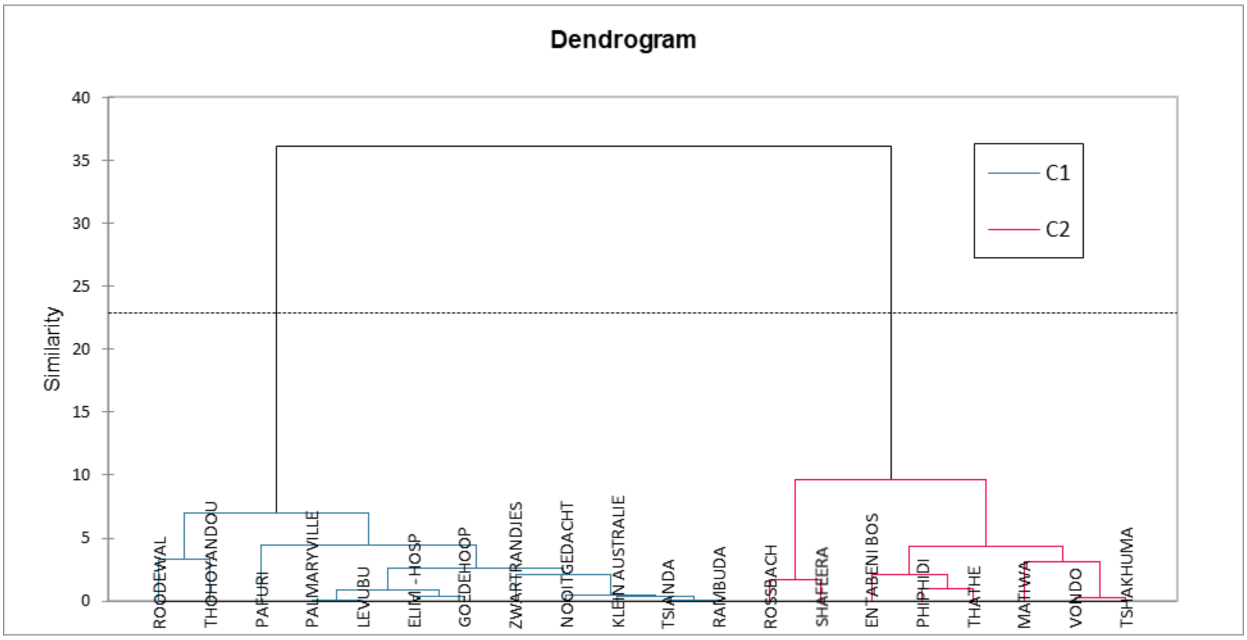

Figure 4.20: Clusters of rainfall stations used in the study

The CCA results confirm there is a strong dependence of rainfall distribution on the study area's topography (Table 4.9). Three topographic factors, which are slope altitude and aspect were considered. Thus, altitude plays a significant role in the spatial distribution of rainfall while using annual series. The spatial distribution of rainfall in the LRC for the study period showed that the northeastern part of the catchment received the least amount of rainfall (Figure 4.16). The shape, height and orientation of the landforms are all contributing factors to the patterns of precipitation we observe. Canonical Correlation Analysis results have confirmed that there is a strong dependence of rainfall distribution on the study area's topography. This means that the study area's topography plays a critical role in determining how rainfall is distributed throughout the region. This information is crucial for researchers and policymakers alike, as it can help them to better understand and manage the area's water resources.

Figure 4.17: Spatial distribution of rainfall in the LRC

Table 4.8: Correlation matrix for rainfall and topographic variables

Variables	AVERAGE_RAINFALL	CV	ASPECT	SLOPE	ALTITUDE
AVERAGE_RAINFALL	1	-0.44	0.53	0.39	0.72
CV	-0.44	1	-0.43	-0.05	-0.58
ASPECT	0.53	-0.43	1	0.21	0.47
SLOPE	0.39	-0.05	0.21	1	0.42
ALTITUDE	0.72	-0.58	0.47	0.42	1

4.7 Summary of the chapter

The general observation is that the CV of rainfall in the studied area varied greatly. Temperature also varied with time with a clear indication of an increasing trend. Topography and climatic drivers influence rainfall distribution in the study area. Changes in rainfall characteristics and temperature impact on seasonal, annual, and spatiotemporal distribution of water availability. The distribution of rainfall in the LRC can be better understood by knowing the altitude and the accompanying parameters such as orientation and slope. Consequently, the availability of water in the area can be comprehended.

CHAPTER FIVE: DROUGHTS AND FLOODS ANALYSIS

5.1 Preamble

This chapter presents the results of flood and drought thresholds, duration, magnitude/intensity and frequency. Drought analysis results are based on SPI, SPEI and SDI. The goodness of fit test is described for flood analysis and the applicability of the method. In addition, a detailed analysis of the patterns and trends in flood/drought occurrence and severity are presented.

5.2 Drought analysis

Based on the number of droughts counted in the time series of SPEI, one can suggest the direction of rainfall trend. For this, several stations in the study area were considered. For all the stations considered there was confirmation that the higher the number of occurrences above and/or below the normal shows whether the area is moving towards a particular condition.

5.2.1 SPI

The time series data covering the study period indicated that drought have occurred in the LRC periodically (Table 5.1). The SPI results are presented in figures 5.1 to 5.3, of more concern were droughts of 1982, 1992, and 2014 – 2016 wherein most provincial governments with the help of the national government declared drought emergencies. For the sake of clarity, only three stations were presented, one from upstream, one from mid-stream and one from downstream. Table 5.1 shows the summary of drought severity and duration over the study period. It shows that over the years there has been an increase in the number of drought events in days. The lower reaches of the catchment are the ones more susceptible to drought days since the period is greater there than the upper reaches. This suggests that rainfall in the study area does not follow the general assertion in South Africa (Reddy, 1986) that rainfall decreases from east to west. In the LRC, rainfall decreases from west to east. As earlier indicated in chapter 4, the Soutpansberg Mountain's presence plays a critical role in the distribution pattern of rainfall in the study area. Drought analysis is critical in this study area. The frequency of droughts is a good indicator of whether an area is transitioning to other climatic conditions such as aridity. Based on this data, a considerable increase in the trend towards below-normal rainfall was observed over the years. Furthermore, there has been a significant decrease in rainfall trends during droughts. As a result, the number of drought episodes is increasing. This gives an indication that the area is transiting towards aridity conditions.

The duration of drought in terms of the SPI show that a maximum of three months in the wet season is common among the drought years. The severity varied across the LRC which decreased from east to west. This is in line with the distribution of rainfall in the catchment as indicated in section 4.2 of Chapter 4. The variability of drought severity has also been supported by studies such as Kabanda (2004), Mazibuko et al. (2021). The latter studies agree that the severity was attributed mainly to the existence of the ENSO events, particularly El Nino.

Table 5.1: Drought severity and duration in the study area using SPI

Number of Drought	Start of Drought	Duration of Drought (days)	Severity of Drought
1	1/1/1965	365	0.684
2	1/1/1968	366	0.058
3	1/1/1970	365	1.15
4	1/1/1979	365	0.116
5	1/1/1982	730	2.3
6	1/1/1986	365	0.768
7	1/1/1989	730	0.78
8	1/1/1992	1096	1.567
9	1/1/2002	730	1.404
10	1/1/2005	365	0.541
11	1/1/2007	365	0.078
12	1/1/2009	730	1.867
13	1/1/2012	2557	9.998

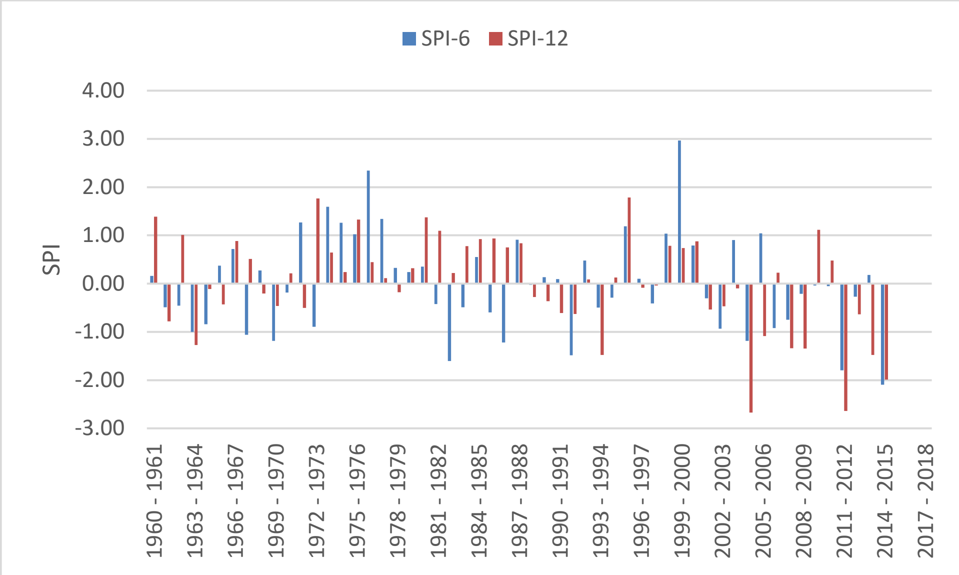

Figure 5.1: SPI for Entabeni Bos

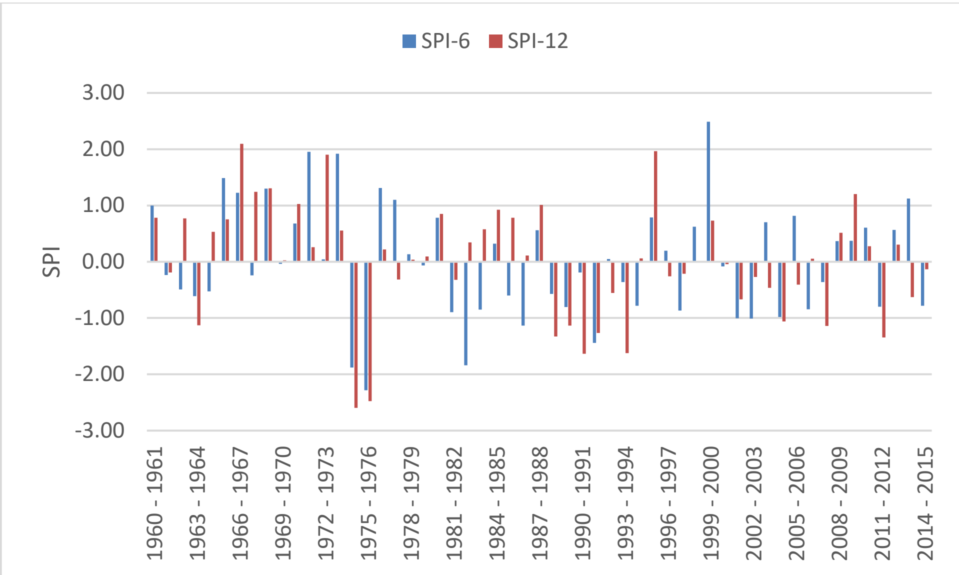

Figure 5.2: SPI for Shafeera

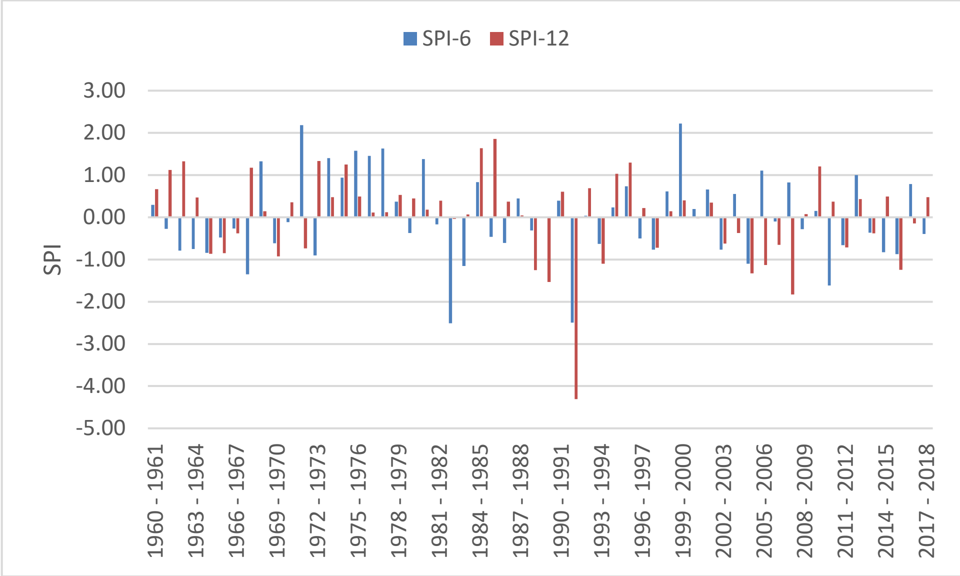

Figure 5.3: SPI for Punda Maria

5.2.2 SPEI

Figure 5.4 presents the average duration and severity of drought in the LRC based on SPEI. Throughout the study period, the intensity of drought remains moderate in the upper reaches of the catchment. Moderate conditions occurred in 1992, 2002, and 2015 for the upper reaches as the lower reaches were experiencing severe droughts. There were no signs of moderate rainy weather at this station. In the year 2000, there was an occurrence of exceptionally heavy rainfall, which led to a notable increase in the overall wetness levels observed during the entire study duration. Extreme rainfall occurred in 1977, 1996 and 2000. The subsequent years were near normal.

Stations in the mid-stream of the catchment of the seldom encountered severe drought conditions. Moderate and severe conditions occurred in 1982, 1992, 1994, 1999, 2002, 2003, and 2015, respectively. These conditions have posed significant challenges for the local communities and have impacted the wildlife and ecosystems in the affected areas. Severe rainy conditions occurred in 1996 and 2000. Moderate rain fell in 1984, 1996, 2000, and 2013. Some years observed near-normal weather.

Stations in the downstream part of the catchment experienced severe drought in 1982, 1992 and 2015. Extreme drought-related difficulties can have negative economic environmental and social impacts in afflicted areas. The impact of the drought had a significant effect on the LRC. This led to a decline in water availability, affecting both the environment and the local communities. Drought conditions were moderate in 2002, 1999, and 2003. The wet cycle occurred when there were monthly temperature changes in the minimum and maximum temperatures. In 1981, extreme wet weather with low drought severity occurred. As a result, extremely rainy weather occurred in 1977, 1996, and 2000.

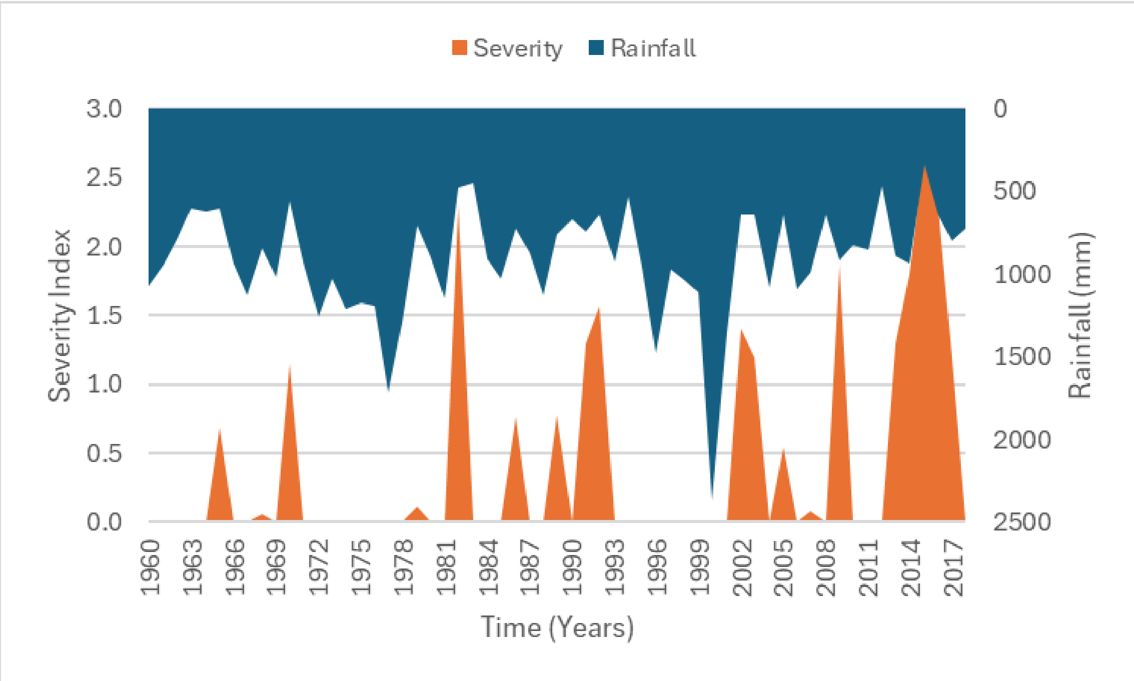

Figure 5.4: Averaged drought duration and severity for LRC

5.2.3 SDI

The analysis of Figure 5.5 reveals noteworthy trends and patterns. Over the study period, the SDI displays considerable variability, with values ranging from -1.98 to 3.39. This wide range indicates the diverse hydrological conditions observed in the LRC over time. Despite this variability, a clear trend emerges when examining the data across the years. The correlation coefficient of 0.87 suggests a strong positive relationship between the SDI-6 (6-month streamflow drought index) and SDI-12 (12-month streamflow drought index). This indicates that the streamflow patterns over these two periods are closely related, meaning that when streamflow is low over 6 months, it is likely also low over 12 months.

For SDI-6 this p-value indicates a 34.2% chance that the observed correlation for the 6-month period could be due to random variation. Because this p-value is greater than 0.05, the correlation is not statistically significant at the conventional 95% confidence level. Similarly for SDI-12, the p-value for the 12 months is even higher at 64.7%, suggesting that the observed correlation could likely be due to random chance. Again, this result is not statistically significant. The data provided does not allow us to confidently predict whether there will be more droughts. The strong correlation coefficient suggests that when drought conditions occur over a shorter period (6 months), they are likely to persist over a longer period (12 months). Although the strong correlation coefficient suggests that drought conditions may persist over 6-month and 12-month periods.

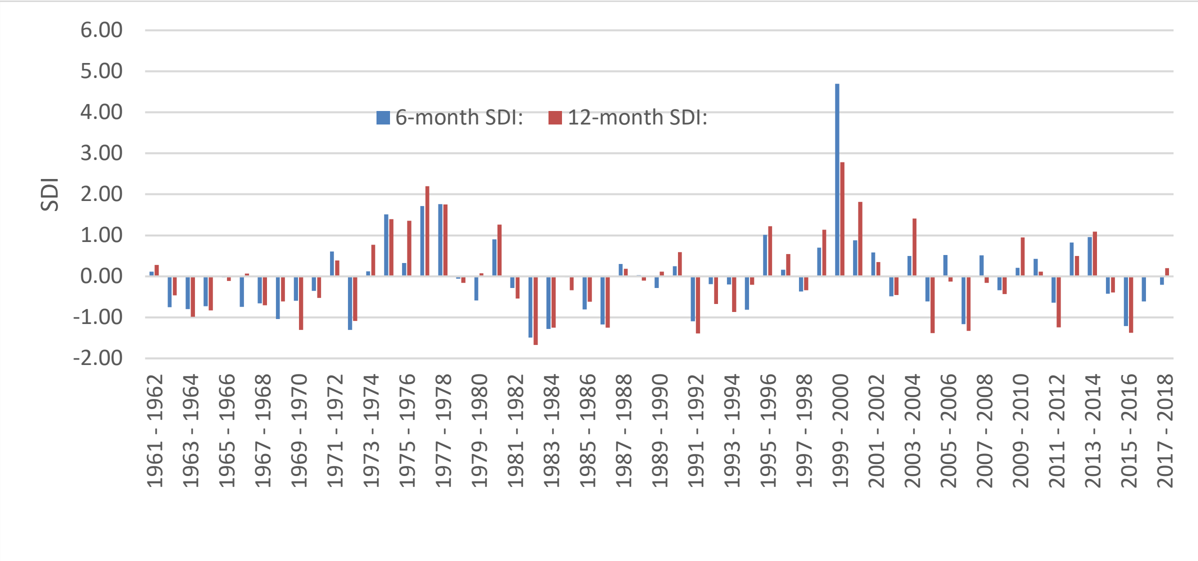

Figure 5.5: Streamflow drought index for the study area

5.3 Floods analysis

This section presents the results and discussion of flood magnitude and return periods using the GEV and LP3 distribution in the LRC for the period used in this study. Table 5.2 shows the summary of statistics and their respective logarithmic transformation useful for estimating flood frequency and magnitude. The data analysis involved the calculation of several statistical parameters such as the total, mean, standard deviation, skewness and coefficient of variation for the highest recorded daily rainfall values in a year.

Two stations (Goodehoop and Mukumbani) showed great disparity in magnitude of 100-year return period between LP3 and GEV. The disparity for both stations above is greater than 150 mm. This could be attributed to the distribution of the annual time series which showed a high degree of variability in rainfall as discussed in chapter 4. The results of flood estimation (magnitude and return period) are consistent with previous studies on the study area. In addition, a longer dataset and the use of predicted impacts of climate change makes the findings more robust. Table 5.3 shows the number of rejections for the goodness-of-fit at a 5% significance level. After following the methods outlined in Chapter 3, the test results were calculated. These results were analysed to determine which distributions should be excluded when there is a clear trend. This was particularly useful when dealing with complex data sets, as it allows for a more accurate interpretation of the results.

Table 5.2: Number of rejections at the 5% significance level for the 3 goodness of fit tests

	EV	LP3
Kolmogorov-Smirnov	**3**	**2**
Anderson-Darling	**4**	**1**
Chi-Squared	**3**	**2**

Figure 5.5 shows the average daily maximum rainfall per annum in the LRC. The data presented indicates a noticeable increase in the quantity of daily maximum rainfall per year in the LRC. This rise in rainfall can have serious implications for the region, including flooding and damage to infrastructure.

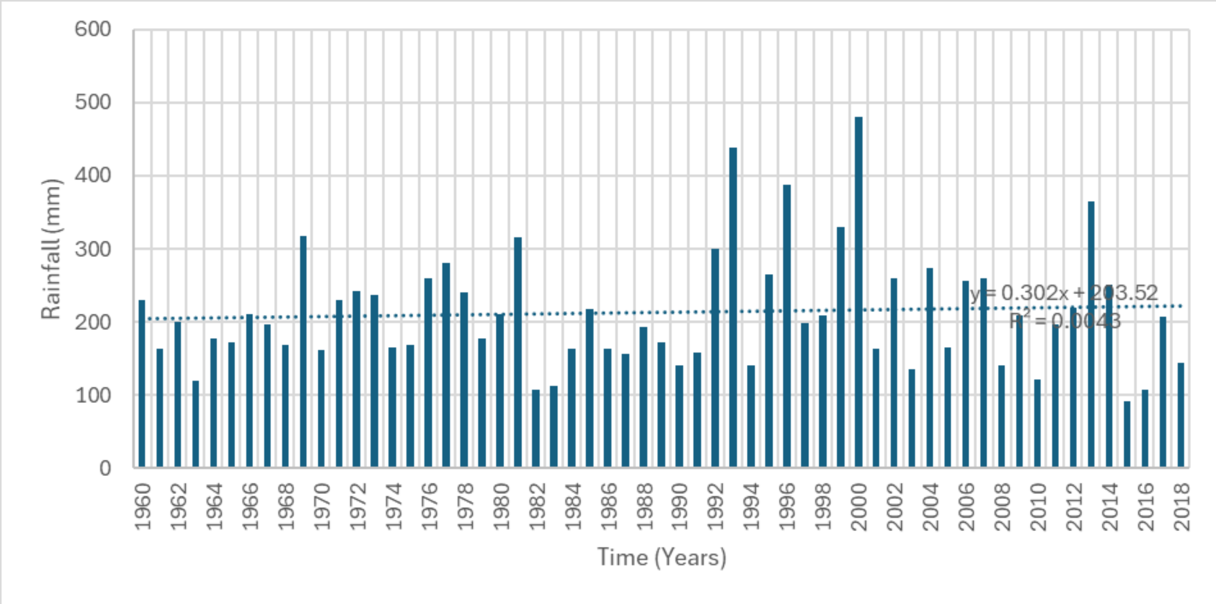

Figure 5.5: Average daily maximum rainfall per annum observed in the LRC during 1961-2018

Table 5.3 shows that data from the Normal and Log-transferred series are positively skewed. These results indicate that the LP3 distribution is a more acceptable fit for the data used in the study area compared to GEV. Figures 5.6 to 5.8 show the comparisons of the LP3 and GEV from upstream to downstream for some of the rainfall stations used in the study. The robustness of the LP3 distribution's applicability in the study area is consistent with findings by Singo et al. (2012). In their study, they examined different methods for flood frequency analysis. On a national scale, Alexander (2002) has also found that the LP3 distribution is most suitable for South African conditions. In certain areas, such as the Upper Thames River Watershed, GEV and LP3 were performed better (Millington et al., 2011). This suggest the statistical parameters involved in the estimation and the hydrological regime played a vital role in the results yielded.

Table 5.3: Computed statistical parameters for annual maximum daily rainfall

Station	Statistical parameter	Computed value	Logarithmic transformation
Pafuri	Sum ($\sum x$)	2312.3	59.6
	Mean ($\bar{x}$)	70.1	1.8
	standard deviation	28.9	0.2
	skewness coefficient	0.5	-0.51
Hanglip	Sum ($\sum x$)	4578.0	109.4
	Mean ($\bar{x}$)	77.6	1.9
	standard deviation	32.4	0.2
	skewness coefficient	1.2	-0.16
Tshakhuma	Sum ($\sum x$)	7338.0	103.6
	Mean ($\bar{x}$)	149.8	2.1
	standard deviation	89.6	0.2
	skewness coefficient	1.8	0.46
Elim	Sum ($\sum x$)	5591.9	113.3
	Mean ($\bar{x}$)	94.8	1.9
	standard deviation	58.5	0.2
	skewness coefficient	2.9	0.65
Thathe Bos	Sum ($\sum x$)	4549.7	75.7
	Mean ($\bar{x}$)	123.0	2.0
	standard deviation	60.7	0.2
	skewness coefficient	1.4	0.34
Matiwa	Sum ($\sum x$)	8681.3	3.94
	Mean ($\bar{x}$)	147.1	2.17
	standard deviation	56.0	1.75
	skewness coefficient	0.9	-0.04
Thohoyandou	Sum ($\sum x$)	3505.1	70.4
	Mean ($\bar{x}$)	97.4	2.0
	standard deviation	41.1	0.2
	skewness coefficient	1.1	0.41

Table 5.3 continues

Station	Statistical parameter	Computed value	Logarithmic transformation
ggffgZdsdgZwaartrandjes	Sum ($\sum x$)	3894.5	3.59
	Mean ($\bar{x}$)	66.0	1.82
	standard deviation	39.5	1.60
	skewness coefficient	3.1	0.50
Punda Maria	Sum ($\sum x$)	4429.4	108.0
	Mean ($\bar{x}$)	75.1	1.8
	standard deviation	37.5	0.2
	skewness coefficient	1.4	0.50
Levubu	Sum ($\sum x$)	5216.9	101.5
	Mean ($\bar{x}$)	96.6	1.9
	standard deviation	65.7	0.4
	skewness coefficient	3.0	-2.93
Goodehoop	Sum ($\sum x$)	5476.5	111.5
	Mean ($\bar{x}$)	92.8	1.9
	standard deviation	67.2	0.3
	skewness coefficient	3.0	0.20
Rambuda	Sum ($\sum x$)	28705.1	141.5
	Mean ($\bar{x}$)	552.0	2.7
	standard deviation	167.0	0.1
	skewness coefficient	0.414	-0.47
Mukumbani	Sum ($\sum x$)	2976.0	52.6
	Mean ($\bar{x}$)	110.2	1.9
	standard deviation	56.4	0.4
	skewness coefficient	0.5	-2.00
Klein Australie	Sum ($\sum x$)	7232.0	119.9
	Mean ($\bar{x}$)	122.6	2.0
	standard deviation	68.7	0.2
	skewness coefficient	1.6	0.294
Noitegedacht	Sum ($\sum x$)	6305.7	116.4
	Mean ($\bar{x}$)	106.9	2.0
	standard deviation	61.3	0.2
	skewness coefficient	1.8	0.423

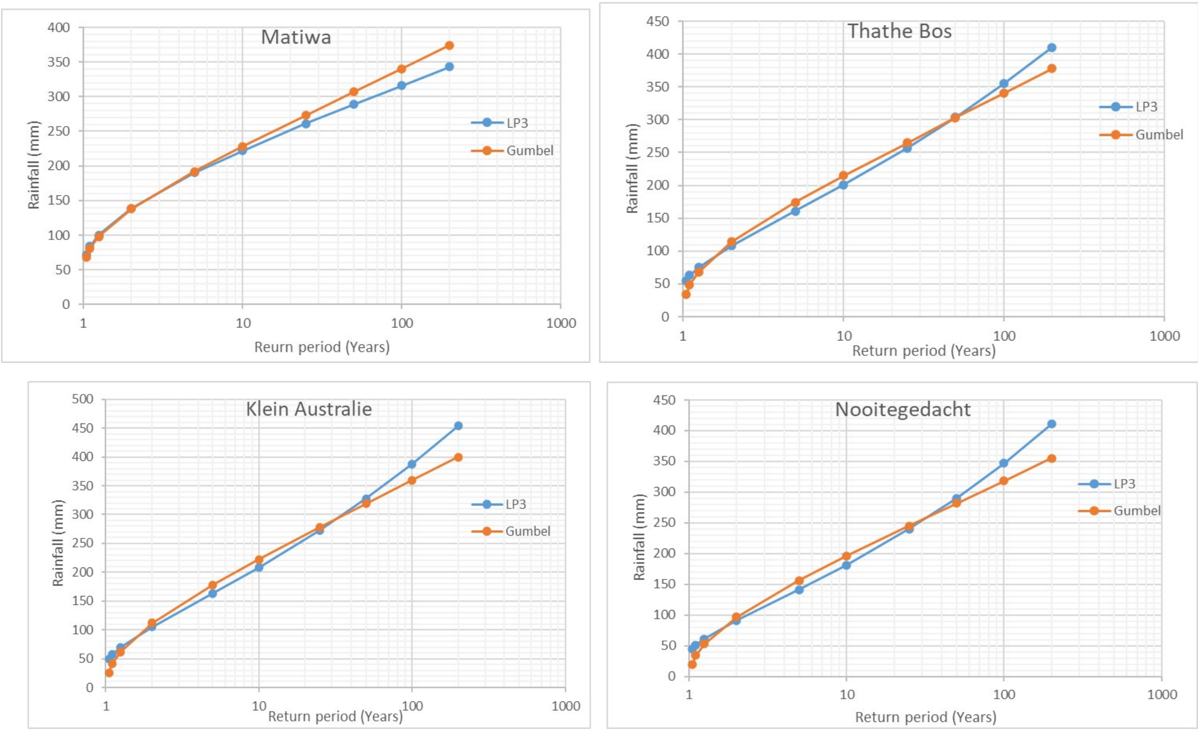

Figure 5.6: Return periods and corresponding flood magnitude upstream

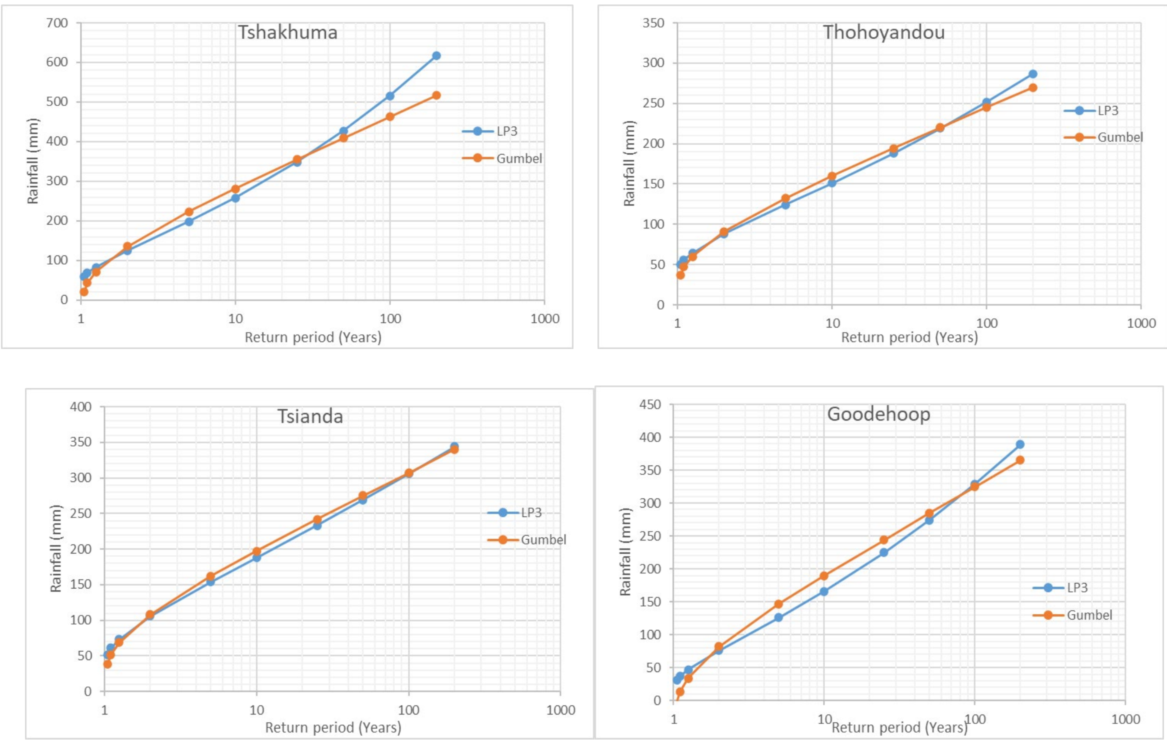

Figure 5.7: Return periods and corresponding flood magnitude mid-stream

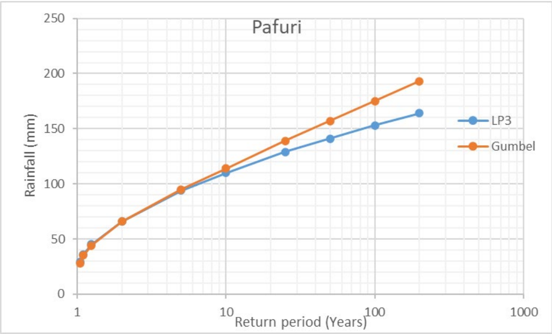

Figure 5.8: Return periods and corresponding flood magnitude downstream

Return periods for streamflow

The recorded flood levels in the area were compared to the mean annual flood calculated using the LP-III method, as shown in Table 5.4. It was observed that the recorded flood levels exceeded the mean annual flood. Based on the available time series data, it has been determined that the largest peak discharge happened in the year 2000. The greatest peak flows were measured at two specific locations, namely A9H012 and A9H013, reaching a staggering 590 and 450 m^3s^{-1}, respectively. These values are significantly higher than the required threshold, indicating a potential risk of flooding in the area.

The A9H012 and A9H013 sites both experienced peak discharges, with values of 418 and 290 m^3s^{-1}, respectively. These values were accompanied by standard deviations of 105 and 57 m^3s^{-1}. The logarithms of peak discharge for A9H012 and A9H013 were found to have average values of 1.89 and 1.51 m^3s^{-1}, respectively. Additionally, the logarithmic skewness coefficients for these stations are 0.42 and -0.28, respectively. Finally, Tables 5.7 display results of LP3 and Gumbel computed discharges at different return periods of 1.05, 1.11, 1.25, 2,5, 10, 25, 50, 100, and 200 years for all stations analysed in this study.

Table 5.4: Number of rejections at the 5% significance level for the 3 goodness of fit tests

	EV	LP3
Kolmogorov-Smirnov	5	2
Anderson-Darling	3	1
Chi-Squared	3	2

In all stations, it has been observed that the LP-III method generated more significant discharges with respect to the EV1 at 1.05, 1.11, and 1.25-year return periods. In contrast, the EV1 method yields greater outcomes compared to the LP-III method when analysing 2, 5, 10, and 25-year return periods. However, at 50, 100, and 200-year periods, LP3 delivers greater discharges than EV1. At the downstream location A9H012, there was a resemblance in the pattern where the discharges calculated utilizing the EV1 method at different return periods are greater in comparison to those calculated using the LP-III method. The Flood Frequency Analysis (FFA) carried out in the study indicated noteworthy outcomes, with the maximum flood discharges escalating from the upstream to downstream owing to the contributions made by the tributaries. The contribution of the significant Latonyanda River, originating from the Soutpansberg Mountain, supports this finding as reported by (Odiyo et al., 2012). Moreover, Section 4.8 indicates that the Lotanyanda area receives high amount of rainfall. There has been an increase in the number of tropical cyclones reported in the last decade. This may associated with the impacts of climate change (Murakami et al., 2020, Knutson et al., 2021). According to Nicholson (2017), it is projected that the occurrence and severity of tropical storms in the Indian Ocean will escalate as a result of global warming. Plate 5.1 shows a flooded Luvuvhu River at gauging station A9H012 in Mhinga Village.

Plate 5.1: Flooded weir in Mhinga Village (A9H012)

The extensive study period has illustrated a noteworthy and statistically significant increase in the yearly peak streamflow, as depicted in Figure 5.8. This upward trend is displayed in the accompanying figures 5.9 and 5.11, which complement Table 5.5 by portraying a consistent and progressive rise in the maximum streamflow data across multiple years of observation. The elevated streamflow levels observed over this duration could potentially entail major consequences for effective water administration, resource allocation, and the crucial prevention of flooding in the locality, as municipalities and environmental agencies may need to reevaluate their existing strategies considering these significant changes.

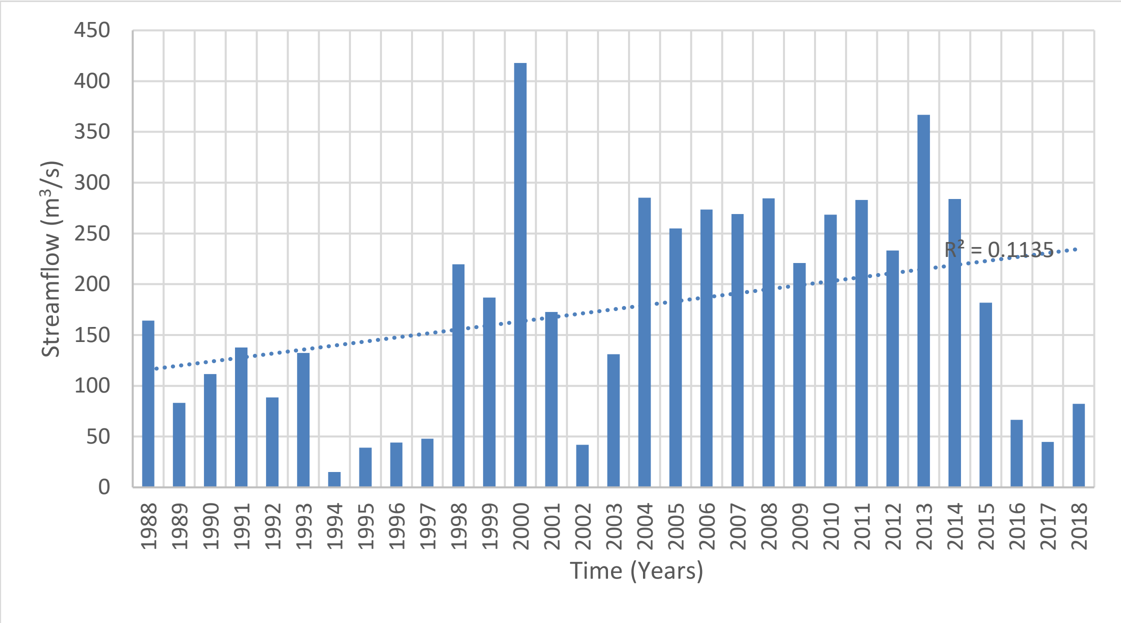

Figure 5.8: Annual maximum daily streamflow observed in the LRC during 1961-2018

Table 5.5: Computed statistical parameters for annual maximum daily streamflow

Station	**Statistical parameter**	**Computed value**	**Logarithmic transformation**
A9H003	Sum ($\sum x$)	712.53	46.70
	Mean ($\bar{x}$)	12.29	0.80
	standard deviation	22.35	0.47
	skewness coefficient	5.46	0.40
A9H006	Sum ($\sum x$)	292.41	12.61
	Mean ($\bar{x}$)	5.04	0.22
	standard deviation	6.24	0.85
	skewness coefficient	1.74	-0.87
A9H012	Sum ($\sum x$)	3670.45	60.51
	Mean ($\bar{x}$)	114.70	1.89
	standard deviation	105.19	0.42
	skewness coefficient	1.89	-0.51
A9H013	Sum ($\sum x$)	1688.19	46.67
	Mean ($\bar{x}$)	54.46	1.51
	standard deviation	57.86	0.48
	skewness coefficient	1.69	-0.28

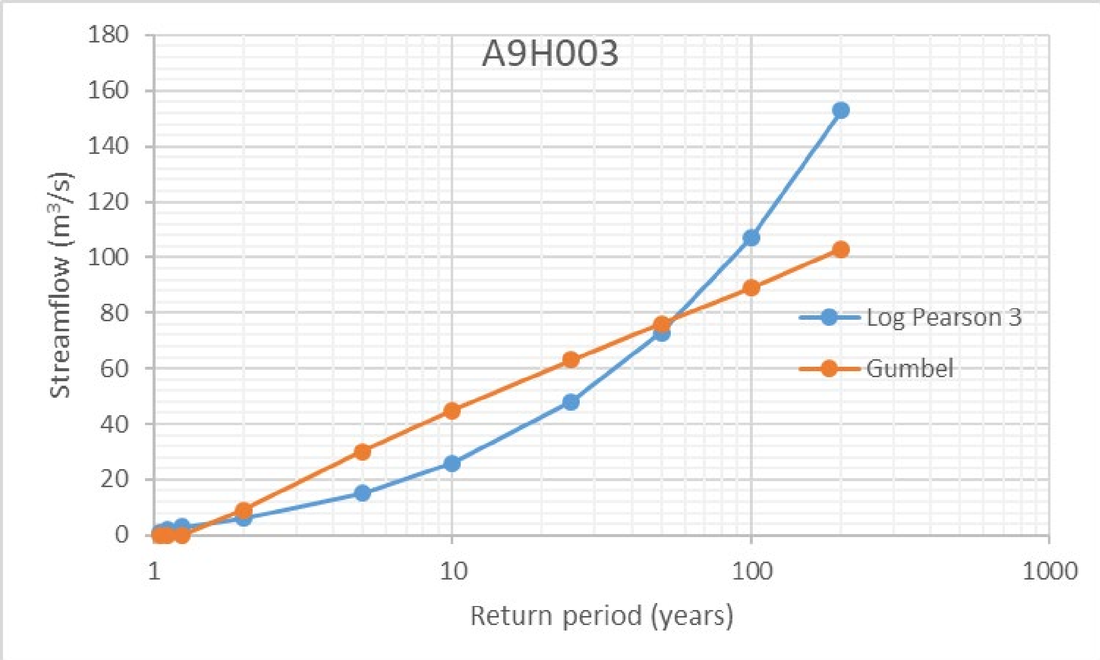

Figure 5.9: Streamflow return periods and corresponding flood magnitude for station A9H004

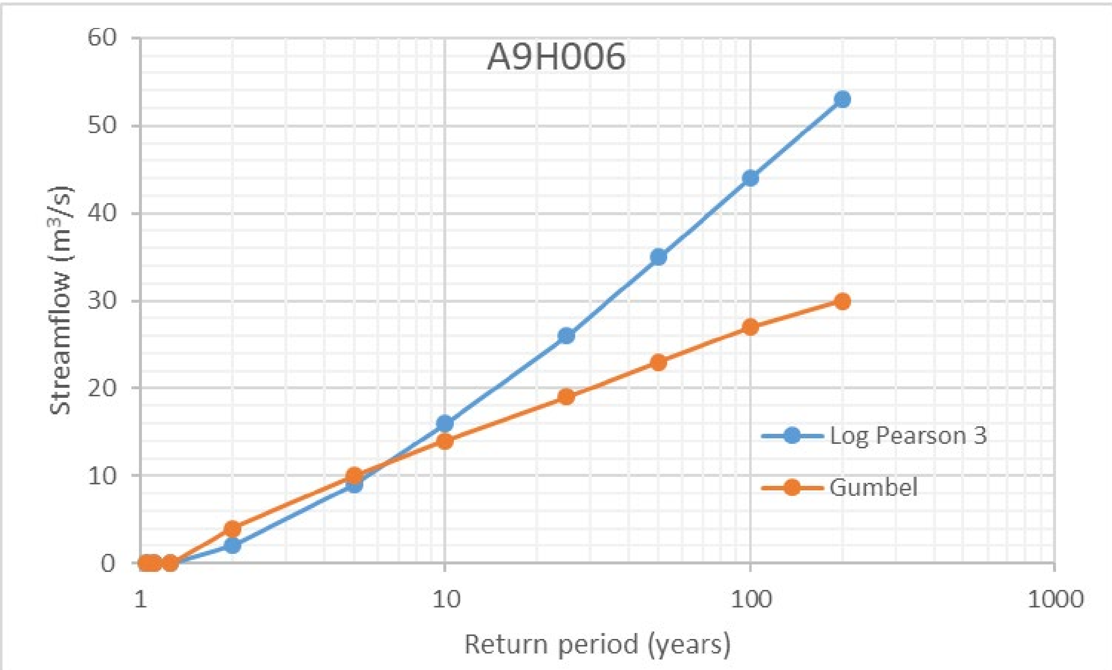

Figure 5.9: Streamflow return periods and corresponding flood magnitude for station A9H006

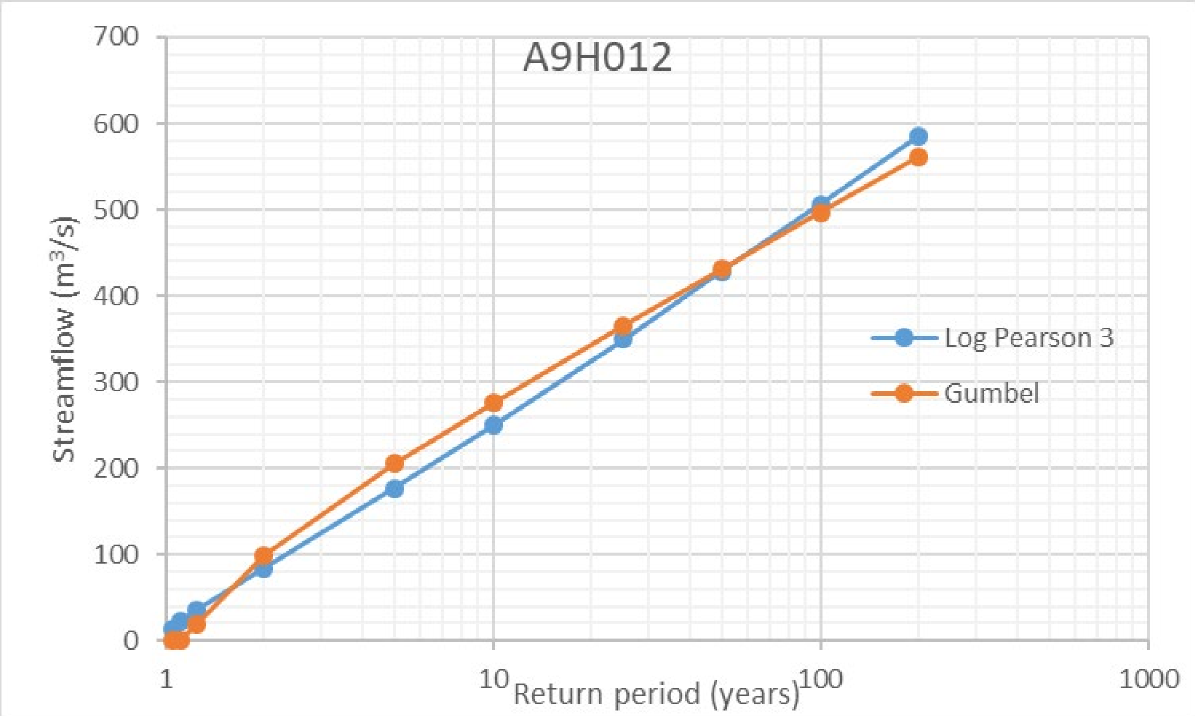

Figure 5.10: Streamflow return periods and corresponding flood magnitude for station A9H012

5.4 Summary of the chapter

The reason for discussing the consequences of droughts and floods in this chapter was to show how they behave in relation to one another. In general, the study found significant year-to-year variability, suggesting that the entire LRC is extremely sensitive to drought and flooding. The results show that the data of both rainfall and streamflow fall below significant drought and flood thresholds. The results also showed that the LRC is vulnerable to flash flooding. In addition, the applicability of using SPI, SPEI and SDI as drought indicators was tested and found suitable for this study. This information is seriously required by disaster response teams in the study area. Thus, drought and flood analysis are becoming increasingly important for water resource managers, policymakers and users as global water supplies approach crisis proportions. Thus, valuable insights into the impact of climate change on water availability and the potential risks associated with extreme weather events are gained.

CHAPTER SIX: SPATIAL-TEMPORAL ARIDITY INDICES AND IMPACTS ON WATER RESOURCES

6.1 Preamble

This chapter presents and discusses the LRC's aridity indices determined using the UNEP Aridity Index. Spatial-temporal maps for various decades were created using historical and future projections. The areas covered by each class of aridity index are discussed. Furthermore, the trends of aridity indices are investigated as well as impacts on water resources.

6.2 Temporal trends and variation of aridity

Figure 6.1 shows the historical annual aridity indices for the stations used in the study. The figure shows there is a distinction among the stations. The individual plots for the stations are presented in Appendix 6. The results show that there are stations that experience evapotranspiration which is lesser than that the amount of precipitation received most part of the study period. The arid indices of most virtual stations decreased from 0.5 in the 1960's to 0.35 in the 1990's and decreased over the decades used in the study. A decrease in the aridity index indicates a move toward drier (arid) conditions. The number of stations with an increased aridity index was relatively small. However, precipitation may not have decreased significantly during the period under study. Temperature, which is the main input into potential evapotranspiration, has increased significantly, as shown in section 4.3 of Chapter 4. This resulted to an increase in the number of stations with a decrease in the aridity index. Most of the stations were classified as semi-arid. Overall, there is a downward trend in the study area since majority of stations had negative Sen’s slope in the historical records used in the study.

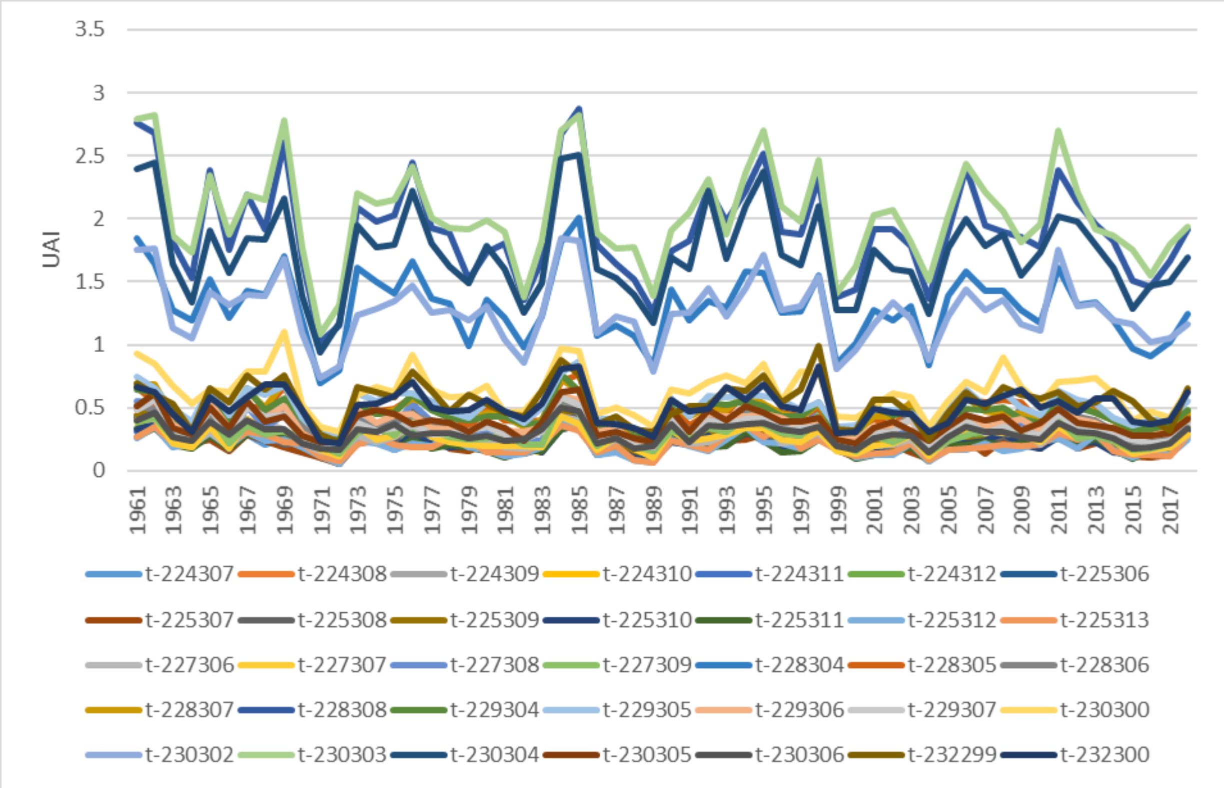

Figure 6.1: Aridity indices for the virtual stations used in the study

Table 6.1 shows the MK trend test and Sen's slope results of the annual aridity indices for all the virtual stations used in the study for the historical period (1961-2020). The results showed that there is a statistically significant (P<0.05 level) decrease in aridity indices of almost all the stations except for station t-227306 that did not show a clear trend. It can be inferred that certain factors within the locality may be influencing the level of aridity in that particular area where the station is located. However, the latter station did not show an overall increase. This suggests that there is an increase in evapotranspiration. The results are in line with the findings by Chai et al. (2021) that reported an increase in aridity of most parts of the world including Southern Africa. This will favour changes in the availability of water resulting in other environmental challenges such land degradation amongst others.

Table 6.1: Mann Kendall trend test and Sen’s slope

Series\Test	Kendall's tau	p-value	Sen's slope
t-224307	-0.156	<0.0001	-0.001
t-224308	-0.173	<0.0001	-0.001
t-224309	-0.176	<0.0001	-0.001
t-224310	-0.080	0.006	-0.001
t-224311	-0.102	0.001	-0.001
t-224312	-0.162	<0.0001	-0.001
t-225306	-0.131	<0.0001	-0.001
t-225307	-0.160	<0.0001	-0.001
t-225308	-0.174	0.021	-0.001
t-225309	-0.192	<0.0001	-0.001
t-225310	-0.155	<0.0001	-0.001
t-225311	-0.113	0.001	-0.001
t-225312	-0.162	<0.0001	-0.001
t-225313	-0.159	<0.0001	-0.001
t-227306	-0.119	0.114	-0.001
t-227307	-0.140	<0.0001	-0.001
t-227308	-0.171	<0.0001	-0.001
t-227309	-0.185	<0.0001	-0.001
t-228304	-0.199	<0.0001	-0.004
t-228305	-0.126	<0.0001	-0.001
t-228306	-0.143	<0.0001	-0.001
t-228307	-0.184	<0.0001	-0.002
t-228308	-0.124	<0.0001	-0.004
t-229304	-0.172	<0.0001	-0.002
t-229305	-0.186	<0.0001	-0.002
t-229306	-0.167	<0.0001	-0.001
t-229307	-0.191	<0.0001	-0.001
t-230300	-0.152	<0.0001	-0.002
t-230302	-0.164	<0.0001	-0.003
t-230303	-0.130	<0.0001	-0.004
t-230304	-0.105	<0.0001	-0.003
t-230305	-0.126	<0.0001	-0.001
t-230306	-0.196	<0.0001	-0.001
t-232299	-0.103	<0.0001	-0.001
t-232300	-0.085	0.000	-0.001

6.3 Spatial variation of aridity

Temporal aridity maps for the study area in Figure 6.2. It shows that the upper reaches of the catchment experience lower potential evapotranspiration while the lower reaches experience higher evapotranspiration. This graphic illustrates the results for the spatial distribution of the aridity indices in the study area. The map displays the different levels of aridity across the LRC, with warmer colours indicating areas with higher aridity and cooler colours representing areas with lower aridity. The results provide valuable insights into the climatic conditions of the region and can inform future research and planning endeavours. Figure 6.2 further revealed an interesting statistic, as it showed that about 60% of the stations analysed were classified as arid or semi-arid. This means that most of the locations studied experience limited rainfall and have dry climates, which can pose challenges for agriculture and other industries that rely on water availability. However, it is important to note that these classifications can change over time due to natural factors such as climate change or human activities like deforestation. Only a small percentage of the stations had an aridity index greater than 1, indicating they were humid. This suggests that higher temperatures are occurring in the lower elevations of the catchment, so the lower reaches experience higher potential evapotranspiration.

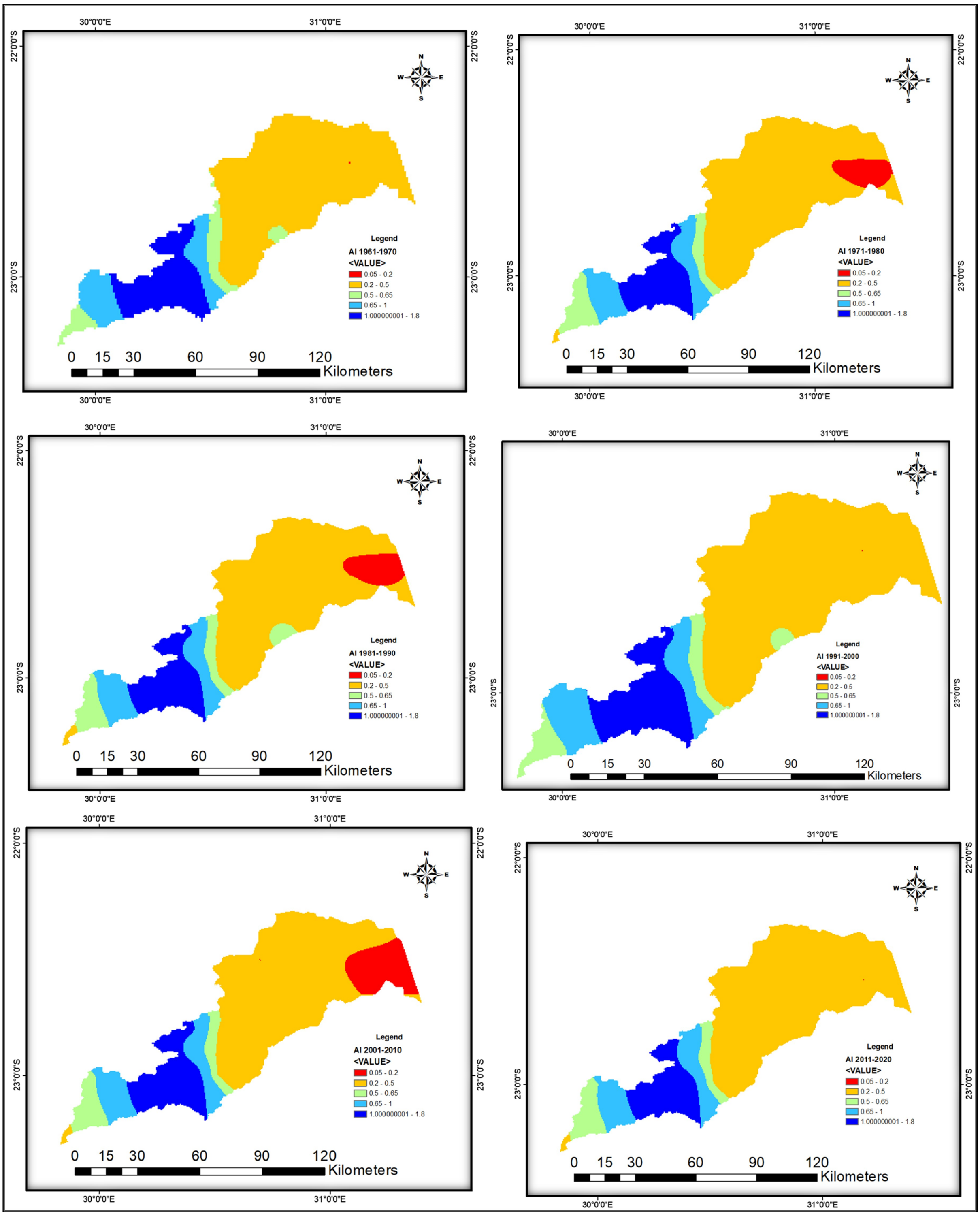

Figure 6.2: Temporal aridity in the study area based on decades

There has been a significant increase in the area covered by lower aridity indices in the LRC i.e. semi-arid and arid (Table 6.2). This means that the region is experiencing more prolonged periods of low rainfall, leading to higher aridity levels.

The impact of this change could have severe consequences for the region's natural ecosystems and its inhabitants, including farmers and other rural communities.

Table 6.2: Area covered by aridity indices in LRC in percentage

Aridity index	Area covered (%)					
	1960s	1970s	1980s	1990s	2000s	2010s
Arid	0.08	4.90	5.39	0.00	9.95	0.00
Semi-arid	69.01	69.18	69.37	68.04	66.82	72.21
Dry sub-humid	5.81	5.72	5.55	6.04	3.37	4.21
Sub-humid	9.86	9.59	9.26	12.29	7.91	11.78
Humid	15.23	10.60	10.44	13.63	11.95	11.80
Total	100.00	100.00	100.00	100.00	100.00	100.00

Figure 6.2 shows that decadal aridity line from the 2000 to 2010 is always below the line from 1991 to 2000. Since the lower value denotes a drier region, this suggests that aridity also scatters in pattern. Relatively low values of all aridity indices increased from 1991 to 2010, indicating that aridity is increasing in pattern.

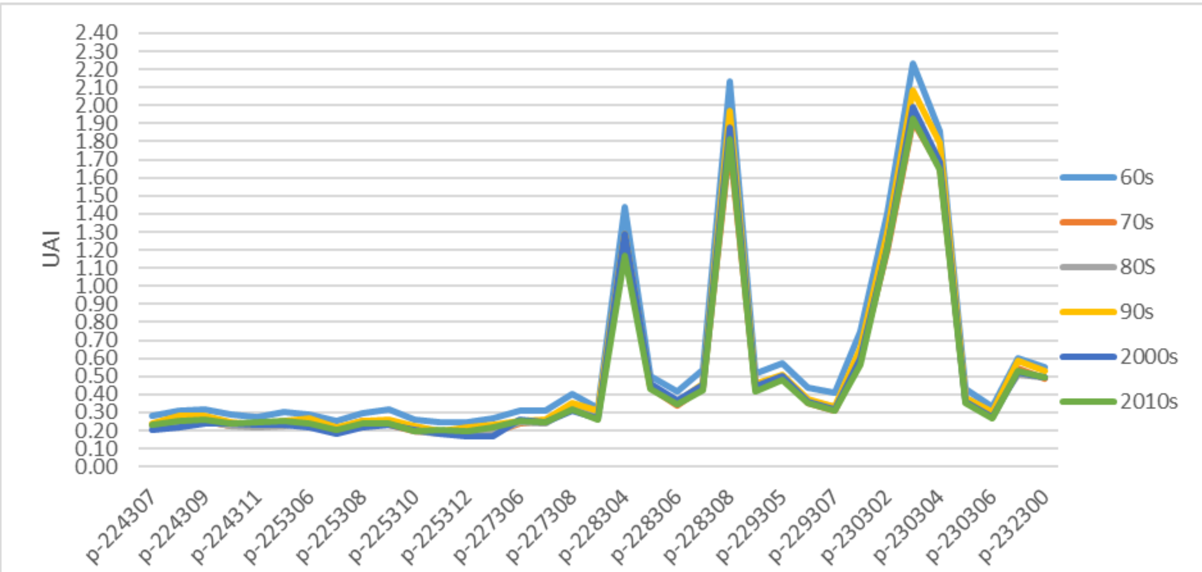

Figure 6.3: Decadal aridity in the study area for historical records

Figure 6.4 shows that the projected arid indices for the LRC for a period of 50 years between 2020 and 2070. Appendix 7 shows plots for individual stations for the projected aridity in the LRC. In Figure 6.4, the projected arid indices for the LRC, which have been calculated for a period of 50 years between 2020 and 2070 ae presented. These indices are a measure of the dryness of an area, and in this case, the LRC region is expected to experience a significant increase in aridity over the next five decades. However, some decades within the projected period will experience an increase in aridity. This may not last longer as there is a great deal of alternative behaviour of the climatic conditions. The trend of arid indices in LRC further confirms that the area will high ETo (Table 6.3).

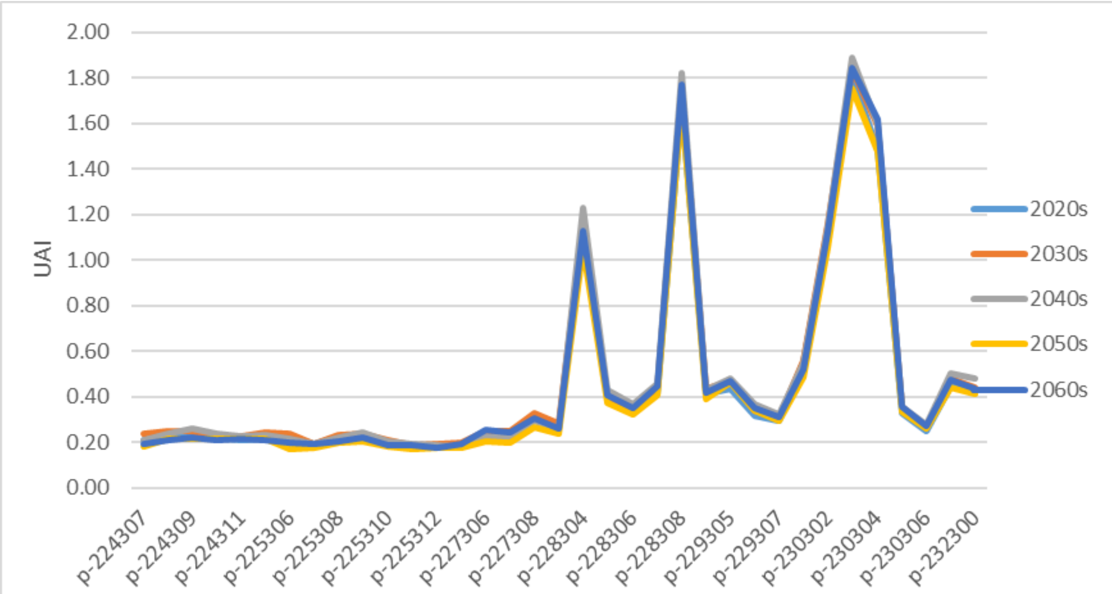

Figure 6.4: Projected decadal aridity in the study area for historical records

Table 6.3: Projected area covered by aridity indices in LRC

Aridity index	Area covered (%)				
	2020s	2030s	2040s	2050s	2060s
Arid	10.10	3.38	7.74	16.85	14.83
Semi-arid	60.98	69.52	63.96	57.06	61.44
Dry sub-humid	6.53	6.40	6.06	5.05	7.07
Sub-humid	10.10	8.42	11.29	11.45	7.74
Humid	12.29	12.29	10.94	9.59	8.92
Total	100	100	100	100	100

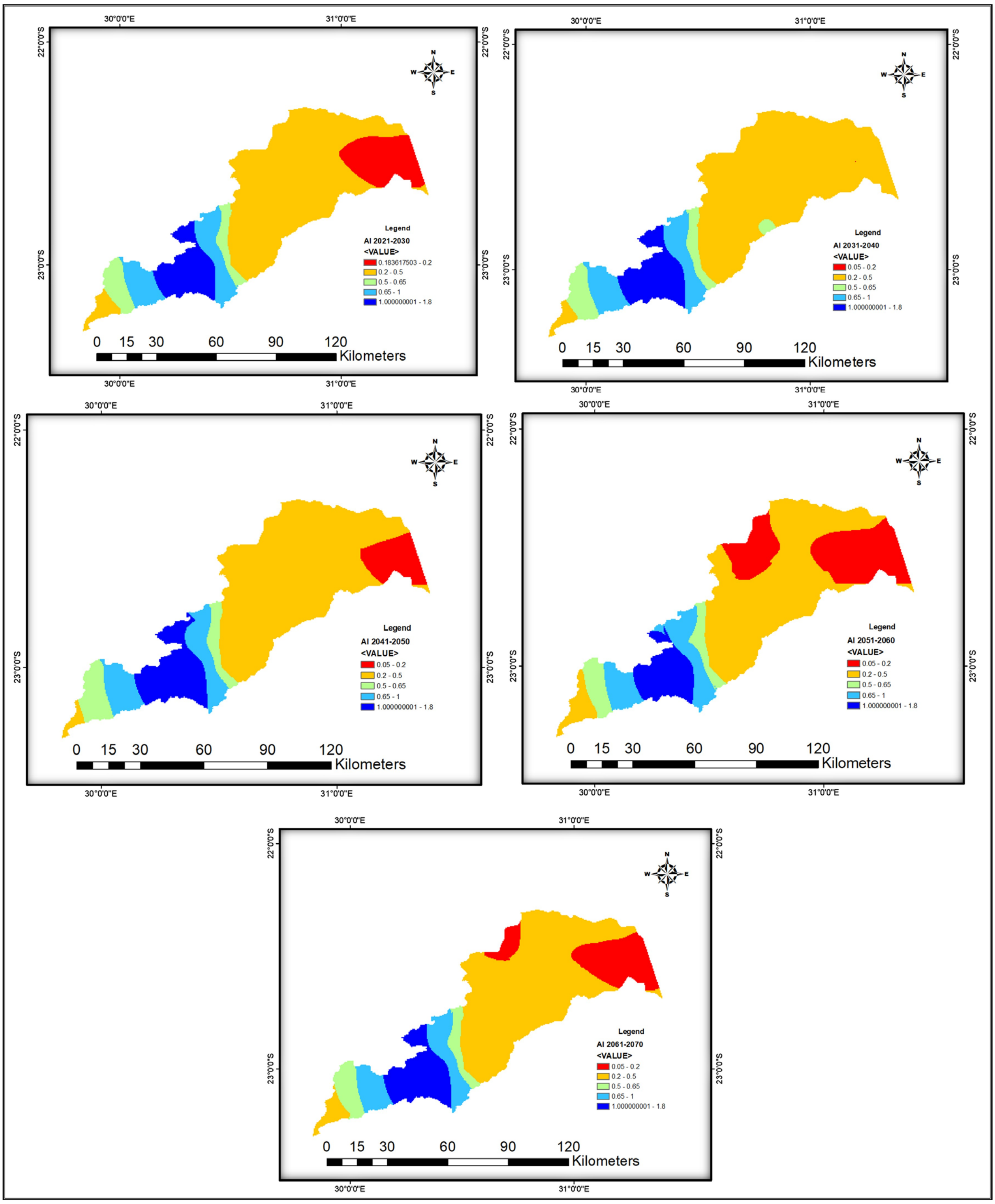

Figure 6.5: Projected aridity for the LRC

Table 4.6 shows that the trend of arid indices in the LRC is an additional piece of evidence that supports the prediction that the area will continue to experience high evapotranspiration rates (ETo). This is in agreement with the study by Mathivha and Mbatha (2022) which found that the LRC has factors favourable for high evaporation rates. This trend, which is indicated by a decrease in the amount of moisture available in the atmosphere, is likely to have significant implications for local ecosystems and water management strategies. Therefore, it is important for researchers and policymakers to closely monitor these trends and develop appropriate responses to address any potential challenges that may arise.

Table 6.4: Mann Kendall trend test and Sen's slope for projected arid indices

Series\Test	Kendall's tau	p-value	Sen's slope
t-224307	-0.136	0.001	-0.001
t-224308	-0.096	0.001	-0.001
t-224309	-0.064	0.035	0.000
t-224310	-0.016	0.637	0.000
t-224311	0.019	0.516	0.000
t-224312	-0.055	0.033	0.000
t-225306	-0.131	0.001	-0.001
t-225307	-0.060	0.123	-0.001
t-225308	-0.096	0.002	-0.001
t-225309	-0.050	0.073	0.000
t-225310	-0.007	0.824	0.000
t-225311	-0.025	0.440	0.000
t-225312	-0.033	0.426	0.000
t-225313	-0.017	0.637	0.000
t-227306	-0.043	0.410	0.000
t-227307	0.006	0.909	0.000
t-227308	-0.055	0.167	0.000
t-227309	-0.069	0.046	-0.001
t-228304	-0.066	0.112	-0.001
t-228305	-0.002	0.969	0.000
t-228306	0.045	0.348	0.001
t-228307	0.060	0.137	0.001
t-228308	0.038	0.322	0.002
t-229304	-0.012	0.743	0.000
t-229305	0.040	0.340	0.001
t-229306	0.071	0.069	0.001
t-229307	0.033	0.339	0.000
t-230300	-0.113	0.000	-0.001
t-230302	-0.014	0.716	0.000
t-230303	0.002	0.960	0.000
t-230304	0.050	0.233	0.001
t-230305	0.030	0.414	0.000
t-230306	0.037	0.278	0.000
t-232299	-0.012	0.740	0.000
t-232300	-0.011	0.800	0.000

6.4 Impacts on water resources

The impacts of aridity are closely tied to the amount of rainfall and streamflow. When there is a lack of rainfall and decreased streamflow, aridity can lead to soil erosion, reduced crop yields, and decreased water availability for human consumption, industrial activities, and wildlife habitats. This can ultimately result in a cycle of drought and desertification, negatively affecting the environment and communities that depend on it.

The upstream areas, located at the beginning of a river system, have a significantly lower level of aridity when compared to the midstream and downstream regions. This is because the upstream areas are in the high rainfall zone and closer to the source of the water, and the water is still in its more natural state. As the water moves downstream, it becomes more affected by the surrounding environment, which can lead to changes in aridity levels.

Examining environmental changes reveals that aridity is not the only factor affecting water resource availability. Seasonal rainfall patterns, temperature fluctuations, and human activities also play significant roles in determining water access for consumption, agriculture, and ecosystem health. Recognizing these factors is essential for effective water management, allowing policymakers and scientists to develop strategies that address water scarcity, promote sustainable use, and enhance ecosystem resilience in the face of climate change. Trends in rainfall and streamflow also exhibit comparable patterns, which imply a broader transformation in the ecosystem. Such changes may have noteworthy consequences on the flora and fauna, in addition to affecting the accessibility of resources for human settlements dependent on these natural systems. The results of the study indicate low rainfall and streamflow variability (Table 4.1 and 4.5) in the upper reaches of the catchment. The mid and lower reaches are dominated by high rainfall variability (Figures 4.1 to 4.6 and Tables 4.1 to 4.3) and streamflow trends (Figures 4.10 to 4.13).

In addition to changes in the amount of rainfall, scientists predict that there will be significant alterations in rainfall patterns, including changes in intensity and frequency. These were also indicated by the results of the current study (Table 5.4).

These alterations in rainfall patterns can lead to more severe occurrences, such as heavy downpours and prolonged periods of rain. These changes can have far-reaching impacts on ecosystems, agriculture, and human societies, increasing flood risks, soil erosion, and water scarcity in certain regions. The changes in rainfall patterns can also affect the timing and availability of water resources.

Changes in temperature and rainfall patterns can have a profound impact on the amount of evapotranspiration that occurs, as well as the quality and quantity of the resulting runoff. These changes in water availability can vary both spatially and temporally, leading to significant fluctuations in the overall availability of water resources. As temperatures rise, evapotranspiration rates can increase, leading to greater water loss from the ecosystem. Additionally, changes in precipitation patterns can influence the amount of water that can infiltrate the soil and replenish groundwater supplies, further affecting the overall availability of water. Taken together, these factors highlight the complex relationship between changes in temperature and rainfall and the availability of water resources.

Figure 6.7 illustrates that the Standardized Drought Index (SDI) in the LRC reveals persistent drought patterns, characterised by moderate to severe drought conditions sustained over an extended duration. The level of aridity within a region serves as both a direct indicator and a predictive tool for assessing the extent of water availability. Conversely, the SDI exceeds the UNEP AI during prolonged drought periods and typical hydrological years. The UNEP AI significantly influences the long-term streamflow in water-stressed catchments. The correlation with the AI, with a value of -0.16. These important observations underscore critical trends in water scarcity and offer essential insights for managing water resources and formulating effective climate adaptation strategies. A comprehensive understanding of these patterns enables policymakers and water scientists to design targeted interventions, such as water conservation measures, drought-resistant crop varieties, and community-based water management programs, to alleviate the impacts of drought on agriculture, ecosystems, and local communities, thereby fostering a more sustainable management approach to vital water resources amidst the challenges posed by climate change.

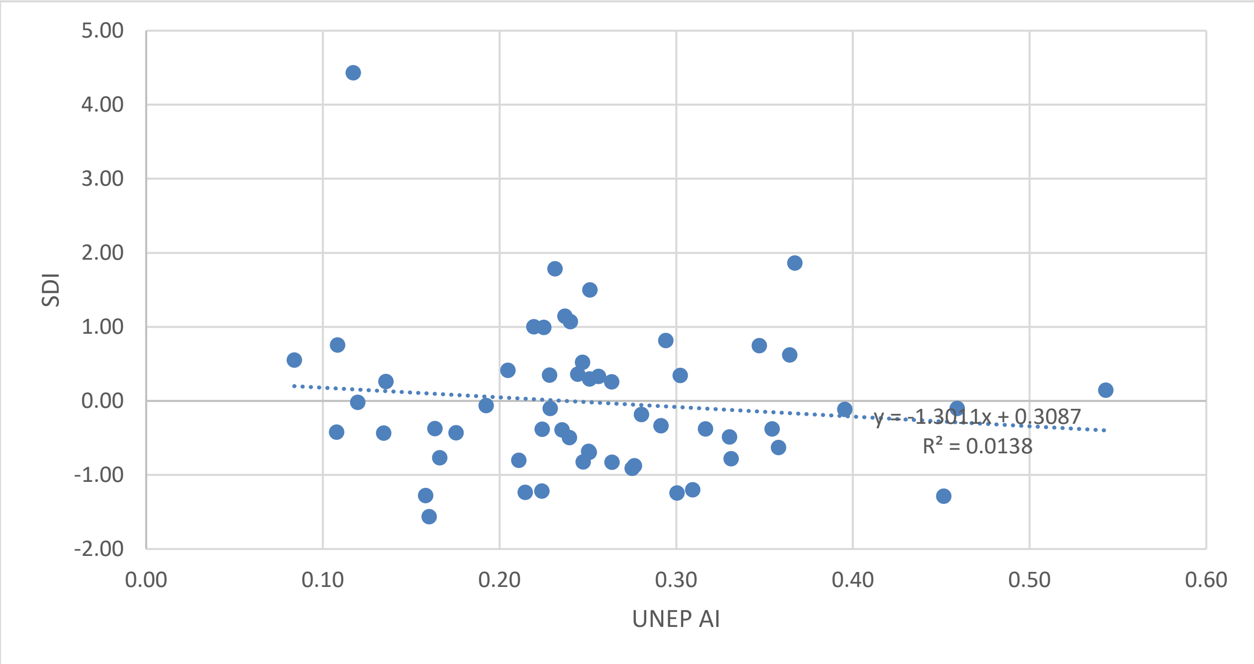

Figure 6.6: SDI versus UNEP AI

The impacts of aridity, characterised by a lack of precipitation and high evaporation rates, can significantly affect water resources. Aridity can decrease water availability for human consumption, agriculture, and natural ecosystems. It can also exacerbate water scarcity and increase the risk of droughts, impacting communities and economies. In addition, aridity can alter the quality of water resources, leading to higher concentrations of pollutants and other contaminants. These impacts highlight the importance of effective water management strategies in arid areas to ensure sustainable use of water resources.

Spatiotemporal variation of aridity is a factor that affects the availability of water resources in the LRC. With increased aridity, water resources become scarce, leading to depletion of groundwater reserves and a decrease in surface water flow. The impact of these variations is significant in the LRC, where water resources are already heavily stressed due to population growth and increased industrialisation. Spatiotemporal variation in drought also affects the quality of water resources by increasing the concentration of pollutants in water bodies. The impacts of these changes on water resources in LRCs are severe and have adverse consequences for agriculture, human consumption, and commercial activities. Therefore, it is necessary to understand the effects of spatiotemporal variation in drought on water resources in LRCs to develop sustainable strategies for water management and conservation.

A similar pattern of results was observed in the study of Lickley and Solomon (2018) that reported drying trends in Southern Africa. It showed that aridity was projected to exceed 10% of the 21st century. This suggests a potentially significant decrease in available water resources, which could have severe implications for the local ecosystems and communities that rely on them.

According to Banda et al. (2022) climate change is an undeniable threat to the stability of the hydrologic system sub-Saharan Africa. The country is already experiencing the effects of global warming through increased temperatures, erratic rainfall patterns, and prolonged droughts. These changes are putting immense pressure on the water resources in the region, affecting water availability, quality, and distribution. These findings are supported by a study by Wright et al. (2021) that revealed more significant warming in the Northern Cape Province and selected districts over Gauteng and Limpopo. Additionally, the frequency and intensity of extreme weather events such as floods and heatwaves have also increased, further exacerbating the vulnerability of the hydrologic system. In addition, the threat of water scarcity is imminent large, and the livelihoods of people who rely on agriculture and livestock are at risk.

6.5 Summary of the chapter

The aridity indices, both historical and projected, for the LRC were determined using the UNEP Aridity Index. Furthermore, spatial and temporal maps for various decades were analysed. The trends and variations of aridity indices are investigated, with a statistically significant decrease observed in almost all virtual stations except for one. Based on the results, it was evident that higher temperatures are occurring in the lower elevations of the catchment area. This, in turn, causes the lower reaches to experience higher potential evapotranspiration. Consequently, the aridity in the LRC is more concentrated in the downstream parts of the catchment. The area covered by humid conditions is decreasing substantially. Thus, indicating a shift towards drier and less humid conditions. The increase in aridity may lead to significant implications for the water resources availability.

CHAPTER SEVEN: CONCLUSIONS AND RECOMMENDATIONS

7.1 Conclusions

The main aim of this study was to determine aridity and impacts on water resources availability in the LRC. Several objectives were set wherein the first objective was to evaluate spatiotemporal interstation variability and trends using pentads and decadal window periods. This was achieved by indicating that there are two classes in the study area i.e. stations with high and stations with low rainfall amount. Some rainfall stations showed a decreasing trend, while others showed an increasing trend. Topography played a pivotal role in these classes, particularly orientation and aspect with a positive correlation coefficient compared to rainfall. The results have affirmed the strong relationship between rainfall distribution and the topography of the study area. The area's topography plays a significant role in influencing rainfall distribution, thereby impacting the overall hydrological processes of the LRC.

Both the Hierarchical Clustering (HC) and the Canonical Correlation Analysis (CCA) were used to study the association of rainfall and other physiographic features in the study area and the results of both methods were found to align and support each other, providing a robust and comprehensive analysis of the data. Thus, the LRC's rainfall is highly variable. Through conducting CCA, it has been confirmed that the topography heavily influences the distribution of rainfall in the study area. The results of this analysis indicate a strong dependence between these two factors, suggesting that changes in the topography may have a significant impact on the rainfall patterns in the region.

The second objective of the study was to assess variations and trends in rainfall, temperature and streamflow over 5-year or 10-year window periods. The findings revealed a significant increasing trend in temperature over time, suggesting a possible manifestation of climate change. Additionally, the study showed that there were noticeable fluctuations in streamflow patterns over the studied periods. The data collected and analysed revealed useful insights into the potential impact of climate change on water resource availability.

Determination of flood and drought thresholds, duration, extent/intensity and frequency in the study area was also performed. The study found significant year-to-year variability, suggesting that the entire LRC is extremely sensitive to drought and flooding. Several events were recorded in the drought history in 58 years from 1961 to 2018; this suggests that the drought occurred every 2 or 3 years on average. Determining floods and droughts in the study area is crucial to understanding the potential impacts of extreme weather events on the economy, environment and society. The study found significant year-to-year variability in floods and drought events, highlighting the need for longer-term monitoring and analysis to accurately assess trends and patterns over time. By identifying these extreme events and understanding their characteristics, policymakers and stakeholders can make informed decisions about land-use planning, infrastructure development and disaster preparedness in the face of climate change. The findings of this study provide valuable insights into the complex interplay between natural and human-driven factors that influence the environmental conditions of a region.

The fourth specific objective focused on determination of aridity indices in the study area. The considered study period shows that the study area falls in different categories of aridity ranging from arid to sub-humid. The fifth specific objective was to assess the impact of spatial-temporal variation of aridity on water resources in the LRC. The projected future conditions show that there will be an increase in arid aridity due to continuous increase in temperature. This shift in weather patterns significantly impacts ecosystems, agriculture, and human communities that rely on water resources. As the trend towards drier and less humid conditions continues, it is crucial that steps are taken to adapt and mitigate the impacts of these changes. There is a strong correlation between drought and aridity in the study area influencing the availability of water resources in the LRC.

7.2 Recommendations

This research study can help authorities and societies protect against flooding. Due to the increasing flood intensity, the return period must be revised for planning purposes. Infrastructure including roads and drainage networks must be properly managed to minimize damage associated with flooding. Further research works to be conducted on trend attribution. Further research will be necessary to fully understand the complex interactions such as at play in this environment.

The study's findings highlight the need for continued monitoring and research to better understand the impacts of climate change on local environments. This information can be valuable for policymakers and planners in the region to consider when designing long-term strategies for water management and land use. Thus, the study underscores the importance of continued research into the impacts of extreme weather events on vulnerable communities and ecosystems.

Further research to understand the complex relationship between climate, geography, and human activity in the study area should sought. Reliable information on the trends in temperature and streamflow is essential for policymakers and stakeholders to develop effective strategies to mitigate the impact of climate change and ensure sustainable use of natural resources. Thus, it is recommended that the monitoring network for hydrometeorological information should be expanded and extended in the LRC to whole area and long period, respectively. By utilizing technology for water resource monitoring and management, the LRC can be preserved as a productive and ecologically viable agricultural region for future generations.

The study highlights the importance of sustainable water management practices to mitigate the effects of drought and ensure the long-term availability of water resources. The potential effects of climate change on rainfall patterns in the region cannot be ignored. However, proactive management techniques can be employed to lessen these impacts. This has far-reaching ramifications for agriculture and water resource management.

REFERENCES

Abida, H. and Ellouze, M. 2008. Probability distribution of flood flows in Tunisia. *Hydrology and Earth System Sciences,* 12(3), 703-714. https://d-nb.info/1149720115/34

Abram, N. J., Henley, B. J., Sen Gupta, A., Lippmann, T. J., Clarke, H., Dowdy, A. J., Sharples, J. J., Nolan, R. H., Zhang, T. and Wooster, M. J. 2021. Connections of climate change and variability to large and extreme forest fires in southeast Australia. *Communications Earth & Environment,* 2(1), 1-17. https://doi.org/10.1038/s43247-020-00065-8

Adamo, S. B. and Crews-Meyer, K. A. 2006. Aridity and desertification: exploring environmental hazards in Jáchal, Argentina. *Applied Geography,* 26(1), 61-85. https://doi.org/10.1016/j.apgeog.2005.09.001

Agnew, C. 1991. Disaster in the arid realm. *Societies: Choices and Environments. Collins Educational, London*, 56-79.

Agnew, M. D. and Palutikof, J. P. 2000. GIS-based construction of baseline climatologies for the Mediterranean using terrain variables. *Climate research,* 14(2), 115-127. https://www.jstor.org/stable/24867279

Ahani, A., Mousavi Nadoushani, S. S. and Moridi, A. 2019. A hybrid regionalization method based on canonical correlation analysis and cluster analysis: a case study in northern Iran. *Hydrology Research,* 50(4), 1076-1095. https://doi.org/10.2166/nh.2019.105

Ahilan, S., O'sullivan, J. and Bruen, M. 2012. Influences on flood frequency distributions in Irish river catchments. *Hydrology and Earth System Sciences,* 16(4), 1137-1150. https://doi.org/10.5194/hess-16-1137-2012,2012.

Ahmed, K., Shahid, S., Wang, X., Nawaz, N. and Khan, N. 2019. Spatiotemporal changes in aridity of Pakistan during 1901–2016. *Hydrology and Earth System Sciences,* 23(7), 3081-3096. https://doi.org/10.5194/hess-23-3081-2019

Akpalu, W. and Hassan, R. M. 2009. *Climate variability and maize yield in South Africa: results from GME and MELE methods*, Intl Food Policy Res Inst. https://econpapers.repec.org/scripts/redir.pf?u=http%3A%2F%2Fwww.ifpri.or g%2Fsites%2Fdefault%2Ffiles%2Fpublications%2Fifpridp00843.pdf;h=repec:fpr:ifprid:843

Alam, A., Bhat, M. S., Farooq, H., Ahmad, B., Ahmad, S. and Sheikh, A. H. 2018. Flood risk assessment of Srinagar city in Jammu and Kashmir, India. *International Journal of Disaster Resilience in the Built Environment*. https://doi.org/10.1108/IJDRBE-02-2017-0012

Alexander, W. 2002. Statistical analysis of extreme floods. *Journal of the South African Institution of Civil Engineering= Joernaal van die Suid-Afrikaanse Instituut van Siviele Ingenieurswese,* 44(1), 20-25. https://saice.org.za/downloads/journal/vol44-1-2002/Alexander2.pdf

Allen, R. G., Pereira, L. S., Raes, D. and Smith, M. 1998. Crop evapotranspiration-Guidelines for computing crop water requirements-FAO Irrigation and drainage paper 56. *Fao, Rome,* 300(9), D05109. https://www.fao.org/4/X0490E/X0490E00.htm

Andersen, F. H. 2008. Hydrological modeling in a semi-arid area using remote sensing data. *Department of Geography and Geology, University of Copenhagen, Copenhagen*. https://www.researchgate.net/publication/234203308_Hydrological_Modelling_in_a_semi-arid_region_using_remote_sensing_data

Araghi, A., Martinez, C. J., Adamowski, J. and Olesen, J. E. 2018. Spatiotemporal variations of aridity in Iran using high-resolution gridded data. *International Journal of Climatology,* 38(6), 2701-2717. https://doi.org/10.1002/joc.5454

Archer, D. 1998. Flood frequency analysis. *Encyclopedia of Hydrology and Water*. https://doi.org/10.1007/1-4020-4497-6_86

Archer, E. R., Engelbrecht, F. A., Hänsler, A., Landman, W., Tadross, M. and Helmschrot, J. 2018. Seasonal prediction and regional climate projections for southern Africa. Klaus Hess Publishers. http://www.biodiversity-plants.de/biodivers_ecol/vol6.php

Arkian, F., Nicholson, S. E. and Ziaie, B. 2018. Meteorological factors affecting the sudden decline in Lake Urmia's water level. *Theoretical and Applied Climatology,* 131, 641-651.

Asfaw, A., Simane, B., Hassen, A. and Bantider, A. 2018. Variability and time series trend analysis of rainfall and temperature in northcentral Ethiopia: A case study in Woleka sub-basin. *Weather and climate extremes,* 19, 29-41. https://doi.org/10.1016/j.wace.2017.12.002

Asheesh, M. 2007. Allocating gaps of shared wáter resources (scarcity index): case study on Palestine-Israel. *Water resources in the Middle East.* Springer. https://doi.org/10.1007/978-3-540-69509-7_24

Ashraf, M. S., Ahmad, I., Khan, N. M., Zhang, F., Bilal, A. and Guo, J. 2021. Streamflow Variations in Monthly, Seasonal, Annual and Extreme Values Using Mann-Kendall, Spearmen's Rho and Innovative Trend Analysis. *Water Resources Management,* 35(1), 243-261. https://dx.doi.org/10.1007/s11269-020-02723-0

Ávila, Á., Guerrero, F. C., Escobar, Y. C. and Justino, F. 2019. Recent precipitation trends and floods in the Colombian Andes. *Water,* 11(2), 379. https://doi.org/10.3390/w11020379

Backeberg, G. and Viljoen, M. Drought management in South Africa. A workshop of the ICID working group on irrigation under drought and water scarcity, Tehran, Iran, 2003. 13-14. http://doi.org/10.22004/ag.econ.28071

Banda, V. D., Dzwairo, R. B., Singh, S. K. and Kanyerere, T. 2021. Trend analysis of selected hydro-meteorological variables for the Rietspruit sub-basin, South Africa. *Journal of Water and Climate Change,* 12(7), 3099-3123. https://doi.org/10.2166/wcc.2021.260

Banda, V. D., Dzwairo, R. B., Singh, S. K. and Kanyerere, T. 2022. Hydrological Modelling and Climate Adaptation under Changing Climate: A Review with a Focus in Sub-Saharan Africa. *Water,* 14(24), 4031. https://doi.org/10.3390/w14244031

Barnes, K. B., Morgan, J. and Roberge, M. 2001. Impervious surfaces and the quality of natural and built environments. *Baltimore: Department of Geography and Environmental Planning, Towson University.* https://citeseerx.ist.psu.edu/document?repid=rep1&type=pdf&doi=f8a7d8f4148029dca5a37cce9f7b67552ad6a95a

Basso, F., Bellotti, A., Bove, E., Faretta, S., Ferrara, A., Mancino, G., Pisante, M., Quaranta, G. and Taberner, M. Degradation processes in the Agri Basin: evaluating environmental sensitivity to desertification at basin scale. Indicators for assessing desertification in the Mediterranean. Proceedings of the International Seminar held in Porto Torres, Italy, 18-20 September, 1998, 2000. Nucleo Ricerca Desertificazion, University of Sassari, 131-145. https://doi.org/10.1016/S0341-8162(99)00062-4

Becerril-Piña, R. and Mastachi-Loza, C. A. 2021. Desertification: Causes and countermeasures. *Life on land*, 219-231. https://doi.org/10.1007/978-3-319-71065-5_81-1

Benaradj, A., Boucherit, H., Bouderbala, A. and Hasnaoui, O. 2022. Biophysical Effects of Evapotranspiration on Steppe Areas: A Case Study in Naâma Region (Algeria). *Climate Change in Asia and Africa: Examining the Biophysical and Social Consequences, and Society's Responses*, 3. http://doi.org/10.5772/intechopen.97614

Berdowski, J., Guicherit, R. and Heij, B. 2001. Dutch National Research Programme on Global Air Pollution and Climate Change: The Climate System. AA Balkema Publishers, Lisse, Exton, PA. https://doi.org/10.1201/9781003211266

Berndtsson, R. 1988. Temporal variability in spatial correlation of daily rainfall. *Water Resources Research,* 24(9), 1511-1517. https://doi.org/10.1029/WR024i009p01511

Bossong, C. 1999. *Overview and technical and practical aspects for use of geostatistics in hazardous-, toxic-, and radioactive-waste-site investigations*, US Department of the Interior, US Geological Survey. https://doi.org/10.3133/wri984145

Botkin, D. B. and Keller, E. A. 2010. *Environmental science: Earth as a living planet*, Wiley Global Education.

Bradley, R. S. and Diaz, H. F. 2021. Late Quaternary Abrupt Climate Change in the Tropics and Sub-Tropics: The Continental Signal of Tropical Hydroclimatic Events (THEs). *Reviews of Geophysics,* 59(4), e2020RG000732. https://doi.org/10.1029/2020RG000732

Brutsaert, W. and Stricker, H. 1979. An advection-aridity approach to estimate actual regional evapotranspiration. *Water resources research,* 15(2), 443-450. https://doi.org/10.1029/WR015i002p00443

Burić, D., Ivanović, R. and Milenković, M. 2018. Indicators of specificity of climate: The example of Podgorica (Montenegro). *Journal of the Geographical*

Institute" Jovan Cvijic", *SASA,* 68(3), 399-403. https://doi.org/10.2298/IJGI180423009B

Busari, O. 2008. Groundwater in the Limpopo Basin: occurrence, use and impact. *Environment, Development and Sustainability,* 10, 943-957. https://doi.org/10.1007/s10668-007-9094-3

Butt, M., Everard, D. and Geldenhuys, C. 1994. The distribution and composition of vegetation types in the Soutpansberg-Blouberg mountain complex. *Report FOR DEA-814 Forestek CSIR, Pretoria, South Africa*. https://doi.org/10.4102/koedoe.v50i1.125

Camberlin, P., Boyard-Micheau, J., Philippon, N., Baron, C., Leclerc, C. and Mwongera, C. 2014. Climatic gradients along the windward slopes of Mount Kenya and their implication for crop risks. Part 1: climate variability. *International Journal of Climatology,* 34(7), 2136-2152. http://doi.org/10.1002/joc.3427

Cammarano, D., Ceccarelli, S., Grando, S., Romagosa, I., Benbelkacem, A., Akar, T., Al-Yassin, A., Pecchioni, N., Francia, E. and Ronga, D. 2019. The impact of climate change on barley yield in the Mediterranean basin. *European Journal of Agronomy,* 106, 1-11. https://doi.org/10.1016/j.eja.2019.03.002

Carroll, N., Frijters, P. and Shields, M. A. 2009. Quantifying the costs of drought: new evidence from life satisfaction data. *Journal of Population Economics,* 22, 445-461. https://www.jstor.org/stable/40344739

Chai, R., Mao, J., Chen, H., Wang, Y., Shi, X., Jin, M., Zhao, T., Hoffman, F. M., Ricciuto, D. M. and Wullschleger, S. D. 2021. Human-caused long-term changes in global aridity. *npj Climate and Atmospheric Science,* 4(1), 65. https://doi.org/10.1038/s41612-021-00223-5

Cheung, A., Cabrera, C., Sarabandi, P., Nair, K., Kiremidjian, A. and Wenzel, H. 2008. The application of statistical pattern recognition methods for damage detection to field data. *Smart materials and structures,* 17(6), 065023. https://www.ipcc.ch/assessment-report/ar4/

Chikoore, H., Vermeulen, J. H. and Jury, M. R. 2015. Tropical cyclones in the mozambique channel: January–March 2012. *Natural Hazards,* 77, 2081-2095. https://doi.org/10.1007/s11069-015-1691-0

Chowdhury, A. 2018. Assessment of intensity and distribution of aridity over Bangladesh using different climate indices with GIS. *Climate change,* 4(16), 743-749. https://doi.org/10.1007/s00704-020-03339-5

Christensen, J. H. and Christensen, O. B. 2007. A summary of the PRUDENCE model projections of changes in European climate by the end of this century. *Climatic change,* 81(1), 7-30.

Clark, P. U., Webb, R. S. and Keigwin, L. D. 1999. *Mechanisms of global climate change at millennial time scales*, American geophysical union.

Clarke, B., Otto, F., Stuart-Smith, R. and Harrington, L. 2022. Extreme weather impacts of climate change: an attribution perspective. *Environmental Research: Climate,* 1(1), 012001.

Cline, W. R. 2007. *Global warming and agriculture: Impact estimates by country*, Peterson Institute. https://www.imf.org/external/pubs/ft/fandd/2008/03/pdf/cline.pdf

Daly, C., Neilson, R. P. and Phillips, D. L. 1994. A statistical-topographic model for mapping climatological precipitation over mountainous terrain. *Journal of Applied Meteorology and Climatology,* 33(2), 140-158. https://doi.org/10.1175/1520-0450(1994)033%3C0140:ASTMFM%3E2.0.CO;2

De Martonne, E. 1926. Une Nouvelle fonction climatologique. *L'Indice d'aridité. Paris: Impr. Gauthier-Villars*.

Dedekind, Z., Engelbrecht, F. A. and Van Der Merwe, J. 2016. Model simulations of rainfall over southern Africa and its eastern escarpment. *Water SA,* 42(1), 129-143. https://doi.org/10.4314/wsa.v42i1.13

Deniz, A., Toros, H. and Incecik, S. 2011. Spatial variations of climate indices in Turkey. *International Journal of climatology,* 31(3), 394-403. https://doi.org/10.1002/joc.2081

Dennis, H. and Nell, W. T. 2002. Precision irrigation in South Africa. http://ageconsearch.umn.edu/

Dieppois, B., Rouault, M. and New, M. 2015. The impact of ENSO on Southern African rainfall in CMIP5 ocean atmosphere coupled climate models. *Climate dynamics,* 45(9), 2425-2442. https://doi.org/10.1007/s00382-015-2480-x

Dlamini, T., Songsom, V., Koedsin, W. and Ritchie, R. J. 2022. Intensity, Duration and Spatial Coverage of Aridity during Meteorological Drought Years over Northeast Thailand. *Climate,* 10(10), 137. https://doi.org/10.3390/cli10100137

Döll, P. 2002. Impact of climate change and variability on irrigation requirements: a global perspective. *Climatic change,* 54(3), 269-293. https://doi.org/10.1023/A:1016124032231

Dube, T., Moyo, P., Ncube, M. and Nyathi, D. 2016. The impact of climate change on agro-ecological based livelihoods in Africa: A review. *Dube T, Moyo P, Mpofu M, Nyathi D (2016), The impact of climate change on agro-ecological based livelihoods in Africa: A review, Journal of Sustainable Development,* 9(1), 256-267. : http://dx.doi.org/10.5539/jsd.v9n1p256

Elbeltagi, A., Althobiani, F., Kamruzzaman, M., Shaid, S., Roy, D. K., Deb, L., Islam, M. M., Kundu, P. K. and Rahman, M. M. 2022. Estimating the standardized precipitation evapotranspiration index using data-driven techniques: A regional study of Bangladesh. *Water,* 14(11), 1764.

Elhag, M. M. 2006. *Causes and impact of desertification in the Butana area of Sudan.* University of the Free State.

Em-Dat 2019. EM-DAT Database. *Retrieved from EM-DAT: The International Disaster*

Databse. https://www.emdat.be/

England Jr, J. F., Cohn, T. A., Faber, B. A., Stedinger, J. R., Thomas Jr, W. O., Veilleux, A. G., Kiang, J. E. and Mason Jr, R. R. 2019. Guidelines for determining flood flow frequency—Bulletin 17C. US Geological Survey.

Faiz, M. A., Liu, D., Fu, Q., Sun, Q., Li, M., Baig, F., Li, T. and Cui, S. 2018. How accurate are the performances of gridded precipitation data products over Northeast China? *Atmospheric Research,* 211, 12-20. https://doi.org/10.1016/j.atmosres.2018.05.006

Falkenmark, M. 2013. The multiform water scarcity dimension. *Water Security.* Routledge. https://doi.org/10.1098/rsta.2012.0410

Field, C. B., Barros, V., Stocker, T. F. and Dahe, Q. 2012. *Managing the risks of extreme events and disasters to advance climate change adaptation: special report of the intergovernmental panel on climate change*, Cambridge University Press.

Forootan, E., Khaki, M., Schumacher, M., Wulfmeyer, V., Mehrnegar, N., Van Dijk, A. I., Brocca, L., Farzaneh, S., Akinluyi, F. and Ramillien, G. 2019. Understanding the global hydrological droughts of 2003–2016 and their relationships with teleconnections. *Science of the Total Environment,* 650**,** 2587-2604. https://doi.org/10.1016/j.scitotenv.2018.09.231

Frame, D. J., Rosier, S. M., Noy, I., Harrington, L. J., Carey-Smith, T., Sparrow, S. N., Stone, D. A. and Dean, S. M. 2020. Climate change attribution and the economic costs of extreme weather events: a study on damages from extreme rainfall and drought. *Climatic Change,* 162**,** 781-797.

Garrity, D. P., Akinnifesi, F. K., Ajayi, O. C., Weldesemayat, S. G., Mowo, J. G., Kalinganire, A., Larwanou, M. and Bayala, J. 2010. Evergreen Agriculture: a robust approach to sustainable food security in Africa. *Food security,* 2(3)**,** 197-214. https://doi.org/10.1007/s12571-010-0070-7

Gbetibouo, G. A. 2009. *Understanding farmers' perceptions and adaptations to climate change and variability: The case of the Limpopo Basin, South Africa*, Intl Food Policy Res Inst. https://oerafrica.org/sites/default/files/oldresources/38093/Understanding%20farmers'%20perceptions%20and%20adaptations%20to%20climate%20change%20and%20variability.pdf

Gentile, M., Courbin, F. and Meylan, G. 2013. Interpolating point spread function anisotropy. *Astronomy & Astrophysics,* 549**,** A1. https://doi.org/10.1051/0004-6361/201219739

Giorgi, F. 2002. Variability and trends of sub-continental scale surface climate in the twentieth century. Part II: AOGCM simulations. *Climate dynamics,* 18(8)**,** 693-708.

Govender, T., Dube, T. and Shoko, C. 2022. Remote sensing of land use-land cover change and climate variability on hydrological processes in Sub-Saharan Africa: Key scientific strides and challenges. *Geocarto International,* 37(25)**,** 10925-10949. https://doi.org/10.1080/10106049.2022.2043451

Greve, P., Orlowsky, B., Mueller, B., Sheffield, J., Reichstein, M. and Seneviratne, S. I. 2014. Global assessment of trends in wetting and drying over land. *Nature geoscience,* 7(10)**,** 716-721. https://doi.org/10.1038/ngeo2247

Greve, P., Roderick, M., Ukkola, A. and Wada, Y. 2019. The aridity index under global warming. *Environmental Research Letters,* 14(12), 124006. https://doi.org/10.1088/1748-9326/ab5046

Griscom, H. R., Miller, S. N., Gyedu-Ababio, T. and Sivanpillai, R. 2010. Mapping land cover change of the Luvuvhu catchment, South Africa for environmental modelling. *GeoJournal,* 75, 163-173. https://doi.org/10.1007/s10708-009-9281-x

Habeeb, R., Almazah, M. M., Hussain, I., Al-Ansari, N., Al-Rezami, A. and Sammen, S. S. 2023. Modified Standardized Precipitation Evapotranspiration Index: spatiotemporal analysis of drought. *Geomatics, Natural Hazards and Risk,* 14(1), 2195532.

Habib, E., Krajewski, W. F. and Ciach, G. J. 2001. Estimation of rainfall interstation correlation. *Journal of Hydrometeorology,* 2(6), 621-629. https://doi.org/10.1175/1525-7541(2001)002%3C0621:EORIC%3E2.0.CO;2

Hadji, F., Marok, A., Belmouhoub, A., Benaabidate, L., Dahmani, B. and Taleb, K. 2010. Water resources and its quality in arid and semi arid areas: the case of the NW of Algeria. *Water resources,* 16(1), 75-85.

Haghighatafshar, S., Becker, P., Moddemeyer, S., Persson, A., Sörensen, J., Aspegren, H. and Jönsson, K. 2020. Paradigm shift in engineering of pluvial floods: From historical recurrence intervals to risk-based design for an uncertain future. *Sustainable Cities and Society,* 61, 102317. https://doi.org/10.1016/j.scs.2020.102317

Haile, A. T. 2010. Rainfall variability and estimation for hydrologic modeling: a remote sensing based study at the source basin of the Upper Blue Nile river. https://doi.org/10.3990/1.9789061642862

Hanel, M., Rakovec, O., Markonis, Y., Máca, P., Samaniego, L., Kyselý, J. and Kumar, R. 2018. Revisiting the recent European droughts from a long-term perspective. *Scientific reports,* 8(1), 1-11. https://doi.org/10.1038/s41598-018-27464-4

Hare, J. D. 1983. Seasonal variation in plant-insect associations: Utilization of Solanum dulcamara by Leptinotarsa decemlineata. *Ecology,* 64(2), 345-361. https://doi.org/10.2307/1937081

Harouna, S. and Carlson, R. 1994. Analysis of an Iowa Aridity Index in relationship to climate and crop yield. *Journal of the Iowa Academy of Science: JIAS,* 101(1), 14-18. https://scholarworks.uni.edu/jias/vol101/iss1/5

Hayes, M. J., Svoboda, M. D., Wiihite, D. A. and Vanyarkho, O. V. 1999. Monitoring the 1996 drought using the standardized precipitation index. *Bulletin of the American meteorological society,* 80(3), 429-438. https://doi.org/10.1175/1520-0477(1999)080%3C0429:MTDUTS%3E2.0.CO;2

Heim Jr, R. R. 2015. An overview of weather and climate extremes–Products and trends. *Weather and Climate Extremes,* 10, 1-9. https://doi.org/10.1016/j.wace.2015.11.001

Hernandez, E. A. and Uddameri, V. 2014. Standardized precipitation evaporation index (SPEI)-based drought assessment in semi-arid south Texas. *Environmental Earth Sciences,* 71(6), 2491-2501. https://doi.org/10.1007/s12665-013-2897-7

Hoekstra, A. Y., Mekonnen, M. M., Chapagain, A. K., Mathews, R. E. and Richter, B. D. 2012. Global monthly water scarcity: blue water footprints versus blue water availability. *PloS one,* 7(2), e32688. https://doi.org/10.1371/journal.pone.0032688

Hoffman, T. and Ashwell, A. 2001. *Nature divided: land degradation in South Africa*, University of Cape Town Press.

Howlett, M. P. and Cuenca, J. S. 2017. The use of indicators in environmental policy appraisal: lessons from the design and evolution of water security policy measures. *Journal of Environmental Policy & Planning,* 19(2), 229-243.

Hulme, M. 2001. Climatic perspectives on Sahelian desiccation: 1973–1998. *Global Environmental Change,* 11(1), 19-29. https://doi.org/10.1016/S0959-3780(00)00042-X

Hunziker, S., Gubler, S., Calle, J., Moreno, I., Andrade, M., Velarde, F., Ticona, L., Carrasco, G., Castellón, Y. and Oria, C. 2017. Identifying, attributing, and overcoming common data quality issues of manned station observations. *International Journal of Climatology,* 37(11), 4131-4145. 10.1002/joc.5037

Illius, A. W. and O'connor, T. G. 1999. On the relevance of nonequilibrium concepts to arid and semiarid grazing systems. *Ecological applications,* 9(3), 798-813.

https://esajournals.onlinelibrary.wiley.com/doi/pdf/10.1890/1051-0761%281999%29009%5B0798%3AOTRONC%5D2.0.CO%3B2

Incoom, A. B. M., Adjei, K. A. and Odai, S. N. 2020. Rainfall variabilities and droughts in the savannah zone of Ghana from 1960-2015. *Scientific African,* 10, e00571. https://doi.org/10.1016/j.sciaf.2020.e00571

Ipcc 2001. *Climate Change 2001: The Scientific Basis. Contribution of Working Group Ito the Third Assessment Report of the*

Intergovernmental Panel on Climate Change, Cambridge, Cambridge University Press. https://www.ipcc.ch/site/assets/uploads/2001/04/doc3d.pdf

Jain, M., Kataria, S., Hirve, M. and Prajapati, R. 2019. Water deficit stress effects and responses in maize. *Plant Abiotic Stress Tolerance: Agronomic, Molecular and Biotechnological Approaches*, 129-151. https://link.springer.com/chapter/10.1007/978-3-030-06118-0_5

Joshi, S., Kumar, K., Joshi, V. and Pande, B. 2014. Rainfall variability and indices of extreme rainfall-analysis and perception study for two stations over Central Himalaya, India. *Natural hazards,* 72, 361-374. https://doi.org/10.1007/s11069-013-1012-4

Joubert, A., Mason, S. J. and Galpin, J. 1996. Droughts over southern Africa in a doubled-CO2 climate. *International Journal of Climatology,* 16(10), 1149-1156. https://doi.org/10.1002/(SICI)1097-0088(199610)16:10<1149::AID-JOC70>3.0.CO;2-V

Kabanda, T. A. 2004. *Climatology of Long-term Drought in the Nothern Region of the Limpopo Province of South Africa.* University of Venda.

Kalisa, W., Igbawua, T., Henchiri, M., Ali, S., Zhang, S., Bai, Y. and Zhang, J. 2019. Assessment of climate impact on vegetation dynamics over East Africa from 1982 to 2015. *Scientific reports,* 9(1), 1-20. https://doi.org/10.1038/s41598-019-53150-0

Kalumba, A., Olwoch, J., Van Aardt, I., Botai, O., Tsela, P., Nsubuga, F. and Adeola, A. 2013. Trend analysis of climate variability over the west bank-East London Area, South Africa (1975-2011). *Journal of Geography and Geology,* 5(4), 131. https://doi.org/10.5539/jgg.v5n4p131

Kampata, J. M., Parida, B. P. and Moalafhi, D. 2008. Trend analysis of rainfall in the headstreams of the Zambezi River Basin in Zambia. *Physics and Chemistry of* *the Earth, Parts A/B/C,* 33(8-13)**,** 621-625. https://doi.org/10.1016/j.pce.2008.06.012

Kenny, G., Ye, W., Flux, T. and Warrick, R. 2001. Climate variations and New Zealand agriculture: the CLIMPACTS system and issues of spatial and temporal scale. *Environment international,* 27(2-3)**,** 189-194. https://doi.org/10.1016/S0160-4120(01)00081-2

Kephe, P. N., Petja, B. M. and Kabanda, T. A. 2016. Spatial and inter-seasonal behaviour of rainfall in the Soutpansberg region of South Africa as attributed to the changing climate. *Theoretical and applied climatology,* 126**,** 233-245. https://doi.org/10.1007/s00704-015-1569-9

Keyantash, J. and Dracup, J. A. 2002. The quantification of drought: an evaluation of drought indices. *Bulletin of the American Meteorological Society,* 83(8)**,** 1167-1180. https://doi.org/10.1175/1520-0477-83.8.1167

Khorram-Manesh, A., Burkle Jr, F. M. and Goniewicz, K. 2024. Pandemics: past, present, and future: multitasking challenges in need of cross-disciplinary, transdisciplinary, and multidisciplinary collaborative solutions. *Osong Public Health and Research Perspectives,* 15(4)**,** 267.

Kizza, M., Rodhe, A., Xu, C.-Y., Ntale, H. K. and Halldin, S. 2009. Temporal rainfall variability in the Lake Victoria Basin in East Africa during the twentieth century. *Theoretical and applied climatology,* 98(1)**,** 119-135. https://doi.org/10.1007/s00704-008-0093-6

Knutson, T. R., Chung, M. V., Vecchi, G., Sun, J., Hsieh, T.-L. and Smith, A. J. 2021. Climate change is probably increasing the intensity of tropical cyclones. *Critical Issues in Climate Change Science, Science Brief Review,* 4570334. https://tyndall.ac.uk/wp-content/uploads/2023/10/ScienceBrief_Review_CYCLONES_Mar2021.pdf

Konapala, G., Mishra, A. K., Wada, Y. and Mann, M. E. 2020. Climate change will affect global water availability through compounding changes in seasonal precipitation and evaporation. *Nature Communications,* 11(1). https://dx.doi.org/10.1038/s41467-020-16757-w

Koster, R. D. and Suarez, M. J. 1999. A simple framework for examining the interannual variability of land surface moisture fluxes. *Journal of Climate,* 12(7), 1911-1917. https://doi.org/10.1175/1520-0442(1999)012%3C1911:ASFFET%3E2.0.CO;2

Kundu, P., Mathivha, F. and Nkuna, T. 2015. *The Use of GIS and Remote Sensing Techniques to Evaluate the Impact of Land Use and Land Cover Change on the Hydrology of Luvuvhu River Catchment in Limpopo Province: Report to the Water Research Commission*, Water Research Commission Pretoria, South Africa. https://www.wrc.org.za/wp-content/uploads/mdocs/2246-1-15.pdf

Kundzewicz, Z., Mata, L., Arnell, N., Döll, P., Kabat, P., Jiménez, B., Miller, K., Oki, T., Sen, Z. and Shiklomanov, I. 2007. Climate Change 2007: Impacts, Adaptation and Vulnerability. Contribution of working group II to the fourth assessment report of the intergovernmental panel on climate change. Cambridge University Press, Cambridge, UK. https://www.ipcc.ch/site/assets/uploads/2018/03/ar4_wg2_full_report.pdf

Kundzewicz, Z. W. and Kaczmarek, Z. 2000. Coping with hydrological extremes. *Water International,* 25(1), 66-75. https://doi.org/10.1080/02508060008686798

Kundzewicz, Z. W. and Robson, A. J. 2004. Change detection in hydrological records—a review of the methodology/revue méthodologique de la détection de changements dans les chroniques hydrologiques. *Hydrological sciences journal,* 49(1), 7-19. https://doi.org/10.1623/hysj.49.1.7.53993

Laity, J. J. 2009. *Deserts and desert environments*, John Wiley & Sons.

Lana, X., Serra, C. and Burgueño, A. 2001. Patterns of monthly rainfall shortage and excess in terms of the standardized precipitation index for Catalonia (NE Spain). *International Journal of Climatology: A Journal of the Royal Meteorological Society,* 21(13), 1669-1691.

Lickley, M. and Solomon, S. 2018. Drivers, timing and some impacts of global aridity change. *Environmental Research Letters,* 13(10), 104010. http://doi.org/10.1088/1748-9326/aae013

Liebmann, B., Hoerling, M. P., Funk, C., Bladé, I., Dole, R. M., Allured, D., Quan, X., Pegion, P. and Eischeid, J. K. 2014. Understanding recent eastern Horn of Africa rainfall variability and change. *Journal of Climate,* 27(23), 8630-8645. https://doi.org/10.1175/JCLI-D-13-00714.1

Lillesand, T., Kiefer, R. W. and Chipman, J. 2015. *Remote sensing and image interpretation*, John Wiley & Sons.

Liu, J., Yang, H., Gosling, S. N., Kummu, M., Flörke, M., Pfister, S., Hanasaki, N., Wada, Y., Zhang, X. and Zheng, C. 2017. Water scarcity assessments in the past, present, and future. *Earth's future,* 5(6), 545-559. https://doi.org/10.1002/2016EF000518

Lynch, S. and Schulze, R. 2006. Rainfall database. *South African atlas of climatology and agrohydrology. WRC report,* 1489(1), 06.

Maema, L. P., Potgieter, M. and Mahlo, S. M. 2016. Invasive alien plant species used for the treatment of various diseases in Limpopo Province, South Africa. *African Journal of Traditional, Complementary and Alternative Medicines,* 13(4), 223-231. https://doi.org/10.21010/ajtcam.v13i4.29

Magakane, R. 2019. *An integrated approach to groundwater exploration using remotely sensed imagery and geophysical techniques: a case study in the Archean basement and Karoo sedimentary basins of Limpopo Province of South Africa.*

Makarieva, A. M., Gorshkov, V. G. and Li, B.-L. 2013. Revisiting forest impact on atmospheric water vapor transport and precipitation. *Theoretical and Applied Climatology,* 111, 79-96. https://doi.org/10.1016%2Fj.heliyon.2022.e11173

Makungo, R. and Mashinye, M. D. 2022. Long-term trends and changes in rainfall magnitude and duration in a semi-arid catchment, South Africa. *Journal of Water and Climate Change,* 13(6), 2319-2336. https://doi.org/10.2166/wcc.2022.427

Malherbe, J., Dieppois, B., Maluleke, P., Van Staden, M. and Pillay, D. 2016. South African droughts and decadal variability. *Natural Hazards,* 80(1), 657-681. https://doi.org/10.1007/s11069-015-1989-

Malik, A., Kumar, A. and Singh, R. P. 2019. Application of heuristic approaches for prediction of hydrological drought using multi-scalar streamflow drought index. *Water Resources Management,* 33, 3985-4006.

Maliva, R. and Missimer, T. 2012. *Arid lands water evaluation and management*, Springer Science & Business Media. https://doi.org/10.1007/978-3-642-29104-3

Maliva, R., Missimer, T., Maliva, R. and Missimer, T. 2012. Aridity and drought. *Arid lands water evaluation and management*, 21-39. https://doi.org/10.1007/978-3-642-29104-3

Manatsa, D. and Matarira, C. 2009. Changing dependence of Zimbabwean rainfall variability on ENSO and the Indian Ocean dipole/zonal mode. *Theoretical and applied climatology,* 98(3), 375-396. https://doi.org/10.1007/s00704-009-0114-0

Mann, M. P., Rizzardo, J. and Satkowski, R. 2004. *Evaluation of methods used for estimating selected streamflow statistics, and flood frequency and magnitude, for small basins in north coastal California*, US Department of the Interior, US Geological Survey. https://doi.org/10.3133/sir20045068

Marani-Barzani, M., Eslamian, S., Amoushahi-Khouzani, M., Gandomkar, A., Rajaei-Rizi, F., Kazemi, M., Dehghan, S., Singh, V. P., Norouzi, H. and Shirvani-Dastgerdi10, H.-R. 2017. Assessment of aridity using geographical information system in zayandeh-roud basin, Isfahan, Iran. *International Journal of Mining Science,* 3(2), 49-61.

Martano, P., Elefante, C. and Grasso, F. 2015. Ten years water and energy surface balance from the CNR-ISAC micrometeorological station in Salento peninsula (southern Italy). *Advances in Science and Research,* 12(1), 121-125. https://doi.org/10.5194/asr-12-121-2015

Mason, J. A. and De Blij, H. 2016. *Physical geography: The global environment*, Oxford University Press.

Masoud, A. M., Pham, Q. B., Alezabawy, A. K. and El-Magd, S. a. A. 2022. Efficiency of geospatial technology and multi-criteria decision analysis for groundwater potential mapping in a Semi-Arid region. *Water,* 14(6), 882. https://doi.org/10.3390/w14060882

Mathivha, F. and Mbatha, N. 2022. Comparison of Long-Term Changes in Non-Linear Aggregated Drought Index Calibrated by MERRA–2 and NDII Soil Moisture Proxies. *Water,* 14(1), 26. https://doi.org/10.3390/w14010026

Mathivha, F., Sigauke, C., Chikoore, H. and Odiyo, J. 2020. Short-term and medium-term drought forecasting using generalized additive models. *Sustainability,* 12(10), 4006. https://doi.org/10.3390/su12104006

Mazibuko, S., Mukwada, G. and Moeletsi, M. 2021. Assessing the frequency of drought/flood severity in the Luvuvhu River catchment, Limpopo Province, South Africa. *Water SA,* 47(2), 172-184.

Mckee, T. B., Doesken, N. J. and Kleist, J. The relationship of drought frequency and duration to time scales. Proceedings of the 8th Conference on Applied Climatology, 1993. Boston, 179-183.

Mengistu, D., Bewket, W. and Lal, R. 2014. Recent spatiotemporal temperature and rainfall variability and trends over the Upper Blue Nile River Basin, Ethiopia. *International Journal of Climatology,* 34(7), 2278-2292. https://doi.org/10.1002/joc.3837

Millington, N., Das, S. and Simonovic, S. P. 2011. The comparison of GEV, log-Pearson type 3 and Gumbel distributions in the Upper Thames River watershed under global climate models. https://ir.lib.uwo.ca/wrrr/40

Misra, A. K. 2014. Climate change and challenges of water and food security. *International Journal of Sustainable Built Environment,* 3(1), 153-165. https://doi.org/10.1016/j.ijsbe.2014.04.006

Mmbando, G. A. and Kleyer, M. 2018. Mapping precipitation, temperature, and evapotranspiration in the Mkomazi River Basin, Tanzania. *Climate,* 6(3), 63. https://doi.org/10.3390/cli6030063

Molden, D. 2013. *Water for food water for life: A comprehensive assessment of water management in agriculture*, Routledge.

Molini, A. Understanding the link between aridity and hydrological extremes: Lessons from hyper-arid climates. EGU General Assembly Conference Abstracts, 2016. EPSC2016-5529.

Monashane, S. C. 2011. *Water supply and sanitation service delivery problems as Praktiseer, Limpopo Province.* North-West University. http://hdl.handle.net/10394/7315

Moorhead, J. E., Gowda, P. H., Singh, V. P., Porter, D. O., Marek, T. H., Howell, T. A. and Stewart, B. 2015. Identifying and evaluating a suitable index for agricultural drought monitoring in the Texas high plains. *JAWRA Journal of the American Water Resources Association,* 51(3), 807-820. https://doi.org/10.1111/jawr.12275

Moral, F. J., Rebollo, F. J., Paniagua, L. L., García-Martín, A. and Honorio, F. 2016. Spatial distribution and comparison of aridity indices in Extremadura, southwestern Spain. *Theoretical and Applied Climatology,* 126**,** 801-814. https://doi.org/10.1007/s00704-015-1615-7

Moreira, E. E., Martins, D. S. and Pereira, L. S. 2015. Assessing drought cycles in SPI time series using a Fourier analysis. *Natural Hazards and Earth System Sciences,* 15(3)**,** 571-585.

Mukwada, G., Mazibuko, S. M., Moeletsi, M. and Robinson, G. M. 2021. Can famine be averted? A spatiotemporal assessment of the impact of climate change on food security in the Luvuvhu River Catchment of South Africa. *Land,* 10(5)**,** 527. https://doi.org/10.3390/land10050527

Muli, J. M. 2014. *The impact of irrigated agriculture in dry lands on the natural environment: a case study of chala ward in taita taveta county, Kenya.* University of Nairobi. http://hdl.handle.net/11295/75298

Muller, M., Schreiner, B., Smith, L., Van Koppen, B., Sally, H., Aliber, M., Cousins, B., Tapela, B., Van Der Merwe-Botha, M. and Karar, E. 2009. Water security in South Africa. *Development Planning Division. Working Paper Series,* 12.

Murad, A., Baker, H., Mahmoud, S. and Gabr, A. 2010. Groundwater level prediction at a pilot area in southeastern part of the UAE using Shallow Seismic Method. *International Journal of Geological and Environmental Engineering,* 4(11)**,** 508-515. https://idc-online.com/technical_references/pdfs/civil_engineering/Groundwater%20Level.pdf

Murakami, H., Delworth, T. L., Cooke, W. F., Zhao, M., Xiang, B. and Hsu, P.-C. 2020. Detected climatic change in global distribution of tropical cyclones. *Proceedings of the National Academy of Sciences,* 117(20)**,** 10706-10714. https://doi.org/10.1073/pnas.1922500117

Musakwa, W., Wang, S., Wei, F., Malapane, O. L., Thomas, M. M., Mavengahama, S., Zeng, H., Wu, B., Zhao, W. and Nyathi, N. A. 2020. Survey of community livelihoods and landscape change along the Nzhelele and Levuvhu river catchments in Limpopo Province, South Africa. *Land,* 9(3)**,** 91. https://doi.org/10.3390/land9030091

Muthoni, F. K., Baijukya, F., Bekunda, M., Sseguya, H., Kimaro, A., Alabi, T., Mruma, S. and Hoeschle-Zeledon, I. 2019a. Accounting for correlation among environmental covariates improves delineation of extrapolation suitability index for agronomic technological packages. *Geocarto International,* 34(4)**,** 368-390. https://doi.org/10.1080/10106049.2017.1404144

Muthoni, F. K., Odongo, V. O., Ochieng, J., Mugalavai, E. M., Mourice, S. K., Hoesche-Zeledon, I., Mwila, M. and Bekunda, M. 2019b. Long-term spatial-temporal trends and variability of rainfall over Eastern and Southern Africa. *Theoretical and Applied Climatology,* 137**,** 1869-1882. https://doi.org/10.1007/s00704-018-2712-1

Ncongwane, K. P., Botai, J. O., Sivakumar, V., Botai, C. M. and Adeola, A. M. 2021. Characteristics and long-term trends of heat stress for South Africa. *Sustainability,* 13(23)**,** 13249. https://doi.org/10.3390/su132313249

Nicholls, N., Drosdowsky, W. and Lavery, B. 1997. Australian rainfall variability and change. *Weather,* 52(3)**,** 66-72. https://doi.org/10.1002/j.1477-8696.1997.tb06274.x

Nicholson, S. E. 2014. Spatial teleconnections in African rainfall: A comparison of 19th and 20th century patterns. *The Holocene,* 24(12)**,** 1840-1848.

Nicholson, S. E. 2015. Long-term variability of the East African 'short rains' and its links to large-scale factors. *International Journal of Climatology,* 35(13)**,** 3979-3990. https://doi.org/10.1002/joc.4259

Nicholson, S. E. 2017. Climate and climatic variability of rainfall over eastern Africa. *Reviews of Geophysics,* 55(3)**,** 590-635. https://doi.org/10.1002/2016RG000544

Nkuna, T. R. 2012. *Hydrological Variations and Trends and Links to Climate Change and Land Use in the Luvuvhi River Catchment, South Africa*.

Nkuna, T. R. and Odiyo, J. O. 2016. The relationship between temperature and rainfall variability in the Levubu sub-catchment, South Africa. *International Journal of Education and Learning Systems,* 1. https://www.iaras.org/iaras/filedownloads/ijes/2016/008-0011.pdf

Odiyo, J., Makungo, R., Nkuna, T. and Chikoore, H. 2020. Hydrological Modelling of Climate Change Impacts for Development of Adaptation Strategies: the Case of Luvuvhu River Catchment, Limpopo, South Africa. *Water Research*

Commission, Pretoria, South Africa. https://www.wrc.org.za/wp-content/uploads/mdocs/2771%20final.pdf

Odiyo, J., Phangisa, J. and Makungo, R. 2012. Rainfall–runoff modelling for estimating Latonyanda River flow contributions to Luvuvhu River downstream of Albasini Dam. *Physics and Chemistry of the Earth, Parts A/B/C,* 50**,** 5-13. https://doi.org/10.1016/j.pce.2012.09.007

Odiyo, J. O., Makungo, R. and Nkuna, T. R. 2015. Long-term changes and variability in rainfall and streamflow in Luvuvhu River Catchment, South Africa. *South African Journal of Science,* 111(7-8)**,** 1-9. http://dx.doi.org/10.17159/SAIS2015/20140169

Odiyo, J. O. and Maluleke, D. 2005. Flood risk on human settlement and agriculture along Luvuvhu River Basin. *Proceedings of the 12th SANCIAHS Conference*.

Oladipo, O. E. 1985. A comparative performance analysis of three meteorological drought indices. *Journal of Climatology,* 5(6)**,** 655-664. https://doi.org/10.1002/joc.3370050607

Orimoloye, I. R. 2023. Livelihood Vulnerability Assessment and Drought Events in South Africa. *Climate Change Impacts on Natural Resources, Ecosystems and Agricultural Systems.* Springer. https://doi.org/10.1007/978-3-031-19059-9_5

Palmer, W. C. 1965. *Meteorological drought*, US Department of Commerce, Weather Bureau.

Paltineanu, C., Tanasescu, N., Chitu, E. and Mihailescu, I. 2007. Relationships between the De Martonne aridity index and water requirements of some representative crops: A case study from Romania. *International agrophysics,* 21(1).

Parry, M. L., Canziani, O., Palutikof, J., Van Der Linden, P. and Hanson, C. 2007. *Climate change 2007-impacts, adaptation and vulnerability: Working group II contribution to the fourth assessment report of the IPCC*, Cambridge University Press.

Pellicciotti, F., Burlando, P. and Vliet, K. V. 2007. Recent trends in precipitation and streamflow in the Aconcagua River Basin, central Chile. *IAHS Publications-Series of Proceedings and Reports,* 318**,** 17-38.

Ponce, V. M. 1995. Management of droughts and floods in the semiarid Brazilian Northeast—The case for conservation. *Journal of soil and water conservation,* 50(5), 422-431.

Puertas Orozco, O. L., Carvajal Escobar, Y. and Quintero Angel, M. 2011. Study of monthly rainfall trends in the upper and Middle Cauca River basin, Colombia. *Dyna,* 78(169), 112-120.

Quesada-Hernandez, L. E., Calvo-Solano, O. D., Hidalgo, H. G., Perez-Briceno, P. M. and Alfaro, E. J. 2019. Dynamical delimitation of the Central American Dry Corridor (CADC) using drought indices and aridity values. *Progress in Physical Geography: Earth and Environment,* 43(5), 627-642. https://doi.org/10.1177/0309133319860224

Raulino, J. B., Silveira, C. S. and Lima Neto, I. E. 2021. Assessment of climate change impacts on hydrology and water quality of large semi-arid reservoirs in Brazil. *Hydrological Sciences Journal,* 66(8), 1321-1336. https://doi.org/10.1080/02626667.2021.1933491

Riddell, E., Boyd, L., Petersen, R. and Heath, R. 2022. Protected areas and the diffuse pollution problem: rivers of the Kruger National Park, South Africa. https://doi.org/10.2166/9781789061123_169

Riedel, T. and Weber, T. K. 2020. The influence of global change on Europe's water cycle and groundwater recharge. *Hydrogeology Journal,* 28(6), 1939-1959.

Rojas, O., Li, Y. and Cumani, R. 2014. *Understanding the drought impact of El Niño on the global agricultural areas: an assessment using FAO's Agricultural Stress Index (ASI)*, Food and Agriculture Organization of the United Nations (FAO).

Rossi, G. 2000. Drought mitigation measures: a comprehensive framework. *Drought and drought mitigation in Europe*, 233-246. https://doi.org/10.1007/978-94-015-9472-1_18

Ryu, Y., Lim, Y.-J., Ji, H.-S., Park, H.-H., Chang, E.-C. and Kim, B.-J. 2017. Applying a coupled hydrometeorological simulation system to flash flood forecasting over the Korean Peninsula. *Asia-Pacific Journal of Atmospheric Sciences,* 53, 421-430. https://doi.org/10.1007/s13143-017-0045-0

Salvati, L., Perini, L., Sabbi, A. and Bajocco, S. 2012. Climate aridity and land use changes: A regional-scale analysis. *Geographical Research,* 50(2), 193-203.

Schilling, J., Hertig, E., Tramblay, Y. and Scheffran, J. 2020. Climate change vulnerability, water resources and social implications in North Africa. *Regional Environmental Change,* 20, 1-12. https://doi.org/10.1007/s10113-020-01597-7

Schmittner, K.-E. and Giresse, P. 1996. Modelling and application of the geomorphic and environmental controls on flash flood flow. *Geomorphology,* 16(4), 337-347. https://doi.org/10.1016/0169-555X(96)00002-5

Schwalm, C. R., Glendon, S. and Duffy, P. B. 2020. RCP8. 5 tracks cumulative CO2 emissions. *Proceedings of the National Academy of Sciences,* 117(33), 19656-19657.

Scordo, A., Maltese, A., Ciraolo, G. and La Loggia, G. 2009. Estimation of the time lag occurring between vegetation indices and aridity indices in a Sicilian semi-arid catchment. *Ital. J. Remote Sens,* 41, 33-46.

Seager, R., Ting, M., Li, C., Naik, N., Cook, B., Nakamura, J. and Liu, H. 2013. Projections of declining surface-water availability for the southwestern United States. *Nature Climate Change,* 3(5), 482-486. https://doi.org/10.1038/nclimate1787

Seo, D., Lakhankar, T., Mejia, J., Cosgrove, B. and Khanbilvardi, R. 2013. Evaluation of Operational National Weather Service Gridded Flash Flood Guidance over the A rkansas R ed R iver B asin. *JAWRA Journal of the American Water Resources Association,* 49(6), 1296-1307. https://doi.org/10.1111/jawr.12087

Shaban, A., Awad, M., Ghandour, A. J. and Telesca, L. 2019. A 32-year aridity analysis: a tool for better understanding on water resources management in Lebanon. *Acta Geophysica,* 67, 1179-1189. https://doi.org/10.1007/s11600-019-00300-7

Shafer, B. and Dezman, L. Development of surface water supply index (SWSI) to assess the severity of drought condition in snowpack runoff areas. 1982. PROCEEDING OF THE WESTERN SNOW CONFERENCE.

Sharma, P. K. 2021. Ecology of Arid Zone Plants with Special Reference to North Eastern Region of Rajasthan and Methods to Conserve Them. https://doi.org/10.46501/IJMTST0711027

Sharma, S., Khadka, N., Hamal, K., Shrestha, D., Talchabhadel, R. and Chen, Y. 2020. How accurately can satellite products (TMPA and IMERG) detect precipitation patterns, extremities, and drought across the Nepalese Himalaya? *Earth and Space Science,* 7(8), e2020EA001315. https://doi.org/10.1029/2020EA001315

Shaw, R., Nguyen, H., Habiba, U. and Takeuchi, Y. 2011. Overview and characteristics of Asian monsoon drought. *Droughts in Asian monsoon region.* Emerald Group Publishing Limited.

Shikwambana, S., Malaza, N. and Shale, K. 2021. Impacts of Rainfall and Temperature Changes on Smallholder Agriculture in the Limpopo Province, South Africa. *Water,* 13(20), 2872. https://doi.org/10.3390/w13202872

Singo, L., Kundu, P., Odiyo, J., Mathivha, F. and Nkuna, T. 2012. Flood frequency analysis of annual maximum stream flows for Luvuvhu River Catchment, Limpopo Province, South Africa.

Smakhtin, V. U. and Hughes, D. 2004. Review, automated estimation and analyses of drought indices in South Asia.

Smakhtin, V. U. and Schipper, E. L. F. 2008. Droughts: The impact of semantics and perceptions. *Water Policy,* 10(2), 131-143. https://doi.org/10.2166/wp.2008.036

Smith, R. B. and Barstad, I. 2004. A linear theory of orographic precipitation. *Journal of the Atmospheric Sciences,* 61(12), 1377-1391. https://doi.org/10.1175/1520-0469(2004)061%3C1377:ALTOOP%3E2.0.CO;2

Smithers, J. and Schulze, R. 2004. The estimation of design rainfalls for South Africa using a regional scale invariant approach. *Water SA,* 30(4), 435-444. 10.4314/wsa.v30i4.5095

Srivastava, A., Grotjahn, R. and Ullrich, P. A. 2020. Evaluation of historical CMIP6 model simulations of extreme precipitation over contiguous US regions. *Weather and Climate Extremes,* 29, 100268. https://doi.org/10.1016/j.wace.2020.100268

Sun, L. 2009. *Blended drought indices for agricultural drought: risk assessment on the Canadian prairies.* Carleton University.

Sun, X., Li, R., Shan, X., Xu, H. and Wang, J. 2021. Assessment of climate change impacts and urban flood management schemes in central Shanghai. *International Journal of Disaster Risk Reduction,* 65, 102563. https://doi.org/10.1016/j.ijdrr.2021.102563

Swift, J. 2019. Pastoral development in Somalia: herding cooperatives as a strategy against desertification and famine. *Desertification.* CRC Press.

Tallaksen, L. M. and Van Lanen, H. A. 2004. Hydrological drought: processes and estimation methods for streamflow and groundwater.

Tang, J., Song, P., Hu, X., Chen, C., Wei, B. and Zhao, S. 2023. Coupled effects of land use and climate change on water supply in SSP–RCP scenarios: A case study of the Ganjiang river Basin, China. *Ecological Indicators,* 154**,** 110745. https://doi.org/10.1016/j.ecolind.2023.110745

Teyso, T. A. and Anjulo, A. 2016. Spatio-temporal variability and trends of rainfall and temperature over Gamo Gofa Zone, Ethiopia. *Journal of Scientific Research and Reports***,** 1-11.

Thangamani, S. and Raviraj, A. 2016. Rainfall variability and trend detection in Dindigul district of Amaravathi Basin. *Current World Environment,* 11(2)**,** 567. http://dx.doi.org/10.12944/CWE.11.2.27

Thompson, R. D. 1975. *The climatology of the arid world*, University of Reading. https://lccn.loc.gov/77358405

Thornthwaite, C. W. 1948. An approach toward a rational classification of climate. *Geographical review,* 38(1)**,** 55-94. https://doi.org/10.2307/210739

Tierney, K. J. 2007. From the margins to the mainstream? Disaster research at the crossroads. *Annu. Rev. Sociol.,* 33(1)**,** 503-525.

Totin, H. S., Zannou, A., Amoussou, E., Afouda, A. and Boko, M. 2014. Progressive aridity impact on the hydrological regime on the Volta River basin in Benin (West Africa). *Hydrology in a Changing World: Environmental and Human Dimensions, Proceedings of FRIEND-Water 2014***,** 17-22.

Trenberth, K. E. 2011. Changes in precipitation with climate change. *Climate research,* 47(1-2)**,** 123-138.

Tsakiris, G. and Vangelis, H. 2005. Establishing a drought index incorporating evapotranspiration. *European water,* 9(10)**,** 3-11. http://danida.vnu.edu.vn/cpis/files/Refs/Drought/Establishing%20a%20Drought%20Index%20Incorporating%20Evapotranspiration.pdf

Tshiala, M. F., Olwoch, J. M. and Engelbrecht, F. A. 2011. Analysis of temperature trends over Limpopo province, South Africa. *Journal of Geography and Geology,* 3(1)**,** 13. http://doi.org/10.5539/jgg.v3n1p13

Tuladhar, D., Dewan, A., Kuhn, M. and Corner, R. J. 2020. Spatio-temporal rainfall variability in the Himalayan mountain catchment of the Bagmati River in Nepal. *Theoretical and Applied Climatology,* 139**,** 599-614. https://www.ipcc.ch/site/assets/uploads/2018/03/ar4_wg2_full_report.pdf

Ullah, S., You, Q., Sachindra, D., Nowosad, M., Ullah, W., Bhatti, A. S., Jin, Z. and Ali, A. 2022. Spatiotemporal changes in global aridity in terms of multiple aridity indices: An assessment based on the CRU data. *Atmospheric Research,* 268**,** 105998. https://doi.org/10.1016/j.atmosres.2021.105998

Unep 1997. World atlas of desertification 2ED. UNEP London.

Upreti, G. 2023. Climate Change and Its Threat to Humanity in the Anthropocene. *Ecosociocentrism: The Earth First Paradigm for Sustainable Living.* Springer.

Van Lanen, H. A., Wanders, N., Tallaksen, L. M. and Van Loon, A. F. 2013. Hydrological drought across the world: impact of climate and physical catchment structure. *Hydrology and Earth System Sciences,* 17(5)**,** 1715-1732. https://doi.org/10.5194/hess-17-1715-2013

Verheye, W. H. 2009. *Land Use, Land Cover and Soil Sciences-Volume V: Dry Lands and Desertification*, EOLSS Publications.

Villiger, L., Wernli, H., Boettcher, M., Hagen, M. and Aemisegger, F. 2022. Lagrangian formation pathways of moist anomalies in the trade-wind region during the dry season: two case studies from EUREC 4 A. *Weather and Climate Dynamics,* 3(1)**,** 59-88. https://doi.org/10.5194/wcd-3-59-2022

Walsh, K. J., Mcbride, J. L., Klotzbach, P. J., Balachandran, S., Camargo, S. J., Holland, G., Knutson, T. R., Kossin, J. P., Lee, T. C. and Sobel, A. 2016. Tropical cyclones and climate change. *Wiley Interdisciplinary Reviews: Climate Change,* 7(1)**,** 65-89. https://doi.org/10.1002/wcc.371

Walton, K. 1969. *The arid zones*, Transaction Publishers.

Walz, Y., Min, A., Dall, K., Duguru, M., De Leon, J.-C. V., Graw, V., Dubovyk, O., Sebesvari, Z., Jordaan, A. and Post, J. 2020. Monitoring progress of the Sendai Framework using a geospatial model: The example of people affected by agricultural droughts in Eastern Cape, South Africa. *Progress in Disaster Science,* 5**,** 100062. https://doi.org/10.1016/j.pdisas.2019.100062

Wang, L., D'odorico, P., Evans, J., Eldridge, D., Mccabe, M., Caylor, K. and King, E. 2012. Dryland ecohydrology and climate change: critical issues and technical advances. *Hydrology and Earth System Sciences,* 16(8), 2585-2603. https://doi.org/10.5194/hess-16-2585-2012

Ward, P. J., De Ruiter, M. C., Mård, J., Schröter, K., Van Loon, A., Veldkamp, T., Von Uexkull, N., Wanders, N., Aghakouchak, A. and Arnbjerg-Nielsen, K. 2020. The need to integrate flood and drought disaster risk reduction strategies. *Water Security,* 11, 100070.

Warner, T. T. 2009. *Desert meteorology*, Cambridge University Press.

Wasti, A., Ray, P., Wi, S., Folch, C., Ubierna, M. and Karki, P. 2022. Climate change and the hydropower sector: A global review. *Wiley Interdisciplinary Reviews: Climate Change,* 13(2), e757. https://doi.org/10.1002/wcc.757

Wazneh, H., Arain, M. A. and Coulibaly, P. 2017. Historical spatial and temporal climate trends in southern Ontario, Canada. *Journal of Applied Meteorology and Climatology,* 56(10), 2767-2787. https://doi.org/10.1175/JAMC-D-16-0290.1

Wheater, H. 2008. Modelling hydrological processes in arid and semi-arid areas: an introduction to the workshop. *Hydrological modelling in arid and semi-arid areas*, 1-20. https://doi.org/10.1017/CBO9780511535734.002

Wilhite, D. A. and Buchanan-Smith, M. 2005. Drought as hazard: understanding the natural and social context. *Drought and water crises: Science, technology, and management issues,* 3, 29.

Wilhite, D. A. and Glantz, M. H. 1985. Understanding: the drought phenomenon: the role of definitions. *Water international,* 10(3), 111-120.

Wolter, K. 1987. The Southern Oscillation in surface circulation and climate over the tropical Atlantic, Eastern Pacific, and Indian Oceans as captured by cluster analysis. *Journal of Applied Meteorology and Climatology,* 26(4), 540-558.

Wooldridge, S. A., Franks, S. W. and Kalma, J. D. 2001. Hydrological implications of the Southern Oscillation: variability of the rainfall-runoff relationship. *Hydrological sciences journal,* 46(1), 73-88.

Wrc 2001. State of Rivers Report: Letaba and Luvuvhu River systems. WRC Report, Number TT 165/01. *Water Research Commission, Pretoria, South Africa.* https://www.dws.gov.za/iwqs/rhp/state_of_rivers/state_of_letluv_01/luvuvhu.html

Wright, C. Y., Kapwata, T., Du Preez, D. J., Wernecke, B., Garland, R. M., Nkosi, V., Landman, W. A., Dyson, L. and Norval, M. 2021. Major climate change-induced risks to human health in South Africa. *Environmental Research,* 196**,** 110973. https://doi.org/10.1016/j.envres.2021.110973

Xu, K., Milliman, J. D. and Xu, H. 2010. Temporal trend of precipitation and runoff in major Chinese Rivers since 1951. *Global and Planetary Change,* 73(3-4)**,** 219-232. https://doi.org/10.1016/j.gloplacha.2010.07.002

Yin, Y., Ma, D., Wu, S. and Pan, T. 2015. Projections of aridity and its regional variability over China in the mid-21st century. *International Journal of Climatology,* 35(14)**,** 4387-4398. https://doi.org/10.1002/joc.4295

Zarch, M. a. A., Sivakumar, B. and Sharma, A. 2015. Assessment of global aridity change. *Journal of Hydrology,* 520**,** 300-313. https://doi.org/10.1016/j.jhydrol.2014.11.033

Zhang, J., Tourian, M. J. and Sneeuw, N. 2020a. Identification of ENSO signature in the boreal hydrological cycle through canonical correlation with sea surface temperature anomalies. *International Journal of Climatology,* 40(15)**,** 6219-6241. https://doi.org/10.1002/joc.6573

Zhang, X., Li, Z., Siddique, K. H., Shayakhmetova, A., Jia, Z. and Han, Q. 2020b. Increasing maize production and preventing water deficits in semi-arid areas: A study matching fertilization with regional precipitation under mulch planting. *Agricultural Water Management,* 241**,** 106347. https://doi.org/10.1016/j.agwat.2020.106347

Zhao, Y., Weng, Z., Chen, H. and Yang, J. 2020. Analysis of the evolution of drought, flood, and drought-flood abrupt alternation events under climate change using the daily SWAP index. *Water,* 12(7)**,** 1969. https://doi.org/10.3390/w12071969

Zomer, R. J., Xu, J. and Trabucco, A. 2022. Version 3 of the global aridity index and potential evapotranspiration database. *Scientific Data,* 9(1)**,** 409. https://doi.org/10.1038/s41597-022-01493-1

APPENDICES

Appendix 1: Raw data used in the study

Appendix 1A Raw rainfall data used in the study

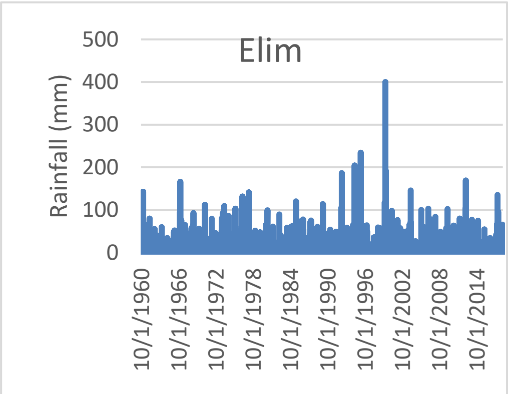
Elim
Rainfall (mm)
500
400
300
200
100
0
10/1/1960
10/1/1966
10/1/1972
10/1/1978
10/1/1984
10/1/1990
10/1/1996
10/1/2002
10/1/2008
10/1/2014

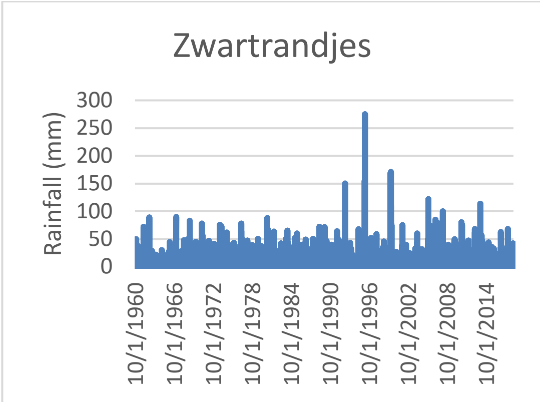
Zwartrandjes
Rainfall (mm)
300
250
200
150
100
50
0
10/1/1960
10/1/1966
10/1/1972
10/1/1978
10/1/1984
10/1/1990
10/1/1996
10/1/2002
10/1/2008
10/1/2014

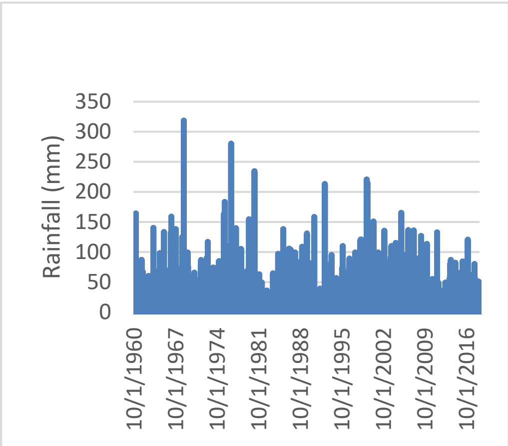
Rainfall (mm)
350
300
250
200
150
100
50
0
10/1/1960
10/1/1967
10/1/1974
10/1/1981
10/1/1988
10/1/1995
10/1/2002
10/1/2009
10/1/2016

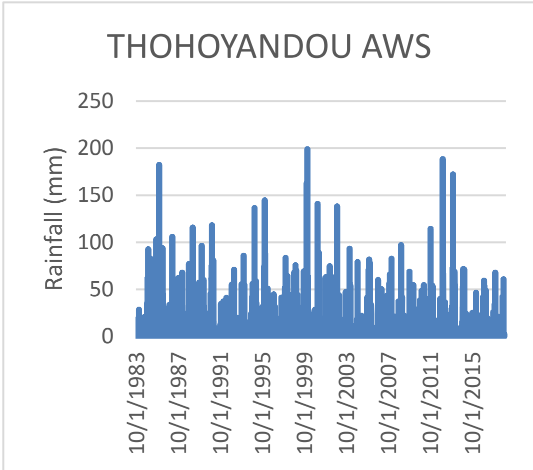
THOHOYANDOU AWS
Rainfall (mm)
250
200
150
100
50
0
10/1/1983
10/1/1987
10/1/1991
10/1/1995
10/1/1999
10/1/2003
10/1/2007
10/1/2011
10/1/2015

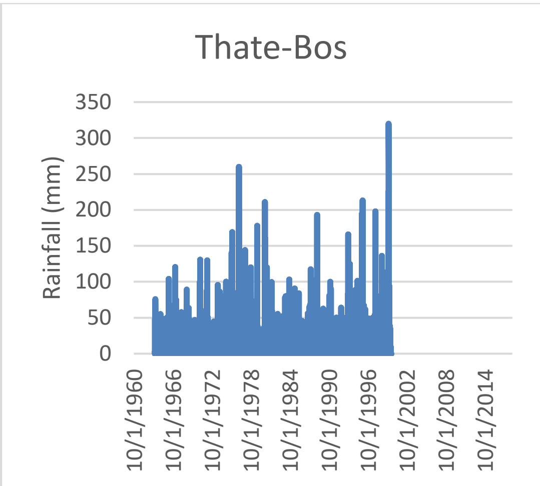
Thate-Bos
Rainfall (mm)
350
300
250
200
150
100
50
0
10/1/1960
10/1/1966
10/1/1972
10/1/1978
10/1/1984
10/1/1990
10/1/1996
10/1/2002
10/1/2008
10/1/2014

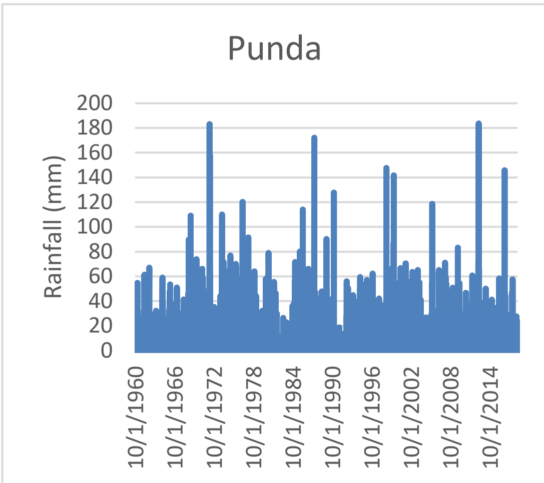
Punda
Rainfall (mm)
200
180
160
140
120
100
80
60
40
20
0
10/1/1960
10/1/1966
10/1/1972
10/1/1978
10/1/1984
10/1/1990
10/1/1996
10/1/2002
10/1/2008
10/1/2014

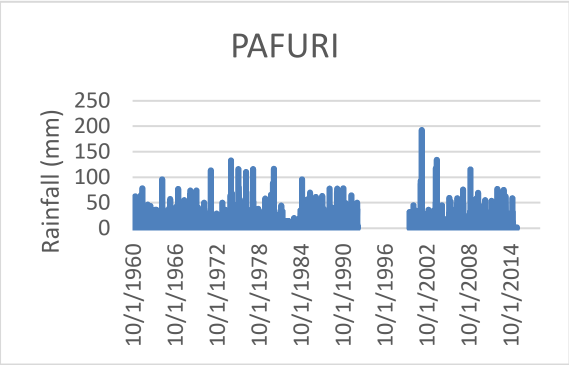
PAFURI
Rainfall (mm)
250
200
150
100
50
0
10/1/1960
10/1/1966
10/1/1972
10/1/1978
10/1/1984
10/1/1990
10/1/1996
10/1/2002
10/1/2008
10/1/2014

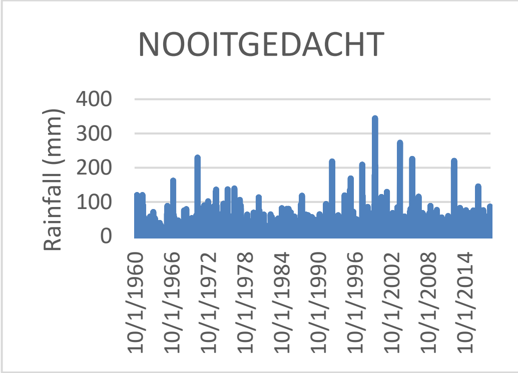
NOOITGEDACHT
Rainfall (mm)
400
300
200
100
0
10/1/1960
10/1/1966
10/1/1972
10/1/1978
10/1/1984
10/1/1990
10/1/1996
10/1/2002
10/1/2008
10/1/2014

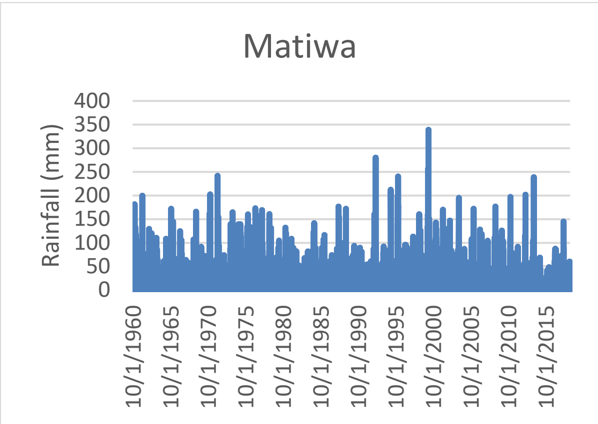
Matiwa
Rainfall (mm)
400
350
300
250
200
150
100
50
0
10/1/1960
10/1/1965
10/1/1970
10/1/1975
10/1/1980
10/1/1985
10/1/1990
10/1/1995
10/1/2000
10/1/2005
10/1/2010
10/1/2015

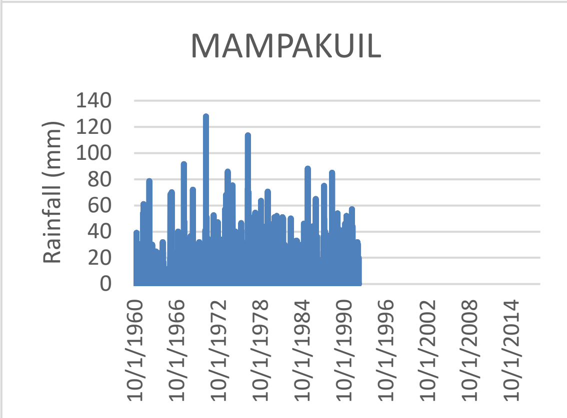
MAMPAKUIL
Rainfall (mm)
140
120
100
80
60
40
20
0
10/1/1960
10/1/1966
10/1/1972
10/1/1978
10/1/1984
10/1/1990
10/1/1996
10/1/2002
10/1/2008
10/1/2014

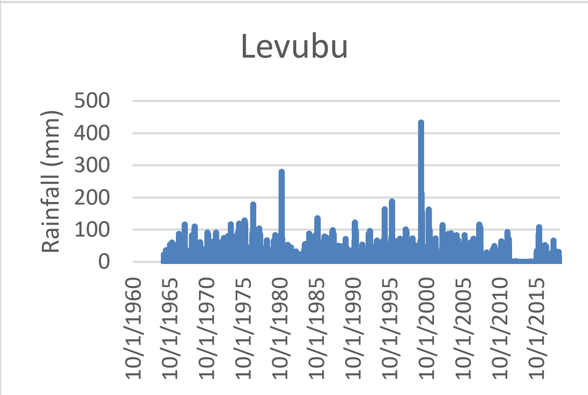
Levubu
Rainfall (mm)
500
400
300
200
100
0
10/1/1960
10/1/1965
10/1/1970
10/1/1975
10/1/1980
10/1/1985
10/1/1990
10/1/1995
10/1/2000
10/1/2005
10/1/2010
10/1/2015

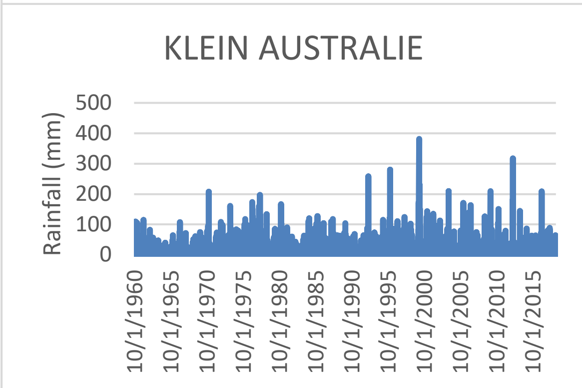
KLEIN AUSTRALIE
Rainfall (mm)
500
400
300
200
100
0
10/1/1960
10/1/1965
10/1/1970
10/1/1975
10/1/1980
10/1/1985
10/1/1990
10/1/1995
10/1/2000
10/1/2005
10/1/2010
10/1/2015

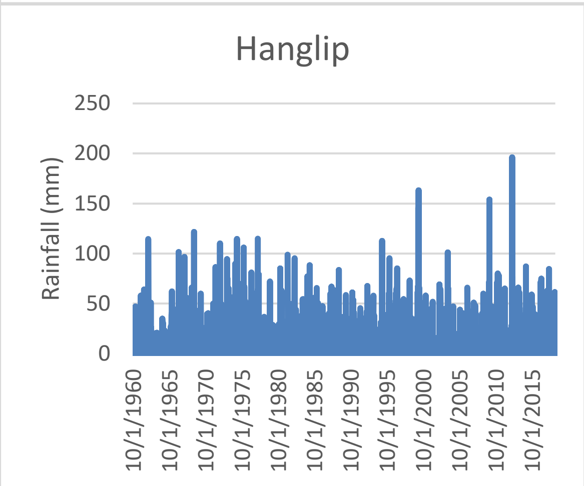
Hanglip
Rainfall (mm)
250
200
150
100
50
0
10/1/1960
10/1/1965
10/1/1970
10/1/1975
10/1/1980
10/1/1985
10/1/1990
10/1/1995
10/1/2000
10/1/2005
10/1/2010
10/1/2015

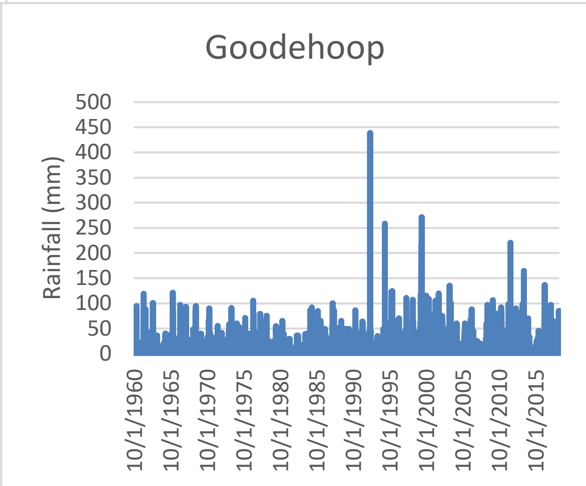
Goodehoop
Rainfall (mm)
500
450
400
350
300
250
200
150
100
50
0
10/1/1960
10/1/1965
10/1/1970
10/1/1975
10/1/1980
10/1/1985
10/1/1990
10/1/1995
10/1/2000
10/1/2005
10/1/2010
10/1/2015

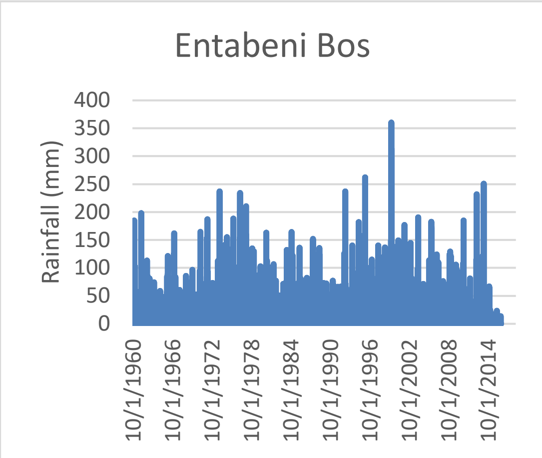
Entabeni Bos
Rainfall (mm)
400
350
300
250
200
150
100
50
0
10/1/1960
10/1/1966
10/1/1972
10/1/1978
10/1/1984
10/1/1990
10/1/1996
10/1/2002
10/1/2008
10/1/2014

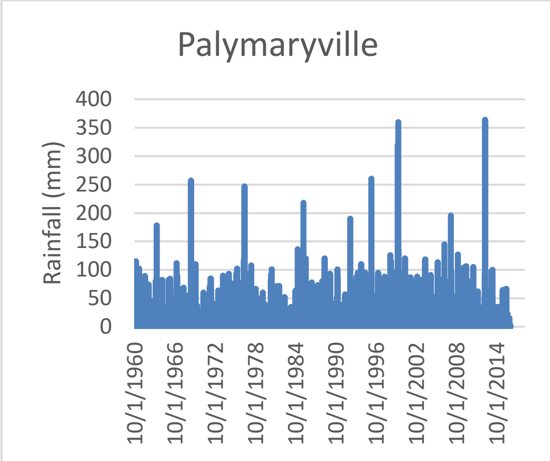
Palymaryville
Rainfall (mm)
400
350
300
250
200
150
100
50
0
10/1/1960
10/1/1966
10/1/1972
10/1/1978
10/1/1984
10/1/1990
10/1/1996
10/1/2002
10/1/2008
10/1/2014

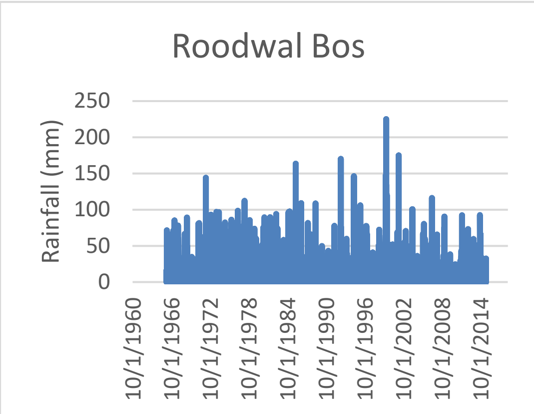
Roodwal Bos
Rainfall (mm)
250
200
150
100
50
0
10/1/1960
10/1/1966
10/1/1972
10/1/1978
10/1/1984
10/1/1990
10/1/1996
10/1/2002
10/1/2008
10/1/2014

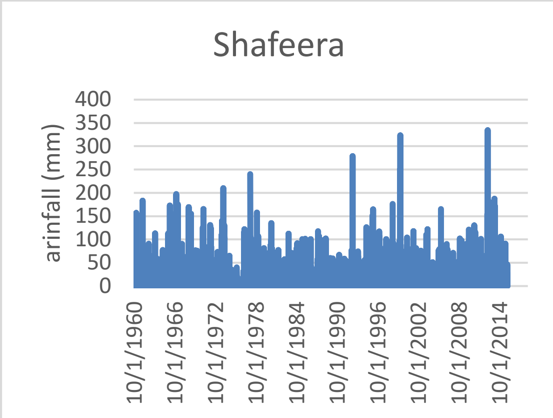
Shafeera
arinfall (mm)
400
350
300
250
200
150
100
50
0
10/1/1960
10/1/1966
10/1/1972
10/1/1978
10/1/1984
10/1/1990
10/1/1996
10/1/2002
10/1/2008
10/1/2014

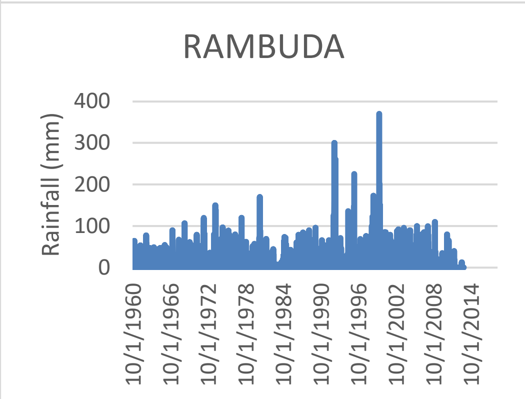
RAMBUDA
Rainfall (mm)
400
300
200
100
0
10/1/1960
10/1/1966
10/1/1972
10/1/1978
10/1/1984
10/1/1990
10/1/1996
10/1/2002
10/1/2008
10/1/2014

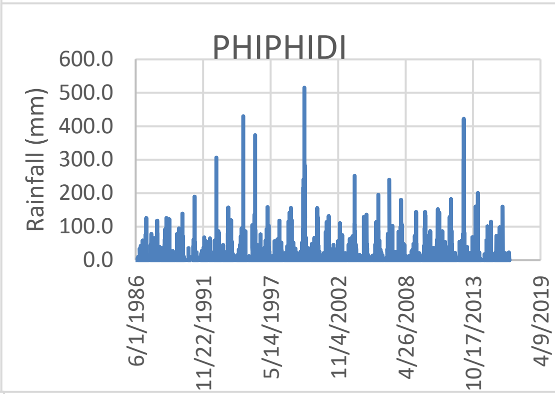
PHIPHIDI
Rainfall (mm)
600.0
500.0
400.0
300.0
200.0
100.0
0.0
6/1/1986
11/22/1991
5/14/1997
11/4/2002
4/26/2008
10/17/2013
4/9/2019

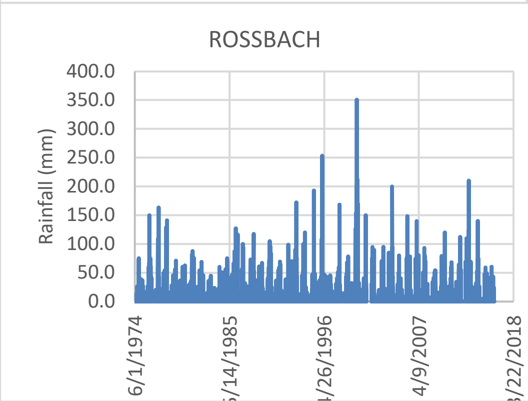
ROSSBACH
Rainfall (mm)
400.0
350.0
300.0
250.0
200.0
150.0
100.0
50.0
0.0
6/1/1974
4/9/2007

Appendix 1B Raw temperature data used in the study

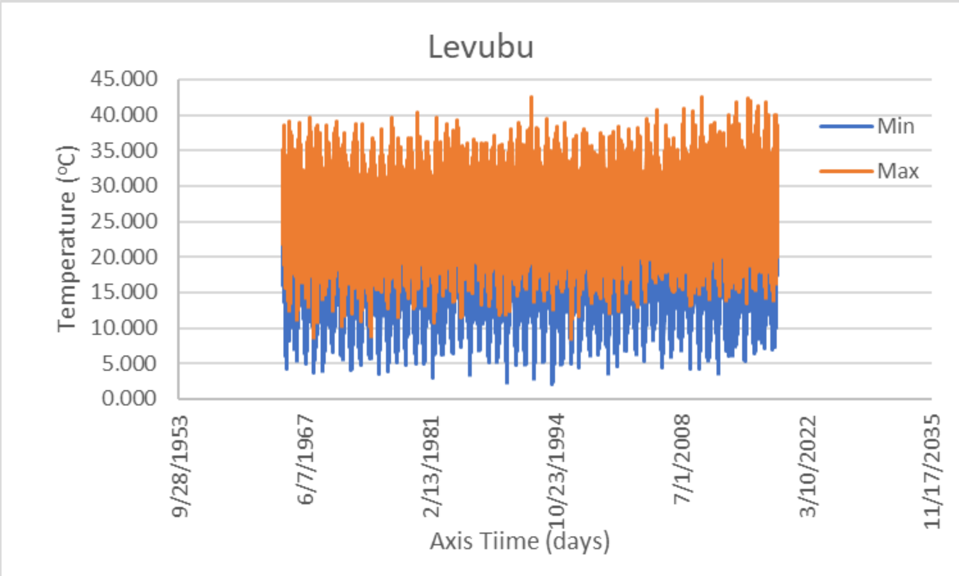

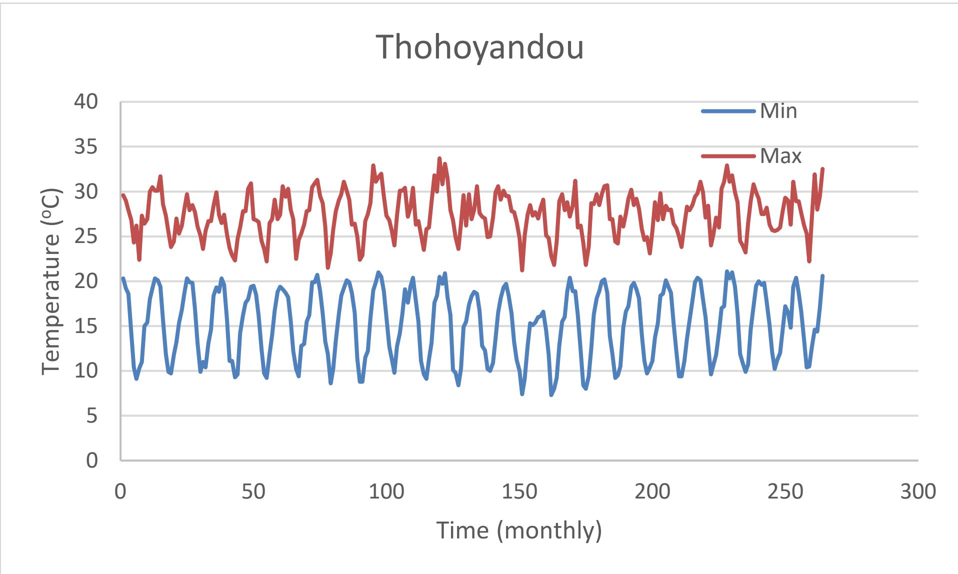

Appendix 1C Raw streamflow data used in the study

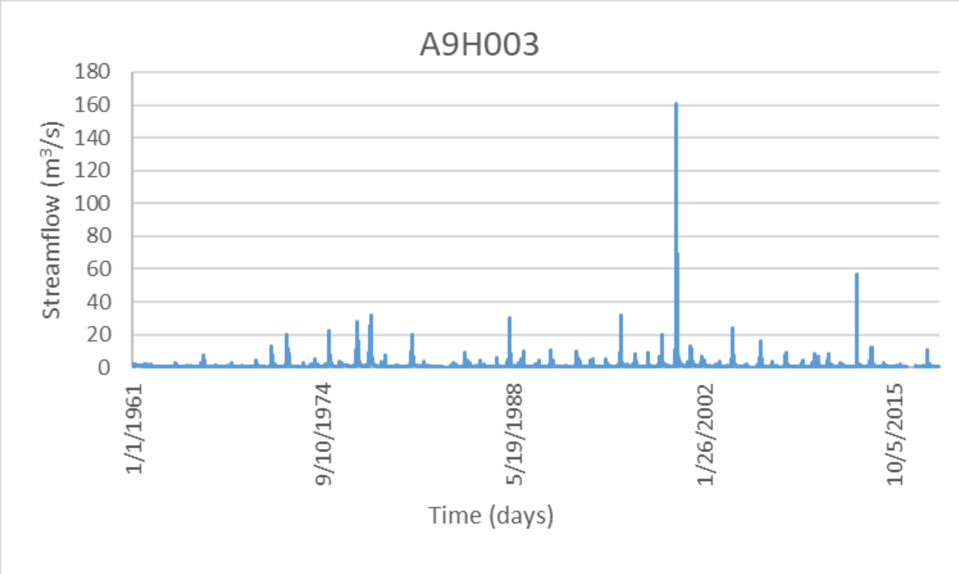

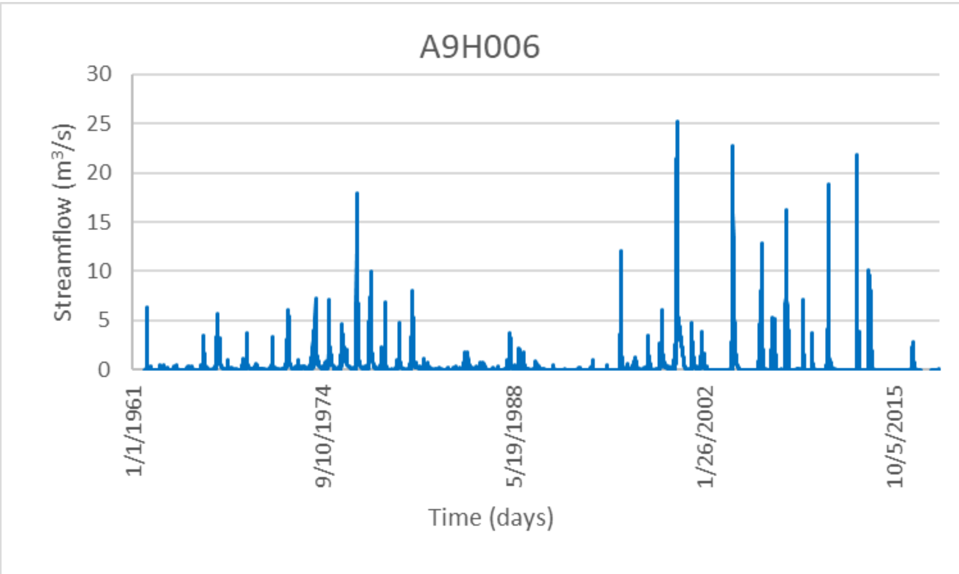

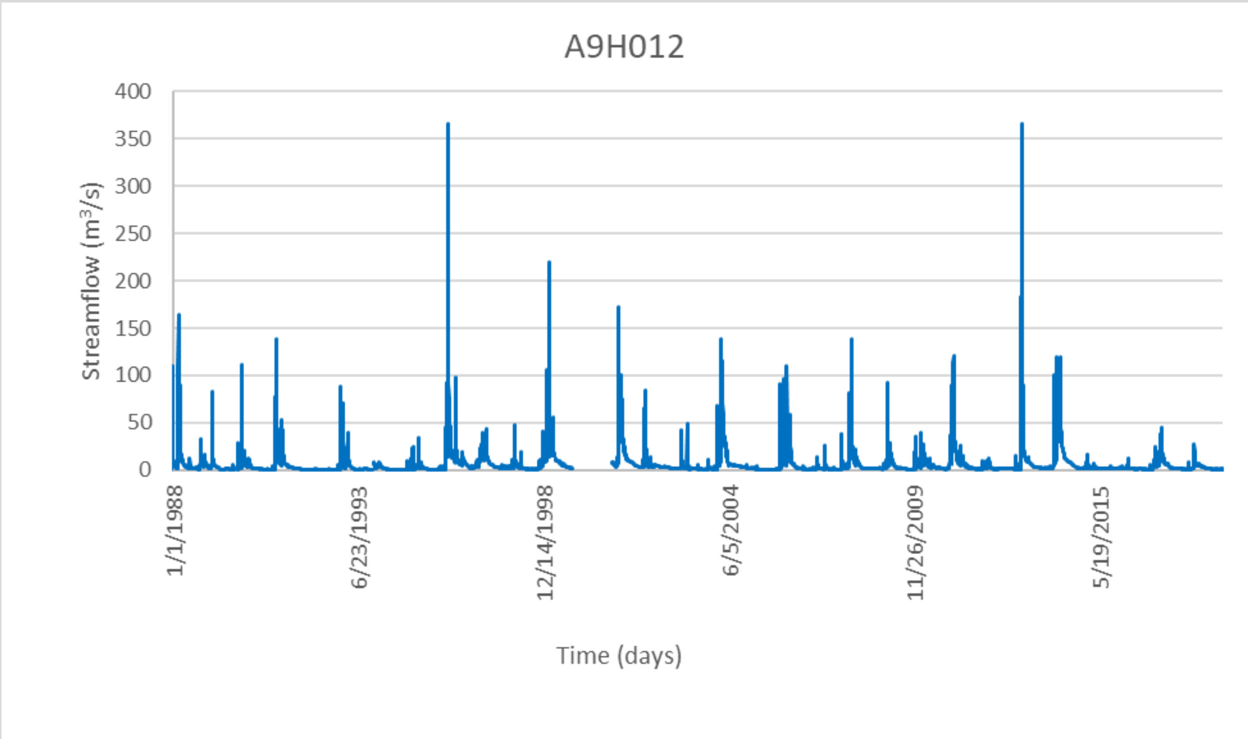
A9H012
400
350
300
250
200
150
100
50
0
Streamflow (m3/s)
1/1/1988
6/23/1993
12/14/1998
6/5/2004
11/26/2009
5/19/2015
Time (days)

Appendix 2: Normality plots

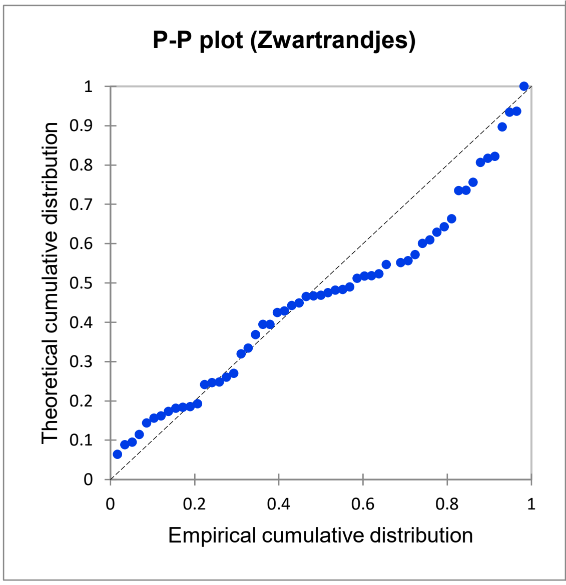

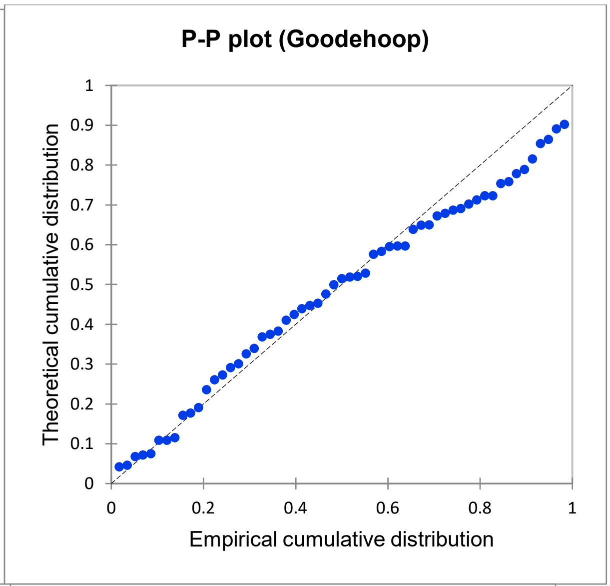

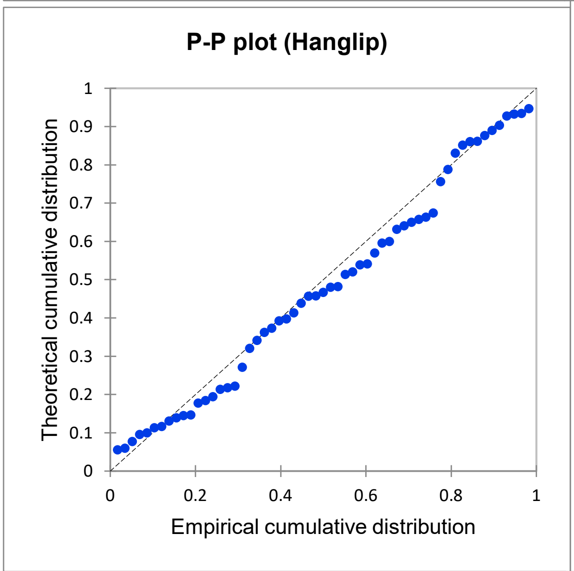

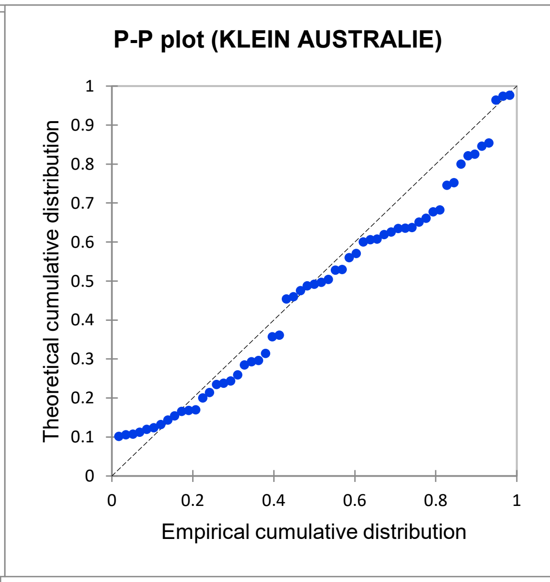

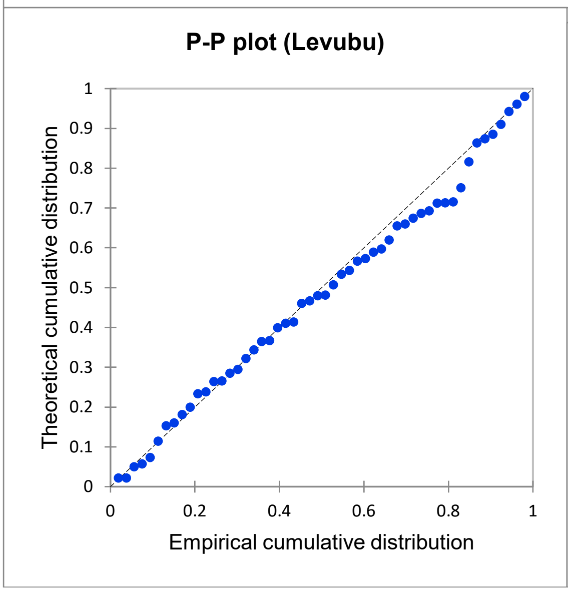

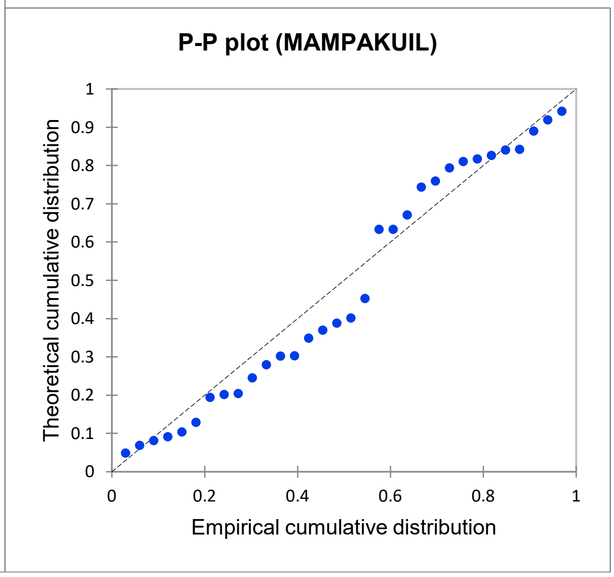

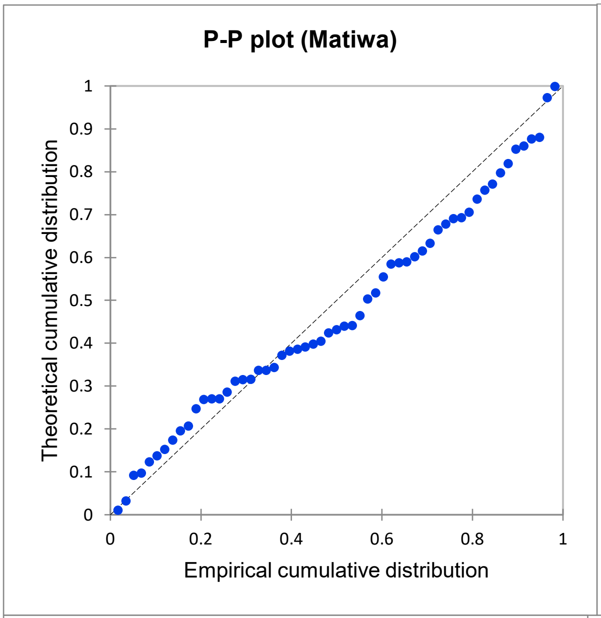
P-P plot (Matiwa)
Theoretical cumulative distribution
Empirical cumulative distribution
0
0.1
0.2
0.3
0.4
0.5
0.6
0.7
0.8
0.9
1
0
0.2
0.4
0.6
0.8
1

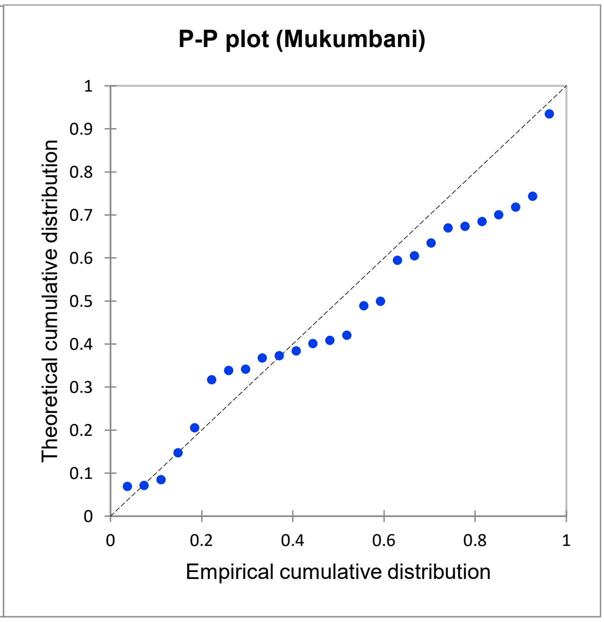
P-P plot (Mukumbani)
Theoretical cumulative distribution
Empirical cumulative distribution
0
0.1
0.2
0.3
0.4
0.5
0.6
0.7
0.8
0.9
1
0
0.2
0.4
0.6
0.8
1

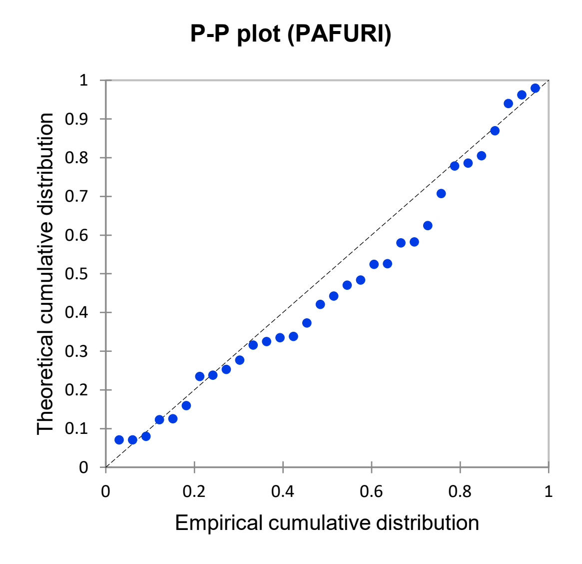
P-P plot (PAFURI)
Theoretical cumulative distribution
Empirical cumulative distribution
0
0.1
0.2
0.3
0.4
0.5
0.6
0.7
0.8
0.9
1
0
0.2
0.4
0.6
0.8
1

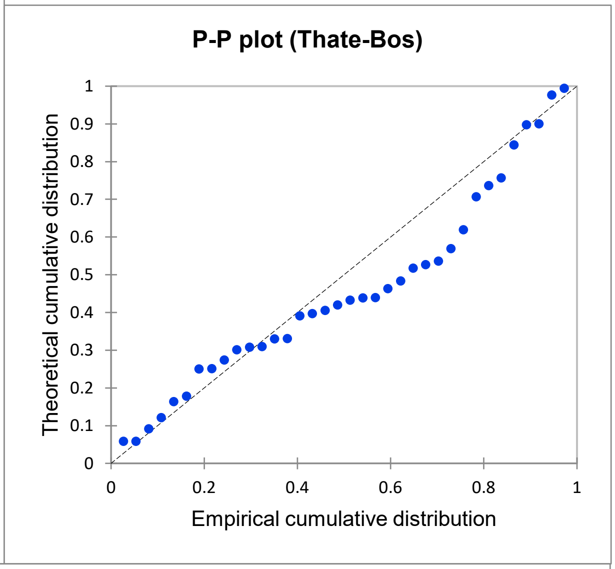
P-P plot (Thate-Bos)
Theoretical cumulative distribution
Empirical cumulative distribution
0
0.1
0.2
0.3
0.4
0.5
0.6
0.7
0.8
0.9
1
0
0.2
0.4
0.6
0.8
1

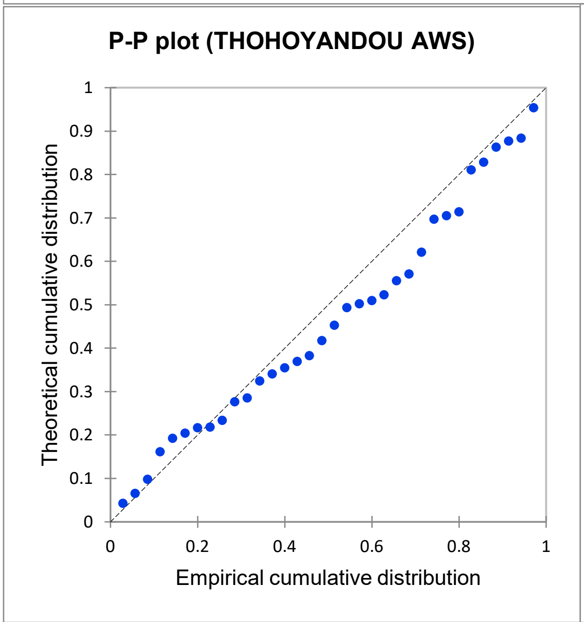
P-P plot (THOHOYANDOU AWS)
Theoretical cumulative distribution
Empirical cumulative distribution
0
0.1
0.2
0.3
0.4
0.5
0.6
0.7
0.8
0.9
1
0
0.2
0.4
0.6
0.8
1

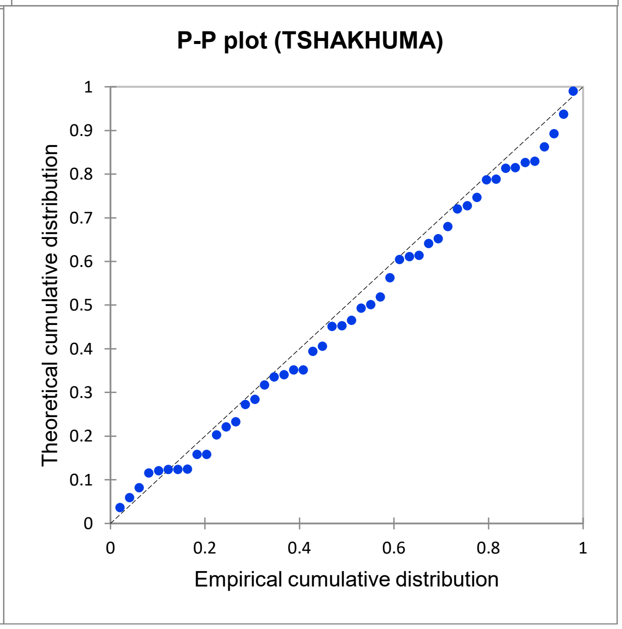
P-P plot (TSHAKHUMA)
Theoretical cumulative distribution
Empirical cumulative distribution
0
0.1
0.2
0.3
0.4
0.5
0.6
0.7
0.8
0.9
1
0
0.2
0.4
0.6
0.8
1

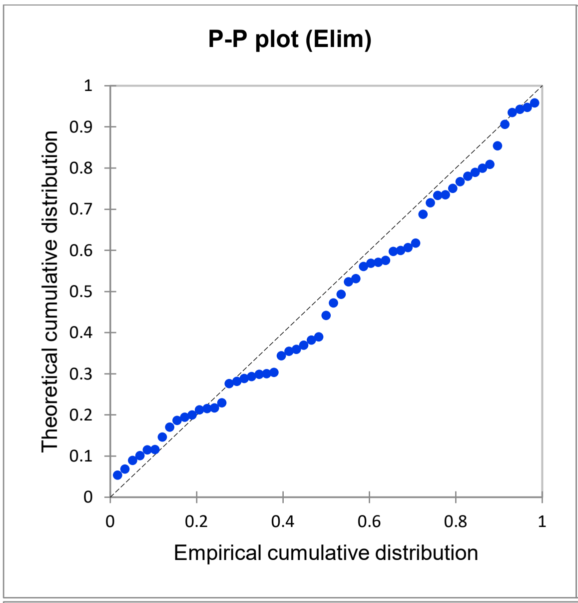
P-P plot (Elim)
Theoretical cumulative distribution
Empirical cumulative distribution

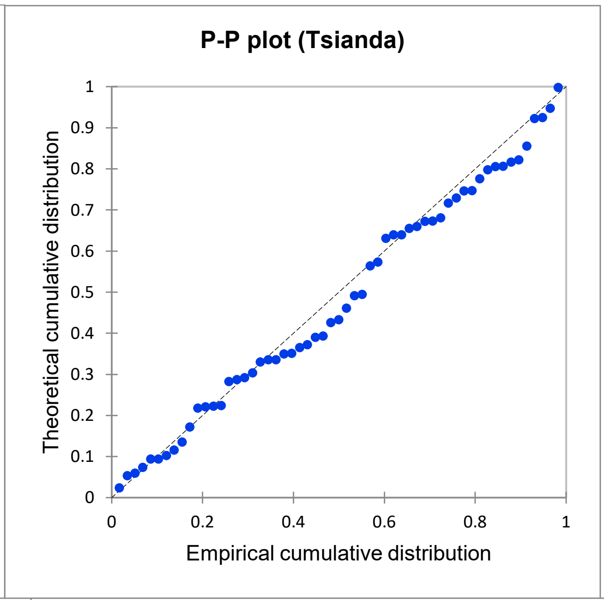
P-P plot (Tsianda)
Theoretical cumulative distribution
Empirical cumulative distribution

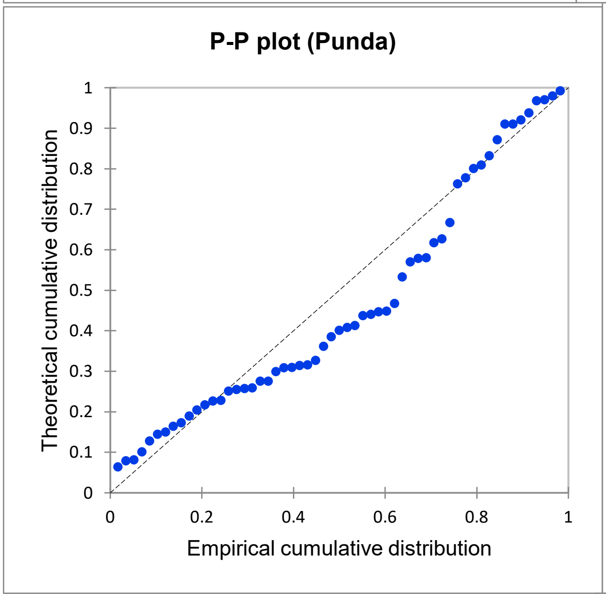
P-P plot (Punda)
Theoretical cumulative distribution
Empirical cumulative distribution

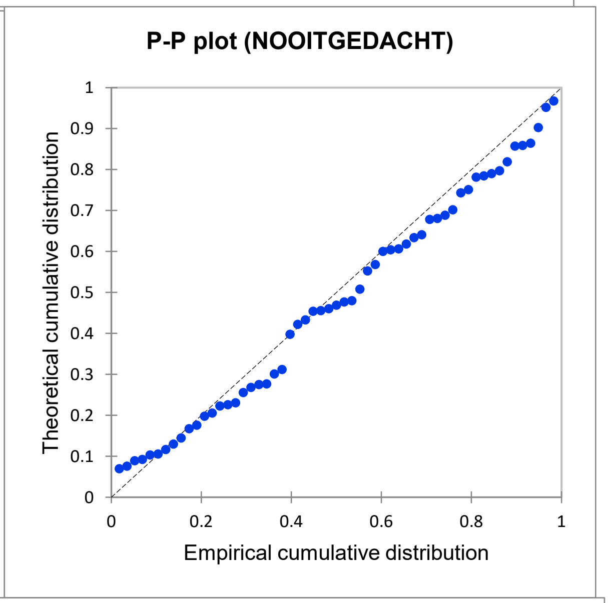
P-P plot (NOOITGEDACHT)
Theoretical cumulative distribution
Empirical cumulative distribution

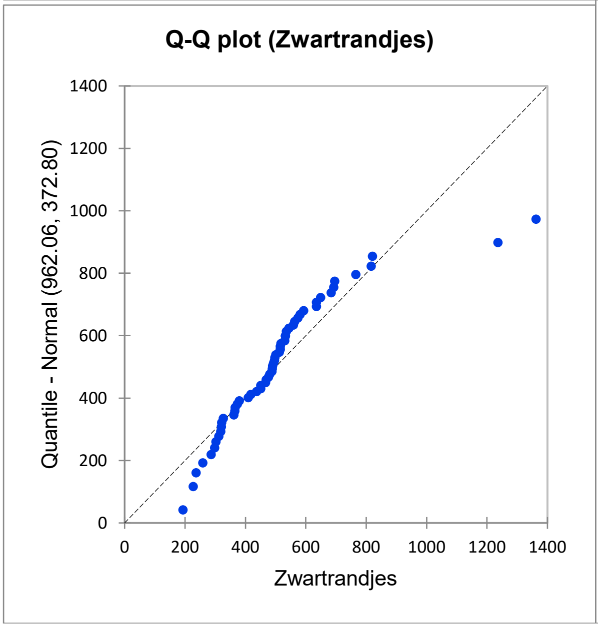
Q-Q plot (Zwartrandjes)
Quantile - Normal (962.06, 372.80)
Zwartrandjes

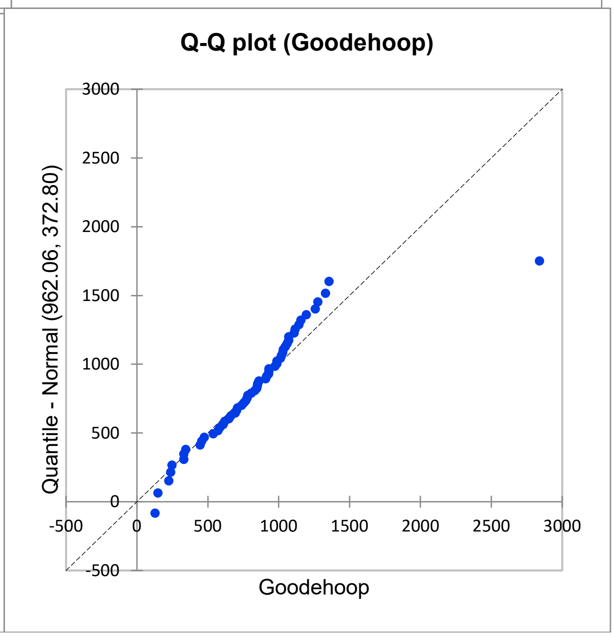
Q-Q plot (Goodehoop)
Quantile - Normal (962.06, 372.80)
Goodehoop

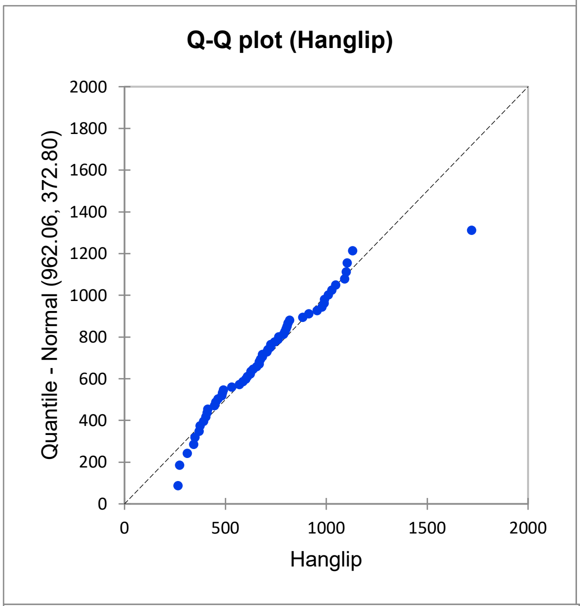
Q-Q plot (Hanglip)
Quantile - Normal (962.06, 372.80)
Hanglip

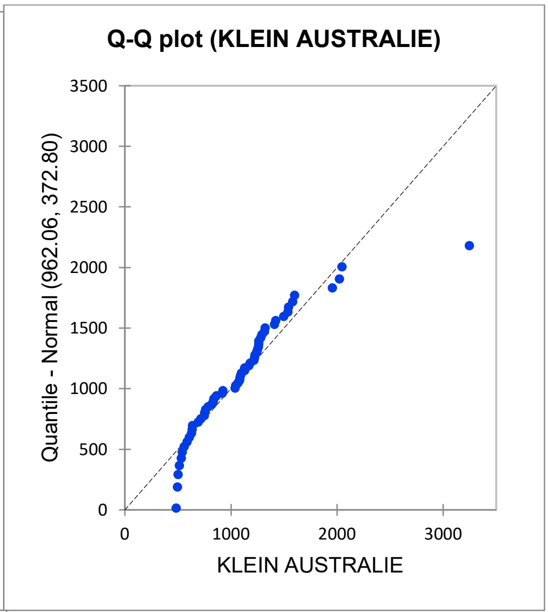
Q-Q plot (KLEIN AUSTRALIE)
Quantile - Normal (962.06, 372.80)
KLEIN AUSTRALIE

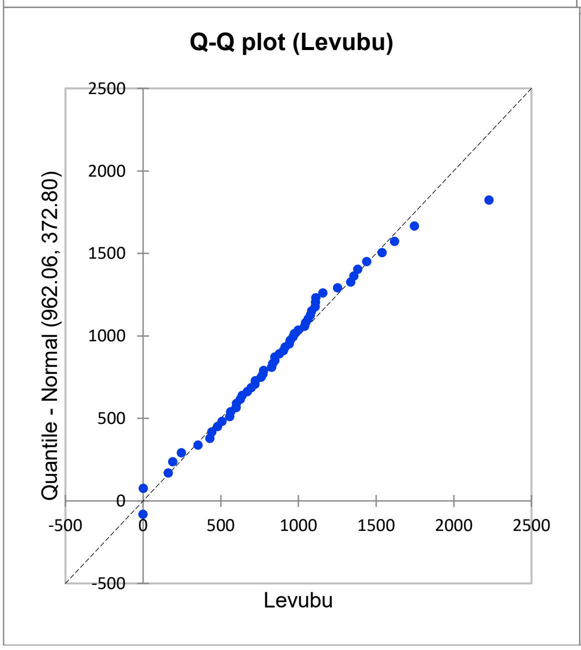
Q-Q plot (Levubu)
Quantile - Normal (962.06, 372.80)
Levubu

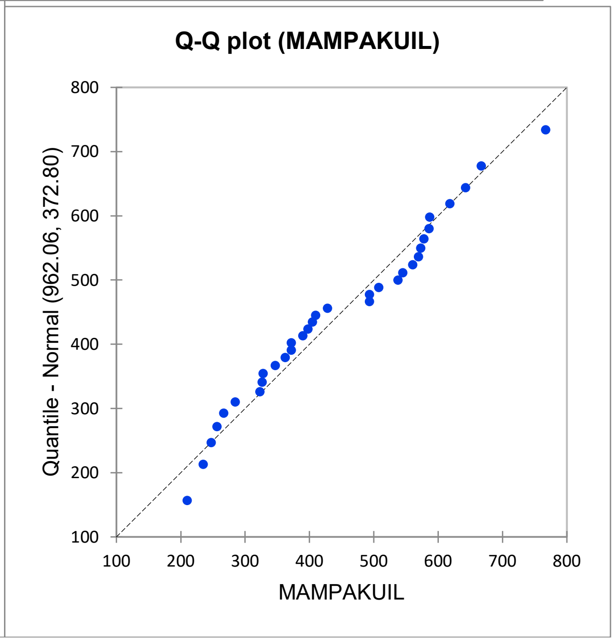
Q-Q plot (MAMPAKUIL)
Quantile - Normal (962.06, 372.80)
MAMPAKUIL

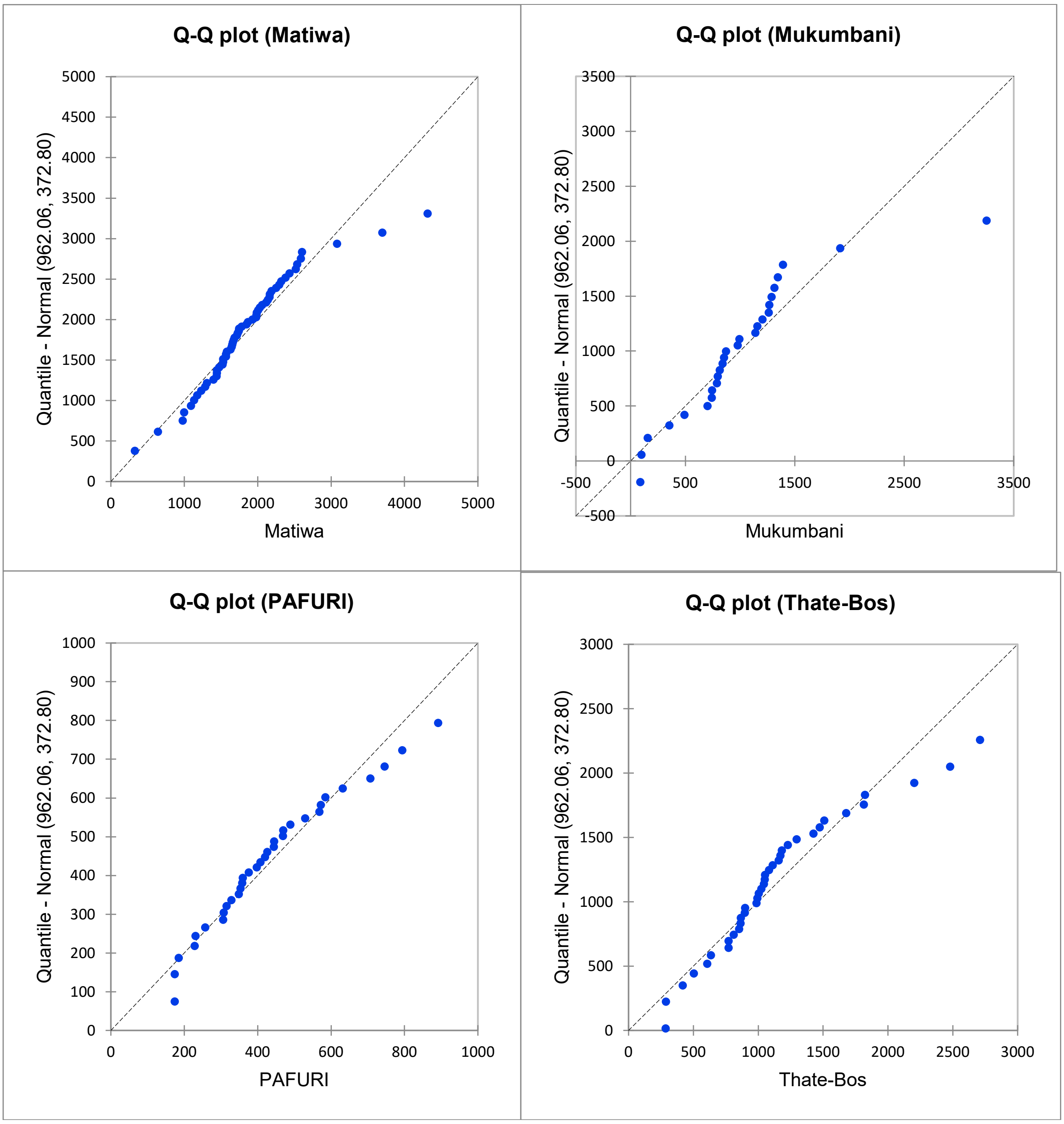
Q-Q plot (Matiwa)
Quantile - Normal (962.06, 372.80)
Matiwa
Q-Q plot (Mukumbani)
Quantile - Normal (962.06, 372.80)
Mukumbani
Q-Q plot (PAFURI)
Quantile - Normal (962.06, 372.80)
PAFURI
Q-Q plot (Thate-Bos)
Quantile - Normal (962.06, 372.80)
Thate-Bos

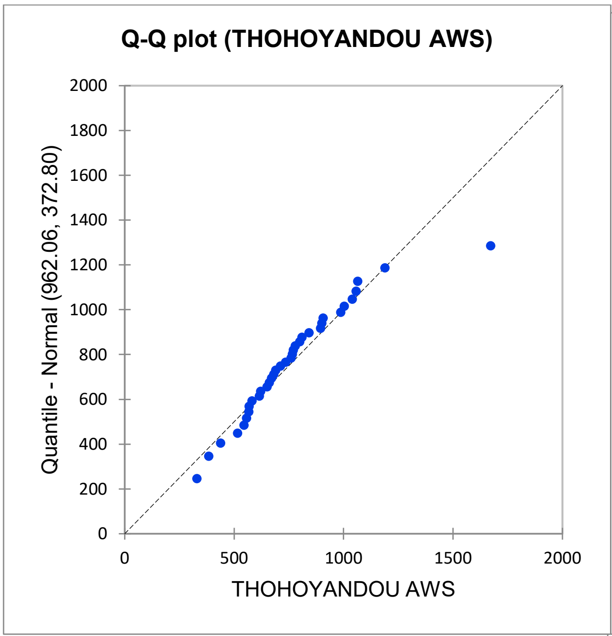
Q-Q plot (THOHOYANDOU AWS)
Quantile - Normal (962.06, 372.80)
2000
1800
1600
1400
1200
1000
800
600
400
200
0
0
500
1000
1500
2000
THOHOYANDOU AWS

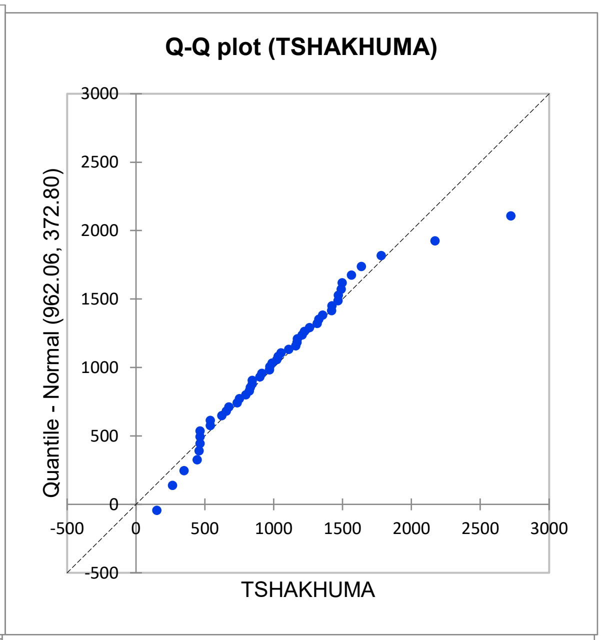
Q-Q plot (TSHAKHUMA)
Quantile - Normal (962.06, 372.80)
3000
2500
2000
1500
1000
500
0
-500
-500
0
500
1000
1500
2000
2500
3000
TSHAKHUMA

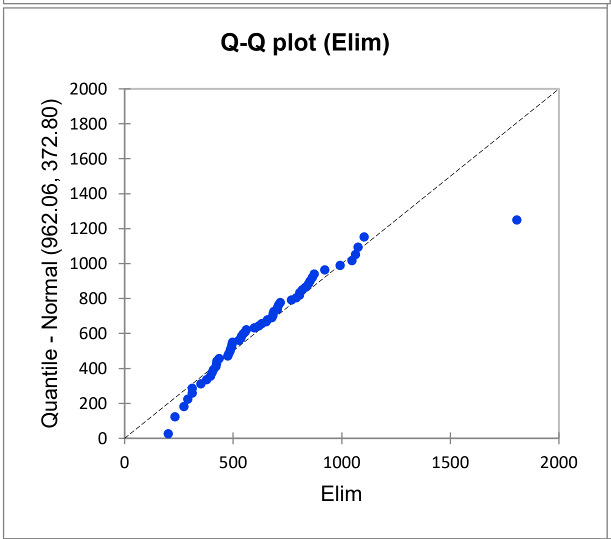
Q-Q plot (Elim)
Quantile - Normal (962.06, 372.80)
2000
1800
1600
1400
1200
1000
800
600
400
200
0
0
500
1000
1500
2000
Elim

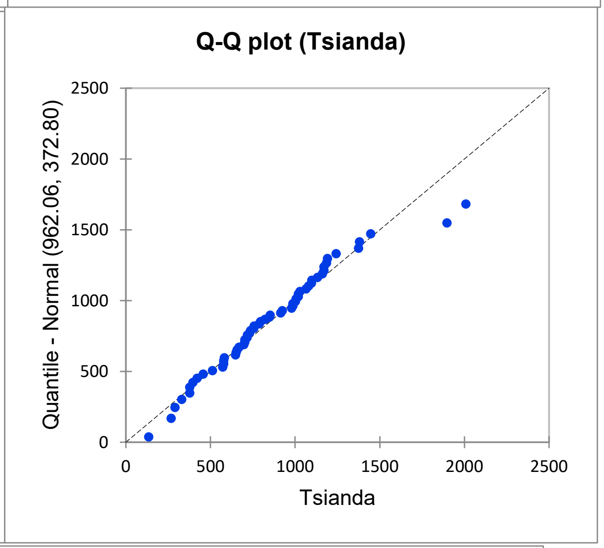
Q-Q plot (Tsianda)
Quantile - Normal (962.06, 372.80)
2500
2000
1500
1000
500
0
0
500
1000
1500
2000
2500
Tsianda

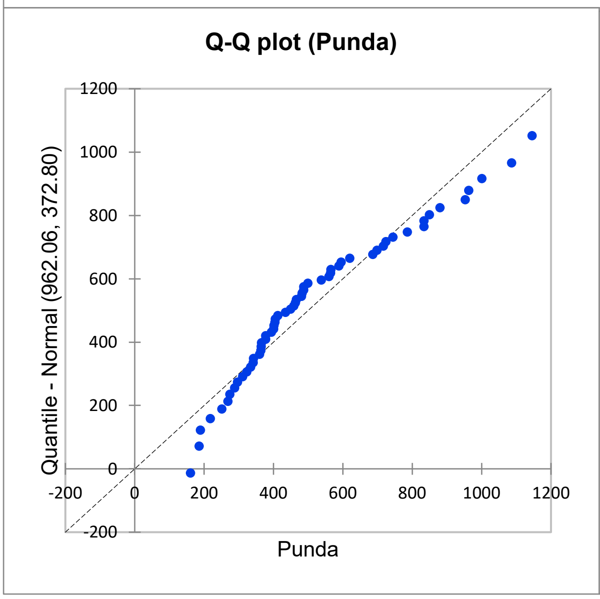
Q-Q plot (Punda)
Quantile - Normal (962.06, 372.80)
1200
1000
800
600
400
200
0
-200
-200
0
200
400
600
800
1000
1200
Punda

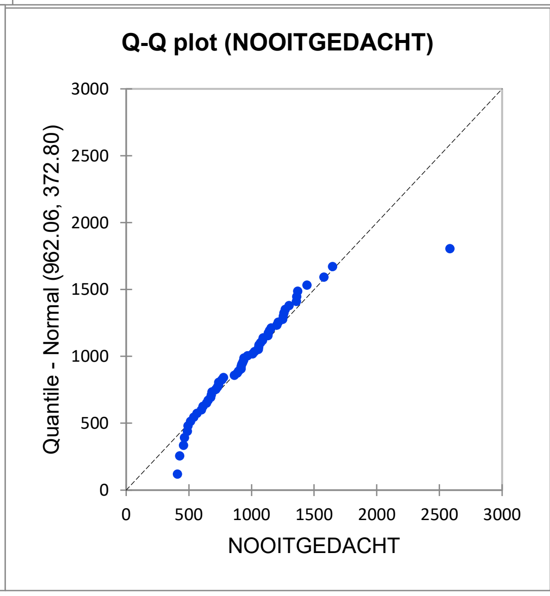
Q-Q plot (NOOITGEDACHT)
Quantile - Normal (962.06, 372.80)
3000
2500
2000
1500
1000
500
0
0
500
1000
1500
2000
2500
3000
NOOITGEDACHT

Appendix 3: Frequency factor table

WEIGHTED SKEW COEFFICIENT Cw	Recurrence Interval In Years							
	1.0101	2	5	10	25	50	100	200
	Percent Chance (>=) = 1-F							
	99	50	20	10	4	2	1	0.5
-0.4	-2.615	0.066	0.855	1.231	1.606	1.834	2.029	2.201
-0.5	-2.686	0.083	0.856	1.216	1.567	1.777	1.955	2.108
-0.6	-2.755	0.099	0.857	1.2	1.528	1.72	1.88	2.016
-0.7	-2.824	0.116	0.857	1.183	1.488	1.663	1.806	1.926
-0.8	-2.891	0.132	0.856	1.166	1.448	1.606	1.733	1.837
-0.9	-2.957	0.148	0.854	1.147	1.407	1.549	1.66	1.749
-1	-3.022	0.164	0.852	1.128	1.366	1.492	1.588	1.664
-1.1	-3.087	0.18	0.848	1.107	1.324	1.435	1.518	1.581
-1.2	-3.149	0.195	0.844	1.086	1.282	1.379	1.449	1.501
-1.3	-3.211	0.21	0.838	1.064	1.24	1.324	1.383	1.424
-1.4	-3.271	0.225	0.832	1.041	1.198	1.27	1.318	1.351
-1.5	-3.33	0.24	0.825	1.018	1.157	1.217	1.256	1.282
-1.6	-3.88	0.254	0.817	0.994	1.116	1.166	1.197	1.216
-1.7	-3.444	0.268	0.808	0.97	1.075	1.116	1.14	1.155
-1.8	-3.499	0.282	0.799	0.945	1.035	1.069	1.087	1.097
-1.9	-3.553	0.294	0.788	0.92	0.996	1.023	1.037	1.044
-2	-3.605	0.307	0.777	0.895	0.959	0.98	0.99	0.995
-2.1	-3.656	0.319	0.765	0.869	0.923	0.939	0.946	0.949
-2.2	-3.705	0.33	0.752	0.844	0.888	0.9	0.905	0.907
-2.3	-3.753	0.341	0.739	0.819	0.855	0.864	0.867	0.869
-2.4	-3.8	0.351	0.725	0.795	0.823	0.83	0.832	0.833
-2.5	-3.845	0.36	0.711	0.711	0.793	0.798	0.799	0.8
-2.6	-3.899	0.368	0.696	0.747	0.764	0.768	0.769	0.769
-2.7	-3.932	0.376	0.681	0.724	0.738	0.74	0.74	0.741
-2.8	-3.973	0.384	0.666	0.702	0.712	0.714	0.714	0.714
-2.9	-4.013	0.39	0.651	0.681	0.683	0.689	0.69	0.69
-3	-4.051	0.396	0.636	0.66	0.666	0.666	0.667	0.667

Appendix 4: Quinquennial (pentad) variability

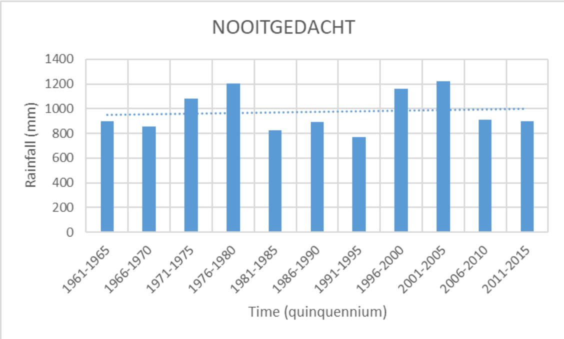

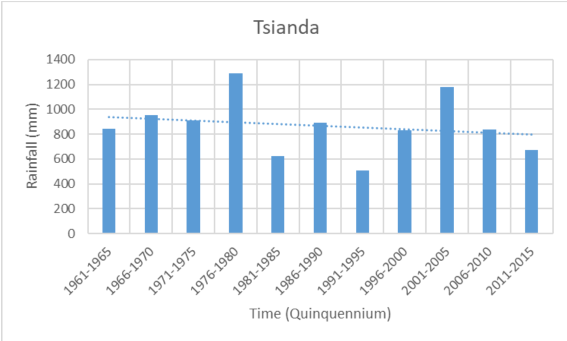

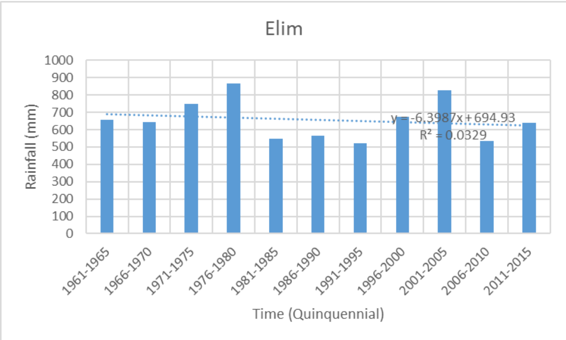

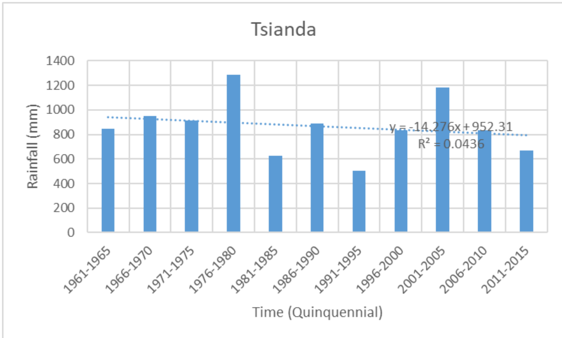

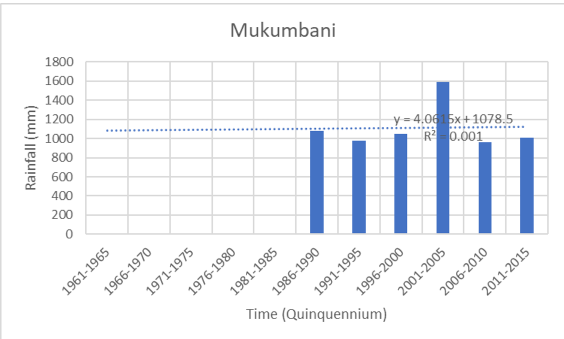

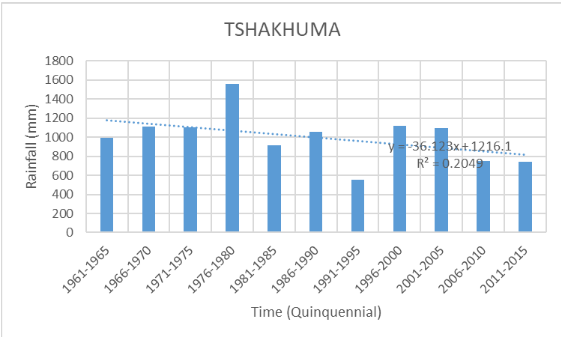

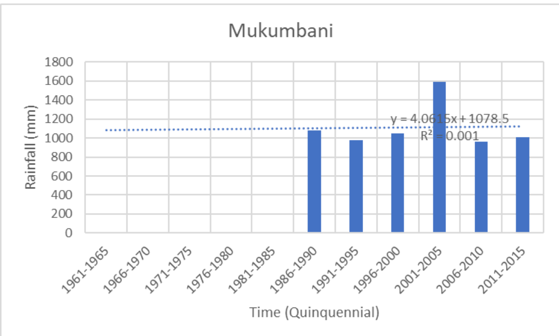

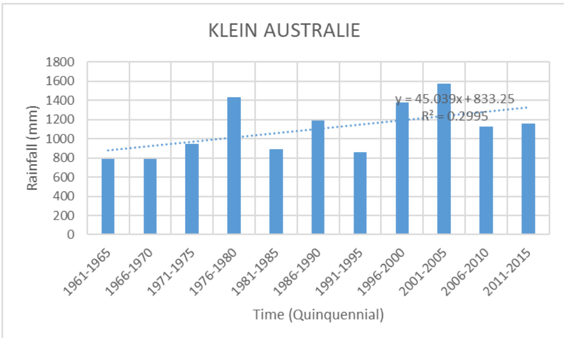

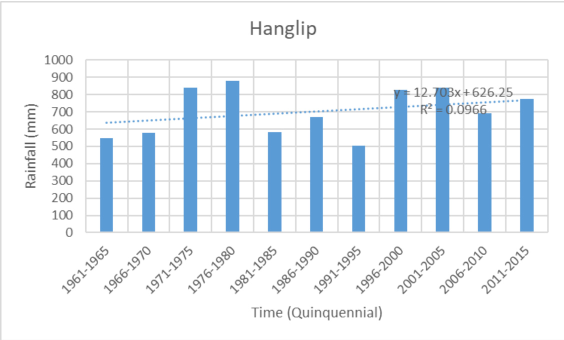
Hanglip
Rainfall (mm)
Time (Quinquennial)
y = 12.703x + 626.25
R² = 0.0966

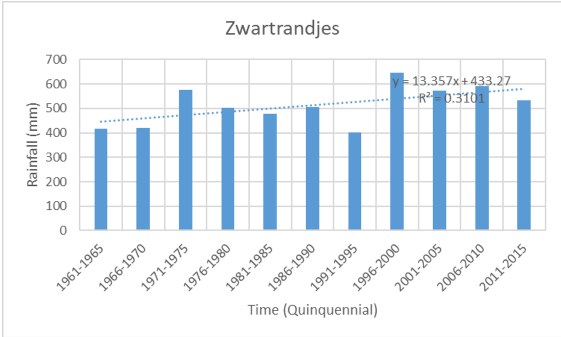
Zwartrandjes
Rainfall (mm)
Time (Quinquennial)
y = 13.357x + 433.27
R² = 0.3101

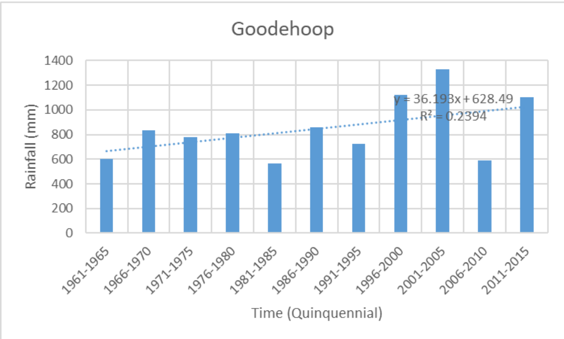
Goodehoop
Rainfall (mm)
Time (Quinquennial)
y = 36.193x + 628.49
R² = 0.2394

Appendix 5: Decadal variability

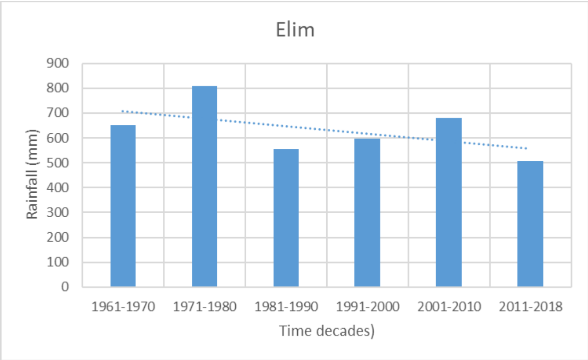

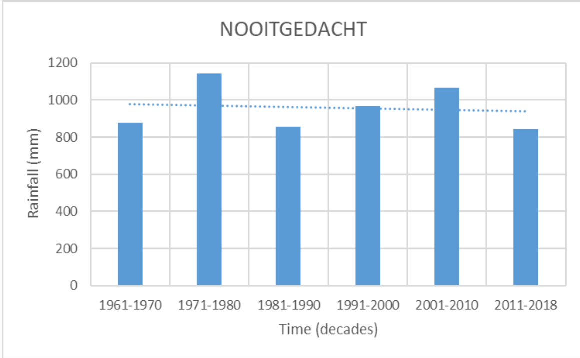

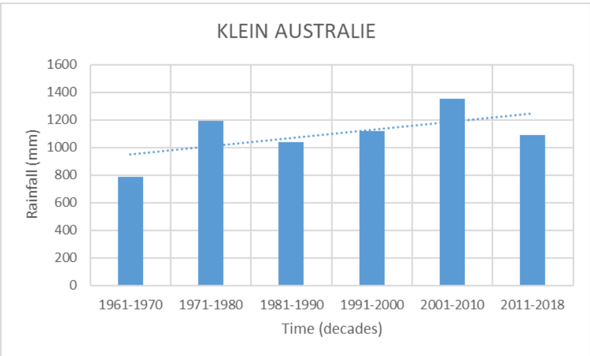

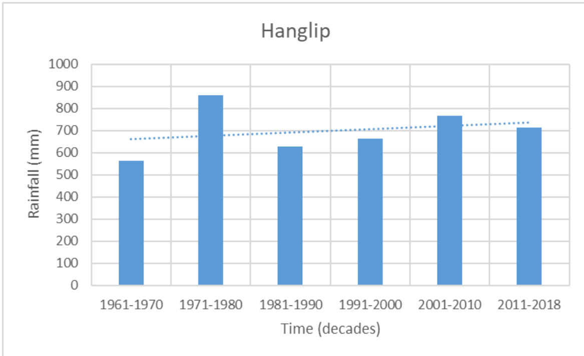

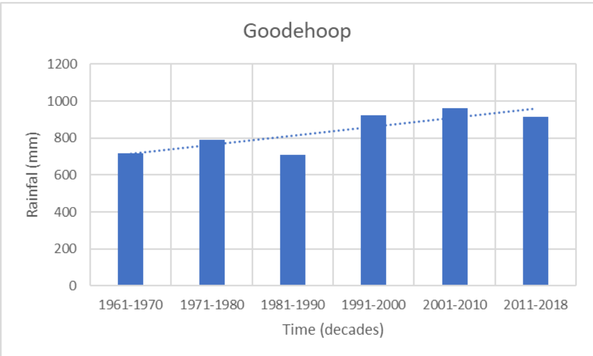

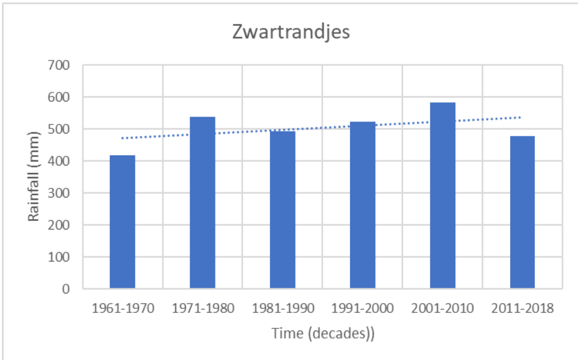

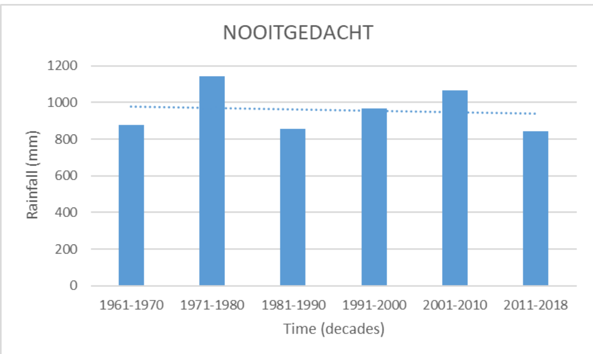

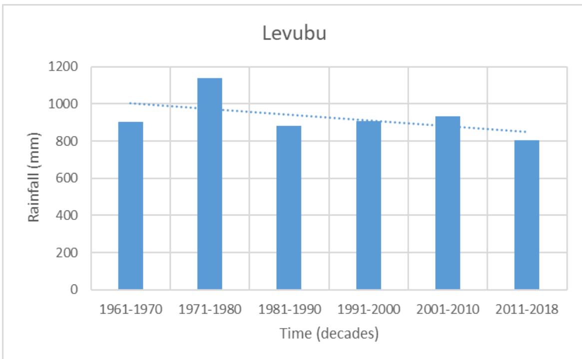

Appendix 6: Historical aridity and their Sen's slope

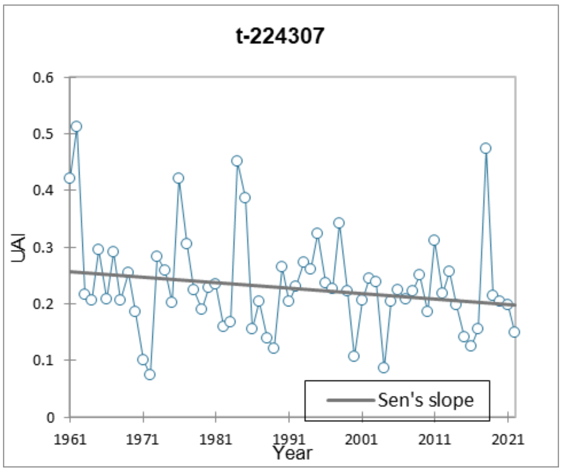

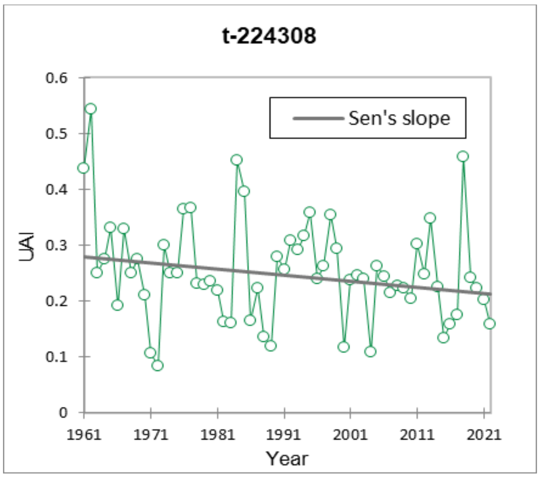

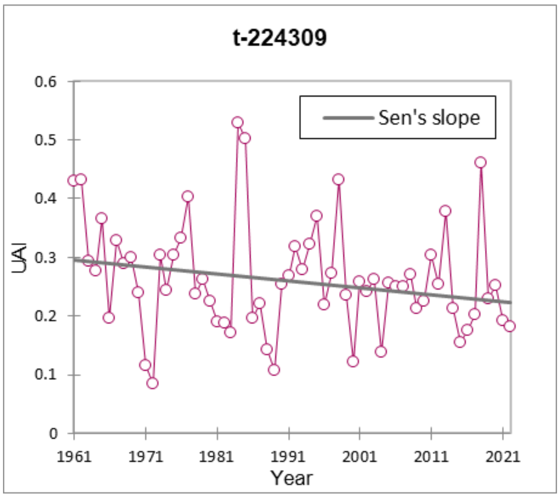

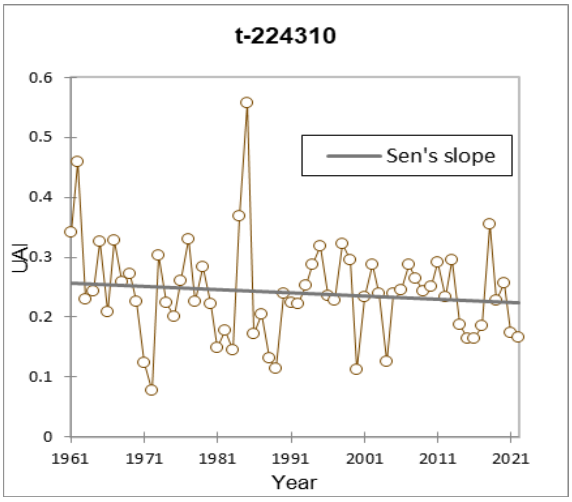

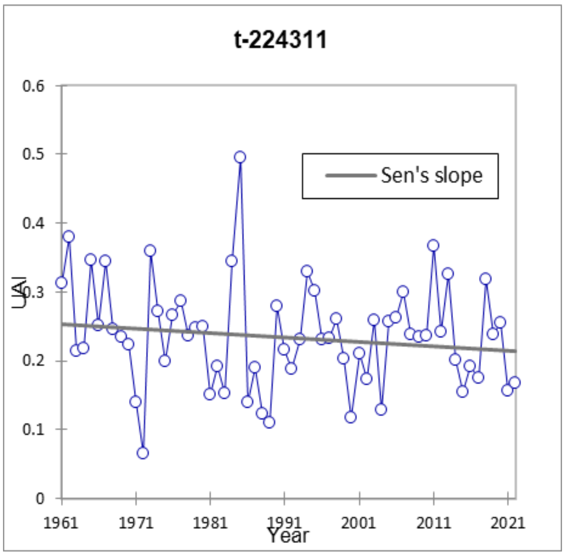

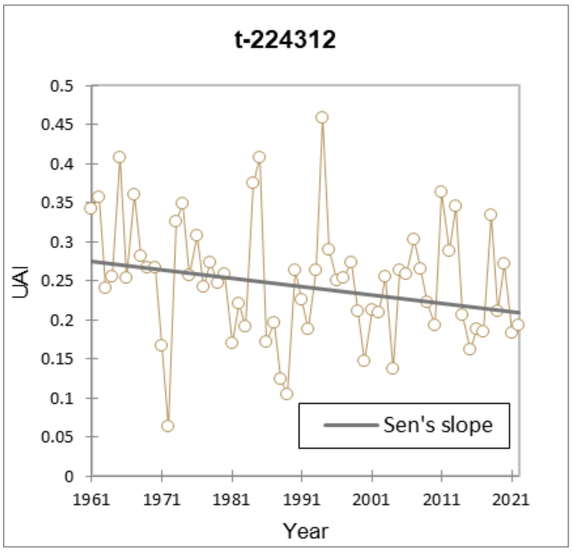

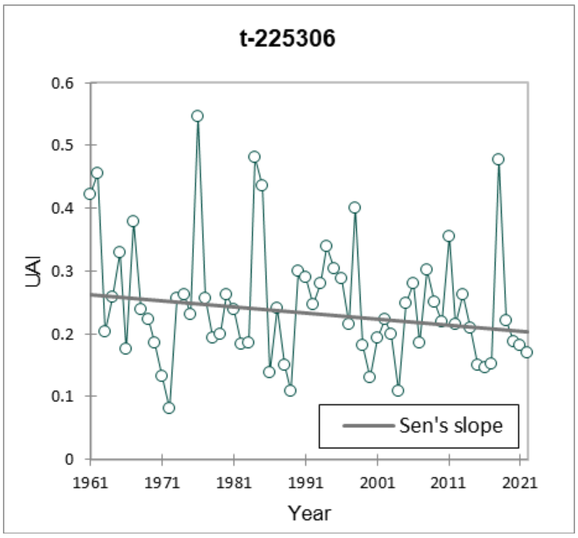
t-225306
UAI
Year
Sen's slope
0
0.1
0.2
0.3
0.4
0.5
0.6
1961
1971
1981
1991
2001
2011
2021

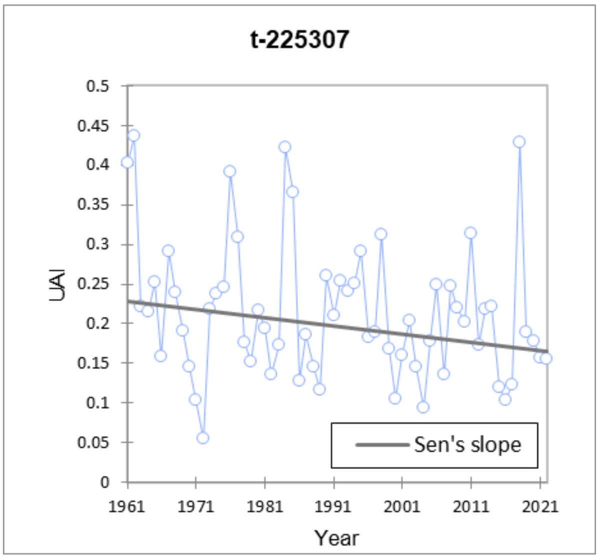
t-225307
UAI
Year
Sen's slope
0
0.05
0.1
0.15
0.2
0.25
0.3
0.35
0.4
0.45
0.5
1961
1971
1981
1991
2001
2011
2021

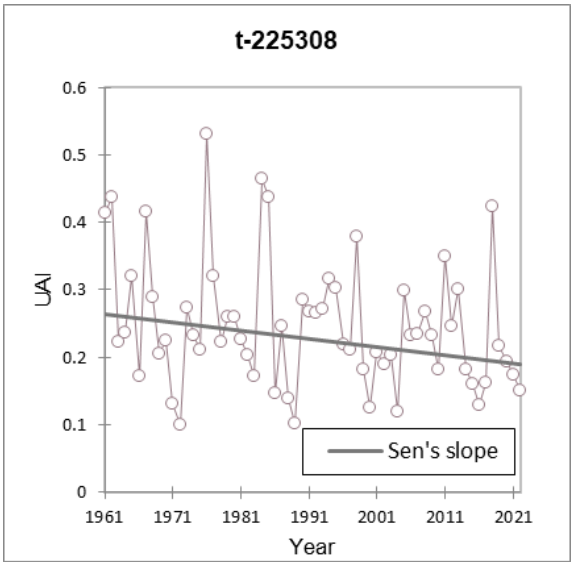
t-225308
UAI
Year
Sen's slope
0
0.1
0.2
0.3
0.4
0.5
0.6
1961
1971
1981
1991
2001
2011
2021

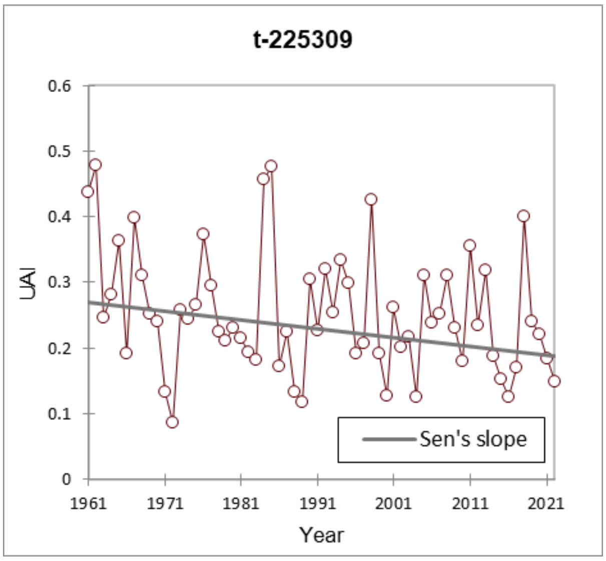
t-225309
UAI
Year
Sen's slope
0
0.1
0.2
0.3
0.4
0.5
0.6
1961
1971
1981
1991
2001
2011
2021

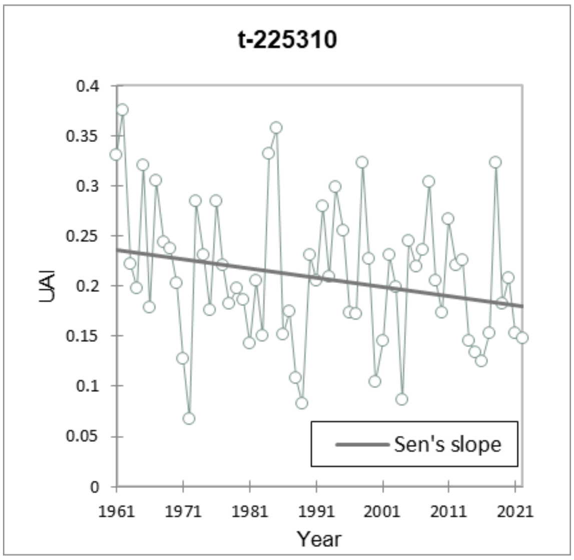
t-225310
UAI
Year
Sen's slope
0
0.05
0.1
0.15
0.2
0.25
0.3
0.35
0.4
1961
1971
1981
1991
2001
2011
2021

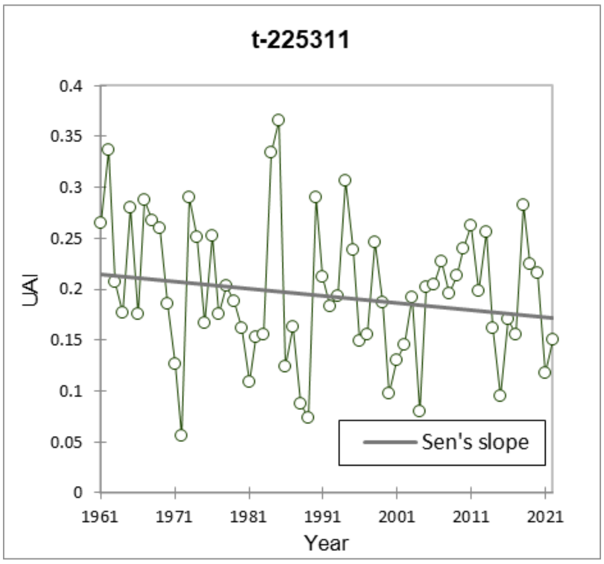
t-225311
UAI
Year
Sen's slope
0
0.05
0.1
0.15
0.2
0.25
0.3
0.35
0.4
1961
1971
1981
1991
2001
2011
2021

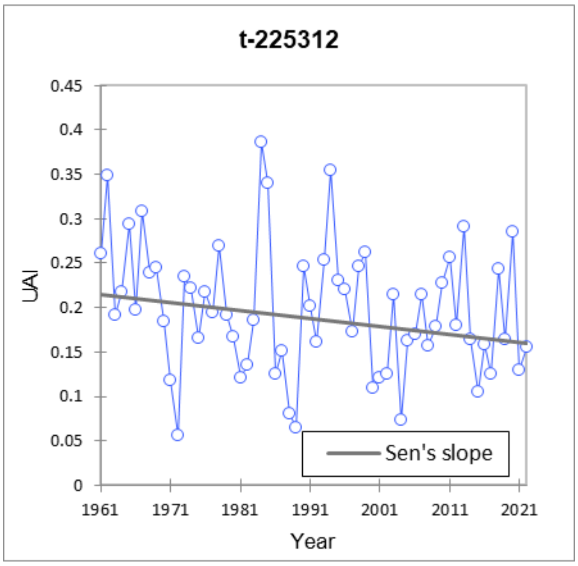
t-225312
0.45
0.4
0.35
0.3
0.25
0.2
0.15
0.1
0.05
0
UAI
Sen's slope
1961
1971
1981
1991
2001
2011
2021
Year

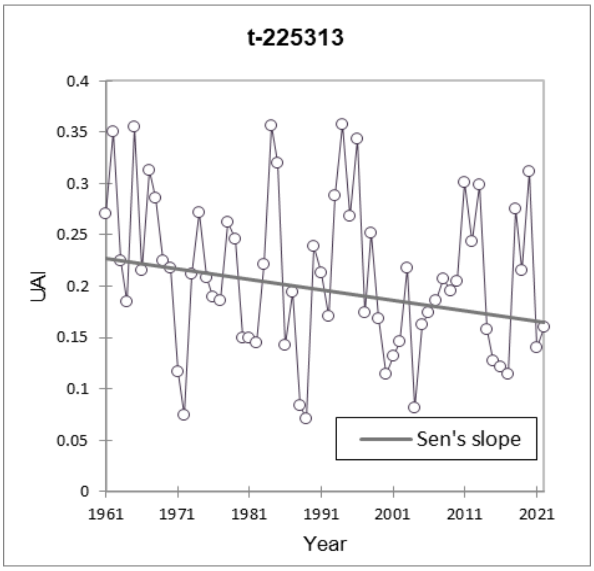
t-225313
0.4
0.35
0.3
0.25
0.2
0.15
0.1
0.05
0
UAI
Sen's slope
1961
1971
1981
1991
2001
2011
2021
Year

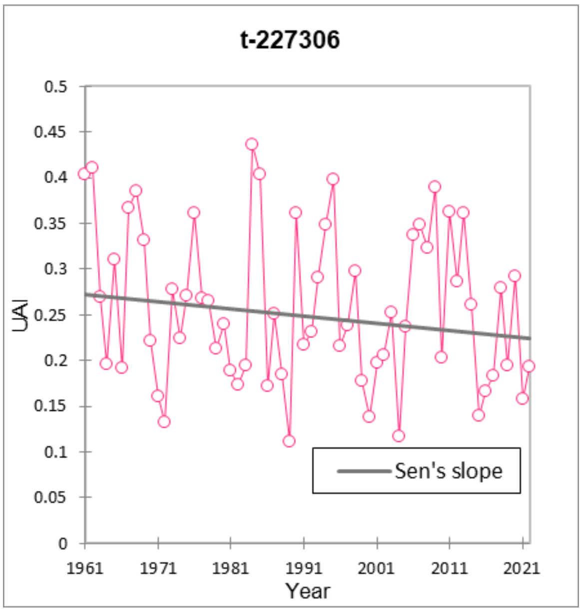
t-227306
0.5
0.45
0.4
0.35
0.3
0.25
0.2
0.15
0.1
0.05
0
UAI
Sen's slope
1961
1971
1981
1991
2001
2011
2021
Year

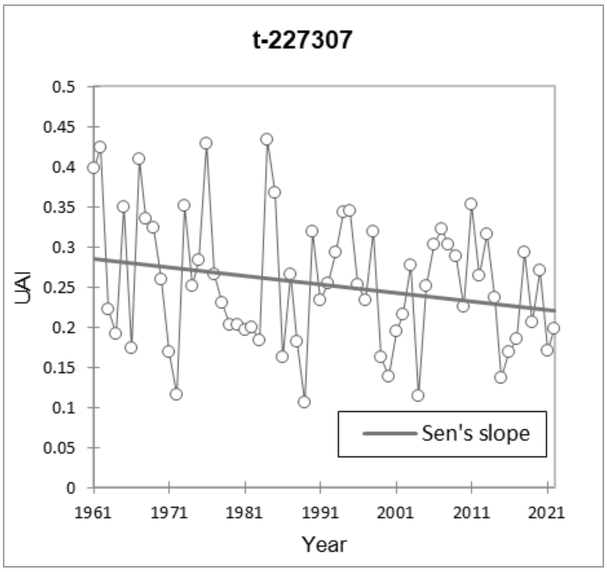
t-227307
0.5
0.45
0.4
0.35
0.3
0.25
0.2
0.15
0.1
0.05
0
UAI
Sen's slope
1961
1971
1981
1991
2001
2011
2021
Year

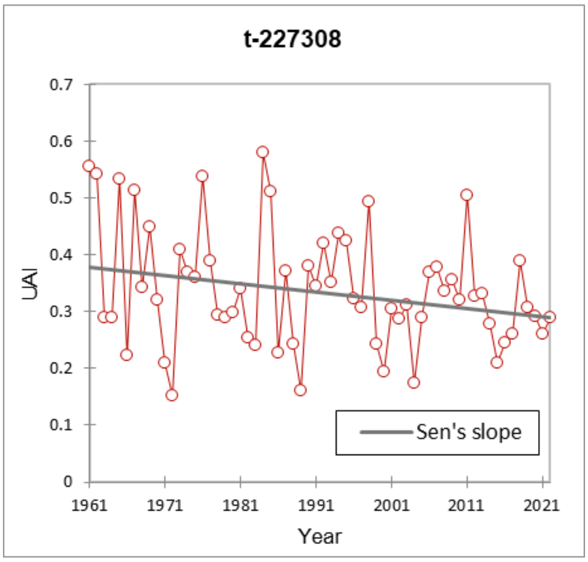
t-227308
0.7
0.6
0.5
0.4
0.3
0.2
0.1
0
UAI
Sen's slope
1961
1971
1981
1991
2001
2011
2021
Year

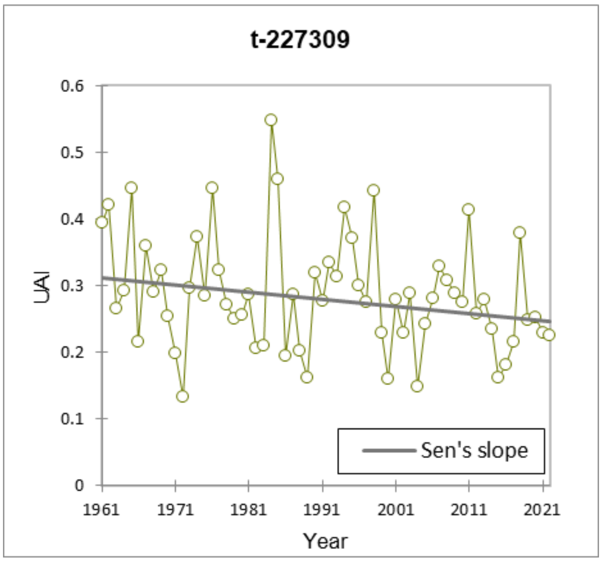
t-227309
0.6
0.5
0.4
0.3
0.2
0.1
0
UAI
Sen's slope
1961
1971
1981
1991
2001
2011
2021
Year

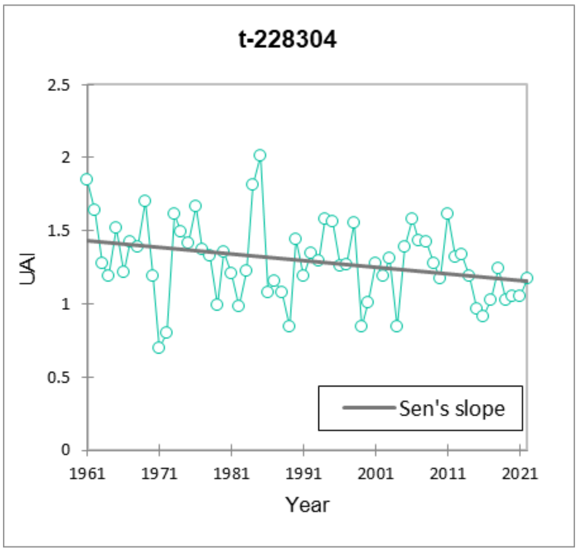
t-228304
UAI
Year
Sen's slope

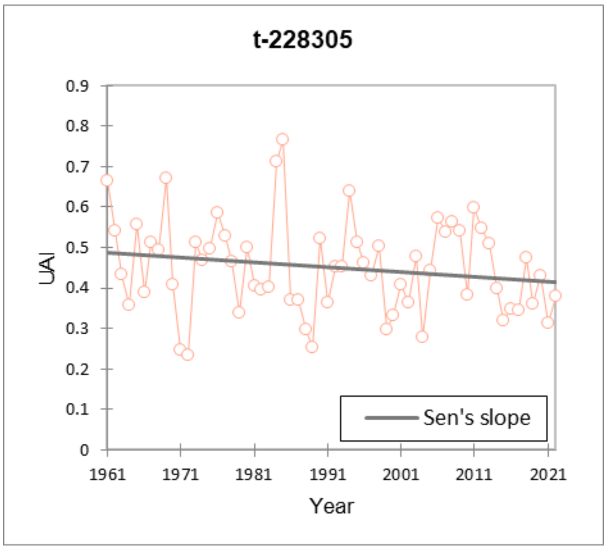
t-228305
UAI
Year
Sen's slope

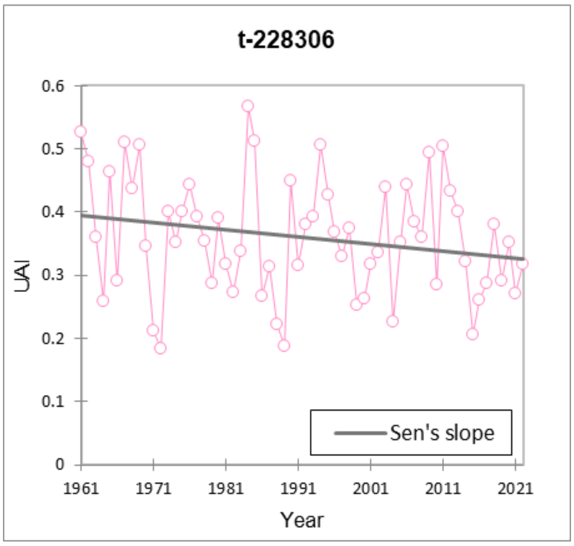
t-228306
UAI
Year
Sen's slope

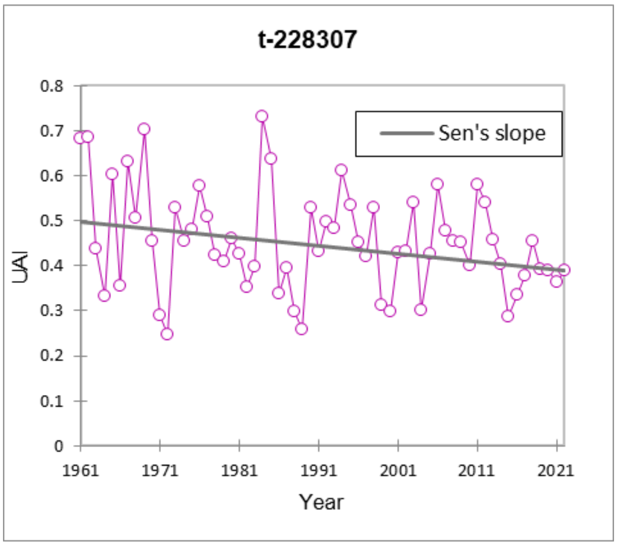
t-228307
UAI
Year
Sen's slope

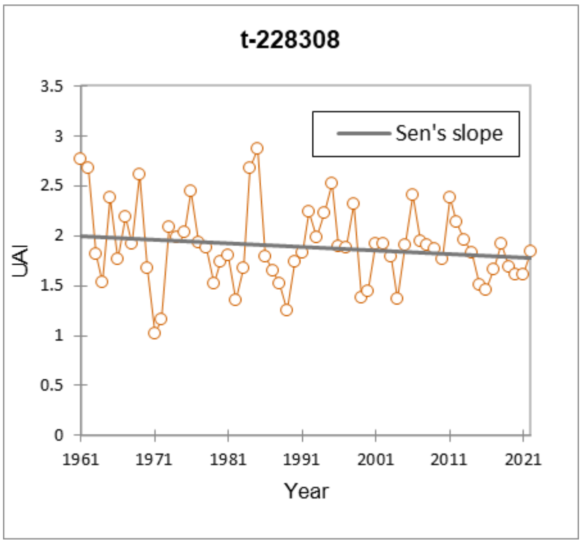
t-228308
UAI
Year
Sen's slope

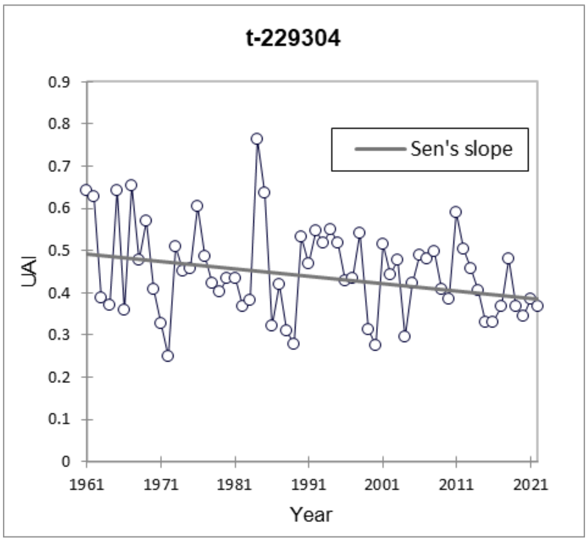
t-229304
UAI
Year
Sen's slope

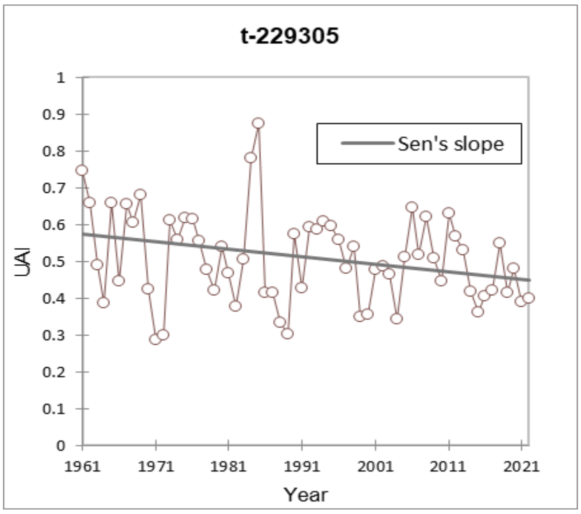
t-229305
Sen's slope
UAI
Year
1961
1971
1981
1991
2001
2011
2021
0
0.1
0.2
0.3
0.4
0.5
0.6
0.7
0.8
0.9
1

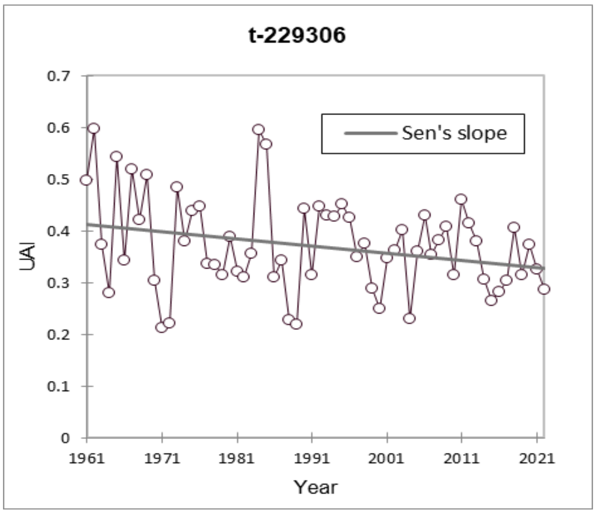
t-229306
Sen's slope
UAI
Year
1961
1971
1981
1991
2001
2011
2021
0
0.1
0.2
0.3
0.4
0.5
0.6
0.7

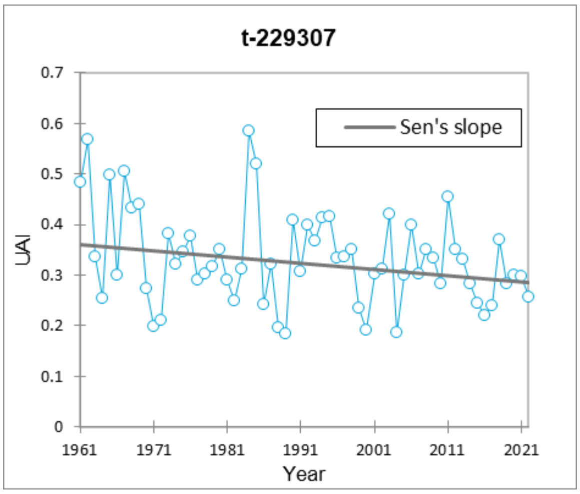
t-229307
Sen's slope
UAI
Year
1961
1971
1981
1991
2001
2011
2021
0
0.1
0.2
0.3
0.4
0.5
0.6
0.7

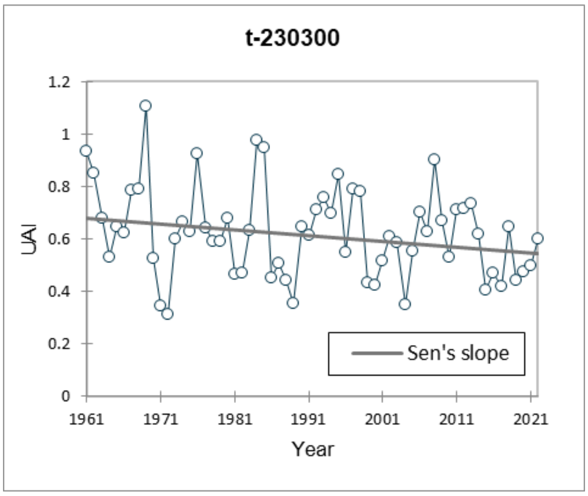
t-230300
Sen's slope
UAI
Year
1961
1971
1981
1991
2001
2011
2021
0
0.2
0.4
0.6
0.8
1
1.2

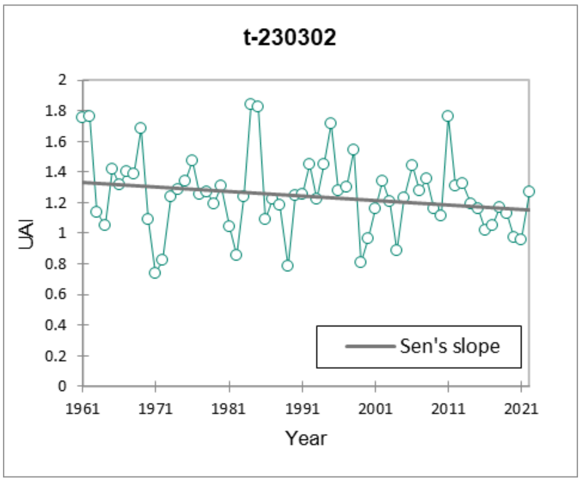
t-230302
Sen's slope
UAI
Year
1961
1971
1981
1991
2001
2011
2021
0
0.2
0.4
0.6
0.8
1
1.2
1.4
1.6
1.8
2

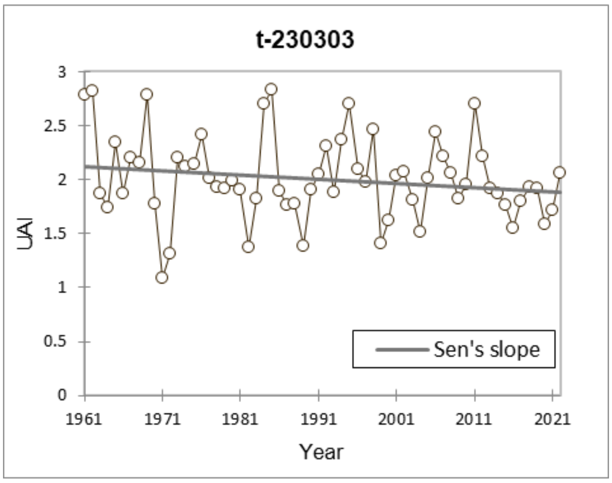
t-230303
Sen's slope
UAI
Year
1961
1971
1981
1991
2001
2011
2021
0
0.5
1
1.5
2
2.5
3

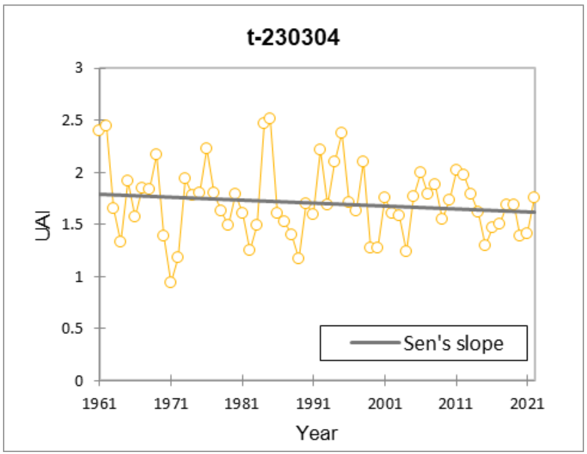
t-230304
Sen's slope
UAI
Year

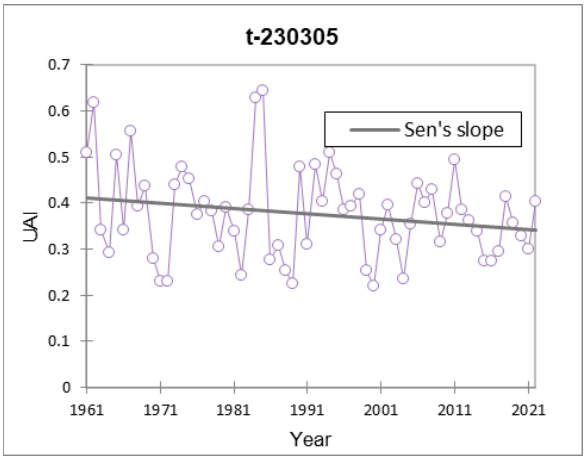
t-230305
Sen's slope
UAI
Year

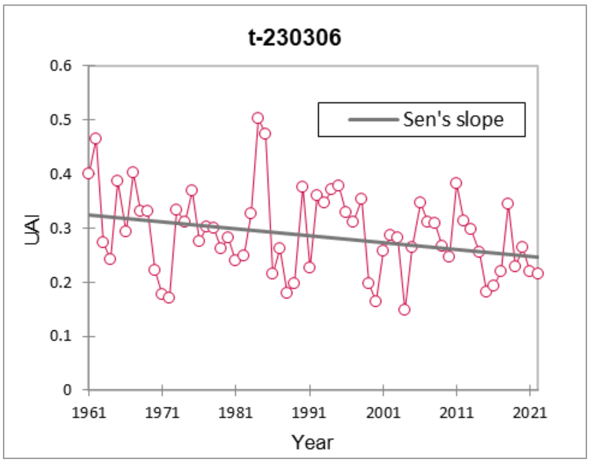
t-230306
Sen's slope
UAI
Year

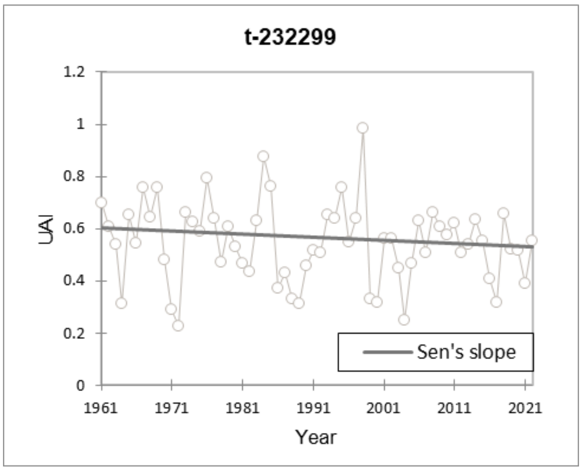
t-232299
Sen's slope
UAI
Year

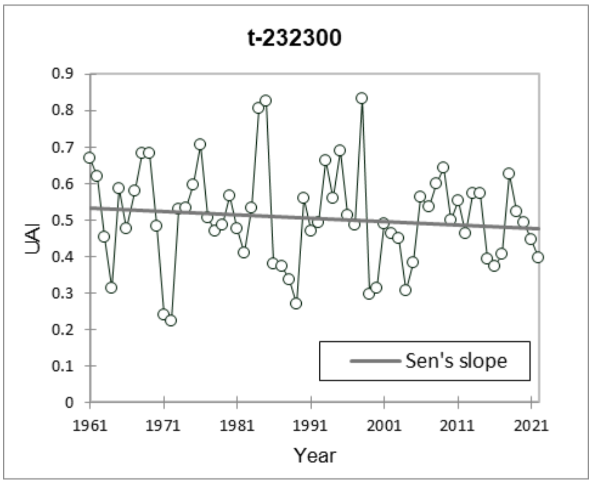
t-232300
Sen's slope
UAI
Year

Appendix 7: Projected aridity and their Sen's slope

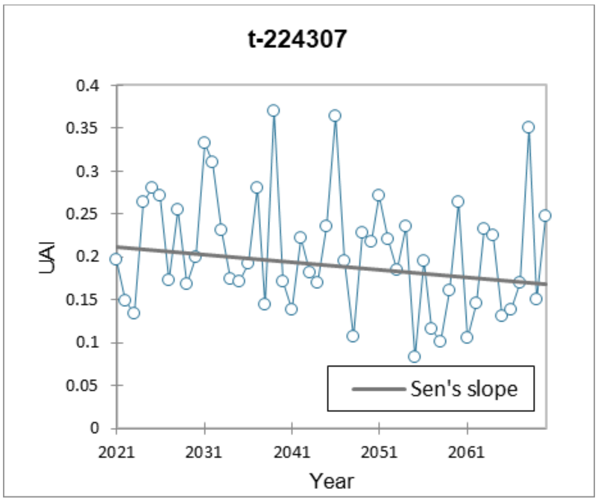

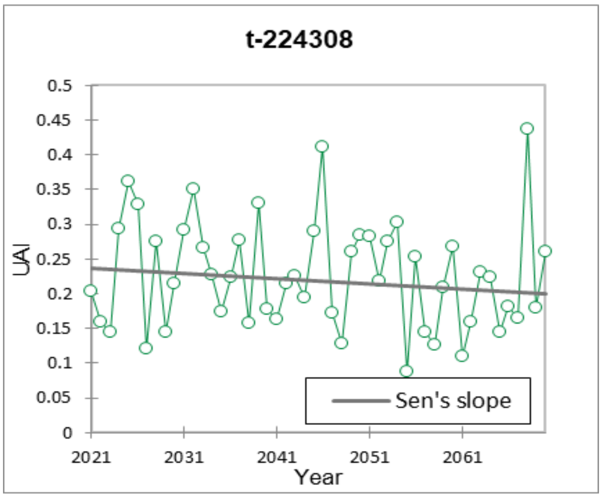

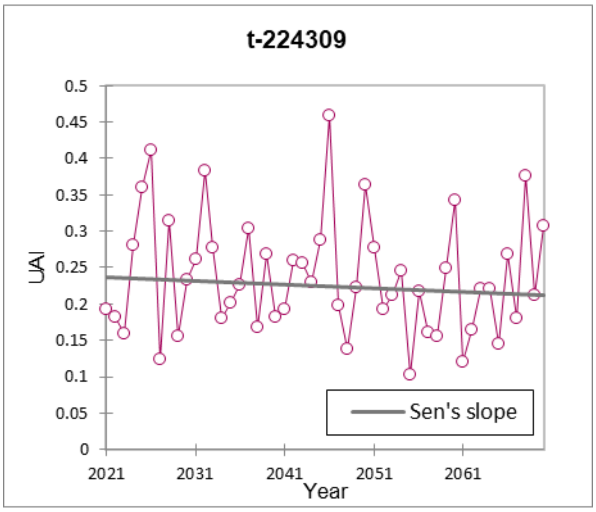

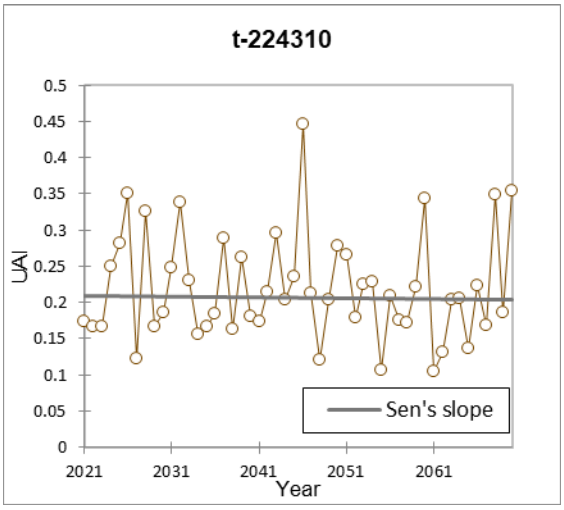

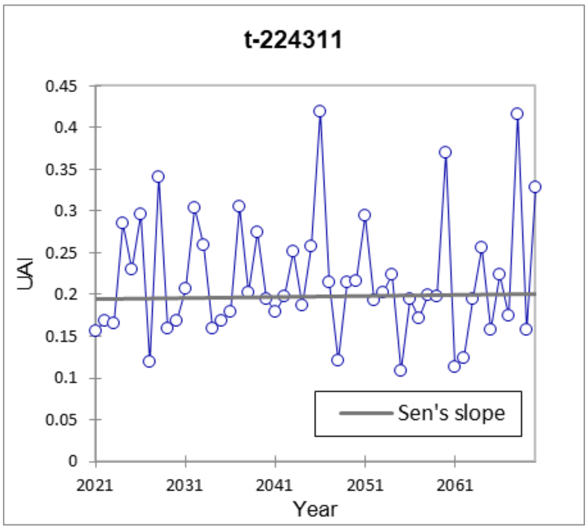

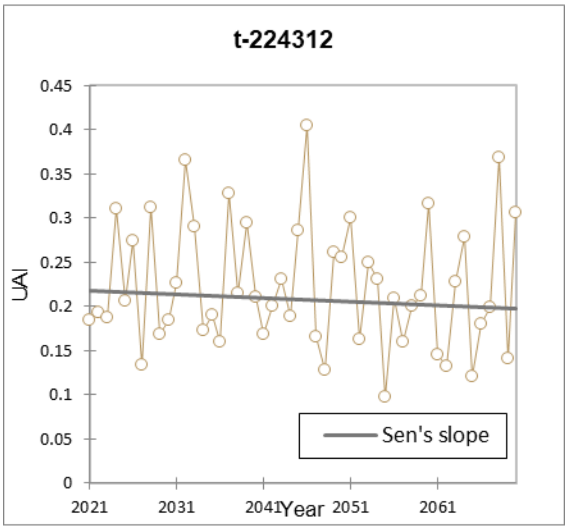

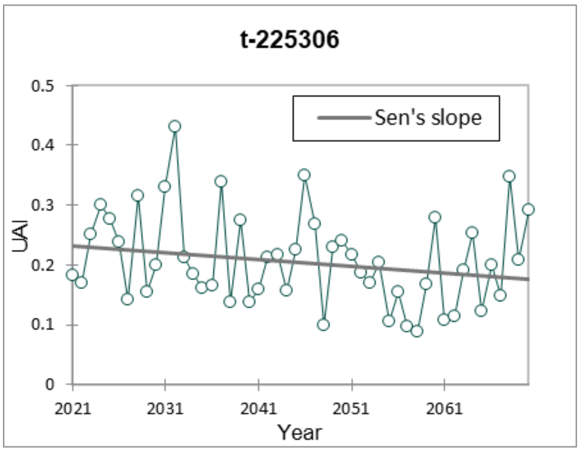
t-225306
Sen's slope
UAI
Year
0.5
0.4
0.3
0.2
0.1
0
2021
2031
2041
2051
2061

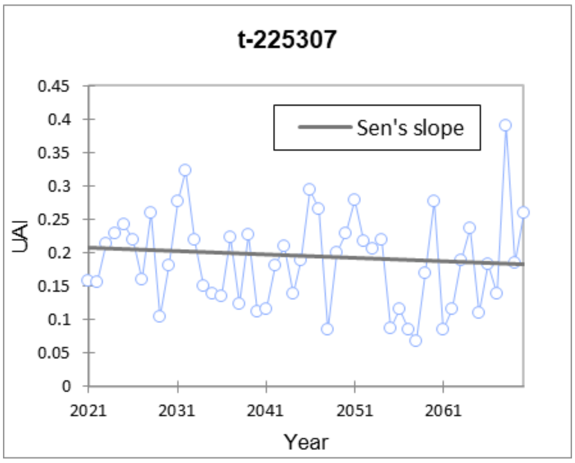
t-225307
Sen's slope
UAI
Year
0.45
0.4
0.35
0.3
0.25
0.2
0.15
0.1
0.05
0
2021
2031
2041
2051
2061

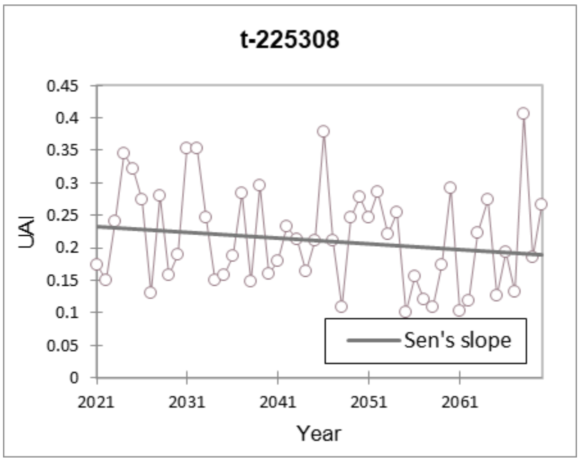
t-225308
Sen's slope
UAI
Year
0.45
0.4
0.35
0.3
0.25
0.2
0.15
0.1
0.05
0
2021
2031
2041
2051
2061

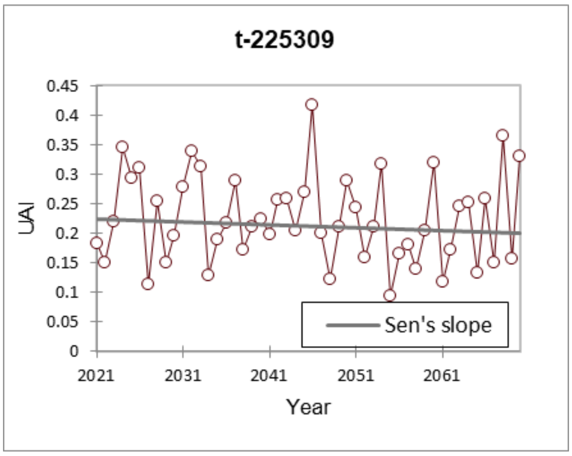
t-225309
Sen's slope
UAI
Year
0.45
0.4
0.35
0.3
0.25
0.2
0.15
0.1
0.05
0
2021
2031
2041
2051
2061

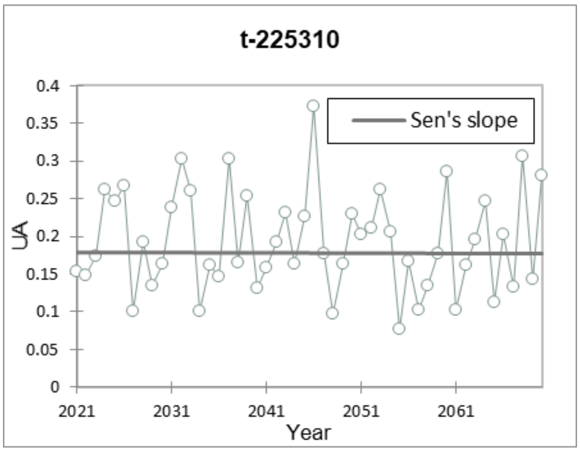
t-225310
Sen's slope
UAI
Year
0.4
0.35
0.3
0.25
0.2
0.15
0.1
0.05
0
2021
2031
2041
2051
2061

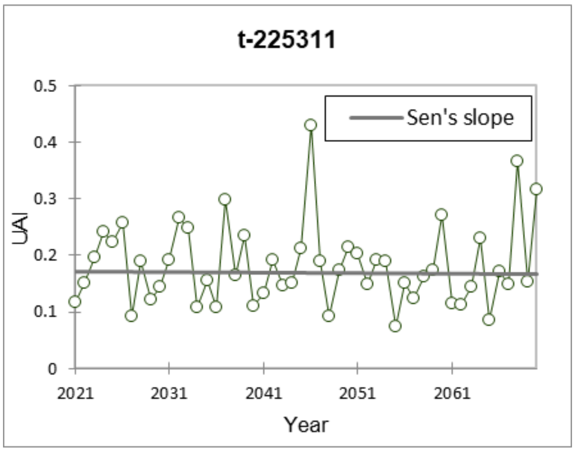
t-225311
Sen's slope
UAI
Year
0.5
0.4
0.3
0.2
0.1
0
2021
2031
2041
2051
2061

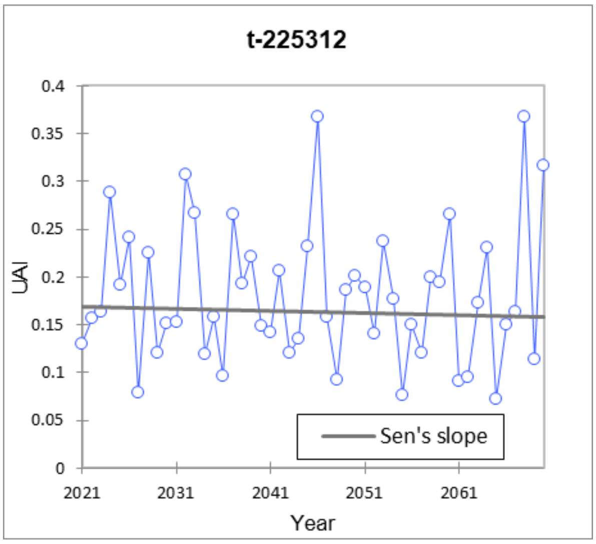
t-225312
UAI
Year
Sen's slope

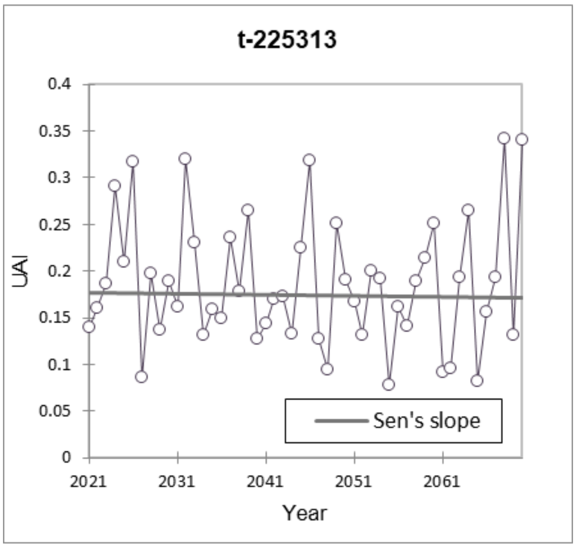
t-225313
UAI
Year
Sen's slope

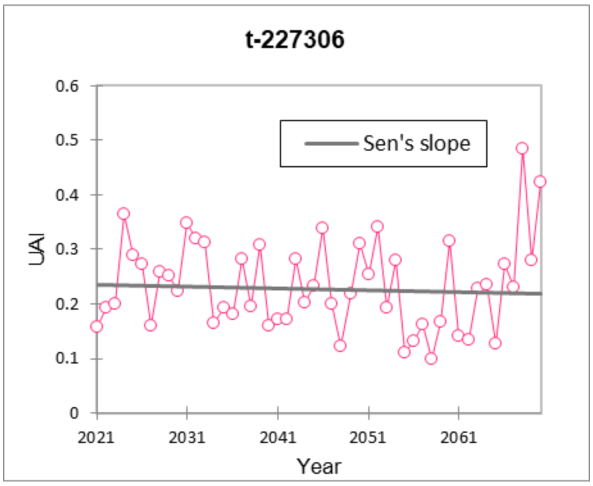
t-227306
UAI
Year
Sen's slope

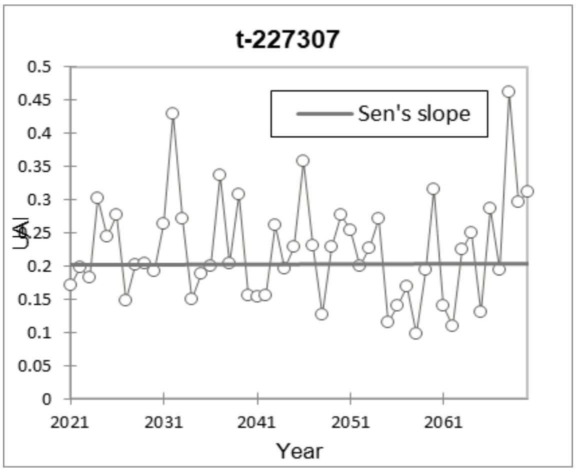
t-227307
UAI
Year
Sen's slope

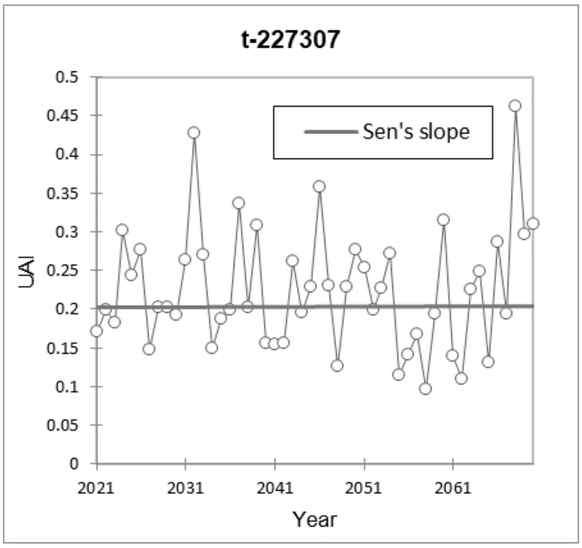
t-227307
UAI
Year
Sen's slope

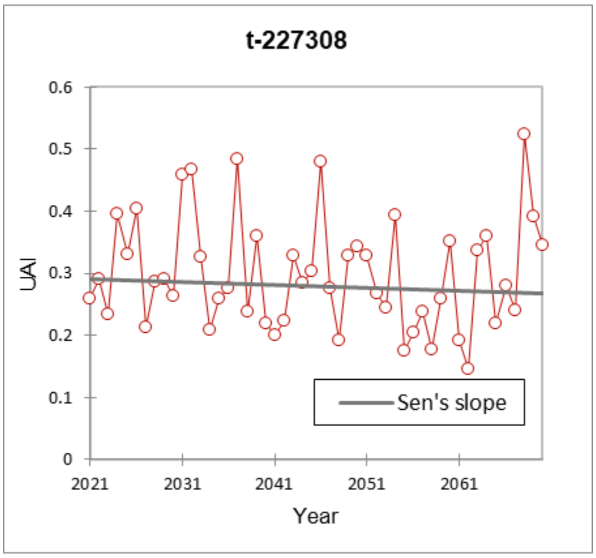
t-227308
UAI
Year
Sen's slope

University of Venda
Creating Future Leaders

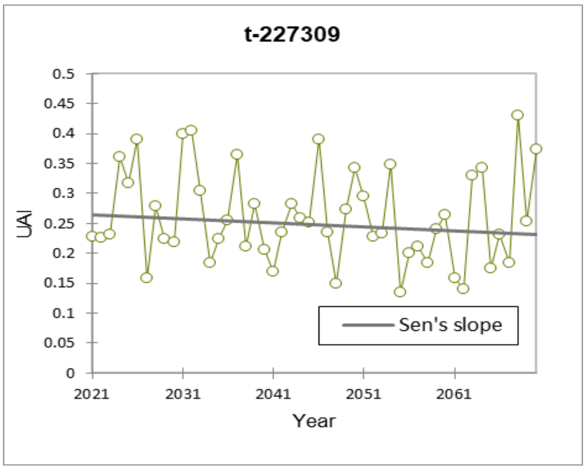

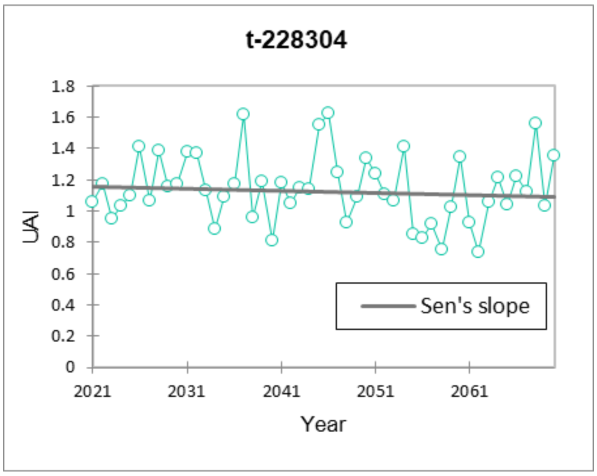

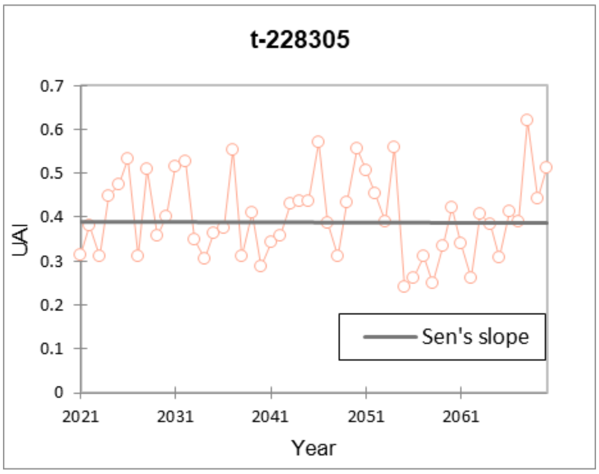

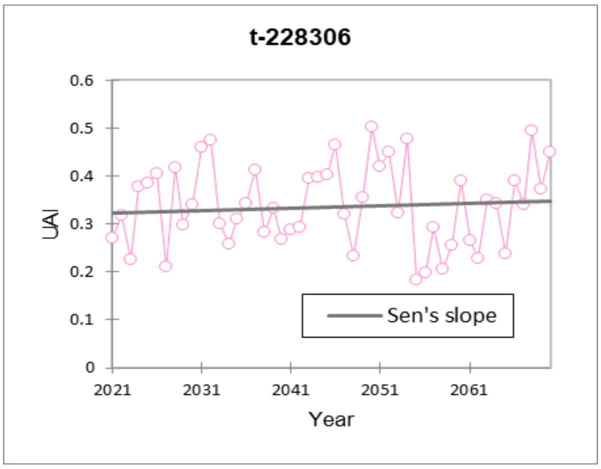

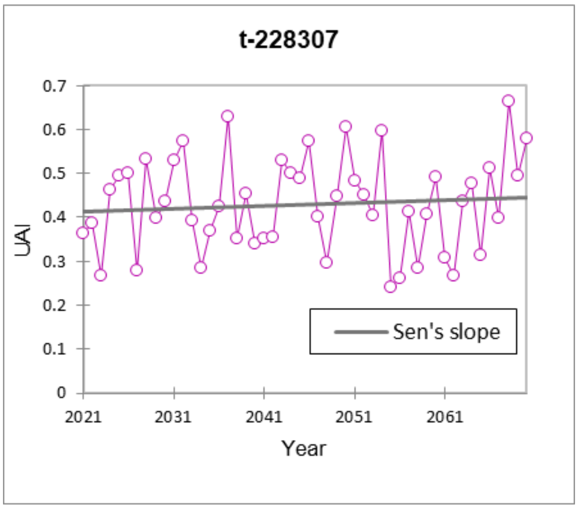

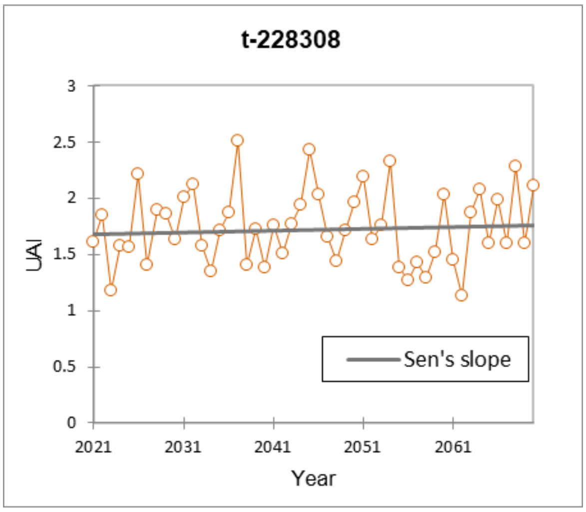

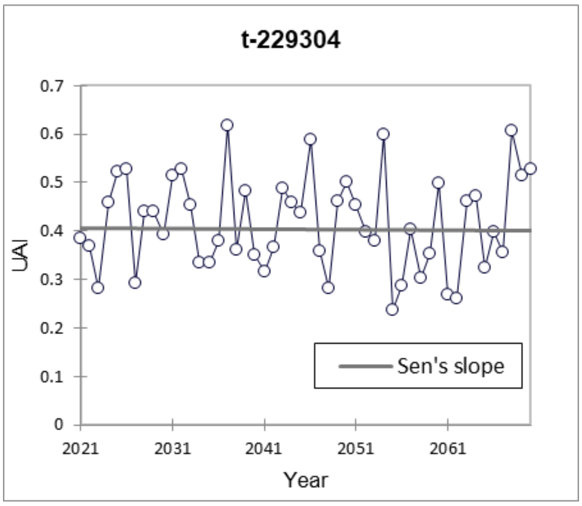
t-229304
0.7
0.6
0.5
0.4
0.3
0.2
0.1
0
UAI
2021
2031
2041
2051
2061
Year
Sen's slope

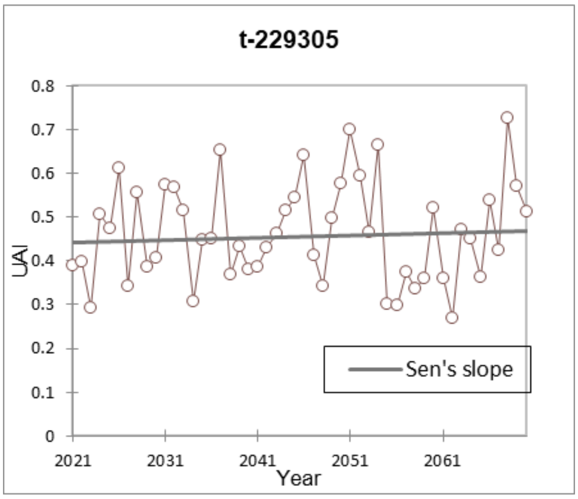
t-229305
0.8
0.7
0.6
0.5
0.4
0.3
0.2
0.1
0
UAI
2021
2031
2041
2051
2061
Year
Sen's slope

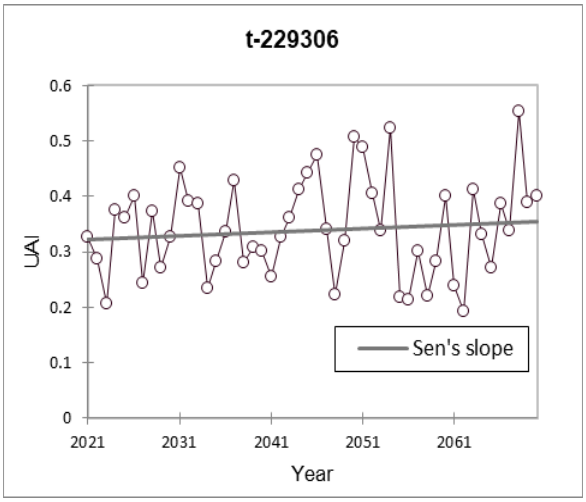
t-229306
0.6
0.5
0.4
0.3
0.2
0.1
0
UAI
2021
2031
2041
2051
2061
Year
Sen's slope

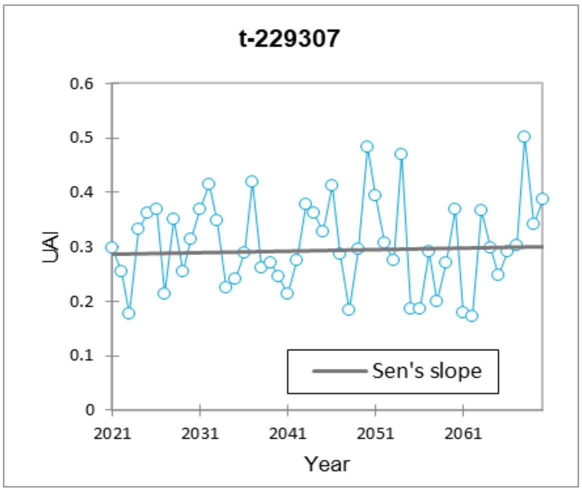
t-229307
0.6
0.5
0.4
0.3
0.2
0.1
0
UAI
2021
2031
2041
2051
2061
Year
Sen's slope

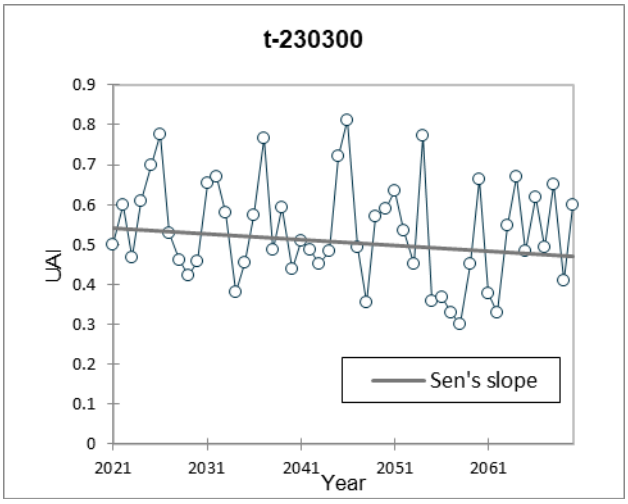
t-230300
0.9
0.8
0.7
0.6
0.5
0.4
0.3
0.2
0.1
0
UAI
2021
2031
2041
2051
2061
Year
Sen's slope

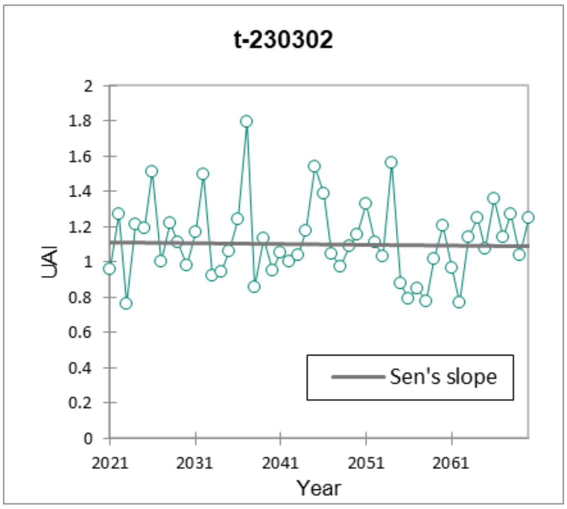
t-230302
2
1.8
1.6
1.4
1.2
1
0.8
0.6
0.4
0.2
0
UAI
2021
2031
2041
2051
2061
Year
Sen's slope

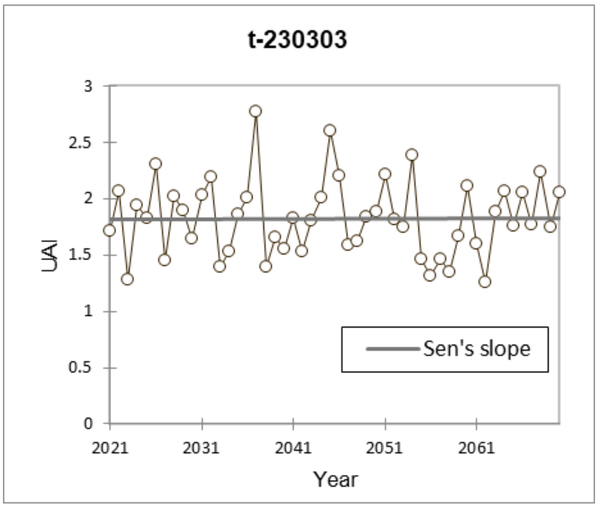
t-230303
UAI
Year
Sen's slope
0
0.5
1
1.5
2
2.5
3
2021
2031
2041
2051
2061

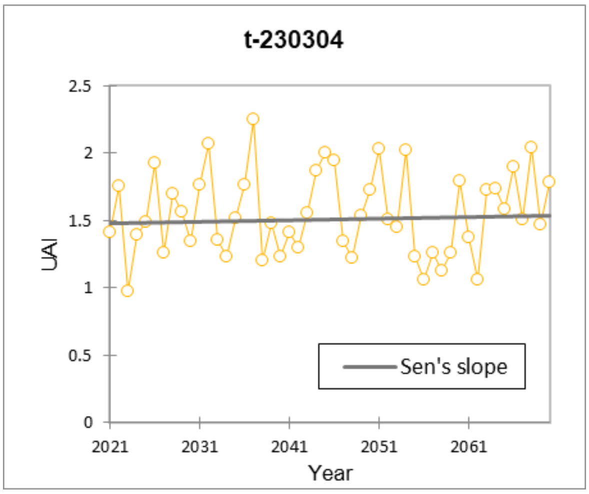
t-230304
UAI
Year
Sen's slope
0
0.5
1
1.5
2
2.5
2021
2031
2041
2051
2061

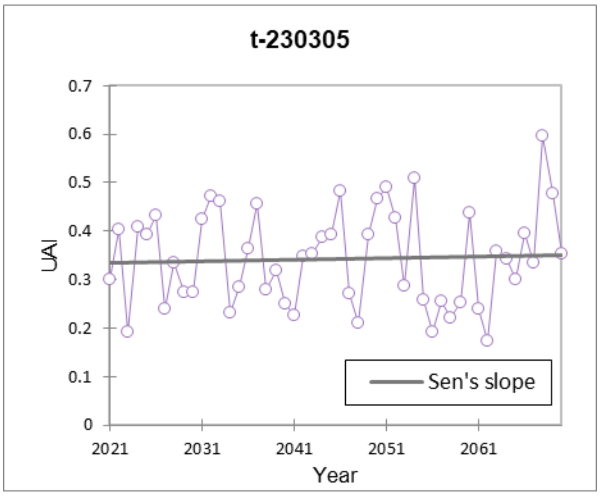
t-230305
UAI
Year
Sen's slope
0
0.1
0.2
0.3
0.4
0.5
0.6
0.7
2021
2031
2041
2051
2061

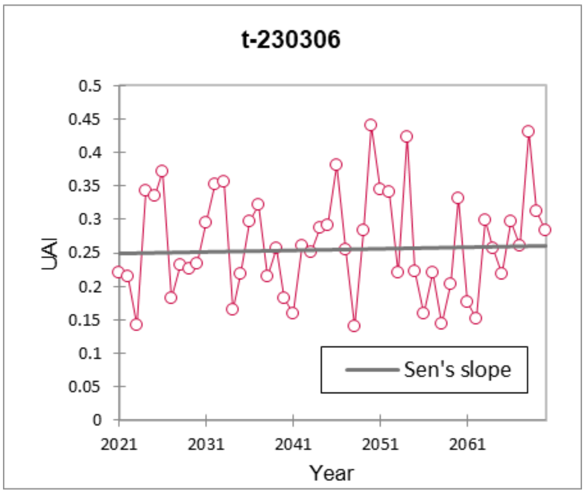
t-230306
UAI
Year
Sen's slope
0
0.05
0.1
0.15
0.2
0.25
0.3
0.35
0.4
0.45
0.5
2021
2031
2041
2051
2061

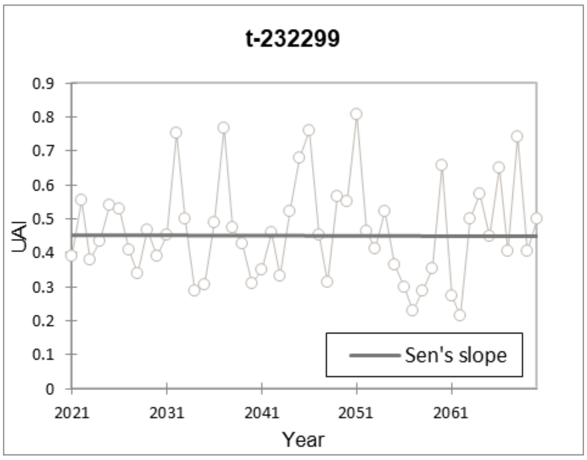
t-232299
UAI
Year
Sen's slope
0
0.1
0.2
0.3
0.4
0.5
0.6
0.7
0.8
0.9
2021
2031
2041
2051
2061

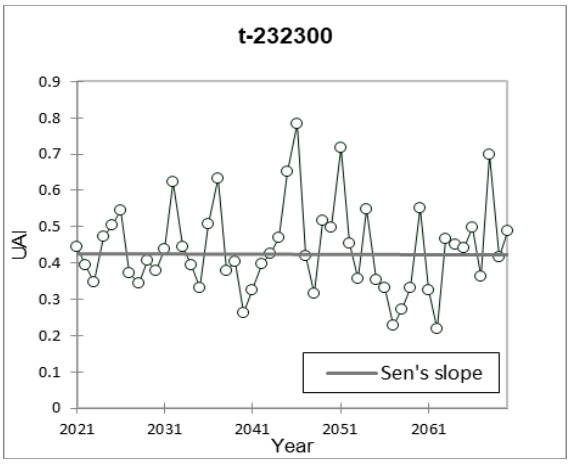
t-232300
UAI
Year
Sen's slope
0
0.1
0.2
0.3
0.4
0.5
0.6
0.7
0.8
0.9
2021
2031
2041
2051
2061